CARDIAC HYPERTROPHY: FROM COMPENSATION TO DECOMPENSATION AND PHARMACOLOGICAL INTERVENTIONS

EDITED BY: Hai-Gang Zhang, Ya Liu and Xiongwen Chen

PUBLISHED IN: Frontiers in Pharmacology

frontiers Research Topics

ISSN 1664-8714
ISBN 978-2-88966-909-7
DOI 10.3389/978-2-88966-909-7

About Frontiers

Frontiers is more than just an open-access publisher of scholarly articles: it is a pioneering approach to the world of academia, radically improving the way scholarly research is managed. The grand vision of Frontiers is a world where all people have an equal opportunity to seek, share and generate knowledge. Frontiers provides immediate and permanent online open access to all its publications, but this alone is not enough to realize our grand goals.

Frontiers Journal Series

The Frontiers Journal Series is a multi-tier and interdisciplinary set of open-access, online journals, promising a paradigm shift from the current review, selection and dissemination processes in academic publishing. All Frontiers journals are driven by researchers for researchers; therefore, they constitute a service to the scholarly community. At the same time, the Frontiers Journal Series operates on a revolutionary invention, the tiered publishing system, initially addressing specific communities of scholars, and gradually climbing up to broader public understanding, thus serving the interests of the lay society, too.

Dedication to Quality

Each Frontiers article is a landmark of the highest quality, thanks to genuinely collaborative interactions between authors and review editors, who include some of the world's best academicians. Research must be certified by peers before entering a stream of knowledge that may eventually reach the public - and shape society; therefore, Frontiers only applies the most rigorous and unbiased reviews.
Frontiers revolutionizes research publishing by freely delivering the most outstanding research, evaluated with no bias from both the academic and social point of view. By applying the most advanced information technologies, Frontiers is catapulting scholarly publishing into a new generation.

What are Frontiers Research Topics?

Frontiers Research Topics are very popular trademarks of the Frontiers Journals Series: they are collections of at least ten articles, all centered on a particular subject. With their unique mix of varied contributions from Original Research to Review Articles, Frontiers Research Topics unify the most influential researchers, the latest key findings and historical advances in a hot research area! Find out more on how to host your own Frontiers Research Topic or contribute to one as an author by contacting the Frontiers Editorial Office: frontiersin.org/about/contact

CARDIAC HYPERTROPHY: FROM COMPENSATION TO DECOMPENSATION AND PHARMACOLOGICAL INTERVENTIONS

Topic Editors:
Hai-Gang Zhang, Army Medical University, China
Ya Liu, Army Medical University, China
Xiongwen Chen, Temple University, United States

Citation: Zhang, H.-G., Liu, Y., Chen, X., eds. (2021). Cardiac Hypertrophy: From Compensation to Decompensation and Pharmacological Interventions. Lausanne: Frontiers Media SA. doi: 10.3389/978-2-88966-909-7

Table of Contents

frontiers in Pharmacology

EDITORIAL
published: 26 April 2021
doi: 10.3389/fphar.2021.665936

Editorial: Cardiac Hypertrophy: From Compensation to Decompensation and Pharmacological Interventions

Ya Liu[1], *Xiongwen Chen*[2]* *and Hai-Gang Zhang*[1]*

[1]Department of Pharmacology, Army Medical University (Third Military Medical University), Chongqing, China, [2]Cardiovascular Research Center, Temple University Lewis Katz School of Medicine, Philadelphia, PA, United States

Keywords: cardiac hypertrophy, cardiac fibrosis, heart failure, cardiac remodeling, heart function

Editorial on the Research Topic

Cardiac Hypertrophy: From Compensation to Decompensation and Pharmacological Interventions

INTRODUCTION

Cardiac hypertrophy is not a single disease, but a complication and a pathological process of many forms of cardiovascular disease, such as hypertension, congestive heart failure, valvular diseases and ischemic diseases, etc. (Yu et al., 2020). It is characterized by abnormal increases in mass and volume of myocardium at the whole heart level, in the size of individual myocyte at cell level, and in synthesis of protein and reprogramming expression of fetal genes at molecule level (Dodge-Kafka et al., 2019; Zhang et al., 2020). Myocardial hypertrophy is an important aspect of myocardial remodeling, which including not only the hypertrophic growth of myocytes but also the proliferation and activation of interstitial fibroblasts to produce intercellular matrix, namely fibrosis (Ge et al., 2021). These three pathological processes, cardiomyocyte hypertrophy, fibrosis and remodeling, are overlapped and closely related to each other.

Cardiac remodeling involves metabolic, mechanical, electrical, and structural alterations (Pitoulis and Terracciano, 2020). It is initially an adaptive response to pressure or volume overload. The myocardium undergoes hypertrophic growth as a compensatory measure aiming to improve myocardial contractility, reduce wall stress and maintain cardiac output. However, increase in mass and volume of myocardial tissue inevitably increase the oxygen consumption and dysfunction of energy metabolism in myocardial tissue (Nakamura and Sadoshima, 2018). Simultaneously, apoptosis, necrosis and autophagic cell death occur in cardiac myocytes, and proliferation and activation arise in fibroblasts, leading to interstitial fibrosis (Zhu and sun, 2018). The continued presence and evolving hypertrophy eventually lead to decompensation of heart function (Messerli et al., 2017; Oldfield et al., 2020). Many studies have demonstrated that ventricular hypertrophy and remodeling is associated with a significantly increased risk of heart failure, malignant arrhythmia, and even sudden death, and is thought to be an independent risk factor for increasing morbidity and mortality of cardiovascular diseases (He et al., 2020). Therefore, clinical guidelines in many countries and organizations have suggested it as primary goal to control or reverse cardiac hypertrophy in the therapeutics of hypertension and chronic heart failure (Di Palo and Barone, 2020).

Multiple signal transduction pathways involving Gq-phospholipase C-diacylglycerol (DAG)/inositol triphosphate (IP_3), mitogen-activated protein kinases, calcineurin-nuclear factor of activated T cells (NFAT), phosphatidylinositol 3-kinase (PI3K)/protein kinase B (AKT), mammalian target of

OPEN ACCESS

Edited and reviewed by:
Francesco Rossi,
University of Campania Luigi Vanvitelli, Italy

***Correspondence:**
Hai-Gang Zhang
hg2ster@gmail.com
hgzhang@tmmu.edu.cn;
Xiongwen Chen
xchen001@temple.edu

Specialty section:
This article was submitted to Cardiovascular and Smooth Muscle Pharmacology, a section of the journal Frontiers in Pharmacology

Received: *09 February 2021*
Accepted: *13 April 2021*
Published: *26 April 2021*

Citation:
Liu Y, Chen X and Zhang H-G (2021) Editorial: Cardiac Hypertrophy: From Compensation to Decompensation and Pharmacological Interventions. Front. Pharmacol. 12:665936. doi: 10.3389/fphar.2021.665936

rapamycin (mTOR), transforming growth factor (TGF)-β, play important roles in the development of cardiac hypertrophy (Nakamura and Sadoshima, 2018), and complex crosstalks and feedbacks among them are present widely. Although the molecular mechanisms underlying cardiac hypertrophy have been extensively studied, there are still many uncharted territories that need to be explored thoroughly, especially the molecular mechanisms that control the transformation from compensation to decompensation.

During the transition from compensated hypertrophy to decompensation and deterioration of systolic heart function, apoptotic and necroptotic loss of cardiomyocytes, contractile dysfunction and massive fibrosis are key points. Heger et al. (2016) have documented in a review article that TGFβ superfamily play a central role. Some modulators of mitochondrial pores and transporters, such as NLR Family Pyrin Domain Containing 3 (NLRP3), adenine nucleotide translocator 1 (ANT1) and various miRNAs, etc., and regulators of adrenoceptor-mediated signaling pathway, such as SMAD4 and β-arrestin, are suggested to be switch molecules for this transition. Zhen et al. (2021) recently reported that signal transducers and transcriptional activation 1 (STAT1) was able to enhance mitochondrial function and prolong the time of compensation period through uncoupling protein 2 (Ucp2)/dynamin-related protein 1 (Drp1) signaling pathway.

In recent years, noncoding RNAs including microRNAs (miRNAs), circular RNAs (circRNAs) and long non-coding RNAs (lncRNAs) have gained more and more attention in the cardiac hypertrophy research field (Heger et al., 2016; He et al., 2020). Multiple miRNAs, such as miR-1, miR-21, miR-132/212, have been uncovered to regulate the process of cardiac hypertrophy *via* influencing the expression of a number of target genes including β1-adrennergic receptor, TGFβ1 receptor III, matrix metalloproteinase-2, connexin 43 (Wang et al., 2016; Mushtaq et al., 2020). Meanwhile, various lncRNAs have been shown to play important roles in both cardiac development and pathological cardiac remodeling. Targeting noncoding RNAs seems to open up a novel strategy for the treatment of cardiac hypertrophy.

This Research Topic aims to provide a platform for discussing about the molecular mechanisms of cardiac hypertrophy and remodeling, as well as the potential drug targets. Nine articles from 5 countries are collected here. Huang et al. reported that cellular communication network factor 5 (CCN5) could inhibit fibroblast-to-myofibroblast transition and suggested it might serve as a potential biomarker for estimating cardiac fibrosis in hypertensive patients as well as a novel therapeutic target. Stafford et al. demonstrated the role of IL-10 signal in the development of cardiac hypertrophy and indicated it might become a therapeutic target. Xiang et al. contributed an interesting review paper focused on the variation of energy metabolism in exercise-induced physiological myocardial hypertrophy, which may antagonize the progress of pathological hypertrophy.

Transfer RNA derived small RNAs (tsRNAs) have recently emerged as important modulators of protein translation and shown to possess varied functions. Cao et al. reviewed that nuclear and mitochondrial tsRNAs, including tRNA halves (tiRNAs), and tRNA fragments (tRFs), exert crucial effects in the development of pathological and decompensated cardiac hypertrophy, implying new therapeutic targets to battle cardiovascular disease.

Thanks to the advantages of multi-target effects, traditional Chinese medicine has attracted growing interests in the treatment of cardiovascular diseases. Yan et al. demonstrated gallic acid could effectively attenuate angiotensin II-induced hypertension and vascular dysfunction through inhibit immunoproteasome. In the article by Li et al., it was found that triptolide, the major active component of the Chinese medicinal herb *Tripterygium wilfordii* Hook F, improved cardiac hypertrophy *via* correction of the unbalanced expression of various cell cycle regulators.

Remarkably, cardiac hypertrophy is not only a complication (result) of multiple cardiovascular diseases, but also a pathological process (reason) of them. Due to the complexity of signaling pathway networks underlying cardiac hypertrophy, it might be difficult to block and reverse cardiac hypertrophy by targeting a single molecule. Therefore, further research needs to be performed, and interventions targeting immune-inflammatory reaction and transcription factors may bring the promise to treat cardiac hypertrophy.

AUTHOR CONTRIBUTIONS

H-GZ surveyed and designed this Research Topic. YL and H-GZ wrote and drafted the editorial manuscript. XC revised the manuscript critically. All authors contributed to the article and approved the submitted version.

REFERENCES

Di Palo, K. E., and Barone, N. J. (2020). Hypertension and Heart Failure. *Heart Fail. Clin.* 16 (1), 99–106. doi:10.1016/j.hfc.2019.09.001

Dodge-Kafka, K., Gildart, M., Tokarski, K., and Kapiloff, M. S. (2019). mAKAPβ Signalosomes - A Nodal Regulator of Gene Transcription Associated with Pathological Cardiac Remodeling. *Cell. Signal.* 63, 109357. doi:10.1016/j.cellsig.2019.109357

Ge, W., Hou, C., Zhang, W., Guo, X., Gao, P., Song, X., et al. (2021). Mep1a Contributes to Ang II-Induced Cardiac Remodeling by Promoting Cardiac Hypertrophy, Fibrosis and Inflammation. *J. Mol. Cell Cardiol.* 152, 52–68. doi:10.1016/j.yjmcc.2020.11.015

He, J., Luo, Y., Song, J., Tan, T., and Zhu, H. (2020). Non-coding RNAs and Pathological Cardiac Hypertrophy. *Adv. Exp. Med. Biol.* 1229, 231–245. doi:10.1007/978-981-15-1671-9_13

Heger, J., Schulz, R., and Euler, G. (2016). Molecular Switches under TGFβ Signalling during Progression from Cardiac Hypertrophy to Heart Failure. *Br. J. Pharmacol.* 173 (1), 3–14. doi:10.1111/bph.13344

Messerli, F. H., Rimoldi, S. F., and Bangalore, S. (2017). The Transition From Hypertension to Heart Failure. *JACC: Heart Fail.* 5 (8), 543–551. doi:10.1016/j.jchf.2017.04.012

Mushtaq, I., Ishtiaq, A., Ali, T., Jan, M. I., and Murtaza, I. (2020). "An Overview of Non-coding RNAs and Cardiovascular System," in *Non-coding RNAs in Cardiovascular Diseases. Advances in Experimental Medicine and Biology*. Editor J. Xiao (Singapore: Springer), vol 1229, 3–45. doi:10.1007/978-981-15-1671-9_1

Nakamura, M., and Sadoshima, J. (2018). Mechanisms of Physiological and Pathological Cardiac Hypertrophy. *Nat. Rev. Cardiol.* 15 (7), 387–407. doi:10.1038/s41569-018-0007-y

Oldfield, C. J., Duhamel, T. A., and Dhalla, N. S. (2020). Mechanisms for the Transition from Physiological to Pathological Cardiac Hypertrophy. *Can. J. Physiol. Pharmacol.* 98 (2), 74–84. doi:10.1139/cjpp-2019-0566

Pitoulis, F. G., and Terracciano, C. M. (2020). Heart Plasticity in Response to Pressure- and Volume-Overload: A Review of Findings in Compensated and Decompensated Phenotypes. *Front. Physiol.* 11, 92. doi:10.3389/fphys.2020.00092

Wang, J., Liew, O., Richards, A., and Chen, Y.-T. (2016). Overview of Micrornas in Cardiac Hypertrophy, Fibrosis, and Apoptosis. *Int. J. Mol. Sci.* 17 (5), 749. doi:10.3390/ijms17050749

Yu, W., Chen, C., and Cheng, J. (2020). The Role and Molecular Mechanism of FoxO1 in Mediating Cardiac Hypertrophy. *ESC Heart Fail.* 7 (6), 3497–3504. doi:10.1002/ehf2.13065

Zhang, X., Lei, F., Wang, X. M., Deng, K. Q., Ji, Y. X., Zhang, Y., et al. (2020). NULP1 Alleviates Cardiac Hypertrophy by Suppressing Nfat3 Transcriptional Activity. *J. Am. Heart. Assoc.* 9 (16), e016419. doi:10.1161/JAHA.120.016419

Zhen, C., Liu, H., Gao, L., Tong, Y., and He, C. (2021). Signal Transducer and Transcriptional Activation 1 Protects against Pressure Overload-induced Cardiac Hypertrophy. *FASEB j.* 35 (1), e21240. doi:10.1096/fj.202000325RRR

Zhu, H., and Sun, A. (2018). Programmed Necrosis in Heart Disease: Molecular Mechanisms and Clinical Implications. *J. Mol. Cell Cardiol.* 116, 125–134. doi:10.1016/j.yjmcc.2018.01.018

Conflict of Interest: The authors declare that the research was conducted in the absence of any commercial or financial relationships that could be construed as a potential conflict of interest.

frontiers in Pharmacology

ORIGINAL RESEARCH
published: 22 July 2020
doi: 10.3389/fphar.2020.01121

Gallic Acid Attenuates Angiotensin II-Induced Hypertension and Vascular Dysfunction by Inhibiting the Degradation of Endothelial Nitric Oxide Synthase

Xiao Yan[1†], Qi-Yu Zhang[2†], Yun-Long Zhang[1], Xiao Han[1], Shu-Bin Guo[1] and Hui-Hua Li[1,2]*

[1] Emergency Medicine Clinical Research Center, Beijing Chao-Yang Hospital, Capital Medical University, and Beijing Key Laboratory of Cardiopulmonary Cerebral Resuscitation, Beijing, China, [2] Department of Cardiology, Institute of Cardiovascular Diseases, First Affiliated Hospital of Dalian Medical University, Dalian, China

OPEN ACCESS

Edited by:
Hai-Gang Zhang,
Army Medical University, China

Reviewed by:
Jie Du,
Capital Medical University, China
Roberta d'Emmanuele di Villa Bianca,
University of Naples Federico II, Italy

***Correspondence:**
Hui-Hua Li
hhli1935@aliyun.com

[†]These authors have contributed equally to this work

Specialty section:
This article was submitted to Cardiovascular and Smooth Muscle Pharmacology, a section of the journal Frontiers in Pharmacology

Received: *01 May 2020*
Accepted: *10 July 2020*
Published: *22 July 2020*

Citation:
Yan X, Zhang Q-Y, Zhang Y-L, Han X, Guo S-B and Li H-H (2020) Gallic Acid Attenuates Angiotensin II-Induced Hypertension and Vascular Dysfunction by Inhibiting the Degradation of Endothelial Nitric Oxide Synthase. Front. Pharmacol. 11:1121. doi: 10.3389/fphar.2020.01121

Hypertension is a major cause of heart attack and stroke. Our recent study revealed that gallic acid (GA) exerts protective effects on pressure overload-induced cardiac hypertrophy and dysfunction. However, the role of GA in angiotensin II (Ang II)-induced hypertension and vascular remodeling remains unknown. C57BL/6J mice were subjected to saline and Ang II infusion. Systolic blood pressure was measured using a tail-cuff system. Vascular remodeling and oxidative stress were examined by histopathological staining. Vasodilatory function was evaluated in the aortic ring. Our findings revealed that GA administration significantly ameliorated Ang II-induced hypertension, vascular inflammation, and fibrosis. GA also abolished vascular endothelial dysfunction and oxidative stress in Ang II-infused aortas. Mechanistically, GA treatment attenuated Ang II-induced upregulation of the immunoproteasome catalytic subunits β2i and β5i leading to reduction of the trypsin-like and chymotrypsin-like activity of the proteasome, which suppressed degradation of endothelial nitric oxide synthase (eNOS) and reduction of nitric oxide (NO) levels. Furthermore, blocking eNOS activity by using a specific inhibitor ($_L$-N^G-nitroarginine methyl ester) markedly abolished the GA-mediated beneficial effect. This study identifies GA as a novel immunoproteasome inhibitor that may be a potential therapeutic agent for hypertension and vascular dysfunction.

Keywords: gallic acid, angiotensin II, hypertension, immunoproteasome, eNOS degradation

INTRODUCTION

Hypertension remains a major risk factor for cardiovascular events, chronic kidney disease, and heart failure (Carey et al., 2018). Recent studies have revealed that vascular inflammation and oxidative stress, which are hallmarks of endothelial dysfunction, contribute to the pathogenesis of hypertension (Wang et al., 2016; Konukoglu and Uzun, 2017; Lang et al., 2019). Importantly, endothelial nitric oxide synthase (eNOS) acts as a key regulator of vasodilation and vasoprotection in physiological and pathological states, respectively (Garcia and Sessa, 2019). eNOS-derived nitric oxide (NO) inhibits

platelet aggregation and adhesion, vascular smooth muscle proliferation, and vascular inflammation (Forstermann and Sessa, 2012). Increasing evidence suggests that sustained hypertensive stimuli such as reactive oxygen species and angiotensin II (Ang II), suppress eNOS expression and NO bioavailability, thereby leading to a reduction of endothelium-dependent vasodilation in the vasculature (Gryglewski et al., 1986; Schrader et al., 2007). Inhibition of basal eNOS activity by administration of $_{L}$-N^{G}-nitroarginine methyl ester (L-NAME) increases vasoconstriction, pathological vascular remodeling, and blood pressure (Ribeiro et al., 1992). In contrast, animal and pre-clinical studies have demonstrated that gene delivery of eNOS is effective in inhibiting vascular injury and promoting endothelial regeneration (Cooney et al., 2007). It is interesting to note that the ubiquitin-proteasome system (UPS) is involved in the regulation of eNOS activity (Stangl et al., 2004). However, the underlying mechanisms by which the proteasome modulates eNOS stability in Ang II-induced hypertension and vascular dysfunction remain unclear.

Natural compounds have been shown to reduce the risk factors of cardiovascular diseases (Pandey and Rizvi, 2009). As a plant-derived phenolic acid, gallic acid (GA) has been shown to exert beneficial effects on myocardial hypertrophy, fibrosis, and oxidative stress in response to various hypertrophic stimuli (Ryu et al., 2016; Yan et al., 2019). We have recently found that GA administration attenuates pressure overload-induced cardiac hypertrophic remodeling by promoting the autophagy-dependent degradation of epidermal growth factor receptor, glycoprotein 130, and calcineurin A (Yan et al., 2019). Moreover, several studies have revealed that GA inhibits hypertension in spontaneously hypertensive rats (SHRs) and L-NAME-treated mice (Kang et al., 2015; Jin et al., 2017a). Intriguingly, an *in vitro* finding demonstrates that GA improves endothelial injury by suppressing the chymotrypsin-like activity of the proteasome (Kam et al., 2014). However, there is little information about the role of GA in the regulation of endothelial dysfunction and hypertension in Ang II-infused mice.

Here, we provide novel evidence that GA administration significantly attenuated Ang II-induced hypertension and vascular remodeling, which was associated with an improvement of endothelium-dependent vascular dysfunction. Furthermore, GA markedly blocked the activity and expression of the immunoproteasome catalytic subunits β2i and β5i, leading to the suppression of eNOS degradation and the reduction of NO levels in Ang II-infused mice. Collectively, these data indicate that GA ameliorates vascular injury likely by inhibiting immunoproteasome-dependent eNOS degradation, and may serve as a promising candidate for treating hypertension.

MATERIALS AND METHODS

Animal Models and Experimental Protocols

Wild-type (WT) C57BL/6 mice (male, 8–12 weeks) were purchased from Jackson Laboratory (Bar Harbor, ME, USA). The procedures were approved by the Animal Care and Use Committee of Capital Medical University (AEE1-2016-045). All investigations were conformed to the Guide for the Care and Use of Laboratory Animals published by the U.S. National Institutes of Health (NIH Publication No.85-23, revised 1996). The Ang II-induced hypertension model was performed by 14-day subcutaneous infusion of Ang II (490 ng/kg/min; Sigma-Aldrich, St. Louis, MO) or saline using osmotic mini-pumps (Alzet MODEL 1007D; DURECT, Cupertino, CA) as previously described (Wang et al., 2016; Lang et al., 2019). The systolic blood pressure (SBP) and heart rate (HR) of mice was gauged by a tail-cuff system (SoftronBP-98A; Softron, Tokyo, Japan).

Mice were orally gavaged with vehicle or GA (Sigma-Aldrich) at doses of 5 or 20 mg/kg body weight (BW) daily and randomly subjected to the saline or Ang II treatment. A specific eNOS inhibitor L-NAME (Sigma-Aldrich) was administrated in the drinking water (1 mg/ml) (Boe et al., 2013). After 2 weeks of Ang II or saline infusion, animals were anaesthetized by intraperitoneal injection of an overdose of pentobarbital (100 mg/kg, Sigma-Aldrich). The aortas were harvested and prepared for further histological and molecular experiments.

Vascular Relaxation Analysis

The thoracic aortas were isolated and cut into 4-mm segments and gently mounted on force transducers (Power Laboratory, AD Instruments, Bella Vista, Australia) in organ chambers. The samples were challenged with 60 mmol/L KCl, and then stimulated by noradrenaline. The vascular responses to increasing concentrations of acetylcholine (ACh) and sodium nitroprusside (SNP) were detected as described previously (Wang et al., 2016; Lang et al., 2019).

Histopathology

The aortic tissues were fixed in 4% paraformaldehyde and embedded in paraffin. Sections (5 μm) were stained with haematoxylin and eosin (H&E) and Masson's trichrome reagent, as well as dihydroethidine (DHE, 1 μM in PBS; Sigma-Aldrich) in accordance with standard procedures (Wang et al., 2016; Lang et al., 2019). Immunohistochemistry staining was performed with the anti-Mac-2 antibody (1:200 dilution; Santa Cruz Biotechnology Inc., Dallas, TX). Images were detected by Nikon Labophot 2 microscope (Nikon, Tokyo, Japan) and analyzed using Image J software (US National Institutes of Health, Bethesda, MD).

Proteasome Activity

The aortic proteasome activity was measured using fluorogenic peptide substrates as previously described (Li et al., 2015; Chen et al., 2019; Li J. et al., 2019). In brief, the protein of aorta was isolated with HEPES buffer (50 mM, pH 7.5) consist of 20 mmol/L KCl, 5 mmol/L $MgCl_2$, and 1 mmol/L dithiothreitol. Z-LLE-AMC (45 μmol/L), Ac-RLR-AMC (40 μmol/L), and Suc-LLVY-AMC (18 μmol/L) were utilized to evaluate the caspase-like, trypsin-like, and chymotrypsin-like activity, respectively. Twenty micrograms of protein were added to 100 μl of the HEPES buffer containing the fluorogenic peptide substrates and incubated for 10 min at 37°C. The fluorescence intensity was gauged with the excitation at 380 nm and emission at 460 nm.

Quantitative Real-Time PCR Analysis

Total RNA was extracted from aorta tissues by Trizol Reagent (Invitrogen, Carlsbad, CA) and reverse-transcribed according to the manufacturer's protocol (Wang et al., 2016; Lang et al., 2019). PCR amplification was performed using 1–2 μg of cDNA and gene-specific primers (Sangon Biotech, Shanghai, China), which are listed in **Supplementary Table 1**. Quantitative real-time PCR (qPCR) was performed with an iCycler IQ system (Bio-Rad, CA), and the transcript quantities were normalized to the amount of glyceraldehyde-3-phosphate dehydrogenase (GAPDH).

Western Blot Analysis

Total proteins were isolated from snap-frozen aorta samples using RIPA buffer containing protease inhibitors (Solarbio Science Technology Co, China). The lysates (40–50 μg) were separated by electrophoresis in 8–12% SDS-PAGE gels, transferred to the polyvinylidene difluoride (PVDF) membranes (Bio-Rad), and incubated with the primary antibodies against β2i (Abcam, London, UK), β5i (Abcam), p-eNOS^{1177} (Cell Signaling Technologies, Boston, MA), eNOS (Cell Signaling Technologies), and GAPDH (Proteintech Group Inc, Rosemont, IL). The horseradish peroxidase-conjugated anti-mouse or anti-rabbit IgG were purchased from Cell Signaling Technologies. All blots were analyzed by the Image J software and normalized to GAPDH.

NO Assay

The aortic and serum NO levels were evaluated using a colorimetric assay kit (Nanjing Jiancheng Biological Company, China) in accordance with the manufacturer's protocol.

Statistical Analysis

All results are presented as mean ± standard error of the mean (SEM). The normality test (Shapiro-Wilk) was used to determine whether the data were normally distributed. The student t test was used to compare the significant difference between two groups in normal distribution. If the data were not normally distributed, the Mann-Whitney test was performed. One-way ANOVA following Newman-Keuls multiple comparison test was performed to evaluate the significance of difference between the means of groups. For blood pressure data and ACh- or SNP-induced vasodilation tests in aortic rings, repeated-measures ANOVA analysis of variance was utilized. If the ANOVA analysis demonstrated a significant effect, *post hoc* comparisons were made pairwise with the Fisher least significant difference test. $P < 0.05$ was considered statistically significant.

RESULTS

GA Reduces Ang II-Induced Hypertension, Vascular Remodeling, and Inflammation

To investigated the functional role of GA in the regulation of blood pressure in Ang II-infused mice, wild-type (WT) mice were treated with different doses of GA (5 or 20 mg/kg BW) and infused with Ang II (490 ng/kg/min). Systolic blood pressure (SBP) was measured by the noninvasive tail-cuff method. We found that Ang II infusion for 2 weeks significantly increased SBP compared with saline-treated controls, whereas this increase was markedly reduced by GA (5 or 20 mg/kg BW) in Ang II-treated mice (**Figure 1A**). The heart rate was not significantly altered in the vehicle- and GA-treated mice after saline or Ang II infusion (**Figure 1B**). Moreover, Ang II-induced increases in aortic wall thickening, collagen deposition, and the accumulation of Mac-2-positive macrophages were also blunted in GA-treated mice (**Figures 1C–E**). Accordingly, Ang II-induced upregulation of the mRNA expression of proinflammatory and fibrotic genes (interleukin [IL]-1β, IL-6, tumor necrosis factor [TNF]-α, monocyte chemoattractant protein-1, α-smooth muscle actin, collagen I, and collagen III) in Ang II-infused aortas was remarkably attenuated in GA-treated mice in a dose-dependent manner (**Figures 1F, G**). These results indicate that the administration of GA improves Ang II-induced hypertension and vascular injury.

GA Blocks Vascular Dysfunction and Oxidative Stress in Ang II-Infused Mice

To determine whether GA treatment suppressed vascular dysfunction, we evaluated *ex vivo* vascular function in vehicle- or GA-treated mice in response to Ang II. Two-week Ang II infusion significantly impaired endothelium-dependent vasodilatation to acetylcholine (ACh) compared with saline control (**Figure 2A**). However, this effect was dose-dependently improved in GA-treated mice (**Figure 2A**). Consistent with previous findings (Wang et al., 2016), there was no statistically significant difference in endothelium-independent vasodilatation to sodium nitroprusside (SNP) between Ang II- and saline-treated mice (**Figure 2B**). Moreover, SNP-induced vasodilatation was not changed in Ang II-infused mice after GA administration (**Figure 2B**). These data suggest that GA prevented endothelial dysfunction in Ang II-infused mice.

Recent studies have found that vascular superoxide production contributes to endothelial dysfunction in the Ang II-treated mouse model (Rajagopalan et al., 1996; Wang et al., 2016). As indicated in **Figure 2C**, Ang II infusion for 2 weeks markedly increased the formation of aortic superoxide as characterized by dihydroethidium (DHE) staining, whereas this effect was abolished in GA-treated mice in a dose-dependent manner. Furthermore, the upregulated mRNA levels of the NADPH oxidase catalytic subunits NOX1, NOX2, and NOX4, and p22^{phox} in Ang II-infused aortas were significantly ameliorated in mice treated with GA (**Figure 2D**). Therefore, these findings illustrate that the GA treatment attenuates Ang II-induced aortic superoxide formation, which is associated with vascular dysfunction.

GA Inhibits eNOS Degradation by Attenuating Immunoproteasome Activity in Ang II-Treated Mice

It is well established that eNOS-derived NO exerts essential effects on vascular dilation (Forstermann and Sessa, 2012). We

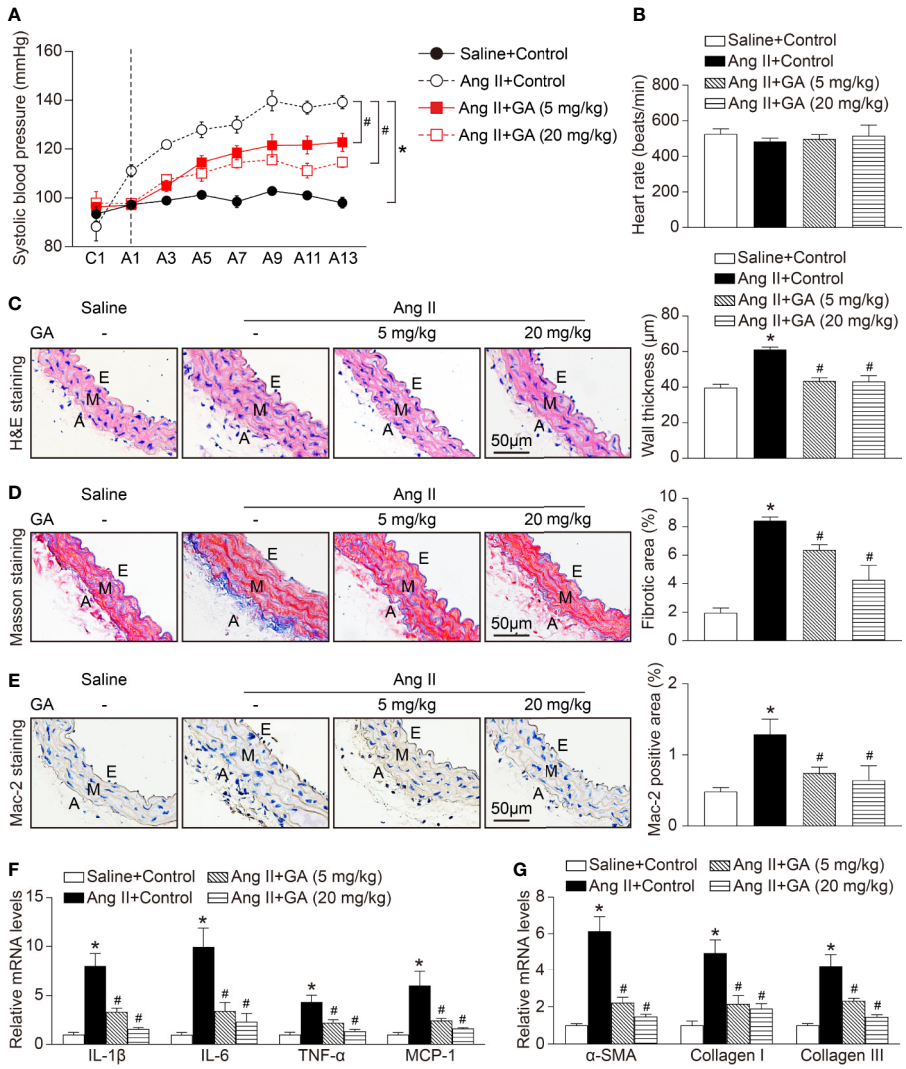

FIGURE 1 | Gallic acid (GA) ameliorates hypertension, vascular inflammation, and fibrosis in Ang II-infused mice. WT mice were orally gavaged with vehicle or GA (5 or 20 mg/kg BW) for 14 days in the presence of saline or Ang II infusion (490 ng·kg^{-1}min^{-1}). **(A)** Average systolic blood pressure of vehicle or GA-treated mice before and after Ang II treatment obtained by telemetry (n=6). **(B)** Heart rate was assessed by the noninvasive tail-cuff method in vehicle- and GA-treated mice after saline and Ang II infusion (n=6). **(C)** Representative images of haematoxylin and eosin (H&E) staining of the thoracic aorta (left), and quantification of the wall thickness of each group (right, n=6). **(D)** Representative images of Masson's trichrome staining of the thoracic aorta (left), and quantification of the percentage of fibrotic area (right, n=6). **(E)** Representative images of immunohistochemical staining of aorta sections with anti-Mac-2 antibody (left), and quantification of Mac-2-positive macrophages (right, n=6). A indicates adventitia; E, endothelium; M, media. Scale bar: 50 μm. **(F)** Quantitative real-time PCR (qPCR) analyses of the mRNA expression of IL-1β, IL-6, TNF-α, and MCP-1 in the aorta (n=6). **(G)** qPCR analyses of α-SMA, collagen I, and collagen III mRNA expression levels (n=6). GAPDH as the internal control. For blood pressure data, repeated-measures ANOVA was used. If the ANOVA analysis demonstrated a significant effect, *post hoc* comparisons were made pairwise with the Fisher least significant difference test. One-way ANOVA following Newman-Keuls multiple comparison test was utilized to evaluate the significance of difference between the means of groups. $^{*}P < 0.05$ versus saline + control, $^{\#}P < 0.05$ versus Ang II + control.

revealed that Ang II infusion for 2 weeks significantly reduced aortic and serum NO levels, and this effect was diminished after GA treatment (**Figures 3A, B**). However, the mRNA level of eNOS, inducible NO synthase (iNOS), Ang II type I receptor (AT1R), and AT2R were not altered in Ang II-infused mice after GA treatment (**Figure 3C** and **Supplementary Figure 1**). It is interesting to note that GA treatment reversed the Ang II-induced downregulation of p-eNOS^{1177} and eNOS protein expression in the aortas (**Figure 3D**) and human umbilical vein endothelial cells (HUVECs) (**Supplementary Figure 2**), suggesting that reduction of eNOS expression occurs at protein level.

Since the proteasome-mediated regulation of eNOS stability contributes to endothelial function and vasodilation in the aorta (Stangl et al., 2004), we then investigated whether GA affects proteasome activity and expression of catalytic subunits. As expected, Ang II infusion significantly induced increase of the trypsin-like and chymotrypsin-like activity of the proteasome as

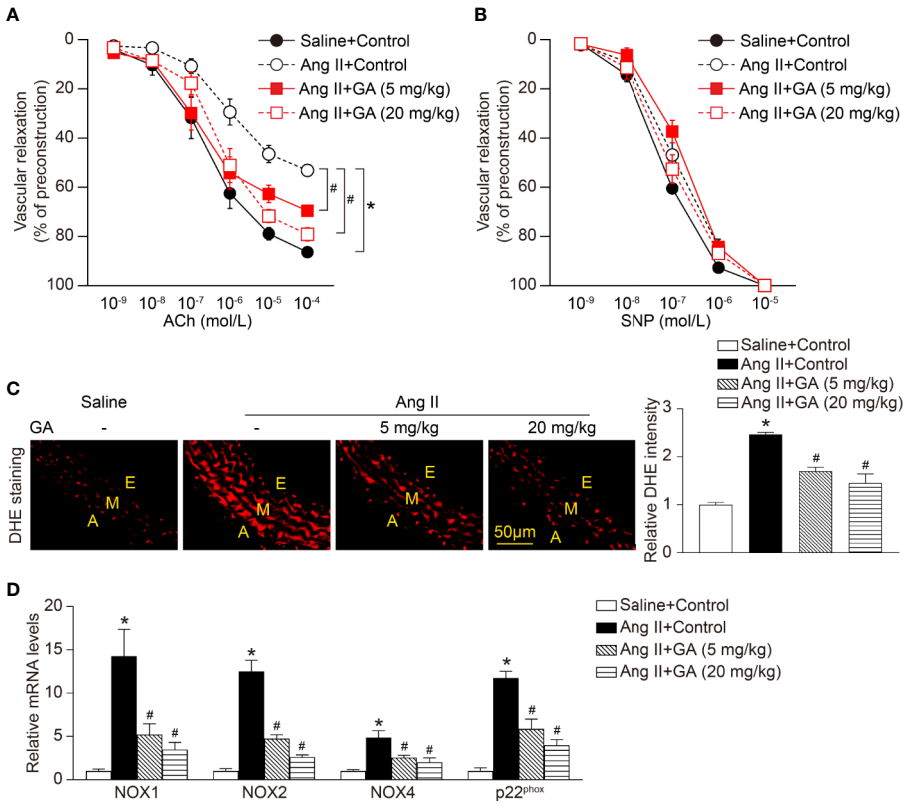

FIGURE 2 | Gallic acid (GA) attenuates Ang II-induced vascular dysfunction and oxidative stress. **(A)** Dose-response curves of endothelium-dependent relaxation (ACh, n=6). **(B)** Dose-response curves of endothelium-independent relaxation in response to SNP (n=6). **(C)** Representative images of DHE staining of the aortic superoxide production (left), and quantification of fluorescence intensity (right, n=6). A indicates adventitia; E, endothelium; M, media. Scale bar: 50 μm. **(D)** Quantitative real-time PCR (qPCR) analyses of the mRNA expression levels of NOX1, NOX2, NOX4, and $p22^{phox}$ (n=4). Glyceraldehyde-3-phosphate dehydrogenase (GAPDH) as an internal control. For ACh- or sodium nitroprusside (SNP)-induced vasodilation tests in aortic rings, repeated-measures ANOVA analysis of variance was utilized. If the analysis of variance demonstrated a significant effect, *post hoc* comparisons were made pairwise with the Fisher least significant difference test. One-way ANOVA following Newman-Keuls multiple comparison test was used to evaluate the significance of difference between the means of groups. $^{*}P < 0.05$ versus saline + control, $^{\#}P < 0.05$ versus Ang II + control.

well as the mRNA levels of the immunoproteasome subunits β2i and β5i, but did not influence other standard and catalytic subunits (β1, β2, β5, and β1i) in the aorta, and the increase was dose-dependently abolished by GA (**Figures 4A, B**). Moreover, GA treatment also markedly reduced the protein levels of β2i and β5i in Ang II-treated aortas and HUVECs (**Figure 4C** and **Supplementary Figure 2**). Overall, these results indicate that GA blunts the Ang II-induced reduction of NO and degradation of eNOS likely by suppressing the activity and expression of β2i and β5i in the aorta.

Blockage of eNOS Activity Diminishes GA-Mediated Protective Effects on Hypertension in Ang II-Treated Mice

To test whether eNOS is involved in Ang II-induced hypertension and vascular dysfunction after GA administration in mice, we treated wild-type mice with GA in the presence or absence of a special eNOS inhibitor (L-NAME) for 2 weeks. In agreement with our previous results (**Figures 1** and **2**), the administration of GA abolished the Ang II-induced increase of SBP and decrease of aortic and serum NO levels (**Figures 5A, C**). The heart rate was not changed in vehicle- or GA-treated mice after Ang II infusion (**Figure 5B**). Ang II-induced increases in aortic thickening, collagen deposition, the accumulation of Mac-2-positive macrophages, and superoxide formation were also ameliorated in GA-treated mice (**Figures 5D–G**). However, these effects were reversed by L-NAME treatment (**Figures 5A, C–F**). Accordingly, L-NAME did not affect the heart rate in Ang II-infused mice (**Figure 5B**). Collectively, these results suggest that GA suppresses hypertension and vascular injury by attenuating the degradation of eNOS after Ang II infusion.

DISCUSSION

In this study, we demonstrated that GA administration significantly ameliorated the Ang II-induced development of hypertension and vascular remodeling in mice. Mechanistically, GA reduced the

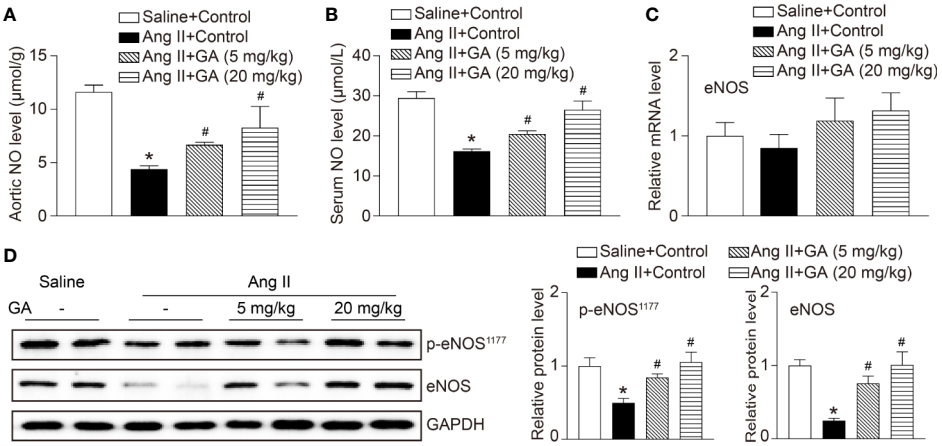

FIGURE 3 | Gallic acid (GA) downregulates the degradation of endothelial nitric oxide synthase (eNOS) and the reduction of nitric oxide (NO) levels in Ang II-treated aortas. **(A)** Measurement of NO levels in the aorta by the colorimetric assay (n=6). **(B)** NO levels in the serum (n=6). **(C)** The qPCR analysis of eNOS mRNA expression in the aorta (n=6). **(D)** Representative immunoblotting analyses of the protein expression of p-eNOS^{1177} and eNOS (left), and quantification of the relative protein levels (right, n=4). Glyceraldehyde-3-phosphate dehydrogenase (GAPDH) as an internal control. One-way ANOVA following Newman-Keuls multiple comparison test was used to evaluate the significance of difference between the means of groups. $^{*}P < 0.05$ versus saline + control, $^{\#}P < 0.05$ versus Ang II + control.

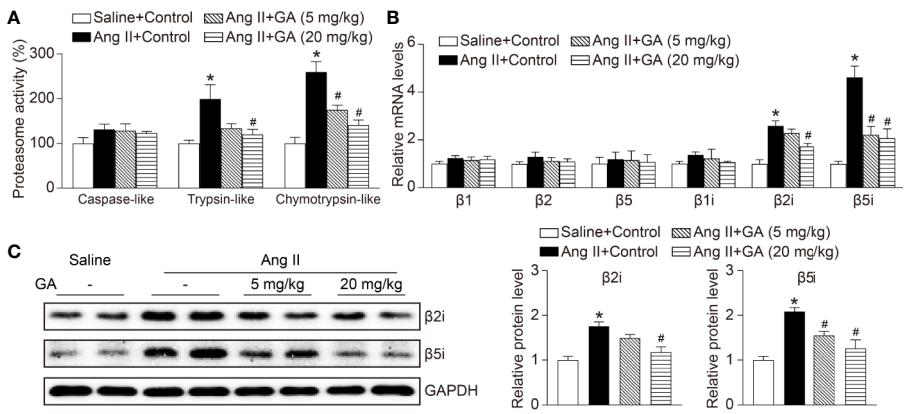

FIGURE 4 | Gallic acid (GA) abolishes immunoproteasome activity and catalytic subunit expression in the aorta after Ang II infusion. **(A)** The caspase-like, trypsin-like, and chymotrypsin-like activity of the proteasome in aortas in response to Ang II infusion with vehicle or GA treatment (n=4). **(B)** Quantitative real-time PCR (qPCR) analyses of the mRNA expression of β1, β2, β5, β1i, β2i, and β5i. **(C)** Representative immunoblotting analyses of the protein expression of β2i and β5i (left), and quantification of the relative protein levels (right, n=4). Glyceraldehyde-3-phosphate dehydrogenase (GAPDH) as an internal control. One-way ANOVA following Newman-Keuls multiple comparison test was used to evaluate the significance of difference between the means of groups. $^{*}P < 0.05$ versus saline + control, $^{\#}P < 0.05$ versus Ang II + control.

activity and expression of the immunoproteasome catalytic subunits β2i and β5i, which abolished the degradation of eNOS, leading to the production of NO and improvement of endothelium-dependent vascular dysfunction (**Figure 6**). Therefore, our study provides evidence that GA represents a novel immunoproteasome inhibitor and may be a potential therapeutic agent for hypertension and vascular dysfunction.

The renin-angiotensin-aldosterone system (RAAS) plays a critical role in the initiation and development of hypertension. As the most powerful vasoconstrictor in the RAAS, Ang II is involved in the regulation of multiple processes, including inflammation, fibrosis, and oxidative stress (Forrester et al., 2018). Current strategies for treating hypertension comprise adrenoceptor antagonists, angiotensin-converting enzyme inhibitors (ACEIs), angiotensin receptor blockers, and mineralocorticoid antagonists; however, their efficacy remains low (Cai and Calhoun, 2017). Thus, there is an urgent need to identify candidate therapeutic approaches for treating hypertensive diseases. GA is a food-derived polyphenol

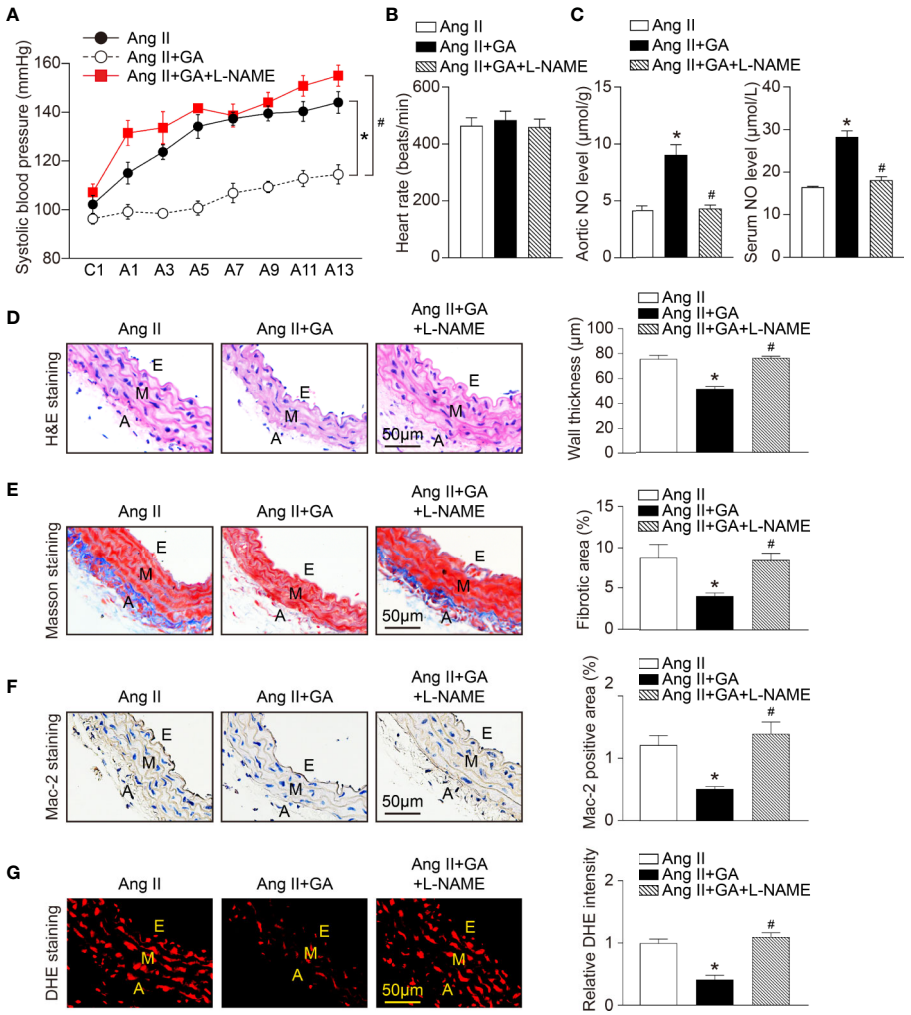

FIGURE 5 | Blocking endothelial nitric oxide synthase (eNOS) activity inhibits gallic acid (GA)-mediated protective effect on Ang II-induced hypertension and vascular remodeling. **(A)** Average systolic blood pressure was gauged by the noninvasive tail-cuff method in vehicle or GA-treated mice before and after Ang II infusion together with $_{L}$-N^{G}-nitroarginine methyl ester (L-NAME) treatment (1 mg/ml drinking water, n=6). **(B)** Heart rate of vehicle or GA-treated mice after Ang II infusion together with L-NAME treatment (n=6). **(C)** Nitric oxide (NO) levels in the aorta (left, n=6) and serum (right, n=6). **(D)** Haematoxylin and eosin (H&E) staining in the aorta (left). Quantification of aortic wall thickness (right, n=6). **(E)** Masson's trichrome staining for aortic fibrosis (left). Quantification of the fibrotic area (right, n=6). **(F)** Immunohistochemical staining of aorta sections with anti-Mac-2 antibody (left), and quantification of Mac-2-positive macrophages (right, n=6). **(G)** Dihydroethidine (DHE) staining of superoxide production in the aorta (left). Quantification of DHE fluorescence intensity (right, n=6). A indicates adventitia; E, endothelium; M, media. Scale bar: 50 μm. For blood pressure data, repeated-measures ANOVA was used. If the ANOVA analysis demonstrated a significant effect, *post hoc* comparisons were made pairwise with the Fisher least significant difference test. After the normality test (Shapiro-Wilk), the student t test was performed to compare the significant difference between two groups in normal distribution, and the Mann-Whitney test was used for the data that were not normally distributed. $^{*}P < 0.05$ versus Ang II, $^{\#}P < 0.05$ versus Ang II + GA.

compound that plays beneficial roles in improving hypertension, vascular dysfunction, and cardiac hypertrophic remodeling in several hypertensive models (Jin et al., 2017a; Jin et al., 2017b). In Ang II-treated H9c2 cells and SHRs, GA attenuates GATA4-induced NOX activity, which reduces oxidative stress and blood pressure (Jin et al., 2017b). Moreover, GA ameliorates L-NAME-induced hypertension and myocardial fibrosis by modulating histone deacetylase 1 and 2 (Jin et al., 2017a). In this study, our data revealed that GA abolished Ang II-induced hypertension and vascular dysfunction, which was associated with the suppression of the activity and expression of the immunoproteasome subunits β2i and β5i, leading to decreased eNOS degradation.

The 26S proteasome accounts for the majority of protein degradation in mammalian cells (Angeles et al., 2012; Thibaudeau and Smith, 2019). As the core part of the UPS, the 26S proteasome is composed of the 20S core protease and 19S regulatory particle. The 20S proteasome contains two pairs of inner β-rings and three catalytic β-subunits including β1 (PMSB6), β2 (PMSB7), and β5 (PMSB5), which exhibit caspase-like, trypsin-like, and chymotrypsin-like activity,

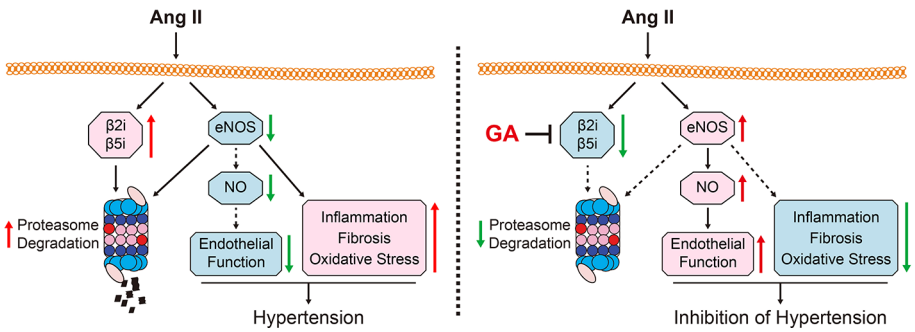

FIGURE 6 | A working diagram of gallic acid (GA)-mediated beneficial effect on the Ang II-infused mouse model. Ang II infusion increases the activity and the expression of the immunoproteasome subunits β2i and β5i, which induces the degradation of endothelial nitric oxide synthase (eNOS) and the reduction of nitric oxide (NO) levels thereby leading to hypertension and impairment of vascular function. Conversely, GA administration attenuates these effects. Ang II, angiotensin II; eNOS, endothelial nitric oxide synthase; GA, gallic acid; NO, nitric oxide.

respectively. After stimulation with interferon-γ or TNF-α, the standard β-subunits of the constitutive proteasome are replaced by their inducible β-counterparts such as β1i (PMSB9 or LMP2), β2i (PMSB10 or MECL-1), and β5i (PMSB8 or LMP7), which form the immunoproteasome (Thibaudeau and Smith, 2019). Previous studies revealed that adverse stimuli activate the immunoproteasome, which is involved in the pathogenesis of cardiovascular diseases including cardiac hypertrophy, ischemia-reperfusion injury, and neointimal formation (Barringhaus and Matsumura, 2007; Li et al., 2015; Guo et al., 2016; Chen et al., 2019). Importantly, our recent studies indicate that Ang II infusion upregulates the activity and expression of immunoproteasome subunits (β2i and β5i) in the heart, atria, retina, and aorta (Li et al., 2015; Li et al., 2018; Wang et al., 2018; Li F. D. et al., 2019; Li J. et al., 2019; Wang et al., 2020). The depletion of β2i or β5i markedly attenuates Ang II-induced blood pressure, cardiac hypertrophy, and atrial fibrillation in mice (Li et al., 2015; Li et al., 2018; Li J. et al., 2019). Furthermore, we revealed that β5i is involved in the modulation of the infiltration of proinflammatory cells into abdominal aortic aneurysm and atherosclerotic lesion, as well as vascular remodeling in ApoE knockout mice (Li F. D. et al., 2019; Wang et al., 2020). It is worth noting that several nutritional factors, such as quercetin, δ-tocotrienol, and resveratrol, are potential proteasome inhibitors, which may represent a strategy for treating cardiovascular diseases (Qureshi et al., 2013; Chen et al., 2019). Here, we provided new evidence that GA administration significantly ameliorated the activity and expression of the immunoproteasome subunits β2i and β5i in Ang II-treated aortas (**Figure 3**). Therefore, these data suggest that GA serves as a novel inhibitor of the immunoproteasome and may reduce eNOS degradation in the aorta.

eNOS has been reported to play critical roles in the modulation of vasodilation, vascular inflammation, leucocyte adhesion, and vascular smooth muscle proliferation (Forstermann and Sessa, 2012). Knockout of eNOS impairs endothelium-dependent relaxation, elevates blood pressure, and induces abnormal vascular remodeling in mice (Forstermann and Sessa, 2012). Furthermore, drugs interfering with the RAAS, such as ACEIs and angiotensin receptor blockers, could improve eNOS dysfunction and vascular oxidative stress (Mancini et al., 1996; Wassmann et al., 2002). Early studies indicated that eNOS function is maintained by multiple mechanisms, including transcriptional and post-transcriptional modulation, post-translational modification, phosphorylation, and protein-protein interactions (Garcia and Sessa, 2019). Recently, increasing evidence has demonstrated that UPS-dependent proteolysis is responsible for the regulation of eNOS degradation (Stangl and Stangl, 2010). Proteasome inhibitors, including MG132, lactacystin, and MLN-273, increase eNOS expression in endothelial cells and in the arterial wall (Stangl et al., 2004; Herrmann et al., 2007; Thomas et al., 2007). In this study, we extended previous findings and revealed that GA markedly protected against the Ang II-induced degradation of eNOS by inhibiting the immunoproteasome subunits β2i and β5i, leading to an improvement of endothelial dysfunction (**Figures 2–4**). Accordingly, blocking eNOS activity with the inhibitor L-NAME significantly reversed these effects (**Figure 5**). Thus, our results indicate that GA attenuates hypertension and vascular remodeling by reducing the immunoproteasome-mediated degradation of eNOS.

In conclusion, this study unveiled a new role for GA in the regulation of hypertension and vascular dysfunction after Ang II stimulation. GA administration abolished the activity and expression of the immunoproteasome subunits β2i and β5i, which attenuated the degradation of eNOS. Thus, our findings suggest that GA is a new immunoproteasome inhibitor and may represent a promising therapeutic option for the treatment of hypertension and vascular remodeling. Further investigations are needed to explore the molecular mechanisms underlying the action of GA to modulate immunoproteasome expression.

DATA AVAILABILITY STATEMENT

The data that support the findings of this study are available from the corresponding author upon reasonable request.

ETHICS STATEMENT

The animal study was reviewed and approved by the Animal Care and Use Committee of Capital Medical University (AEE1-2016-045) and conformed to the US National Institutes of Health Guide for the Care and Use of Laboratory Animals.

AUTHOR CONTRIBUTIONS

XY, Q-YZ, Y-LZ, and XH conducted the experiments. XY and Q-YZ analyzed the data. XY, S-BG, and H-HL designed the study. XY and H-HL wrote the manuscript and provided the funding for the study. XY and H-HL had primary responsibility for the final content. All authors contributed to the article and approved the submitted version.

FUNDING

This work was supported by grants from the China Postdoctoral Science Foundation (2020M670384 to XY) and the National Natural Science Foundation of China (81703217 to XY, 81630009 and 81330003 to H-HL).

SUPPLEMENTARY MATERIAL

The Supplementary Material for this article can be found online at: https://www.frontiersin.org/articles/10.3389/fphar.2020.01121/full#supplementary-material

SUPPLEMENTARY FIGURE S1 | Effect of GA administration on mRNA expression levels of iNOS, AT1R, and AT2R. qPCR analyses ofthe mRNA expression of iNOS, AT1R, and AT2R in the aorta (n=6). GAPDH as the internal control. One-way ANOVA following Newman-Keuls multiple comparison test was utilized to evaluate the significance of difference between the means of groups.

SUPPLEMENTARY FIGURE S2 | Effect of GA treatment on protein expression of p-eNOS1177, eNOS, β2i, and β5i in vitro. Representative immunoblotting analyses of the protein expression ofp-eNOS^{1177}, eNOS, β2i, and β5iin confluent HUVEC streated with GA (10 μm) after 24 h of Ang II (100 nm) stimulation (left), and quantification of the relative protein levels (right, n=3). After the normality test (Shapiro-Wilk), the student t test was used to compare the significant difference between two groups in normal distribution, and the Mann-Whitney test was utilized for the data that were not normally distributed. *P < 0.05 versus Ang II, #P < 0.05 versus Ang II + GA.

REFERENCES

Angeles, A., Fung, G., and Luo, H. (2012). Immune and non-immune functions of the immunoproteasome. *Front. Biosci. (Landmark Ed)* 17, 1904–1916. doi: 10.2741/4027

Barringhaus, K. G., and Matsumura, M. E. (2007). The proteasome inhibitor lactacystin attenuates growth and migration of vascular smooth muscle cells and limits the response to arterial injury. *Exp. Clin. Cardiol.* 12 (3), 119–124.

Boe, A. E., Eren, M., Murphy, S. B., Kamide, C. E., Ichimura, A., Terry, D., et al. (2013). Plasminogen activator inhibitor-1 antagonist TM5441 attenuates Nomega-nitro-L-arginine methyl ester-induced hypertension and vascular senescence. *Circulation* 128 (21), 2318–2324. doi: 10.1161/CIRCULATIONAHA.113.003192

Cai, A., and Calhoun, D. A. (2017). Resistant Hypertension: An Update of Experimental and Clinical Findings. *Hypertension* 70 (1), 5–9. doi: 10.1161/HYPERTENSIONAHA.117.08929

Carey, R. M., Muntner, P., Bosworth, H. B., and Whelton, P. K. (2018). Prevention and Control of Hypertension: JACC Health Promotion Series. *J. Am. Coll. Cardiol.* 72 (11), 1278–1293. doi: 10.1016/j.jacc.2018.07.008

Chen, C., Zou, L. X., Lin, Q. Y., Yan, X., Bi, H. L., Xie, X., et al. (2019). Resveratrol as a new inhibitor of immunoproteasome prevents PTEN degradation and attenuates cardiac hypertrophy after pressure overload. *Redox Biol.* 20, 390–401. doi: 10.1016/j.redox.2018.10.021

Cooney, R., Hynes, S. O., Sharif, F., Howard, L., and O'Brien, T. (2007). Effect of gene delivery of NOS isoforms on intimal hyperplasia and endothelial regeneration after balloon injury. *Gene Ther.* 14 (5), 396–404. doi: 10.1038/sj.gt.3302882

Forrester, S. J., Booz, G. W., Sigmund, C. D., Coffman, T. M., Kawai, T., Rizzo, V., et al. (2018). Angiotensin II Signal Transduction: An Update on Mechanisms of Physiology and Pathophysiology. *Physiol. Rev.* 98 (3), 1627–1738. doi: 10.1152/physrev.00038.2017

Forstermann, U., and Sessa, W. C. (2012). Nitric oxide synthases: regulation and function. *Eur. Heart J.* 33 (7), 829–837. doi: 10.1093/eurheartj/ehr304

Garcia, V., and Sessa, W. C. (2019). Endothelial NOS: perspective and recent developments. *Br. J. Pharmacol.* 176 (2), 189–196. doi: 10.1111/bph.14522

Gryglewski, R. J., Palmer, R. M., and Moncada, S. (1986). Superoxide anion is involved in the breakdown of endothelium-derived vascular relaxing factor. *Nature* 320 (6061), 454–456. doi: 10.1038/320454a0

Guo, C. X., Jiang, X., Zeng, X. J., Wang, H. X., Li, H. H., Du, F. H., et al. (2016). Soluble receptor for advanced glycation end-products protects against ischemia/reperfusion-induced myocardial apoptosis via regulating the ubiquitin proteasome system. *Free Radic. Biol. Med.* 94, 17–26. doi: 10.1016/j.freeradbiomed.2016.02.011

Herrmann, J., Saguner, A. M., Versari, D., Peterson, T. E., Chade, A., Olson, M., et al. (2007). Chronic proteasome inhibition contributes to coronary atherosclerosis. *Circ. Res.* 101 (9), 865–874. doi: 10.1161/CIRCRESAHA.107.152959

Jin, L., Lin, M. Q., Piao, Z. H., Cho, J. Y., Kim, G. R., Choi, S. Y., et al. (2017a). Gallic acid attenuates hypertension, cardiac remodeling, and fibrosis in mice with NG-nitro-L-arginine methyl ester-induced hypertension via regulation of histone deacetylase 1 or histone deacetylase 2. *J. Hypertens.* 35 (7), 1502–1512. doi: 10.1097/HJH.0000000000001327

Jin, L., Piao, Z. H., Sun, S., Liu, B., Kim, G. R., Seok, Y. M., et al. (2017b). Gallic Acid Reduces Blood Pressure and Attenuates Oxidative Stress and Cardiac Hypertrophy in Spontaneously Hypertensive Rats. *Sci. Rep.* 7 (1), 15607. doi: 10.1038/s41598-017-15925-1

Kam, A., Li, K. M., Razmovski-Naumovski, V., Nammi, S., Chan, K., and Li, G. Q. (2014). Gallic acid protects against endothelial injury by restoring the depletion of DNA methyltransferase 1 and inhibiting proteasome activities. *Int. J. Cardiol.* 171 (2), 231–242. doi: 10.1016/j.ijcard.2013.12.020

Kang, N., Lee, J. H., Lee, W., Ko, J. Y., Kim, E. A., Kim, J. S., et al. (2015). Gallic acid isolated from Spirogyra sp. improves cardiovascular disease through a vasorelaxant and antihypertensive effect. *Environ. Toxicol. Pharmacol.* 39 (2), 764–772. doi: 10.1016/j.etap.2015.02.006

Konukoglu, D., and Uzun, H. (2017). Endothelial Dysfunction and Hypertension. *Adv. Exp. Med. Biol.* 956, 511–540. doi: 10.1007/5584_2016_90

Lang, P. P., Bai, J., Zhang, Y. L., Yang, X. L., Xia, Y. L., Lin, Q. Y., et al. (2019). Blockade of intercellular adhesion molecule-1 prevents angiotensin II-induced hypertension and vascular dysfunction. *Lab. Invest.* 100 (3), 378–386. doi: 10.1038/s41374-019-0320-z

Li, N., Wang, H. X., Han, Q. Y., Li, W. J., Zhang, Y. L., Du, J., et al. (2015). Activation of the cardiac proteasome promotes angiotension II-induced hypertrophy by down-regulation of ATRAP. *J. Mol. Cell Cardiol.* 79, 303–314. doi: 10.1016/j.yjmcc.2014.12.007

Li, J., Wang, S., Bai, J., Yang, X. L., Zhang, Y. L., Che, Y. L., et al. (2018). Novel Role for the Immunoproteasome Subunit PSMB10 in Angiotensin II-Induced Atrial Fibrillation in Mice. *Hypertension* 71 (5), 866–876. doi: 10.1161/HYPERTENSIONAHA.117.10390

Li, F. D., Nie, H., Tian, C., Wang, H. X., Sun, B. H., Ren, H. L., et al. (2019). Ablation and Inhibition of the Immunoproteasome Catalytic Subunit LMP7 Attenuate Experimental Abdominal Aortic Aneurysm Formation in Mice. *J. Immunol.* 202 (4), 1176–1185. doi: 10.4049/jimmunol.1800197

Li, J., Wang, S., Zhang, Y. L., Bai, J., Lin, Q. Y., Liu, R. S., et al. (2019). Immunoproteasome Subunit beta5i Promotes Ang II (Angiotensin II)-Induced Atrial Fibrillation by Targeting ATRAP (Ang II Type I Receptor-Associated Protein) Degradation in Mice. *Hypertension* 73 (1), 92–101. doi: 10.1161/HYPERTENSIONAHA.118.11813

Mancini, G. B., Henry, G. C., Macaya, C., O'Neill, B. J., Pucillo, A. L., Carere, R. G., et al. (1996). Angiotensin-converting enzyme inhibition with quinapril improves endothelial vasomotor dysfunction in patients with coronary artery disease. The TREND (Trial on Reversing ENdothelial Dysfunction) Study. *Circulation* 94 (3), 258–265. doi: 10.1161/01.cir.94.3.258

Pandey, K. B., and Rizvi, S. I. (2009). Plant polyphenols as dietary antioxidants in human health and disease. *Oxid. Med. Cell Longev.* 2 (5), 270–278. doi: 10.4161/oxim.2.5.9498

Qureshi, A. A., Khan, D. A., Mahjabeen, W., Papasian, C. J., and Qureshi, N. (2013). Nutritional Supplement-5 with a Combination of Proteasome Inhibitors (Resveratrol, Quercetin, delta-Tocotrienol) Modulate Age-Associated Biomarkers and Cardiovascular Lipid Parameters in Human Subjects. *J. Clin. Exp. Cardiol.* 4 (3), 238. doi: 10.4172/2155-9880.1000238

Rajagopalan, S., Kurz, S., Munzel, T., Tarpey, M., Freeman, B. A., Griendling, K. K., et al. (1996). Angiotensin II-mediated hypertension in the rat increases vascular superoxide production via membrane NADH/NADPH oxidase activation. Contribution to alterations of vasomotor tone. *J. Clin. Invest.* 97 (8), 1916–1923. doi: 10.1172/JCI118623

Ribeiro, M. O., Antunes, E., de Nucci, G., Lovisolo, S. M., and Zatz, R. (1992). Chronic inhibition of nitric oxide synthesis. A new model of arterial hypertension. *Hypertension* 20 (3), 298–303. doi: 10.1161/01.hyp.20.3.298

Ryu, Y., Jin, L., Kee, H. J., Piao, Z. H., Cho, J. Y., Kim, G. R., et al. (2016). Gallic acid prevents isoproterenol-induced cardiac hypertrophy and fibrosis through regulation of JNK2 signaling and Smad3 binding activity. *Sci. Rep.* 6:34790. doi: 10.1038/srep34790

Schrader, L. I., Kinzenbaw, D. A., Johnson, A. W., Faraci, F. M., and Didion, S. P. (2007). IL-6 deficiency protects against angiotensin II induced endothelial dysfunction and hypertrophy. *Arterioscler. Thromb. Vasc. Biol.* 27 (12), 2576–2581. doi: 10.1161/ATVBAHA.107.153080

Stangl, K., and Stangl, V. (2010). The ubiquitin-proteasome pathway and endothelial (dys)function. *Cardiovasc. Res.* 85 (2), 281–290. doi: 10.1093/cvr/cvp315

Stangl, V., Lorenz, M., Meiners, S., Ludwig, A., Bartsch, C., Moobed, M., et al. (2004). Long-term up-regulation of eNOS and improvement of endothelial function by inhibition of the ubiquitin-proteasome pathway. *FASEB J.* 18 (2), 272–279. doi: 10.1096/fj.03-0054com

Thibaudeau, T. A., and Smith, D. M. (2019). A Practical Review of Proteasome Pharmacology. *Pharmacol. Rev.* 71 (2), 170–197. doi: 10.1124/pr.117.015370

Thomas, S., Kotamraju, S., Zielonka, J., Harder, D. R., and Kalyanaraman, B. (2007). Hydrogen peroxide induces nitric oxide and proteosome activity in endothelial cells: a bell-shaped signaling response. *Free Radic. Biol. Med.* 42 (7), 1049–1061. doi: 10.1016/j.freeradbiomed.2007.01.005

Wang, L., Zhao, X. C., Cui, W., Ma, Y. Q., Ren, H. L., Zhou, X., et al. (2016). Genetic and Pharmacologic Inhibition of the Chemokine Receptor CXCR2 Prevents Experimental Hypertension and Vascular Dysfunction. *Circulation* 134 (18), 1353–1368. doi: 10.1161/CIRCULATIONAHA.115.020754

Wang, S., Li, J., Bai, J., Li, J. M., Che, Y. L., Lin, Q. Y., et al. (2018). The immunoproteasome subunit LMP10 mediates angiotensin II-induced retinopathy in mice. *Redox Biol.* 16, 129–138. doi: 10.1016/j.redox.2018.02.022

Wang, S., Li, J., Wang, T., Bai, J., Zhang, Y. L., Lin, Q. Y., et al. (2020). Ablation of Immunoproteasome beta5i Subunit Suppresses Hypertensive Retinopathy by Blocking ATRAP Degradation in Mice. *Mol. Ther.* 28 (1), 279–292. doi: 10.1016/j.ymthe.2019.09.025

Wassmann, S., Hilgers, S., Laufs, U., Bohm, M., and Nickenig, G. (2002). Angiotensin II type 1 receptor antagonism improves hypercholesterolemia-associated endothelial dysfunction. *Arterioscler. Thromb. Vasc. Biol.* 22 (7), 1208–1212. doi: 10.1161/01.atv.0000022847.38083.b6

Yan, X., Zhang, Y. L., Zhang, L., Zou, L. X., Chen, C., Liu, Y., et al. (2019). Gallic Acid Suppresses Cardiac Hypertrophic Remodeling and Heart Failure. *Mol. Nutr. Food Res.* 63 (5), e1800807. doi: 10.1002/mnfr.201800807

Conflict of Interest: The authors declare that the research was conducted in the absence of any commercial or financial relationships that could be construed as a potential conflict of interest.

frontiers in Pharmacology

REVIEW
published: 29 July 2020
doi: 10.3389/fphar.2020.01133

Energy Metabolism in Exercise-Induced Physiologic Cardiac Hypertrophy

Kefa Xiang[†], *Zhen Qin*[†*], *Huimin Zhang* and *Xia Liu*[*]

Department of Clinical Pharmacy, School of Pharmacy, Second Military Medical University, Shanghai, China

Physiologic hypertrophy of the heart preserves or enhances systolic function without interstitial fibrosis or cell death. As a unique form of physiological stress, regular exercise training can trigger the adaptation of cardiac muscle to cause physiological hypertrophy, partly due to its ability to improve cardiac metabolism. In heart failure (HF), cardiac dysfunction is closely associated with early initiation of maladaptive metabolic remodeling. A large amount of clinical and experimental evidence shows that metabolic homeostasis plays an important role in exercise training, which is conducive to the treatment and recovery of cardiovascular diseases. Potential mechanistic targets for modulation of cardiac metabolism have become a hot topic at present. Thus, exploring the energy metabolism mechanism in exercise-induced physiologic cardiac hypertrophy may produce new therapeutic targets, which will be helpful to design novel effective strategies. In this review, we summarize the changes of myocardial metabolism (fatty acid metabolism, carbohydrate metabolism, and mitochondrial adaptation), metabolically-related signaling molecules, and probable regulatory mechanism of energy metabolism during exercise-induced physiological cardiac hypertrophy.

Keywords: energy metabolism, exercise, physiologic cardiac hypertrophy, signaling molecules, regulatory mechanism

OPEN ACCESS

Edited by:
Hai-Gang Zhang,
Army Medical University, China

Reviewed by:
Yi Zhun Zhu,
Fudan University, China
Pei Luo,
Macau University of Science and Technology, Macau

***Correspondence:**
Xia Liu
lxflying@aliyun.com
Zhen Qin
qinzhen@smmu.edu.cn

[†]*These authors have contributed equally to this work*

Specialty section:
This article was submitted to Cardiovascular and Smooth Muscle Pharmacology, a section of the journal Frontiers in Pharmacology

Received: *25 May 2020*
Accepted: *13 July 2020*
Published: *29 July 2020*

Citation:
Xiang K, Qin Z, Zhang H and Liu X (2020) Energy Metabolism in Exercise-Induced Physiologic Cardiac Hypertrophy. Front. Pharmacol. 11:1133. doi: 10.3389/fphar.2020.01133

INTRODUCTION

The health benefits of exercise are indisputable. Exercise not only reduces cardiac risk factors and improves cardiac function, but also reduces mortality and morbidity from various cardiovascular diseases (Lavie et al., 2015; Tao et al., 2015; Ostman et al., 2017; Acosta-Manzano et al., 2020; Bersaoui et al., 2020). Some researchers have demonstrated the cardiac protective effect of regular exercise on patients with cardiovascular disease (Ellison et al., 2012), and endurance training can

Abbreviations: ATGL, adipose triglyceride lipase; GPCRs, G-protein-coupled receptors; FAT/CD36, fatty acid translocases; FATP, fatty acid transporters; FA-CoA, acetyl CoA; ACC, Acetyl coenzyme A carboxylase; PPARα/β, peroxisome proliferators-activated receptor α/β; PGC-1α/β, Peroxisome proliferator-activated receptor-γ coactivator-1α/β; OXPHOS, oxidative phosphorylation; ETC, electron transfer chain; FAO, fatty acid oxidation; ERR, estrogen-related receptors; NRF-1, nuclear receptor factor 1; eNOS, endothelial nitric oxide synthase; LCFA, long-chain fatty acids; PI3K, phosphatidylinositol 3 kinase; IRS, insulin receptor substrate; IGF-1R, insulin-like growth factor-1 receptor; PKC-α, protein kinase C-α; O-GlcNAcylization, O-junction of monosaccharide β-N-acetyl-glucosamine; HDAC, histone deacetylase; MCU, mitochondrial calcium uniporter; VEGFs, vascular endothelial growth factors; CST, chronic swimming training; PAAC, partial aortic constriction; AMPK, Adenosine 5'-monophosphate (AMP)-activated protein kinase.

improve cardiac performance by transforming pathological cardiac hypertrophy into a physiological state (Garciarena et al., 2009). However, the exact mechanism of this cardiac adaptation is not fully understood.

Notably, exercise can induce physiological cardiac hypertrophy (Ellison et al., 2012; Xiao et al., 2014; Xiao et al., 2016). In this state, myocardial hypertrophy has normal or enhanced contractile function, considered adaptive, and is not a risk factor for heart failure (Shimizu and Minamino, 2016). Physiological cardiac hypertrophy is characterized by mild heart growth, its mass is usually 10%-20% higher than that of normalized heart (Maillet et al., 2013). The physiological hypertrophy of myocardium induced by exercise training is different from pathological hypertrophy at the stimulation mode, structure, and molecular level (McMullen and Jennings, 2007). In a study of myocardial gene expression profile in rats, it was shown that during exercise-induced physiological myocardial hypertrophy, the glucose signal of cardiomyocytes was significantly different, while there was no significant change in pathological hypertrophy (Kong et al., 2005). A large number of studies have proved that the metabolic coordination is an essential condition for myocardial adaptive growth (Turpeinen et al., 1996; Peterzan et al., 2017; Fulghum and Hill, 2018; Gibb and Hill, 2018; Heallen et al., 2020), but it is not clear whether the regulation of myocardial energy metabolism can reverse myocardial remodeling and improve myocardial function. Therefore, the study of energy metabolism in exercise-induced physiological cardiac hypertrophy is beneficial to the exploration of exercise-induced cardiac adaptation and might be a unique research perspective for interventions in heart failure and other cardiovascular diseases. This review describes the variation of energy metabolism in exercise-induced physiological myocardial hypertrophy from three aspects: fatty acid metabolism, carbohydrate metabolism, and mitochondrial adaptation, and summarizes the related signal molecules (**Figure 1**) and possible regulatory pathways of this energy metabolism (**Figure 2**).

CHANGES OF MYOCARDIAL METABOLISM IN EXERCISE-INDUCED PHYSIOLOGIC CARDIAC HYPERTROPHY

The heart has to keep contracting to provide the body with the oxygen and nutrients it needs. Under normal physiological conditions, due to the small storage of high energy phosphate in cardiac myocytes, normal heart function depends on the tight coupling of intracellular ATP production and myocardial contraction (Kolwicz et al., 2013), and ATP is mainly derived from the catabolism of glucose and fatty acids. Glucose oxidation is a key source of myocardial ATP. In healthy adults, the heart obtains about 50%-70% of myocardial acetyl CoA derived ATP from fatty acids (Lopaschuk et al., 1994). When endogenous fatty acid supply is reduced, intracellular triacylglycerol hydrolyzes the fatty acid back through specific lipases including adipose triglyceride lipase (ATGL) (Haemmerle et al., 2011; Kienesberger et al., 2012) for fatty acid oxidation and subsequent ATP generation. The efficient absorption and recycling of fatty acids by the heart is the key to ensuring ATP supply and systolic function (Kim and Dyck, 2016), and glycolysis produces less than 10% of total ATP in healthy hearts (Lygate et al., 2013). The main pathway for ATP resynthesis is mitochondrial oxidative phosphorylation (>98%), which is driven by the reduction equivalent NADH and FADH2 produced by fatty acid oxidation, pyruvate oxidation, and Krebs cycle. In a healthy heart, the hydrolysis rate of ATP matches the rate of ATP resynthesis, and the tissue content of ATP is very constant, even though the conversion rate of ATP is greatly raised (Stanley and Chandler, 2002). The elevated acute load during exercise has a strong effect on myocardial metabolism (Gibala et al., 1998). In the heart, exercise boosts contractility and oxygen consumption, which is 10 times higher than the resting rate (Olver et al., 2015). Although the heart can take advantage of substrates including carbohydrates, lipids, amino acids, and ketone bodies, to provide energy, while its substrate preference vary under both

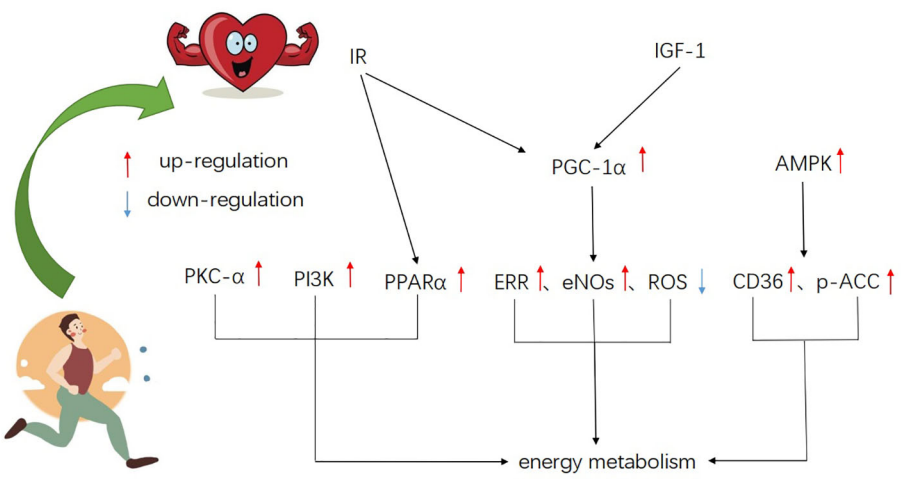

FIGURE 1 | A schematic of the major signaling molecules of metabolism in exercise-induced physiological myocardial hypertrophy, showing integration and cross-talk of various pathways.

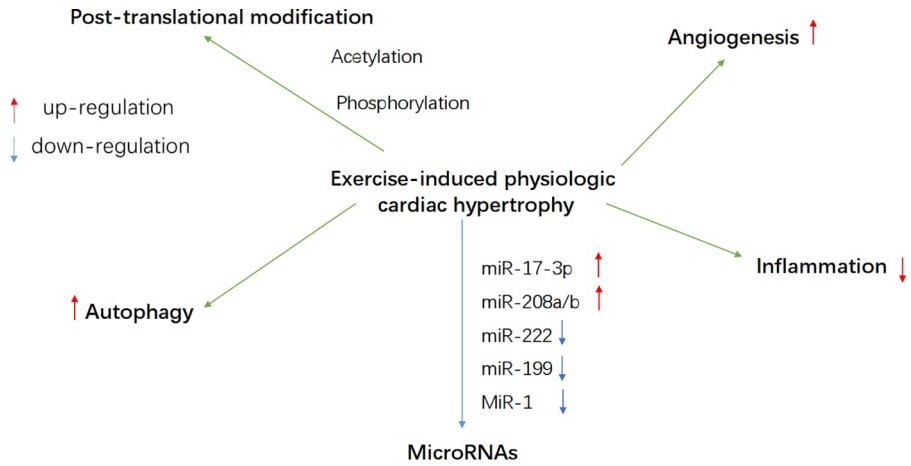

FIGURE 2 | A schematic overview of probable regulatory mechanism of energy metabolism during exercise-induced heart growth, such as autophagy, post-translational modification, microRNAs, angiogenesis, and inflammation.

physiological and pathological stress (Ritterhoff and Tian, 2017). The changes of substrate utilization and mitochondrial adaptation induced by exercise in physiological cardiomyocytes are effective guarantees to maintain the normal myocardial cells function.

Fatty Acid Metabolism

Exercise heightens fat catabolism in adipose tissue and increases triglycerides and free fatty acids in plasma, thus promoting the utilization of fatty acids. It was found that the myocardial hypertrophy of female mice after exercise was significantly enhanced compared with that of male mice, which may be related to the heightened level of free fatty acid in plasma caused by exercise (Foryst-Ludwig et al., 2011). During exercise, hormone-mediated lipid interpretation of fatty acid metabolites in adipose tissue during exercise potentially promotes cardiac physiological growth by activating G-protein-coupled receptors (GPCRs), Akt, or nuclear receptors (Foryst-Ludwig et al., 2015). Not only did free fatty acids increase rapidly with exercise (Frandsen et al., 2019), but they also seemed to remain elevated during exercise adaptation, and the elevated levels of free fatty acids in plasma were considered sufficient to promote cardiac fat catabolism (Pels et al., 1985; Monleon et al., 2014). The uptake of free fatty acids by cardiomyocytes was achieved through plasma membrane transporters, fatty acid translocases (FAT/CD36), fatty acid transporters (FATP), and to a lesser extent, transmembrane diffusion. CD36 deficiency will result in defective fatty acid uptake (Tanaka et al., 1997; Abumrad and Goldberg, 2016). In exercise-induced physiological myocardial hypertrophy, fatty acid and glucose oxidation are enhanced, accompanied by increasing gene expression of encoding fatty acid transporters, fatty acid binding proteins, and lipid metabolic pathways (Strøm et al., 2005; Dobrzyn et al., 2013; Nakamura and Sadoshima, 2018). After fatty acid uptake and conjugation with acetyl CoA (FA-CoA), FA-CoA enters the mitochondria, *via* the carnitine acyl transferase shuttle (CPT-1 and CPT-2) (Abel and Doenst, 2011). CPT-I and CPT-II are responsible for the input of mitochondrial fatty acids and control the rate-limiting steps of the mitochondrial fatty acid oxidation pathway (Lehman et al., 2000). The up-regulated expressions of CPT-I and CPT-II were found in a mice model of exercise training and CPT-II mRNA expression was significantly heightened in exercise-induced physiologic myocardial hypertrophy (Iemitsu et al., 2003). Acetyl coenzyme A carboxylase (ACC) is a key enzyme in fatty acid synthesis. An increase in ACC phosphorylation was observed in cardiomyocytes during moderate exercise training, including the phosphorylation of ACC-1 (265 kDa) and ACC-2 (280 kDa) (Coven et al., 2003). It is possible that ACC phosphorylation reduces the generation of malonyl coenzyme A, thereby indirectly lightening its inhibition of CPT-I activity, increasing the level of free fatty acids in plasma (Awan and Saggerson, 1993; Abu-Elheiga et al., 2001), and playing an important role in regulating fatty acid oxidation (Lopaschuk et al., 1994).

Carbohydrate Metabolism

Glucose uptake in the heart was found to be transversely distributed, and the subendocardial layer is about 30% higher than the epicardial layer. The altered transmural distribution of glucose uptake after exercise probably reflects the metabolic adaptation of different myocardial layers to the physiologic growth of cardiomyocytes induced by exercise (Takala et al., 1983; Kainulainen et al., 1985; Kainulainen et al., 1989). It was found that exercise training elevated GLUT4 mRNA levels of left ventricle in rats (Vettor et al., 2014). The myocardial glucose uptake was significantly higher in the exercise group than that in the rest group (Gertz et al., 1988; Kemppainen et al., 2002). In addition, experimental studies have demonstrated that the elevation of catecholamine and intracellular calcium concentration can raise GLUT4 translocation in the heart (Rattigan et al., 1991), while exercise can activate the sympathetic nerve, elevate catecholamine levels in the body, strengthen calcium concentration

and myocardial contractility in cardiomyocytes. These mechanisms may all play a role in promoting glucose uptake during exercise. At the same time, studies have indicated that the glucose utilization rate of cardiomyocytes in the exercise group is significantly lower than that in the control group (Monleon et al., 2014). At present, only pyruvate kinase activity has been found to be elevated in exercise-adapted rat hearts (York et al., 1975; Stuewe et al., 2000), but little is known about the effect of exercise on rate-limiting enzymes in glycolysis pathway. Glycolysis, aerobic oxidation of glucose and glycogen synthesis, were all enhanced *in vitro* perfusion hearts of exercise-adapted mice (Riehle et al., 2014). However, in exercise-adapted rats, basal myocardial glycolysis was reduced despite increased myocardial glucose and palmitate oxidation (Burelle et al., 2004). Differences between the two studies may be due to differences in animal models (such as rodent species, exercise type) or differences in cardiac perfusion regiments (matrix levels, hormone addition). It was found that the glycogen accumulation in the perfused heart of exercise training adapted mice (Riehle et al., 2014) may be due to the increased glucose uptake stimulated by insulin (Jensen and Richter, 2012). The cardiac glycogen is a potential source of myocardial energy (Aguiar et al., 2017), and glycogen resynthesis after exercise contributes to glucose homeostasis. Recent studies have manifested that cardiac-specific expression of a kinase-deficient 6-phosphofructo-2-kinase/fructose-2,6-bisphosphatase transgene lowered glycolytic rate and regulated the expression of genes known to promote cardiac growth (Boström et al., 2010; Bezzerides et al., 2016; Gibb et al., 2017). These researches further illustrated that depressed glycolytic activity appeared to be important in exercise-induced physiological cardiac hypertrophy. These experimental results showed that although glucose uptake, aerobic oxidation, and glycogen synthesis are all prolonged in exercise-induced hypertrophic myocardium, cardiomyocytes still give priority to fatty acid oxidation to provide energy. Metabolic adaptation maintains the balance between glucose and fatty acid catabolism on the premise of improving the efficiency of cardiac energy production.

Mitochondrial Adaptation

The role of mitochondria in physiological myocardial hypertrophy cannot be ignored. Exercise training promoted mitochondrial biosynthesis in the heart (Vettor et al., 2014), which was related to exercise-induced cardiac hypertrophy (White et al., 1987; Rimbaud et al., 2009a; Abel and Doenst, 2011). A recent study showed that a single exhausting exercise in untrained or trained rats resulted in increasing levels of cytochrome C, Caspase3, and mitochondrial DNA deletion (Huang et al., 2009), suggesting that mitochondrial damage may be an indirect signal to activate mitochondrial biogenesis. It was found that mitochondrial DNA synthesis, electron transport chain related enzyme activity and citrate synthase activity all increased in the hearts of swimming training mice (Riehle et al., 2014). The energy consumption of the heart during exercise is several times higher than that of the resting state, which is related to the increasing of oxygen consumption and mitochondrial ATP production rate. Meanwhile, the myocardial mitochondrial ATP production rate must be highly matched with the ATP decomposition rate. Swimming training induced the enhancement of mitochondrial respiration and ATP production in physiological myocardial hypertrophy of mice (Ascensão et al., 2011), and some experiments proved that the mitochondrial respiration of isolated myocardium of mice also increased after exercise training, which was consistent with the change of gene expression of fatty acid utilization (O'Neill et al., 2007). In addition, exercise training promotes myocardial physiological hypertrophy while carrying out adaptive remodeling of mitochondria (Bo et al., 2010). Eight weeks of exercise conditioned training increased the number of myocardial mitochondria, especially the smaller ones (Dworatzek et al., 2014). In mice, exercise strongly promotes the division of myocardial mitochondria, thereby enhancing the function of mitochondria; these mitochondrial changes occur in a manner dependent on adrenergic signals (Coronado et al., 2018). In cardiomyocytes, mitochondria are considered to be the main source of reactive oxygen species. Under normal/basic conditions, ROS is produced as a by-product of mitochondrial electron transfer activity and is buffered by antioxidant systems. Exercise-induced reactive oxygen species may have beneficial effects on heart growth (Sadoshima, 2006; Alleman et al., 2014; Schieber and Chandel, 2014), probably because ROS, a second messenger to change redox sensitive enzymes, contributes to exercise-induced mitochondrial adaptive signal transduction.

The above studies showed that the adjustment of myocardial energy metabolism contributes to exercise-induced physiological myocardial hypertrophy. Although fatty acids seem to favor energy production, the heart has the ability to respond quickly to variation in matrix availability, ensuring that ATP production continues to meet its energy needs (Taegtmeyer et al., 2004; Hue and Taegtmeyer, 2009; Smith et al., 2018). Therefore, exercise training is related to the regulation of fatty acid, glucose metabolism and mitochondrial adaptation, which may further promote the coordination of myocardial metabolic flexibility and myocyte physiological hypertrophy. However, the specific mechanism is still not well understood and needs further study.

THE SIGNALING MOLECULES OF METABOLISM IN EXERCISE-INDUCED PHYSIOLOGICAL MYOCARDIAL HYPERTROPHY

PGC-1α

Peroxisome proliferator-activated receptor-γ coactivator-1α (PGC-1α) is a transcriptional coactivator initially identified as a cold-inducing factor involved in the mitochondrial biogenesis of brown adipocytes (Puigserver et al., 1998). PGC-1α is required for the normal reserve of fatty acid oxidation (FAO) (Lehman et al., 2008; Peterzan et al., 2017), and PGC-1β for the normal expression of OXPHOS gene (Vianna et al., 2006). PGC-1α/β promotes coordination of gene transcription, mitochondrial biosynthesis, and growth signal at various levels of oxidative metabolism (Rowe et al., 2010). The expression of PGC-1α increases in exercise-induced myocardial hypertrophy, which promotes the production of

mitochondria and the ability of fatty acid oxidation (FAO) (O'Neill et al., 2007; Watson et al., 2007; Riehle et al., 2014). The cardiac function of adult PGC-1α/β-deficient mice does not show obvious abnormalities, but the expression of genes related to the mitochondrial energy transmission pathway (including FAO, tricarboxylic acid cycle, ETC/OXPHOS) in the gene expression profile is significantly and widely down-regulated (Martin et al., 2014). It is probably that PGC-1α/β is not necessary to maintain mitochondrial density and cardiac function in the basal state (Vega et al., 2015), but in the process of exercise-induced physiological myocardial growth, it is necessary to maintain the high volume respiratory function of hypertrophic myocardial mitochondria by driving the expression of genes related to mitochondrial energy conduction and ATP synthesis pathway. PGC-1α also promotes a broader mitochondrial biological response through interaction with estrogen-related receptors (ERR) and nuclear receptor factor 1 (NRF-1) (Scarpulla et al., 2012). Studies have demonstrated that, ERR directly activates mitochondrial energy metabolism involving TCA cycle, electron transfer, and oxidative phosphorylation in cardiomyocytes (Dufour et al., 2007). In the exercise training experiment, endothelial nitric oxide synthase (eNOS) in left ventricular murine tissue (Kojda et al., 2001; Zhang et al., 2007) elevates the gene expression of PGC-1α (Vettor et al., 2014). In addition, it is also found that PGC-1α plays an important role in protecting cardiomyocytes from ROS-mediated injury. In the hearts of PGC-1α knockout mice, the basic mRNA expression levels of ROS detoxifying enzymes such as cytoplasmic copper/zinc-SOD1, mitochondrial Mn-SOD, and peroxisome catalase were significantly reduced (St-Pierre et al., 2006). However, whether ERR, eNOS and ROS play a role in cardiac exercise adaptation by affecting the expression of PGC-1α needs further study.

PPARα

The content of PPARα and PPARβ in cardiomyocytes are the highest, while the expression level of PPARγ is low (Vega et al., 2015). Although both PPARα and PPARβ were initially considered to be regulators of peroxisome β-oxidation (Issemann and Green, 1990), it was later found that only the activation of PPARα in cardiomyocytes regulated the uptake, oxidation and storage of fatty acids in the heart (Gulick et al., 1994; Brandt et al., 1998; Mascaró et al., 1998). Research finds that Cn works by activating PPARα to promote mitochondrial energy production and myocardial growth (White et al., 1987; Turpeinen et al., 1996). Initially, the increasing expression of myocardial peroxisome proliferator-activated receptor (PPARα) was detected during treadmill training in mice (Dobrzyn et al., 2013). Later, it was found that the level of PPARα also increased in exercise-induced physiologic hypertrophic cardiomyocytes (Youtz et al., 2014). In addition, some experiments found that gene expression of PPARα was reduced in pathological cardiac hypertrophy, suggesting that upregulation of PPAR-α expression may limit pathological cardiac hypertrophy (Barger et al., 2000). However, another study explained that the elevating levels of PPARα may be the result of physiological hypertrophy (Rimbaud et al., 2009b). These results further illustrated that PPARα may play an important role in inhibiting the transformation from physiological growth to pathological hypertrophy of cardiomyocytes.

AMPK

In skeletal muscle, AMPK is activated during exercise to increase metabolism (Winder and Hardie, 1996; Winder et al., 1997). AMPK also acts as an important energy sensor and metabolic regulator in the heart (Bairwa et al., 2016). When activated by increasing energy demand, its role is to boost the intake and catabolism of fatty acids (Hardie, 2004). The increase in myocardial stromal metabolism during exercise can be explained by the activation of AMPK (Coven et al., 2003). The activation of AMPK can enhance the uptake of long-chain fatty acids (LCFA) in wild-type cardiomyocytes (Habets et al., 2007) but not the uptake in CD36 knockout cardiomyocytes (Samovski et al., 2015), promote the transport of CD36 to the plasma membrane (Luiken et al., 2003; Kim and Dyck, 2016), indicating that AMPK promotes the CD36 expression and transport to raise fatty acid supply. In addition, AMPK plays a role in myocardial metabolism by phosphorylating ACC, a key enzyme that activate fatty acid metabolism (Nagendran et al., 2013; Hardie et al., 2016). It was found that CD36 expression and ACC phosphorylation are up-regulated in physiologically hypertrophic myocardium induced by exercise training (Strøm et al., 2005; Dolinsky and Dyck, 2006). Thus, AMPK may strengthen the energy supply of exercise-induced myocardial hypertrophy through interaction with CD36 and ACC.

PI3K

Mitochondrial-associated factor phosphatidylinositol 3 kinase (PI3K) signaling and its downstream effectors Akt and GSK-3β promote myocardial physiological hypertrophy growth and maintain normal cardiac function (McMullen et al., 2003). Although PI3K inhibition can reduce the size of the heart and prevent the adaptation of mitochondria to physiological hypertrophy (Shioi et al., 2000). However, the downregulation of the effector Akt by PI3K is not necessary for mitochondria to adapt to cardiac hypertrophy, suggesting that there is an independent PI3K signaling pathway in the induction of physiological hypertrophy and may be related to the regulation of mitochondrial metabolism (O'Neill et al., 2007). It was found that the repolarization of K^+ current amplitude of ventricular myocytes in PI3K cultured group and swimming training induced physiological cardiac hypertrophy group are both higher than that of the wild type, while the expression of transcripts encoding K^+, Ca^{2+}, and other ion channel subunits is elevated, which is parallel to the increased cardiomyocyte size and total cellular RNA expression. It is suggested that the steady-state regulation of physiological myocardial hypertrophy and excitability induced by exercise may be related to myocardial PI3Kα signal (Yang et al., 2010), and the normal maintenance of myocardial electrical function is inseparable from energy.

Therefore, PI3K may be related to the energy regulation of maintaining electrical excitation homeostasis in exercise-induced physiological myocardial hypertrophy.

IGF-1R and IR

Insulin-like growth factor-1 receptor (IGF-1R) has been proved to be an important condition for inducing myocardial physiological growth in mice (McMullen et al., 2004; Kim et al., 2008). In heart-specific IR knockout mice, the expression of PPARα decreased, the level of PGC-1α did not change. Meanwhile, the mitochondrial respiration and ATP synthesis rate were impaired (Boudina et al., 2009). The deletion of insulin receptor substrate (IRS), which is necessary for IGF-1R and IR signal transduction, preventing the activation of PGC-1α, but increasing the capacity of mitochondria after exercise (Riehle et al., 2014). These results provide evidence that the coordination of growth procedures and metabolic reprogramming may occur in insulin-like growth factor-1 and insulin triggered signaling pathways.

PKC-α

Experiments with swimming-trained mice have shown that activation of PKC-α suppresses apoptosis, promotes the growth of physiological cardiomyocytes and improves cardiac function (Naskar et al., 2014). Excessive activation of PKC-α in the liver affects glucose and fatty acid metabolism. In myocardium, PKC-α activation protects myocardium by improving cardiac mitochondrial function (Nowak and Bakajsova, 2013). These related researches of PKC-α indicated that the role of PKC-α in exercise-induced physiological hypertrophy may be associated with the regulation of metabolism.

THE PROBABLE REGULATORY MECHANISM OF ENERGY METABOLISM DURING EXERCISE-INDUCED HEART GROWTH

Autophagy

The recycling of cell components by autophagy has become an important process of adaptive response to exercise (Halling and Pilegaard, 2017). Many beneficial effects of exercise may be related to autophagy, especially physiological myocardial hypertrophy caused by exercise. It was found that the activity of autophagy increased significantly in the heart of exercise-induced physiologically hypertrophic rats (Qi et al., 2020). Some previous studies have shown that autophagy/mitophagy plays an important role in the adaptation of skeletal muscle to endurance exercise and interacts with mitochondrial organisms (He et al., 2012; Vainshtein et al., 2015; Ju et al., 2016). A team found that mitochondrial autophagy-related proteins Beclin1, LC3, and Bnip3 are significantly up-regulated during acute exercise (Li et al., 2016a). Therefore, there may be a certain interaction between autophagy and metabolism in exercise-induced physiological hypertrophic cardiomyocytes.

Post-Translational Modification

Post-translational modification refers to the process of covalent processing of the translated proteins. There are more than 20 post-translational modification processes in eukaryotic cells, such as acetylation, phosphorylation, ubiquitination, and methylation. The mitochondrial proteome consists of approximately 1100 to 1500 proteins, most of which are encoded by nuclear DNA and transferred to mitochondria after post-translational modification (Zhou et al., 2013). Studies have found that metabolic adjustment of myocardium during exercise may be related to ACC phosphorylation in fatty acid metabolism (Coven et al., 2003). By activating PKC-δ and simultaneously inhibiting PKC-α phosphorylation, the PKC subtype is reversed, resulting in impaired cardiac function during physiological hypertrophy (Naskar et al., 2014). In addition, a research shows that the protein O-GlcNAcylization in physiologically growing cardiomyocytes in swimming trained mice is reduced as a whole compared to sedentary mice (Belke, 2011). The O-junction of monosaccharide β-N-acetyl-glucosamine (O-GlcNAcylization) is a post-translational modification on serine and threonine residues, which is an important mechanism for regulating various cellular processes (Mailleux et al., 2016). Another study compared the low and high running ability of rats. The author mentioned the difference in the level of cardiac O-GlcNAcylization of several mitochondrial proteins, among which the O-GlcNAc levels of complex I and complex IV proteins in the low-volume group are higher than high capacity group (Johnsen et al., 2013). Therefore, O-GlcNAcylization may play a role in mitochondrial adaptation to exercise-induced cardiac hypertrophy. Meanwhile, in the physiological cardiac hypertrophy induced by aerobic exercise, PPARβ and histone deacetylase (HDAC) I and II were found to be elevated, accompanied by the interaction between metabolism and epigenetic genes (Soci et al., 2016). Deacetylase (HDAC) affects the acetylation of histones, and exercise training can accelerate the up-regulation of HDAC gene expression and increase the acetylation of histones in cardiomyocytes (Medford et al., 2013; Konhilas et al., 2015; Bernardo et al., 2018). In addition, myocardium-specific histone deacetylase HDAC3 (a member of HDAC I) plays a unique role in maintaining cardiac function and modulating fatty acid metabolism by regulating histone acetylation in the promoter region of myocardial energy gene (Montgomery et al., 2008). These studies indicated that posttranslational modification may play a complementary role in regulating cardiac growth and myocardial energy metabolism.

MicroRNAs

MicroRNAs are small non-coding RNA molecules with a length of about 22 nucleotides, which activate the post-transcriptional gene expression by binding to target messenger RNA to promote its degradation. Some animal and human studies have shown that the levels of microRNAs in exercise-induced cardiac hypertrophy have been altered (**Table 1**). Among them, the expressions of miR-17-3p, miR-30, miR-21, miR-27a/b, miR-144, miR-145 (Wang et al., 2018), miR-29 (Soci et al., 2011),

TABLE 1 | Overview of microRNA levels altered in exercise-induced physiologic cardiac hypertrophy and their cellular targets.

MicroRNA	Cellular Target	Animal Model and Exercise Modality	References
miR-17-3p	TIMP3, PTEN	Mice, swimming exercise	(Wang et al., 2018)
miR-30	P53, Drp-1	Mice, treadmill running	(Wang et al., 2018)
miR-21	PDCD4	Mice, treadmill running	(Wang et al., 2018)
miR-27a/b	ACE	Rats, swimming exercise	(Wang et al., 2018)
miR-144	PTEN	Rats, swimming exercise	(Wang et al., 2018)
miR-145	TSC2	Rats, swimming exercise	(Wang et al., 2018)
miR-29	collagen	Rats, swimming exercise	(Soci et al., 2011)
miR-19b	PTEN, MuRF, Bcl2, Atrogin-1, αCryB	Rats, swimming exercise	(Ramasamy et al., 2015)
miR-208b	THRAP1, Myostatin	Rats, swimming exercise	(Ramasamy et al., 2015; Soci et al., 2016)
miR-133b	CyclinD, NelfA, RhoA, Ccd42	Rats, swimming exercise	(Ramasamy et al., 2015)
miR-100	IGF1R, Akt, mTOR	Rats, swimming exercise	(Ramasamy et al., 2015)
miR-22	CDK6, Sir1, Sp1	Rats, swimming exercise	(Ramasamy et al., 2015)
miR-99b	IGF1R, Akt, mTOR	Rats, swimming exercise	(Ramasamy et al., 2015)
miR-181a	MAPK1, TNFα, GATA4	Rats, swimming exercise	(Ramasamy et al., 2015)
miR-191a	Egr1, Cd4, Casp4, SOCS4, p53	Rats, swimming exercise	(Ramasamy et al., 2015)
miR-1	Bcl-2	Mice, treadmill running	(Zaglia et al., 2017; Wang et al., 2018).
miR-133	Calcineurin, PI3K/Akt signaling	Rats, swimming exercise	(Wang et al., 2018)
miR-124	PI3K	Rats, swimming exercise	(Wang et al., 2018)
miR-143	ACE2	Rats, swimming exercise	(Wang et al., 2018)
miR-341	c-Myb	Mice, treadmill running	(Martinelli et al., 2014)
miR-199	PGC1α	Mice, treadmill running	(Li et al., 2016b; Schüttler et al., 2019)
miR-222	P27, Hipk1, Hmbox1	Mice, swimming exercise	(Schüttler et al., 2019)
miR-214	SERCA2a	Rats, leg flexing exercise	(Melo et al., 2015)
miR-26b-5p	LC3B, Beclin1, SQSTM1	Rats, swimming exercise	(Qi et al., 2020)
miR204-5p	LC3B, Beclin1, SQSTM1	Rats, swimming exercise	(Qi et al., 2020)
miR-497-3p	LC3B, Beclin1, SQSTM1	Rats, swimming exercise	(Qi et al., 2020)

miR-19b, miR-208b, and miR-133b (Ramasamy et al., 2015) were up-regulated. MiR-1, miR-133, miR-124, miR-143 (Wang et al., 2018), miR-341 (Martinelli et al., 2014), miR-100, miR-22, miR-99b, miR-181a, miR-191a (Ramasamy et al., 2015), miR-214 (Melo et al., 2015), miR-199, miR-222 (Schüttler et al., 2019), miR-26b-5p, miR-204-5p, and miR-497-3p (Qi et al., 2020) were down-regulated. MicroRNAs regulate gene expression in hypertrophic myocardium induced by exercise training, in which miR-17-3p and miR-222 may induce cardiomyocyte metabolism and mitochondrial adaptation (Schüttler et al., 2019). Furthermore, inhibition of endogenous miR-199 inducing physiological myocardial hypertrophy may be related to up-regulation of PGC-1α mRNA expression (Li et al., 2016b). MiR-1 suppresses the translation of MCU (a kind of mitochondrial calcium transporter), reduces the uptake of mitochondrial Ca^{2+} in cardiomyocyte, and increases the production of metabolic energy (Zaglia et al., 2017). Inhibition of miR-208b increases the expression of epigenetic target proteins, which may stimulate the interaction between metabolism and cell growth (Soci et al., 2016). In addition, in a study on the relationship between miRNAs and exercise-induced physiological cardiac hypertrophy, KEGG pathway analysis showed that 12 up-regulated miRNAs are associated with fatty acid degradation, fatty acid metabolism, and fatty acid elongation (Xu et al., 2017). These researches indicated that microRNAs may have a certain effect on metabolism in maintaining exercise-induced physiological myocardial hypertrophy. However, the roles of lncRNAs and circRNAs in physiological cardiac hypertrophy have not been reported (Wang et al., 2020).

Angiogenesis

VEGFs are main regulators of myocardial angiogenesis. Some studies have found that inhibition of VEGFs signal transduction leads to capillary thinning and early heart failure (Izumiya et al., 2006; Sano et al., 2007), indicating that cardiomyocytes may produce angiogenic factors to maintain capillary density, oxygen supply, and function. The number of myocardial capillaries increased significantly in physiological myocardial hypertrophy (Anversa et al., 1983; Oka et al., 2014), while the capillary density was attenuated in pathological myocardial hypertrophy (Anversa and Capasso, 1991; Beltrami et al., 1994), suggesting that the number of myocardial capillaries is controlled by the myocardium, and the decrease in capillary density may cause hypoxia or even contraction dysfunction. Therefore, the growth of physiologically hypertrophic cardiomyocytes induced by exercise may be related to angiogenesis providing a good oxygen supply for myocardial metabolism.

Inflammation

There are total 59 genetic variation in the study of physiological cardiac hypertrophy in swimming mice or treadmill rats, only two genes (Cd74 and Col3a1) are changed in both mice and rat models. The immune-function related gene Col3a1 was down-regulated in response to exercise in mice (1.6, 3.1-fold) and rats (1.8-fold) but up-regulated in most pathological cardiac hypertrophy models (Galindo et al., 2009). In the study of cardiac cell RNA sequencing, it was found that one of the most significant difference in the physiologically hypertrophic myocardium induced by swimming training was the severe downregulation of the autoimmunity pathway, accompanied

by the obvious selective splice of exon variants (AS) (Song et al., 2012). In addition, in a study using high-density oligonucleotide microarray to detect myocardial gene expression profiles in physiologically and pathologically hypertrophic rats, inflammation-related genes (such as pancreatitis-associated proteins and arachidonic acid 12 lipoxygenase) increased in the pathological process, but not in physiological hypertrophy (Kong et al., 2005). At the molecular level, the up-regulated expression of Rho kinase promoted inflammation. Fasudil is an inhibitor of Rho kinase. It was found that fasudil could significantly reduce the left ventricular dysfunction of pathological myocardial hypertrophy caused by partial aortic constriction (PAAC), but has no significant regulatory effect on left ventricular hypertrophy induced by chronic swimming training (CST). These results suggest that Rho kinase is involved in PAAC-induced pathological myocardial hypertrophy (Balakumar and Singh, 2006). However, it is not ruled out that the regulatory effect of Rho kinase on physiological hypertrophy is not obvious due to the down-regulation of immune pathway in physiological cardiac hypertrophy induced by CST. It remains further explored whether the down-regulation of this immune pathway affects the energy metabolism of the myocardium.

CONCLUSIONS

Metabolic remodeling is closely related to the occurrence and development of cardiac hypertrophy and other heart diseases. Exploring the energy metabolism mechanism of cardiomyocytes may lead to new therapeutic targets, which will be helpful to design new effective methods and strategies for the treatment of heart failure (Bøgh et al., 2020; Makrecka-Kuka et al., 2020; Zuurbier et al., 2020). As we all know, physical exercise has a protective effect on the heart, and can even partially compensate for heart damage and improve heart function. Combined with the metabolic adaptation pathway observed in the studies of myocardial physiological hypertrophy induced by exercise, we can further explore how exercise-induced metabolic adaptation coordinate cell signals and gene expression, which may be helpful to guide exercise training scientifically, maximize the benefits of exercise, improve heart health, and develop new treatment strategies for the treatment of heart failure caused by various complex reasons and aging in the future.

AUTHOR CONTRIBUTIONS

KX and ZQ contributed equally to this work. KX wrote the manuscript. ZQ and HZ analyzed concerned literatures. XL and ZQ revised the manuscript. All authors agree to be accountable for the content of the work.

FUNDING

This study was sponsored by the National Natural Science Foundation of China (81773726 to XL), National Science and Technology Major Project (2018ZX09711002-003-015 to XL), Shanghai Sailing Program (19YF1459500 to ZQ) and Science and Technology Innovation Action Plan Project (19401900100 to XL and 19431901400 to ZQ).

REFERENCES

Abel, E. D., and Doenst, T. (2011). Mitochondrial adaptations to physiological vs. pathological cardiac hypertrophy. *Cardiovasc. Res.* 90 (2), 234–242. doi: 10.1093/cvr/cvr015

Abu-Elheiga, L., Matzuk, M. M., Abo-Hashema, K. A., and Wakil, S. J. (2001). Continuous fatty acid oxidation and reduced fat storage in mice lacking acetyl-CoA carboxylase 2. *Science* 291 (5513), 2613–2616. doi: 10.1126/science.1056843

Abumrad, N. A., and Goldberg, I. J. (2016). CD36 actions in the heart: Lipids, calcium, inflammation, repair and more? *Biochim. Biophys. Acta* 1861 (10), 1442–1449. doi: 10.1016/j.bbalip.2016.03.015

Acosta-Manzano, P., Rodriguez-Ayllon, M., Acosta, F. M., Niederseer, D., and Niebauer, J. (2020). Beyond general resistance training. Hypertrophy versus muscular endurance training as therapeutic interventions in adults with type 2 diabetes mellitus: A systematic review and meta-analysis. *Obes. Rev.* 21 (6), e13007. doi: 10.1111/obr.13007

Aguiar, R. R., Vale, D. F., Silva, R. M. D., Muniz, Y. P., Antunes, F., Logullo, C., et al. (2017). A possible relationship between gluconeogenesis and glycogen metabolism in rabbits during myocardial ischemia. *Acad. Bras. Cienc.* 89 (3), 1683–1690. doi: 10.1590/0001-3765201720160773

Alleman, R. J., Katunga, L. A., Nelson, M. A., Brown, D. A., and Anderson, E. J. (2014). The "Goldilocks Zone" from a redox perspective-Adaptive vs. deleterious responses to oxidative stress in striated muscle. *Front. Physiol.* 5, 358. doi: 10.3389/fphys.2014.00358

Anversa, P., and Capasso, J. M. (1991). Loss of intermediate-sized coronary arteries and capillary proliferation after left ventricular failure in rats. *Am. J. Physiol.* 260 (5 Pt 2), H1552–H1560. doi: 10.1152/ajpheart.1991.260.5.H1552

Anversa, P., Levicky, V., Beghi, C., McDonald, S. L., and Kikkawa, Y. (1983). Morphometry of exercise-induced right ventricular hypertrophy in the rat. *Circ. Res.* 52 (1), 57–64. doi: 10.1161/01.res.52.1.57

Ascensão, A., Lumini-Oliveira, J., Oliveira, P. J., and Magalhães, J. (2011). Mitochondria as a target for exercise-induced cardioprotection. *Curr. Drug Targets* 12 (6), 860–871. doi: 10.2174/138945011795529001

Awan, M. M., and Saggerson, E. D. (1993). Malonyl-CoA metabolism in cardiac myocytes and its relevance to the control of fatty acid oxidation. *Biochem. J.* 295 (Pt 1), 61–66. doi: 10.1042/bj2950061

Bairwa, S. C., Parajuli, N., and Dyck, J. R. (2016). The role of AMPK in cardiomyocyte health and survival. *Biochim. Biophys. Acta* 1862 (12), 2199–2210. doi: 10.1016/j.bbadis.2016.07.001

Balakumar, P., and Singh, M. (2006). Differential role of rho-kinase in pathological and physiological cardiac hypertrophy in rats. *Pharmacology* 78 (2), 91–97. doi: 10.1159/000095784

Barger, P. M., Brandt, J. M., Leone, T. C., Weinheimer, C. J., and Kelly, D. P. (2000). Deactivation of peroxisome proliferator-activated receptor-alpha during cardiac hypertrophic growth. *J. Clin. Invest.* 105 (12), 1723–1730. doi: 10.1172/jci9056

Belke, D. D. (2011). Swim-exercised mice show a decreased level of protein O-GlcNAcylation and expression of O-GlcNAc transferase in heart. *J. Appl. Physiol. (1985)* 111 (1), 157–162. doi: 10.1152/japplphysiol.00147.2011

Beltrami, C. A., Finato, N., Rocco, M., Feruglio, G. A., Puricelli, C., Cigola, E., et al. (1994). Structural basis of end-stage failure in ischemic cardiomyopathy in humans. *Circulation* 89 (1), 151–163. doi: 10.1161/01.cir.89.1.151

Bernardo, B. C., Ooi, J. Y. Y., Weeks, K. L., Patterson, N. L., and McMullen, J. R. (2018). Understanding Key Mechanisms of Exercise-Induced Cardiac

Protection to Mitigate Disease: Current Knowledge and Emerging Concepts. *Physiol. Rev.* 98 (1), 419–475. doi: 10.1152/physrev.00043.2016

Bersaoui, M., Baldew, S. M., Cornelis, N., Toelsie, J., and Cornelissen, V. A. (2020). The effect of exercise training on blood pressure in African and Asian populations: A systematic review and meta-analysis of randomized controlled trials. *Eur. J. Prev. Cardiol.* 27 (5), 457–472. doi: 10.1177/2047487319871233

Bezzerides, V. J., Platt, C., Lerchenmüller, C., Paruchuri, K., Oh, N. L., Xiao, C., et al. (2016). CITED4 induces physiologic hypertrophy and promotes functional recovery after ischemic injury. *JCI Insight* 1 (9), e85904. doi: 10.1172/jci.insight.85904

Bo, H., Zhang, Y., and Ji, L. L. (2010). Redefining the role of mitochondria in exercise: a dynamic remodeling. *Ann. N. Y. Acad. Sci.* 1201, 121–128. doi: 10.1111/j.1749-6632.2010.05618.x

Bøgh, N., Hansen, E. S. S., Omann, C., Lindhardt, J., Nielsen, P. M., Stephenson, R. S., et al. (2020). Increasing carbohydrate oxidation improves contractile reserves and prevents hypertrophy in porcine right heart failure. *Sci. Rep.* 10 (1), 8158. doi: 10.1038/s41598-020-65098-7

Boström, P., Mann, N., Wu, J., Quintero, P. A., Plovie, E. R., Panáková, D., et al. (2010). C/EBPβ controls exercise-induced cardiac growth and protects against pathological cardiac remodeling. *Cell* 143 (7), 1072–1083. doi: 10.1016/j.cell.2010.11.036

Boudina, S., Bugger, H., Sena, S., O'Neill, B. T., Zaha, V. G., Ilkun, O., et al. (2009). Contribution of impaired myocardial insulin signaling to mitochondrial dysfunction and oxidative stress in the heart. *Circulation* 119 (9), 1272–1283. doi: 10.1161/circulationaha.108.792101

Brandt, J. M., Djouadi, F., and Kelly, D. P. (1998). Fatty acids activate transcription of the muscle carnitine palmitoyltransferase I gene in cardiac myocytes via the peroxisome proliferator-activated receptor alpha. *J. Biol. Chem.* 273 (37), 23786–23792. doi: 10.1074/jbc.273.37.23786

Burelle, Y., Wambolt, R. B., Grist, M., Parsons, H. L., Chow, J. C., Antler, C., et al. (2004). Regular exercise is associated with a protective metabolic phenotype in the rat heart. *Am. J. Physiol. Heart Circ. Physiol.* 287 (3), H1055–H1063. doi: 10.1152/ajpheart.00925.2003

Coronado, M., Fajardo, G., Nguyen, K., Zhao, M., Kooiker, K., Jung, G., et al. (2018). Physiological Mitochondrial Fragmentation Is a Normal Cardiac Adaptation to Increased Energy Demand. *Circ. Res.* 122 (2), 282–295. doi: 10.1161/circresaha.117.310725

Coven, D. L., Hu, X., Cong, L., Bergeron, R., Shulman, G. I., Hardie, D. G., et al. (2003). Physiological role of AMP-activated protein kinase in the heart: graded activation during exercise. *Am. J. Physiol. Endocrinol. Metab.* 285 (3), E629–E636. doi: 10.1152/ajpendo.00171.2003

Dobrzyn, P., Pyrkowska, A., Duda, M. K., Bednarski, T., Maczewski, M., Langfort, J., et al. (2013). Expression of lipogenic genes is upregulated in the heart with exercise training-induced but not pressure overload-induced left ventricular hypertrophy. *Am. J. Physiol. Endocrinol. Metab.* 304 (12), E1348–E1358. doi: 10.1152/ajpendo.00603.2012

Dolinsky, V. W., and Dyck, J. R. (2006). Role of AMP-activated protein kinase in healthy and diseased hearts. *Am. J. Physiol. Heart Circ. Physiol.* 291 (6), H2557–H2569. doi: 10.1152/ajpheart.00329.2006

Dufour, C. R., Wilson, B. J., Huss, J. M., Kelly, D. P., Alaynick, W. A., Downes, M., et al. (2007). Genome-wide orchestration of cardiac functions by the orphan nuclear receptors ERRalpha and gamma. *Cell Metab.* 5 (5), 345–356. doi: 10.1016/j.cmet.2007.03.007

Dworatzek, E., Mahmoodzadeh, S., Schubert, C., Westphal, C., Leber, J., Kusch, A., et al. (2014). Sex differences in exercise-induced physiological myocardial hypertrophy are modulated by oestrogen receptor beta. *Cardiovasc. Res.* 102 (3), 418–428. doi: 10.1093/cvr/cvu065

Ellison, G. M., Waring, C. D., Vicinanza, C., and Torella, D. (2012). Physiological cardiac remodelling in response to endurance exercise training: cellular and molecular mechanisms. *Heart* 98 (1), 5–10. doi: 10.1136/heartjnl-2011-300639

Foryst-Ludwig, A., Kreissl, M. C., Sprang, C., Thalke, B., Böhm, C., Benz, V., et al. (2011). Sex differences in physiological cardiac hypertrophy are associated with exercise-mediated changes in energy substrate availability. *Am. J. Physiol. Heart Circ. Physiol.* 301 (1), H115–H122. doi: 10.1152/ajpheart.01222.2010

Foryst-Ludwig, A., Kreissl, M. C., Benz, V., Brix, S., Smeir, E., Ban, Z., et al. (2015). Adipose Tissue Lipolysis Promotes Exercise-induced Cardiac Hypertrophy Involving the Lipokine C16:1n7-Palmitoleate. *J. Biol. Chem.* 290 (39), 23603–23615. doi: 10.1074/jbc.M115.645341

Frandsen, J., Vest, S. D., Ritz, C., Larsen, S., Dela, F., and Helge, J. W. (2019). Plasma free fatty acid concentration is closely tied to whole body peak fat oxidation rate during repeated exercise. *J. Appl. Physiol. (1985)* 126 (6), 1563–1571. doi: 10.1152/japplphysiol.00995.2018

Fulghum, K., and Hill, B. G. (2018). Metabolic Mechanisms of Exercise-Induced Cardiac Remodeling. *Front. Cardiovasc. Med.* 5, 127. doi: 10.3389/fcvm.2018.00127

Galindo, C. L., Skinner, M. A., Errami, M., Olson, L. D., Watson, D. A., Li, J., et al. (2009). Transcriptional profile of isoproterenol-induced cardiomyopathy and comparison to exercise-induced cardiac hypertrophy and human cardiac failure. *BMC Physiol.* 9, 23. doi: 10.1186/1472-6793-9-23

Garciarena, C. D., Pinilla, O. A., Nolly, M. B., Laguens, R. P., Escudero, E. M., Cingolani, H. E., et al. (2009). Endurance training in the spontaneously hypertensive rat: conversion of pathological into physiological cardiac hypertrophy. *Hypertension* 53 (4), 708–714. doi: 10.1161/hypertensionaha.108.126805

Gertz, E. W., Wisneski, J. A., Stanley, W. C., and Neese, R. A. (1988). Myocardial substrate utilization during exercise in humans. Dual carbon-labeled carbohydrate isotope experiments. *J. Clin. Invest.* 82 (6), 2017–2025. doi: 10.1172/jci113822

Gibala, M. J., MacLean, D. A., Graham, T. E., and Saltin, B. (1998). Tricarboxylic acid cycle intermediate pool size and estimated cycle flux in human muscle during exercise. *Am. J. Physiol.* 275 (2), E235–E242. doi: 10.1152/ajpendo.1998.275.2.E235

Gibb, A. A., and Hill, B. G. (2018). Metabolic Coordination of Physiological and Pathological Cardiac Remodeling. *Circ. Res.* 123 (1), 107–128. doi: 10.1161/circresaha.118.312017

Gibb, A. A., Epstein, P. N., Uchida, S., Zheng, Y., McNally, L. A., Obal, D., et al. (2017). Exercise-Induced Changes in Glucose Metabolism Promote Physiological Cardiac Growth. *Circulation* 136 (22), 2144–2157. doi: 10.1161/circulationaha.117.028274

Gulick, T., Cresci, S., Caira, T., Moore, D. D., and Kelly, D. P. (1994). The peroxisome proliferator-activated receptor regulates mitochondrial fatty acid oxidative enzyme gene expression. *Proc. Natl. Acad. Sci. U.S.A.* 91 (23), 11012–11016. doi: 10.1073/pnas.91.23.11012

Habets, D. D., Coumans, W. A., Voshol, P. J., den Boer, M. A., Febbraio, M., Bonen, A., et al. (2007). AMPK-mediated increase in myocardial long-chain fatty acid uptake critically depends on sarcolemmal CD36. *Biochem. Biophys. Res. Commun.* 355 (1), 204–210. doi: 10.1016/j.bbrc.2007.01.141

Haemmerle, G., Moustafa, T., Woelkart, G., Büttner, S., Schmidt, A., van de Weijer, T., et al. (2011). ATGL-mediated fat catabolism regulates cardiac mitochondrial function via PPAR-α and PGC-1. *Nat. Med.* 17 (9), 1076–1085. doi: 10.1038/nm.2439

Halling, J. F., and Pilegaard, H. (2017). Autophagy-Dependent Beneficial Effects of Exercise. *Cold Spring Harb. Perspect. Med.* 7 (8), a029777. doi: 10.1101/cshperspect.a029777

Hardie, D. G., Schaffer, B. E., and Brunet, A. (2016). AMPK: An Energy-Sensing Pathway with Multiple Inputs and Outputs. *Trends Cell Biol.* 26 (3), 190–201. doi: 10.1016/j.tcb.2015.10.013

Hardie, D. G. (2004). AMP-activated protein kinase: the guardian of cardiac energy status. *J. Clin. Invest.* 114 (4), 465–468. doi: 10.1172/jci22683

He, C., Bassik, M. C., Moresi, V., Sun, K., Wei, Y., Zou, Z., et al. (2012). Exercise-induced BCL2-regulated autophagy is required for muscle glucose homeostasis. *Nature* 481 (7382), 511–515. doi: 10.1038/nature10758

Heallen, T. R., Kadow, Z. A., Wang, J., and Martin, J. F. (2020). Determinants of Cardiac Growth and Size. *Cold Spring Harb. Perspect. Biol.* 12 (3), a037150. doi: 10.1101/cshperspect.a037150

Huang, C. C., Lin, T. J., Chen, C. C., and Lin, W. T. (2009). Endurance training accelerates exhaustive exercise-induced mitochondrial DNA deletion and apoptosis of left ventricle myocardium in rats. *Eur. J. Appl. Physiol.* 107 (6), 697–706. doi: 10.1007/s00421-009-1177-4

Hue, L., and Taegtmeyer, H. (2009). The Randle cycle revisited: a new head for an old hat. *Am. J. Physiol. Endocrinol. Metab.* 297 (3), E578–E591. doi: 10.1152/ajpendo.00093.2009

Iemitsu, M., Miyauchi, T., Maeda, S., Sakai, S., Fujii, N., Miyazaki, H., et al. (2003). Cardiac hypertrophy by hypertension and exercise training exhibits different

gene expression of enzymes in energy metabolism. *Hypertens. Res.* 26 (10), 829–837. doi: 10.1291/hypres.26.829

Issemann, I., and Green, S. (1990). Activation of a member of the steroid hormone receptor superfamily by peroxisome proliferators. *Nature* 347 (6294), 645–650. doi: 10.1038/347645a0

Izumiya, Y., Shiojima, I., Sato, K., Sawyer, D. B., Colucci, W. S., and Walsh, K. (2006). Vascular endothelial growth factor blockade promotes the transition from compensatory cardiac hypertrophy to failure in response to pressure overload. *Hypertension* 47 (5), 887–893. doi: 10.1161/01.Hyp.0000215207.54689.31

Jensen, T. E., and Richter, E. A. (2012). Regulation of glucose and glycogen metabolism during and after exercise. *J. Physiol.* 590 (5), 1069–1076. doi: 10.1113/jphysiol.2011.224972

Johnsen, V. L., Belke, D. D., Hughey, C. C., Hittel, D. S., Hepple, R. T., Koch, L. G., et al. (2013). Enhanced cardiac protein glycosylation (O-GlcNAc) of selected mitochondrial proteins in rats artificially selected for low running capacity. *Physiol. Genomics* 45 (1), 17–25. doi: 10.1152/physiolgenomics.00111.2012

Ju, J. S., Jeon, S. I., Park, J. Y., Lee, J. Y., Lee, S. C., Cho, K. J., et al. (2016). Autophagy plays a role in skeletal muscle mitochondrial biogenesis in an endurance exercise-trained condition. *J. Physiol. Sci.* 66 (5), 417–430. doi: 10.1007/s12576-016-0440-9

Kainulainen, H., Takala, T. E., Hassinen, I. E., and Vihko, V. (1985). Redistribution of glucose uptake by chronic exercise, measured in isolated perfused rat hearts. *Pflugers Arch.* 403 (3), 296–300. doi: 10.1007/bf00583603

Kainulainen, H., Virtanen, P., Ruskoaho, H., and Takala, T. E. (1989). Training increases cardiac glucose uptake during rest and exercise in rats. *Am. J. Physiol.* 257 (3 Pt 2), H839–H845. doi: 10.1152/ajpheart.1989.257.3.H839

Kemppainen, J., Fujimoto, T., Kalliokoski, K. K., Viljanen, T., Nuutila, P., and Knuuti, J. (2002). Myocardial and skeletal muscle glucose uptake during exercise in humans. *J. Physiol.* 542 (Pt 2), 403–412. doi: 10.1113/jphysiol.2002.018135

Kienesberger, P. C., Pulinilkunnil, T., Sung, M. M., Nagendran, J., Haemmerle, G., Kershaw, E. E., et al. (2012). Myocardial ATGL overexpression decreases the reliance on fatty acid oxidation and protects against pressure overload-induced cardiac dysfunction. *Mol. Cell Biol.* 32 (4), 740–750. doi: 10.1128/mcb.06470-11

Kim, T. T., and Dyck, J. R. (2016). The role of CD36 in the regulation of myocardial lipid metabolism. *Biochim. Biophys. Acta* 1861 (10), 1450–1460. doi: 10.1016/j.bbalip.2016.03.018

Kim, J., Wende, A. R., Sena, S., Theobald, H. A., Soto, J., Sloan, C., et al. (2008). Insulin-like growth factor I receptor signaling is required for exercise-induced cardiac hypertrophy. *Mol. Endocrinol.* 22 (11), 2531–2543. doi: 10.1210/me.2008-0265

Kojda, G., Cheng, Y. C., Burchfield, J., and Harrison, D. G. (2001). Dysfunctional regulation of endothelial nitric oxide synthase (eNOS) expression in response to exercise in mice lacking one eNOS gene. *Circulation* 103 (23), 2839–2844. doi: 10.1161/01.cir.103.23.2839

Kolwicz, S. C.Jr., Purohit, S., and Tian, R. (2013). Cardiac metabolism and its interactions with contraction, growth, and survival of cardiomyocytes. *Circ. Res.* 113 (5), 603–616. doi: 10.1161/circresaha.113.302095

Kong, S. W., Bodyak, N., Yue, P., Liu, Z., Brown, J., Izumo, S., et al. (2005). Genetic expression profiles during physiological and pathological cardiac hypertrophy and heart failure in rats. *Physiol. Genomics* 21 (1), 34–42. doi: 10.1152/physiolgenomics.00226.2004

Konhilas, J. P., Chen, H., Luczak, E., McKee, L. A., Regan, J., Watson, P. A., et al. (2015). Diet and sex modify exercise and cardiac adaptation in the mouse. *Am. J. Physiol. Heart Circ. Physiol.* 308 (2), H135–H145. doi: 10.1152/ajpheart.00532.2014

Lavie, C. J., Arena, R., Swift, D. L., Johannsen, N. M., Sui, X., Lee, D. C., et al. (2015). Exercise and the cardiovascular system: clinical science and cardiovascular outcomes. *Circ. Res.* 117 (2), 207–219. doi: 10.1161/circresaha.117.305205

Lehman, J. J., Barger, P. M., Kovacs, A., Saffitz, J. E., Medeiros, D. M., and Kelly, D. P. (2000). Peroxisome proliferator-activated receptor gamma coactivator-1 promotes cardiac mitochondrial biogenesis. *J. Clin. Invest.* 106 (7), 847–856. doi: 10.1172/jci10268

Lehman, J. J., Boudina, S., Banke, N. H., Sambandam, N., Han, X., Young, D. M., et al. (2008). The transcriptional coactivator PGC-1alpha is essential for maximal and efficient cardiac mitochondrial fatty acid oxidation and lipid homeostasis. *Am. J. Physiol. Heart Circ. Physiol.* 295 (1), H185–H196. doi: 10.1152/ajpheart.00081.2008

Li, H., Miao, W., Ma, J., Xv, Z., Bo, H., Li, J., et al. (2016a). Acute Exercise-Induced Mitochondrial Stress Triggers an Inflammatory Response in the Myocardium via NLRP3 Inflammasome Activation with Mitophagy. *Oxid. Med. Cell Longev.* 2016:1987149. doi: 10.1155/2016/1987149

Li, Z., Liu, L., Hou, N., Song, Y., An, X., Zhang, Y., et al. (2016b). miR-199-sponge transgenic mice develop physiological cardiac hypertrophy. *Cardiovasc. Res.* 110 (2), 258–267. doi: 10.1093/cvr/cvw052

Lopaschuk, G. D., Belke, D. D., Gamble, J., Itoi, T., and Schönekess, B. O. (1994). Regulation of fatty acid oxidation in the mammalian heart in health and disease. *Biochim. Biophys. Acta* 1213 (3), 263–276. doi: 10.1016/0005-2760(94)00082-4

Luiken, J. J., Coort, S. L., Willems, J., Coumans, W. A., Bonen, A., van der Vusse, G. J., et al. (2003). Contraction-induced fatty acid translocase/CD36 translocation in rat cardiac myocytes is mediated through AMP-activated protein kinase signaling. *Diabetes* 52 (7), 1627–1634. doi: 10.2337/diabetes.52.7.1627

Lygate, C. A., Schneider, J. E., and Neubauer, S. (2013). Investigating cardiac energetics in heart failure. *Exp. Physiol.* 98 (3), 601–605. doi: 10.1113/expphysiol.2012.064709

Maillet, M., van Berlo, J. H., and Molkentin, J. D. (2013). Molecular basis of physiological heart growth: fundamental concepts and new players. *Nat. Rev. Mol. Cell Biol.* 14 (1), 38–48. doi: 10.1038/nrm3495

Mailleux, F., Gélinas, R., Beauloye, C., Horman, S., and Bertrand, L. (2016). O-GlcNAcylation, enemy or ally during cardiac hypertrophy development? *Biochim. Biophys. Acta* 1862 (12), 2232–2243. doi: 10.1016/j.bbadis.2016.08.012

Makrecka-Kuka, M., Korzh, S., Videja, M., Vilks, K., Cirule, H., Kuka, J., et al. (2020). Empagliflozin Protects Cardiac Mitochondrial Fatty Acid Metabolism in a Mouse Model of Diet-Induced Lipid Overload. *Cardiovasc. Drugs Ther.* [Epub ahead of print]. doi: 10.1007/s10557-020-06989-9

Martin, O. J., Lai, L., Soundarapandian, M. M., Leone, T. C., Zorzano, A., Keller, M. P., et al. (2014). A role for peroxisome proliferator-activated receptor γ coactivator-1 in the control of mitochondrial dynamics during postnatal cardiac growth. *Circ. Res.* 114 (4), 626–636. doi: 10.1161/circresaha.114.302562

Martinelli, N. C., Cohen, C. R., Santos, K. G., Castro, M. A., Biolo, A., Frick, L., et al. (2014). An analysis of the global expression of microRNAs in an experimental model of physiological left ventricular hypertrophy. *PloS One* 9 (4), e93271. doi: 10.1371/journal.pone.0093271

Mascaró, C., Acosta, E., Ortiz, J. A., Marrero, P. F., Hegardt, F. G., and Haro, D. (1998). Control of human muscle-type carnitine palmitoyltransferase I gene transcription by peroxisome proliferator-activated receptor. *J. Biol. Chem.* 273 (15), 8560–8563. doi: 10.1074/jbc.273.15.8560

McMullen, J. R., and Jennings, G. L. (2007). Differences between pathological and physiological cardiac hypertrophy: novel therapeutic strategies to treat heart failure. *Clin. Exp. Pharmacol. Physiol.* 34 (4), 255–262. doi: 10.1111/j.1440-1681.2007.04585.x

McMullen, J. R., Shioi, T., Zhang, L., Tarnavski, O., Sherwood, M. C., Kang, P. M., et al. (2003). Phosphoinositide 3-kinase(p110alpha) plays a critical role for the induction of physiological, but not pathological, cardiac hypertrophy. *Proc. Natl. Acad. Sci. U.S.A.* 100 (21), 12355–12360. doi: 10.1073/pnas.1934654100

McMullen, J. R., Shioi, T., Huang, W. Y., Zhang, L., Tarnavski, O., Bisping, E., et al. (2004). The insulin-like growth factor 1 receptor induces physiological heart growth via the phosphoinositide 3-kinase(p110alpha) pathway. *J. Biol. Chem.* 279 (6), 4782–4793. doi: 10.1074/jbc.M310405200

Medford, H. M., Porter, K., and Marsh, S. A. (2013). Immediate effects of a single exercise bout on protein O-GlcNAcylation and chromatin regulation of cardiac hypertrophy. *Am. J. Physiol. Heart Circ. Physiol.* 305 (1), H114–H123. doi: 10.1152/ajpheart.00135.2013

Melo, S. F., Barauna, V. G., Júnior, M. A., Bozi, L. H., Drummond, L. R., Natali, A. J., et al. (2015). Resistance training regulates cardiac function through modulation of miRNA-214. *Int. J. Mol. Sci.* 16 (4), 6855–6867. doi: 10.3390/ijms16046855

Monleon, D., Garcia-Valles, R., Morales, J. M., Brioche, T., Olaso-Gonzalez, G., Lopez-Grueso, R., et al. (2014). Metabolomic analysis of long-term spontaneous exercise in mice suggests increased lipolysis and altered glucose metabolism when animals are at rest. *J. Appl. Physiol. (1985)* 117 (10), 1110–1119. doi: 10.1152/japplphysiol.00585.2014

Montgomery, R. L., Potthoff, M. J., Haberland, M., Qi, X., Matsuzaki, S., Humphries, K. M., et al. (2008). Maintenance of cardiac energy metabolism by histone deacetylase 3 in mice. *J. Clin. Invest.* 118 (11), 3588–3597. doi: 10.1172/jci35847

Nagendran, J., Waller, T. J., and Dyck, J. R. (2013). AMPK signalling and the control of substrate use in the heart. *Mol. Cell Endocrinol.* 366 (2), 180–193. doi: 10.1016/j.mce.2012.06.015

Nakamura, M., and Sadoshima, J. (2018). Mechanisms of physiological and pathological cardiac hypertrophy. *Nat. Rev. Cardiol.* 15 (7), 387–407. doi: 10.1038/s41569-018-0007-y

Naskar, S., Datta, K., Mitra, A., Pathak, K., Datta, R., Bansal, T., et al. (2014). Differential and conditional activation of PKC-isoforms dictates cardiac adaptation during physiological to pathological hypertrophy. *PloS One* 9 (8), e104711. doi: 10.1371/journal.pone.0104711

Nowak, G., and Bakajsova, D. (2013). Assessment of mitochondrial functions and cell viability in renal cells overexpressing protein kinase C isozymes. *J. Vis. Exp.* (71), 4301. doi: 10.3791/4301

Oka, T., Akazawa, H., Naito, A. T., and Komuro, I. (2014). Angiogenesis and cardiac hypertrophy: maintenance of cardiac function and causative roles in heart failure. *Circ. Res.* 114 (3), 565–571. doi: 10.1161/circresaha.114.300507

Olver, T. D., Ferguson, B. S., and Laughlin, M. H. (2015). Molecular Mechanisms for Exercise Training-Induced Changes in Vascular Structure and Function: Skeletal Muscle, Cardiac Muscle, and the Brain. *Prog. Mol. Biol. Transl. Sci.* 135, 227–257. doi: 10.1016/bs.pmbts.2015.07.017

O'Neill, B. T., Kim, J., Wende, A. R., Theobald, H. A., Tuinei, J., Buchanan, J., et al. (2007). A conserved role for phosphatidylinositol 3-kinase but not Akt signaling in mitochondrial adaptations that accompany physiological cardiac hypertrophy. *Cell Metab.* 6 (4), 294–306. doi: 10.1016/j.cmet.2007.09.001

Ostman, C., Jewiss, D., and Smart, N. A. (2017). The Effect of Exercise Training Intensity on Quality of Life in Heart Failure Patients: A Systematic Review and Meta-Analysis. *Cardiology* 136 (2), 79–89. doi: 10.1159/000448088

Pels, A. E. 3, White, T. P., and Block, W. D. (1985). Effects of exercise training on plasma lipids and lipoproteins in rats. *J. Appl. Physiol. (1985)* 58 (2), 612–618. doi: 10.1152/jappl.1985.58.2.612

Peterzan, M. A., Lygate, C. A., Neubauer, S., and Rider, O. J. (2017). Metabolic remodeling in hypertrophied and failing myocardium: a review. *Am. J. Physiol. Heart Circ. Physiol.* 313 (3), H597–h616. doi: 10.1152/ajpheart.00731.2016

Puigserver, P., Wu, Z., Park, C. W., Graves, R., Wright, M., and Spiegelman, B. M. (1998). A cold-inducible coactivator of nuclear receptors linked to adaptive thermogenesis. *Cell* 92 (6), 829–839. doi: 10.1016/s0092-8674(00)81410-5

Qi, J., Luo, X., Ma, Z., Zhang, B., Li, S., and Zhang, J. (2020). Downregulation of miR-26b-5p, miR-204-5p, and miR-497-3p Expression Facilitates Exercise-Induced Physiological Cardiac Hypertrophy by Augmenting Autophagy in Rats. *Front. Genet.* 11, 78. doi: 10.3389/fgene.2020.00078

Ramasamy, S., Velmurugan, G., Shanmugha Rajan, K., Ramprasath, T., and Kalpana, K. (2015). MiRNAs with apoptosis regulating potential are differentially expressed in chronic exercise-induced physiologically hypertrophied hearts. *PloS One* 10 (3), e0121401. doi: 10.1371/journal.pone.0121401

Rattigan, S., Appleby, G. J., and Clark, M. G. (1991). Insulin-like action of catecholamines and Ca2+ to stimulate glucose transport and GLUT4 translocation in perfused rat heart. *Biochim. Biophys. Acta* 1094 (2), 217–223. doi: 10.1016/0167-4889(91)90012-m

Riehle, C., Wende, A. R., Zhu, Y., Oliveira, K. J., Pereira, R. O., Jaishy, B. P., et al. (2014). Insulin receptor substrates are essential for the bioenergetic and hypertrophic response of the heart to exercise training. *Mol. Cell Biol.* 34 (18), 3450–3460. doi: 10.1128/mcb.00426-14

Rimbaud, S., Garnier, A., and Ventura-Clapier, R. (2009a). Mitochondrial biogenesis in cardiac pathophysiology. *Pharmacol. Rep.* 61 (1), 131–138. doi: 10.1016/s1734-1140(09)70015-5

Rimbaud, S., Sanchez, H., Garnier, A., Fortin, D., Bigard, X., Veksler, V., et al. (2009b). Stimulus specific changes of energy metabolism in hypertrophied heart. *J. Mol. Cell Cardiol.* 46 (6), 952–959. doi: 10.1016/j.yjmcc.2009.01.013

Ritterhoff, J., and Tian, R. (2017). Metabolism in cardiomyopathy: every substrate matters. *Cardiovasc. Res.* 113 (4), 411–421. doi: 10.1093/cvr/cvx017

Rowe, G. C., Jiang, A., and Arany, Z. (2010). PGC-1 coactivators in cardiac development and disease. *Circ. Res.* 107 (7), 825–838. doi: 10.1161/circresaha.110.223818

Sadoshima, J. (2006). Redox regulation of growth and death in cardiac myocytes. *Antioxid. Redox Signal* 8 (9–10), 1621–1624. doi: 10.1089/ars.2006.8.1621

Samovski, D., Sun, J., Pietka, T., Gross, R. W., Eckel, R. H., Su, X., et al. (2015). Regulation of AMPK activation by CD36 links fatty acid uptake to β-oxidation. *Diabetes* 64 (2), 353–359. doi: 10.2337/db14-0582

Sano, M., Minamino, T., Toko, H., Miyauchi, H., Orimo, M., Qin, Y., et al. (2007). p53-induced inhibition of Hif-1 causes cardiac dysfunction during pressure overload. *Nature* 446 (7134), 444–448. doi: 10.1038/nature05602

Scarpulla, R. C., Vega, R. B., and Kelly, D. P. (2012). Transcriptional integration of mitochondrial biogenesis. *Trends Endocrinol. Metab.* 23 (9), 459–466. doi: 10.1016/j.tem.2012.06.006

Schieber, M., and Chandel, N. S. (2014). ROS function in redox signaling and oxidative stress. *Curr. Biol.* 24 (10), R453–R462. doi: 10.1016/j.cub.2014.03.034

Schüttler, D., Clauss, S., Weckbach, L. T., and Brunner, S. (2019). Molecular Mechanisms of Cardiac Remodeling and Regeneration in Physical Exercise. *Cells* 8 (10), 1128. doi: 10.3390/cells8101128

Shimizu, I., and Minamino, T. (2016). Physiological and pathological cardiac hypertrophy. *J. Mol. Cell Cardiol.* 97, 245–262. doi: 10.1016/j.yjmcc.2016.06.001

Shioi, T., Kang, P. M., Douglas, P. S., Hampe, J., Yballe, C. M., Lawitts, J., et al. (2000). The conserved phosphoinositide 3-kinase pathway determines heart size in mice. *EMBO J.* 19 (11), 2537–2548. doi: 10.1093/emboj/19.11.2537

Smith, R. L., Soeters, M. R., Wüst, R. C. I., and Houtkooper, R. H. (2018). Metabolic Flexibility as an Adaptation to Energy Resources and Requirements in Health and Disease. *Endocr. Rev.* 39 (4), 489–517. doi: 10.1210/er.2017-00211

Soci, U. P., Fernandes, T., Hashimoto, N. Y., Mota, G. F., Amadeu, M. A., Rosa, K. T., et al. (2011). MicroRNAs 29 are involved in the improvement of ventricular compliance promoted by aerobic exercise training in rats. *Physiol. Genomics* 43 (11), 665–673. doi: 10.1152/physiolgenomics.00145.2010

Soci, U. P. R., Fernandes, T., Barauna, V. G., Hashimoto, N. Y., de Fátima Alves Mota, G., Rosa, K. T., et al. (2016). Epigenetic control of exercise training-induced cardiac hypertrophy by miR-208. *Clin. Sci. (Lond)* 130 (22), 2005–2015. doi: 10.1042/cs20160480

Song, H. K., Hong, S. E., Kim, T., and Kim, D. H. (2012). Deep RNA sequencing reveals novel cardiac transcriptomic signatures for physiological and pathological hypertrophy. *PloS One* 7 (4), e35552. doi: 10.1371/journal.pone.0035552

Stanley, W. C., and Chandler, M. P. (2002). Energy metabolism in the normal and failing heart: potential for therapeutic interventions. *Heart Fail Rev.* 7 (2), 115–130. doi: 10.1023/a:1015320423577

St-Pierre, J., Drori, S., Uldry, M., Silvaggi, J. M., Rhee, J., Jäger, S., et al. (2006). Suppression of reactive oxygen species and neurodegeneration by the PGC-1 transcriptional coactivators. *Cell* 127 (2), 397–408. doi: 10.1016/j.cell.2006.09.024

Strøm, C. C., Aplin, M., Ploug, T., Christoffersen, T. E., Langfort, J., Viese, M., et al. (2005). Expression profiling reveals differences in metabolic gene expression between exercise-induced cardiac effects and maladaptive cardiac hypertrophy. *FEBS J.* 272 (11), 2684–2695. doi: 10.1111/j.1742-4658.2005.04684.x

Stuewe, S. R., Gwirtz, P. A., Agarwal, N., and Mallet, R. T. (2000). Exercise training enhances glycolytic and oxidative enzymes in canine ventricular myocardium. *J. Mol. Cell Cardiol.* 32 (6), 903–913. doi: 10.1006/jmcc.2000.1131

Taegtmeyer, H., Golfman, L., Sharma, S., Razeghi, P., and van Arsdall, M. (2004). Linking gene expression to function: metabolic flexibility in the normal and diseased heart. *Ann. N. Y. Acad. Sci.* 1015, 202–213. doi: 10.1196/annals.1302.017

Takala, T. E., Ruskoaho, H. J., and Hassinen, I. E. (1983). Transmural distribution of cardiac glucose uptake in rat during physical exercise. *Am. J. Physiol.* 244 (1), H131–H137. doi: 10.1152/ajpheart.1983.244.1.H131

Tanaka, T., Sohmiya, K., and Kawamura, K. (1997). Is CD36 deficiency an etiology of hereditary hypertrophic cardiomyopathy? *J. Mol. Cell Cardiol.* 29 (1), 121–127. doi: 10.1006/jmcc.1996.0257

Tao, L., Bei, Y., Zhang, H., Xiao, J., and Li, X. (2015). Exercise for the heart: signaling pathways. *Oncotarget* 6 (25), 20773–20784. doi: 10.18632/oncotarget.4770

Turpeinen, A. K., Kuikka, J. T., Vanninen, E., Vainio, P., Vanninen, R., Litmanen, H., et al. (1996). Athletic heart: a metabolic, anatomical, and functional study. *Med. Sci. Sports Exerc.* 28 (1), 33–40. doi: 10.1097/00005768-199601000-00011

Vainshtein, A., Tryon, L. D., Pauly, M., and Hood, D. A. (2015). Role of PGC-1α during acute exercise-induced autophagy and mitophagy in skeletal muscle. *Am. J. Physiol. Cell Physiol.* 308 (9), C710–C719. doi: 10.1152/ajpcell.00380.2014

Vega, R. B., Horton, J. L., and Kelly, D. P. (2015). Maintaining ancient organelles: mitochondrial biogenesis and maturation. *Circ. Res.* 116 (11), 1820–1834. doi: 10.1161/circresaha.116.305420

Vettor, R., Valerio, A., Ragni, M., Trevellin, E., Granzotto, M., Olivieri, M., et al. (2014). Exercise training boosts eNOS-dependent mitochondrial biogenesis in mouse heart: role in adaptation of glucose metabolism. *Am. J. Physiol. Endocrinol. Metab.* 306 (5), E519–E528. doi: 10.1152/ajpendo.00617.2013

Vianna, C. R., Huntgeburth, M., Coppari, R., Choi, C. S., Lin, J., Krauss, S., et al. (2006). Hypomorphic mutation of PGC-1beta causes mitochondrial dysfunction and liver insulin resistance. *Cell Metab.* 4 (6), 453–464. doi: 10.1016/j.cmet.2006.11.003

Wang, L., Lv, Y., Li, G., and Xiao, J. (2018). MicroRNAs in heart and circulation during physical exercise. *J. Sport Health Sci.* 7 (4), 433–441. doi: 10.1016/j.jshs.2018.09.008

Wang, L., Wang, J., Li, G., and Xiao, J. (2020). Non-coding RNAs in Physiological Cardiac Hypertrophy. *Adv. Exp. Med. Biol.* 1229, 149–161. doi: 10.1007/978-981-15-1671-9_8

Watson, P. A., Reusch, J. E., McCune, S. A., Leinwand, L. A., Luckey, S. W., Konhilas, J. P., et al. (2007). Restoration of CREB function is linked to completion and stabilization of adaptive cardiac hypertrophy in response to exercise. *Am. J. Physiol. Heart Circ. Physiol.* 293 (1), H246–H259. doi: 10.1152/ajpheart.00734.2006

White, F. C., McKirnan, M. D., Breisch, E. A., Guth, B. D., Liu, Y. M., and Bloor, C. M. (1987). Adaptation of the left ventricle to exercise-induced hypertrophy. *J. Appl. Physiol. (1985)* 62 (3), 1097–1110. doi: 10.1152/jappl.1987.62.3.1097

Winder, W. W., and Hardie, D. G. (1996). Inactivation of acetyl-CoA carboxylase and activation of AMP-activated protein kinase in muscle during exercise. *Am. J. Physiol.* 270 (2 Pt 1), E299–E304. doi: 10.1152/ajpendo.1996.270.2.E299

Winder, W. W., Wilson, H. A., Hardie, D. G., Rasmussen, B. B., Hutber, C. A., Call, G. B., et al. (1997). Phosphorylation of rat muscle acetyl-CoA carboxylase by AMP-activated protein kinase and protein kinase A. *J. Appl. Physiol. (1985)* 82 (1), 219–225. doi: 10.1152/jappl.1997.82.1.219

Xiao, J., Xu, T., Li, J., Lv, D., Chen, P., Zhou, Q., et al. (2014). Exercise-induced physiological hypertrophy initiates activation of cardiac progenitor cells. *Int. J. Clin. Exp. Pathol.* 7 (2), 663–669.

Xiao, J., Chen, P., Qu, Y., Yu, P., Yao, J., Wang, H., et al. (2016). Telocytes in exercise-induced cardiac growth. *J. Cell Mol. Med.* 20 (5), 973–979. doi: 10.1111/jcmm.12815

Xu, J., Liu, Y., Xie, Y., Zhao, C., and Wang, H. (2017). Bioinformatics Analysis Reveals MicroRNAs Regulating Biological Pathways in Exercise-Induced Cardiac Physiological Hypertrophy. *BioMed. Res. Int.* 2017:2850659. doi: 10.1155/2017/2850659

Yang, K. C., Foeger, N. C., Marionneau, C., Jay, P. Y., McMullen, J. R., and Nerbonne, J. M. (2010). Homeostatic regulation of electrical excitability in physiological cardiac hypertrophy. *J. Physiol.* 588 (Pt 24), 5015–5032. doi: 10.1113/jphysiol.2010.197418

York, J. W., Penney, D. G., and Oscai, L. B. (1975). Effects of physical training on several glycolytic enzymes in rat heart. *Biochim. Biophys. Acta* 381 (1), 22–27. doi: 10.1016/0304-4165(75)90185-3

Youtz, D. J., Isfort, M. C., Eichenseer, C. M., Nelin, T. D., and Wold, L. E. (2014). In vitro effects of exercise on the heart. *Life Sci.* 116 (2), 67–73. doi: 10.1016/j.lfs.2014.08.015

Zaglia, T., Ceriotti, P., Campo, A., Borile, G., Armani, A., Carullo, P., et al. (2017). Content of mitochondrial calcium uniporter (MCU) in cardiomyocytes is regulated by microRNA-1 in physiologic and pathologic hypertrophy. *Proc. Natl. Acad. Sci. U.S.A.* 114 (43), E9006–e9015. doi: 10.1073/pnas.1708772114

Zhang, Q. J., Li, Q. X., Zhang, H. F., Zhang, K. R., Guo, W. Y., Wang, H. C., et al. (2007). Swim training sensitizes myocardial response to insulin: role of Akt-dependent eNOS activation. *Cardiovasc. Res.* 75 (2), 369–380. doi: 10.1016/j.cardiores.2007.04.015

Zhou, L. Y., Liu, J. P., Wang, K., Gao, J., Ding, S. L., Jiao, J. Q., et al. (2013). Mitochondrial function in cardiac hypertrophy. *Int. J. Cardiol.* 167 (4), 1118–1125. doi: 10.1016/j.ijcard.2012.09.082

Zuurbier, C. J., Bertrand, L., Beauloye, C. R., Andreadou, I., Ruiz-Meana, M., Jespersen, N. R., et al. (2020). Cardiac metabolism as a driver and therapeutic target of myocardial infarction. *J. Cell Mol. Med.* 24 (11), 5937–5954. doi: 10.1111/jcmm.15180

Conflict of Interest: The authors declare that the research was conducted in the absence of any commercial or financial relationships that could be construed as a potential conflict of interest.

frontiers in Pharmacology

MINI REVIEW
published: 21 August 2020
doi: 10.3389/fphar.2020.01314

New Insights and Current Approaches in Cardiac Hypertrophy Cell Culture, Tissue Engineering Models, and Novel Pathways Involving Non-Coding RNA

*Nina Kastner†, Katrin Zlabinger†, Andreas Spannbauer, Denise Traxler, Julia Mester-Tonczar, Ena Hašimbegović and Mariann Gyöngyösi**

Department of Cardiology, Medical University of Vienna, Vienna, Austria

OPEN ACCESS

Edited by:
Hai-Gang Zhang, Army Medical University, China

Reviewed by:
Yong Zhang, Harbin Medical University, China
Ning Zhang, Affiliated Hospital of Qingdao University, China

***Correspondence:**
Mariann Gyöngyösi
mariann.gyongyosi@meduniwien.ac.at

†These authors have contributed equally to this work

Specialty section:
This article was submitted to Cardiovascular and Smooth Muscle Pharmacology, a section of the journal Frontiers in Pharmacology

Received: *04 June 2020*
Accepted: *07 August 2020*
Published: *21 August 2020*

Citation:
Kastner N, Zlabinger K, Spannbauer A, Traxler D, Mester-Tonczar J, Hašimbegović E and Gyöngyösi M (2020) New Insights and Current Approaches in Cardiac Hypertrophy Cell Culture, Tissue Engineering Models, and Novel Pathways Involving Non-Coding RNA. Front. Pharmacol. 11:1314. doi: 10.3389/fphar.2020.01314

Cardiac hypertrophy is an ongoing clinical challenge, as risk factors such as obesity, smoking and increasing age become more widespread, which lead to an increasing prevalence of developing hypertrophy. Pathological hypertrophy is a maladaptive response to stress conditions, such as pressure overload, and involve a number of changes in cellular mechanisms, gene expression and pathway regulations. Although several important pathways involved in the remodeling and hypertrophy process have been identified, further research is needed to achieve a better understanding and explore new and better treatment options. More recently discovered pathways showed the involvement of several non-coding RNAs, including micro RNAs (miRNAs), long non-coding RNAs (lncRNAs), and circular RNAs (circRNAs), which either promote or inhibit the remodeling process and pose a possible target for novel therapy approaches. *In vitro* modeling serves as a vital tool for this further pathway analysis and treatment testing and has vastly improved over the recent years, providing a less costly and labor-intensive alternative to *in vivo* animal models.

Keywords: cardiac hypertrophy, disease modeling, hypertrophy induction, non-coding RNA, tissue engineering

INTRODUCTION

Left ventricular hypertrophy is a consequence of hypertension in up to 30% of patients (Cramariuc and Gerdts, 2016). Due to widespread risk factors such as obesity and smoking, the prevalence of hypertension and subsequent myocardial hypertrophy is rising, which poses a significant public health burden in an aging population (Benjamin et al., 2018). This development combined with the relative paucity of direct treatment options for cardiac hypertrophy makes continued research and the identification of novel therapeutic target molecules absolutely vital. Cardiac hypertrophy is an adaptive process which develops in response to physiological but also pathological processes, leading to heart muscle and cell hypertrophic growth with increased rigidity of the heart structures, and impaired diastolic function leading to heart failure with preserved ejection fraction (HFpEF) (Loonat et al., 2019; Zhao et al., 2020). Hypertrophic growth involves cardiomyocyte enlargement

rather than division, as adult cardiomyocytes have lost the ability to divide (Porrello et al., 2013). Pathological hypertrophy leads to the loss of functional cardiomyocytes (Nakamura and Sadoshima, 2018) and can subsequently progress to heart failure with reduced ejection fraction (HFrEF) (Tham et al., 2015). The main focus in hypertrophy research lies in the investigation of signaling pathways, gene expression analysis, and production of certain proteins and transcription factors, which influence or are responsible for the remodeling process. Many pathways have been identified to be involved in the development of cardiac hypertrophy including calcineurin/nuclear factor of activated T cells (NFAT), mitogen-activated protein kinase ERK, small guanosine triphosphate (GTP)-binding proteins (Ras, Rho), PKC, transcriptional regulation, cell surface level control, miRNA, and many more (Stansfield et al., 2014). Hypertrophic signaling pathways are initiated through mechanical stimulation such as pressure overload and neurohumoral mechanisms including the release of signaling factors such as growth factors, hormones, cytokines, and chemokines (Heineke and Molkentin, 2006).

Non-coding RNAs are RNAs that do not code for a protein and are not translated, however they have been shown to interfere with and regulate numerous physiological and pathophysiological pathways. There are different classes of non-coding RNAs, include microRNAs (miRNAs), long non-coding RNAs (lncRNAs) and circular RNAs (circRNAs), depending on their structure, length and function (Jaé and Dimmeler, 2020). MiRNAs are small RNAs with a length of approximately 22 nucleotides, which can inhibit mRNA translation and signal mRNA degradation (O'Brien et al., 2018). LncRNAs comprise of over 200 nucleotides and they can induce structural changes in DNA and chromatin, therefore regulating gene expression, and bind miRNAs thereby inhibiting their function (Dhanoa et al., 2018). Similarly, circRNAs also act as a sponge for miRNAs, however their structural properties are different to other non-coding RNAs, as they are circularized and are more robust resistant to RNAses (Yu and Kuo, 2019).

The purpose of this mini-review is to summarize the developments in myocardial hypertrophy models, new pathways, tissue engineering and non-coding RNAs relevant in myocardial hypertrophy induction and progression.

CARDIAC HYPERTROPHY CELL CULTURE AND TISSUE ENGINEERING MODELS

Cell culture models are essential for the investigation of pathological and physiological pathways in cardiac diseases. In contrast, *in vivo* animal models more closely simulate human physiological and pathological conditions. In cardiac research the most popular animal models are rodents such as rats and mice (Zuppinger, 2019). However, they differ from human physiology in some key aspects, such as faster heart rates and stem cell phenotypes (Ginis et al., 2004; Jochmans-Lemoine et al., 2015). Several large animal models using pigs, sheep, or dogs have been established to more accurately simulate human pathophysiology and cardiac hypertrophy with HFpEF and HFrEF, but very high cost and labor intensity limit their use for specialized research questions (Spannbauer et al., 2019). Sophisticated *in vitro* models are therefore an important tool to elucidate new remodeling and hypertrophy pathways and identify molecules of interest before proceeding to costly translational models.

The most widely used technique is a 2D monolayer cell culture, which allowed the discovery of several important hypertrophy pathways and cellular mechanisms, but lacks the complexity of interactivity between cells and cell types with electrical and paracrine factors (Zuppinger, 2016). To achieve a more realistic *in vitro* model of cardiac hypertrophy where native *in vivo* niche conditions can be imitated, cell culture techniques have vastly improved in recent years, giving rise to 3D cultures and organoids (Dutta et al., 2017). Cardiac organoids have been developed and have steadily improved, however the optimal ratio of cardiomyocytes, fibroblasts and endothelial cells is the subject of ongoing debate (Nugraha et al., 2019). The most prominent techniques for producing cardiac organoids include the use of hydrogels such as collagen, cell sheet technology where cells are cultured and subsequently stacked in different layers and hanging drop culture (Dutta et al., 2017; Nugraha et al., 2019). Despite their many advantages, it is important to note that cardiac organoids in their current state are still far from the complexity of the organs they are meant to represent and are also unable to capture organism-wide processes like immune response or neurohumoral feedback mechanisms (Iakobachvili and Peters, 2017), which also limit their use in modeling of *in vivo* myocardial hypertrophy.

METHODS OF CARDIAC HYPERTROPHY INDUCTION

In vitro cardiac hypertrophy can be induced by various methods such as chemical stimulation or mechanical stress induction. Mechanical stress induction is achieved by pressure overload *in vivo* and simulated by stretching of cardiomyocytes *in vitro*. On a cellular level, an activation of different oncogenes such as c-fos, c-myc, c-jun, and Egr-1, also called immediate-early genes, and activation of heat shock protein-70 are triggered and lead to subsequent upregulation of hypertrophy inducing genes ANP, BNP, and β-MHC (Rysä et al., 2018).

Pharmacological agents that are used for hypertrophy induction are for example phenylephrine (Jain et al., 2018), angiotensin II (Gelinas et al., 2018), noradrenaline (Guven, 2018), endothelin-1 (Zlabinger et al., 2019), and isoproterenol (Zhang et al., 2016). These agents interfere with a known pathway that is crucial in remodeling and subsequent cardiac hypertrophy. Angiotensin II was described to play a role in cardiac hypertrophy induction over 40 years ago, as it is part of the Renin-Angiotensin-Aldosterone-System. Endothelin-1 was discovered to have a higher protein and mRNA expression in dilated cardiomyopathy and influence matrix metalloproteinase 9 (Mmp9) expression levels (Hathaway et al., 2015). Further, a significant difference in mortality and pathogenesis has been reported in patients with a gene variation of the endothelin type

A receptor gene (polymorphisms G231A and C1363T) (Herrmann et al., 2001; Telgmann et al., 2007). Noradrenaline is a stress induced neurotransmitter, which has been shown to be involved in cardiac hypertrophy and damage due to toxic effects on cardiomyocytes (Jain et al., 2015). Isoproterenol is a β-agonist and activates the Renin-Angiotensin-Aldosterone-System, thus inducing hypertrophic pathways (Leenen et al., 2001). All these pharmacologic agents induce hypertrophy by binding to specific G-coupled receptors on the cell membrane, which then induce diacylglycerol (DAG) and subsequently protein kinase C (PKC). PKC plays an important role in internal Ca^{2+} mobilization, which allows hypertrophic induction through NFAT or calmodulin-dependent kinase (CaMK) pathway interference (Heineke and Molkentin, 2006).

Induction of hypertrophy by all of these chemical agents show a similar modeling time of 24 h, which may be extended to 48 h depending on the used cell type (Zhang et al., 2016; Zlabinger et al., 2019; Zhao et al., 2020). The concentration needs to be optimized by testing different dilutions before the experiment, however the general used concentrations are 20 μM phenylephrine (Gelinas et al., 2018), 100 nM angiotensin II (Zlabinger et al., 2019), 10 μM isoproterenol (Zhang et al., 2016), and 10 nM endothelin-1 (Loonat et al., 2019).

CELLS SOURCES AND MODELS FOR *IN VITRO* CARDIAC HYPERTROPHY MODELING

Establishing a cardiac hypertrophy model needs to incorporate several decisions about induction models, cell sources, pathways of interest and cell culture types. **Table 1** gives a broad overview about established approaches, while also mentioning the investigated pathway of the respective study. It is evident that a preferred choice of cell source are rat cardiomyocytes, which are mostly cultured in a 2D cell culture and the induction of hypertrophy is often performed chemically with pharmacological agents such as angiotensin II or isoproterenol. These approaches are based on availability of the cell source, as rat or also murine tissue for cell extraction is more easily accessible and animal care is cheaper to maintain than with larger animals. Further, chemical induction is a relatively easy method for hypertrophy induction compared to mechanical stress induction, which presumably is why it is often preferred.

When considering which hypertrophy model to choose for a study, various factors need to be considered beforehand. The most prominent factor in research is often time and cost effectiveness, which acts in favor of 2D chemically stimulated cultures, however this is not the best option in quality of results in some cases. The analysis of certain genes, proteins and non-coding RNAs might be insufficient in chemical stimulated cell hypertrophy models, as these do not trigger all the pathways that would be activated *in vivo*, which can lead to a false read-out and interpretations (Carreño et al., 2006). 3D models, such as organoids, can be stimulated mechanically and show a better comparability to *in vivo* conditions. These also allow to investigate the crosstalk between different cell types, especially the three main types within the heart cardiomyocytes, fibroblast, and endothelial cells, which are often not considered in regular 2D models. Fibroblasts especially play an important role in fibrosis and remodeling during hypertrophy processes and are therefore important to investigate (Travers et al., 2016). Organoids appear as the most ideal option in regard to

TABLE 1 | Overview over different approaches of hypertrophy induction methods and used cell sources in *in vitro* models and the investigated pathway of the study.

Cell source	Hypertrophy Model	Involved pathways	Reference
Neonatal rat ventricular myocytes (NRVM)	2D Cell culture, Chemical hypertrophy, Ang II, PE	AMPK pathway, O-GlcNAc signalling	(Gelinas et al., 2018)
Adult rat ventricular myocytes (ARVM)	2D Cell culture, Chemical hypertrophy, PE	AMPK pathway, O-GlcNAc signalling	(Gelinas et al., 2018)
Neonatal rat cardiomyocytes	2D Cell culture, Chemical hypertrophy, PE	Protein kinase D (PKD) knockdown, AKT/mTOR signaling pathway, autophagy	(Zhao et al., 2020)
Murine neonatal cardiomyocytes	Micro ridges vs 2D cell culture, Chemical hypertrophy, PE	Cardiomyocyte morphology on 3D surfaces – F-Actin, Myomesin, Actinin	(Jain et al., 2018)
H9c2 cardiomyocytes	2D Cell culture, Chemical hypertrophy, Iso	ANP, BNP, ROS, 3-nitrotyrosine and p67 (phox), MMP, (p)ERK1/2, (p)p38, (p)JNK	(Zhang et al., 2016)
Primary neonatal rat ventricular myocytes	2D Cell culture, Chemical hypertrophy, PE, ET1, Iso, Ang II	Myocyte area, protein-bound SRB fluorescence	(Loonat et al., 2019)
hiPSC from dermal fibroblasts edited with Crispr/Cas9	2D Cell culture/3D matrigel mattress, Mutational hypertrophy, heterozygous Ca-sensitizing TnT-I79N mutation	TnT-I79N protein levels, cytosolic Ca buffering and electrophysiology	(Wang et al., 2017)
Rat ventricular cardiomyocytes	2D Cell culture, Chemical hypertrophy, Ang II	GATA4 and miR-26a (also β-MHC and ANF)	(Liu et al., 2016)
Neonatal rat ventricular myocytes	2D Cell culture, Chemical hypertrophy, Ang II	β-catenin, NFATc3, WNT pathway	(Jiang et al., 2018)
H9c2 cardiomyocytes	2D Cell culture, Chemical hypertrophy, NA	Mitochondrial KATP channel, mitochondrial membrane potential, oxidant status, total antioxidant status, superoxide dismutase	(Guven, 2018)
Porcine cardiac progenitor cells	2D Cell culture, Chemical hypertrophy, Ang II, ET1	MiR-21, MiR-29a, GATA4, and MEF2c Expression	(Zlabinger et al., 2019)

Ang II, Angiotensin II; PE, Phenylephrine; Iso, Isoproterenol; ET1, Endothelin-1; NA, Noradrenaline.

simulating hypertrophy conditions *in vivo*, while still considering the principles of 3R (replacement, reduction, and refinement). Improving and also simplifying organoid technology should be the goal in translational research, so it can be used more widely for disease modeling such as cardiac hypertrophy instead of animal models.

NEW PATHWAYS IN CARDIAC HYPERTROPHY INVOLVING NON-CODING RNAS

Among some well-known and established pathways in cardiac hypertrophy new signaling cascades have been identified over the last few years, especially with the rise of non-coding RNAs. Non-coding RNAs include amongst others miRNAs, lncRNAs, and circRNA. Some have been shown to play a role in remodeling and hypertrophy induction, either in promoting or inhibiting the process (Wehbe et al., 2019). These non-coding RNAs have also been investigated as potential treatment targets in cardiac hypertrophy, which may lead to new therapeutic approach for patients in the future (Li et al., 2018).

miRNAs Influence Hypertrophy Pathways

MiRNAs are small non-coding RNAs with a length of approximately 22 nucleotides and interfere with mRNAs through complementary binding causing degradation or inhibition of transcription (Fabian and Sonenberg, 2012; Wehbe et al., 2019).

Pro-Hypertrophic miRNAs

Recently, Zhang et al. showed that miRNA-29 played a significant role, as overexpression seemed to inhibit angiotensin II induced LV hypertrophy in a mouse model. Collagen I and III secretion and TGFβ and pSMAD2/3 levels were downregulated indicating that hypertrophy was indeed hindered (Zhang et al., 2020). MiRNA-26a also seems to show anti-hypertrophic effects in rat models and in cell culture, as it targets the 3'-UTR of the GATA4 mRNA (Liu et al., 2016). Similar effects on remodeling can be seen with miRNA-101, as an overexpression in a rat hypertrophy model showed reduced gene expression and protein levels of known hypertrophy related genes like Rab1a, ANF, and b-MHC and reduced relative cell areas (Wei et al., 2015). MiRNA-133 downregulation has been found to aid hypertrophy development, however restoring the expression during hypertrophy induction only reduced fibrosis and apoptosis, but not hypertrophy signaling itself (Abdellatif, 2010).

Anti-Hypertrophic miRNAs

On the other hand, miRNAs can also induce or help induce hypertrophy, as shown with, e.g., miRNA-22. MiRNA-22 overexpression has been shown to be able to induce hypertrophy *in vitro* by modulating PTEN levels without adding any other stimulating agent and further showed to be crucial for phenylephrine and angiotensin II hypertrophy induction (Xu et al., 2012; Huang et al., 2013). MiRNA-217 similarly promotes cardiac hypertrophy interfering with PTEN levels. Additionally, catalysis of histone 3 lysine 9 dimethylation (H3K9me2) and mRNA downregulation of euchromatic histone–lysine N-methyltransferases (EHMT1/2) have been described to imitate fetal heart associated conditions further leading to hypertrophy development (Inagawa et al., 2013; Thienpont et al., 2017). MiR-155 is another player that has been identified to promote cardiac hypertrophy, by causing an inflammatory response with macrophage migration and signaling (Heymans et al., 2013). Additionally, miRNA-200c has been identified to interfere in MAPK/ERK pathway upregulation by targeting dual-specific phosphatase-1 (DUSP-1) (Singh et al., 2017).

LncRNAs and circRNAs: Importance in Remodeling Pathways

LncRNAs can regulate promotors, enhancers and insulators by conformation changes and forming secondary structures further influencing expression of other genes. Moreover, lncRNAs can modulate miRNAs by acting as a sponge and therefore influence genes post-transcriptionally. The lncRNA myosin heavy-chain-associated RNA transcripts (MHRT) has been described to influence hypertrophy induction, as it antagonizes chromatin-remodeling factor Brg1, which further activates β-MHC. MHRT is encoded in the same gene locus (beta-cardiac muscle myosin heavy chain gene) as miRNA-208, which promotes cardiac hypertrophy (Callis et al., 2009; Han et al., 2011; Han et al., 2014). Another prominent lncRNA, identified by Wang et al. (2014a), is cardiac hypertrophy related factor (CHRF). The authors showed that CHRF was upregulated in cardiac hypertrophy and heart failure. CHRF acts as a sponge for a miRNA-489, therefore de-represses the myeloid differentiation primary response gene 88 (Myd88) and subsequently induces remodeling (Wang et al., 2014a). Cardiac-apoptosis-related lncRNA (CARL) has also been shown be strongly expressed in hypertrophy remodeling by inhibiting miR-539 (Muthusamy et al., 2014; Wang et al., 2014b).

CircRNAs are circularized RNAs which are covalently closed. They are more stable than linear RNAs due to this structural feature and have recently gained an increasing research attention. However, they have not been as excessively studied as miRNAs and lncRNAs, leaving room for further studies on circRNAs in hypertrophy remodeling and in cardiovascular diseases in general (Hansen et al., 2013; Ottaviani and Martins, 2017; Li et al., 2018). CircRNAs can, similarly to lncRNAs, act as a sponge for miRNAs, thereby inhibiting them. CircRNA ciRS-7/CDR1as has been identified as a sponge for miR-7, which has been shown to be upregulated in patients with left ventricular hypertrophy (Hansen et al., 2013; Kaneto et al., 2017). The heart-related circRNA (HRCR) has also been found to inhibit miRNA-233 in the same way, therefore de-repressing the activity-regulated cytoskeleton-associated protein (K. Wang et al., 2016).

CircRNAs and LncRNAs provide a new approach for treatment due to their sponging properties and they may present a new biomarker for predicting the severity of the remodeling process and in heart failure. However, some

challenges for non-coding RNAs as therapeutic option must still be faced, including off-target effects and delivery (Dong et al., 2018).

CONCLUSIONS AND OUTLOOK

Cardiac hypertrophy will remain an ever-present clinical challenge due to several widespread risk factors in an increasingly aging patient population. Advanced and refined tissue engineering approaches give an opportunity to study pathological pathways extensively without requiring *in vivo* animal studies, which are more costly, time- and labor-intensive. These approaches allow the identification of possible biomarkers and the testing of therapies in a setting that mimics *in vivo* conditions more closely, although not perfectly as some factors like immune interactions are still lacking. The induction of cardiac hypertrophy *in vitro* is predominantly performed with pharmacological agents, such as angiotensin II, as mechanical stress induction poses a greater challenge.

Several well-known pathways which are involved in hypertrophic remodeling have been identified, including newer additions mostly revolving around non-coding RNAs like miRNAs, lncRNAs, and circRNAs. Non-coding RNAs that aid or negatively interfere with cardiac hypertrophy have been identified by inhibiting other factors (supporting or inhibitory) in the hypertrophy signaling cascades. There have been dozens of studies on a great number of different factors involved in this complex pathological process. Further, also epigenetic modifications have been discovered to be regulated and influenced to some degree by non-coding RNAs, which are involved in cardiac hypertrophy (Dong et al., 2018). However, it is important to further investigate and develop even more advanced tissue engineering options to allow a more profound understanding of remodeling pathways and subsequently the development of new pharmacological targets and treatment approaches.

AUTHOR CONTRIBUTIONS

NK and KZ wrote the main body of the manuscript. AS, JM-T, EH, and DT assisted with literature research and comments regarding language and style. AS and MG revised the manuscript and assisted with structural conceptualization.

REFERENCES

Abdellatif, M. (2010). The Role of MicroRNA-133 in Cardiac Hypertrophy Uncovered. *Circ. Res.* 106 (1), 16–18. doi: 10.1161/CIRCRESAHA.109.212183

Benjamin, E. J., Virani, S. S., Callaway, C. W., Chamberlain, A. M., Chang, A. R., Cheng, S., et al. (2018). Heart Disease and Stroke Statistics-2018 Update: A Report From the American Heart Association. *Circulation* 137 (12), e67–492. doi: 10.1161/CIR.0000000000000558

Callis, T. E., Pandya, K., Seok, H. Y., Tang, R.-H., Tatsuguchi, M., Huang, Z.-P., et al. (2009). MicroRNA-208a Is a Regulator of Cardiac Hypertrophy and Conduction in Mice. *J. Clin. Invest.* 119 (9), 2772–2786. doi: 10.1172/JCI36154

Carreño, J. E., Apablaza, F., Ocaranza, M. P., and Jalil, J. E. (2006). Cardiac hypertrophy: molecular and cellular events. *Rev. Espanola Cardiol.* 59 (5), 473–486. doi: 10.1016/S1885-5857(06)60796-2

Cramariuc, D., and Gerdts, E. (2016). Epidemiology of Left Ventricular Hypertrophy in Hypertension: Implications for the Clinic. *Expert Rev. Cardiovasc. Ther.* 14 (8), 915–926. doi: 10.1080/14779072.2016.1186542

Dhanoa, J. K., Sethi, R. S., Verma, R., Arora, J. S., and Mukhopadhyay, C. S. (2018). Long Non-Coding RNA: Its Evolutionary Relics and Biological Implications in Mammals: A Review. *J. Anim. Sci. Technol.* 60, 25. doi: 10.1186/s40781-018-0183-7

Dong, Y., Xu, S., Liu, J., Ponnusamy, M., Zhao, Y., Zhang, Y., et al. (2018). Non-Coding RNA-Linked Epigenetic Regulation in Cardiac Hypertrophy. *Int. J. Biol. Sci.* 14 (9), 1133–1141. doi: 10.7150/ijbs.26215

Dutta, D., Heo, I., and Clevers, H. (2017). Disease Modeling in Stem Cell-Derived 3D Organoid Systems. *Trends Mol. Med.* 23 (5), 393–410. doi: 10.1016/j.molmed.2017.02.007

Fabian, M. R., and Sonenberg, N. (2012). The Mechanics of MiRNA-Mediated Gene Silencing: A Look under the Hood of MiRISC. *Nat. Struct. Mol. Biol.* 19 (6), 586–593. doi: 10.1038/nsmb.2296

Gelinas, R., Mailleux, F., Dontaine, J., Bultot, L., Demeulder, B., Ginion, A., et al. (2018). AMPK Activation Counteracts Cardiac Hypertrophy by Reducing O-GlcNAcylation. *Nat. Commun.* 9 (1), 374. doi: 10.1038/s41467-017-02795-4

Ginis, I., Luo, Y., Miura, T., Thies, S., Brandenberger, R., Gerecht-Nir, S., et al. (2004). Differences between Human and Mouse Embryonic Stem Cells. *Dev. Biol.* 269 (2), 360–380. doi: 10.1016/j.ydbio.2003.12.034

Guven, C. (2018). The Effect of Diazoxide on Norepinephrine-Induced Cardiac Hypertrophy, in Vitro. *Cell. Mol. Biol. (Noisy-Le-Grand France)* 64 (10), 50–54. doi: 10.14715/cmb/2018.64.10.8

Han, P., Hang, C. T., Yang, J., and Chang, C.-P. (2011). Chromatin Remodeling in Cardiovascular Development and Physiology. *Circ. Res.* 108 (3), 378–396. doi: 10.1161/CIRCRESAHA.110.224287

Han, P., Li, W., Lin, C.-H., Yang, J., Shang, C., Nuernberg, S. T., et al. (2014). A Long Noncoding RNA Protects the Heart from Pathological Hypertrophy. *Nature* 514 (7520), 102–106. doi: 10.1038/nature13596

Hansen, T. B., Jensen, T.II, Clausen, B. H., Bramsen, J. B., Finsen, B., Damgaard, C. K., et al. (2013). Natural RNA Circles Function as Efficient MicroRNA Sponges. *Nature* 495 (7441), 384–388. doi: 10.1038/nature11993

Hathaway, C. K., Grant, R., Hagaman, J. R., Hiller, S., Li, F., Xu, L., et al. (2015). Endothelin-1 Critically Influences Cardiac Function via Superoxide-MMP9 Cascade. *Proc. Natl. Acad. Sci. U. S. A.* 112 (16), 5141–5146. doi: 10.1073/pnas.1504557112

Heineke, J., and Molkentin, J. D. (2006). Regulation of Cardiac Hypertrophy by Intracellular Signalling Pathways. *Nat. Rev. Mol. Cell Biol.* 7 (8), 589–600. doi: 10.1038/nrm1983

Herrmann, S., Schmidt-Petersen, K., Pfeifer, J., Perrot, A., Bit-Avragim, N., Eichhorn, C., et al. (2001). A Polymorphism in the Endothelin-A Receptor Gene Predicts Survival in Patients with Idiopathic Dilated Cardiomyopathy. *Eur. Heart J.* 22 (20), 1948–1953. doi: 10.1053/euhj.2001.2626

Heymans, S., Corsten, M. F., Verhesen, W., Carai, P., van Leeuwen, R. E. W., Custers, K., et al. (2013). Macrophage MicroRNA-155 Promotes Cardiac Hypertrophy and Failure. *Circulation* 128 (13), 1420–1432. doi: 10.1161/CIRCULATIONAHA.112.001357

Huang, Z.-P., Chen, J., Seok, H. Y., Zhang, Z., Kataoka, M., Hu, X., et al. (2013). MicroRNA-22 Regulates Cardiac Hypertrophy and Remodeling in Response to Stress. *Circ. Res.* 112 (9), 1234–1243. doi: 10.1161/CIRCRESAHA.112.300682

Iakobachvili, N., and Peters, P. J. (2017). Humans in a Dish: The Potential of Organoids in Modeling Immunity and Infectious Diseases. *Front. Microbiol.* 8, 2402. doi: 10.3389/fmicb.2017.02402

Inagawa, M., Nakajima, K., Makino, T., Ogawa, S., Kojima, M., Ito, S., et al. (2013). Histone H3 Lysine 9 Methyltransferases, G9a and GLP Are Essential for Cardiac Morphogenesis. *Mech. Dev.* 130 (11–12), 519–531. doi: 10.1016/j.mod.2013.07.002

Jaé, N., and Dimmeler, S. (2020). Noncoding RNAs in Vascular Diseases. *Circ. Res.* 126 (9), 1127–1145. doi: 10.1161/CIRCRESAHA.119.315938

Jain, A., Atale, N., Kohli, S., Bhattacharya, S., Sharma, M., and Rani, V. (2015). An Assessment of Norepinephrine Mediated Hypertrophy to Apoptosis Transition in Cardiac Cells: A Signal for Cell Death. *Chem. Biol. Interact.* 225, 54–62. doi: 10.1016/j.cbi.2014.11.017

Jain, A., Hasan, J., Desingu, P. A., Sundaresan, N. R., and Chatterjee, K. (2018). Engineering an in Vitro Organotypic Model for Studying Cardiac Hypertrophy. *Colloids Surf. B. Biointerf.* 165, 355–362. doi: 10.1016/j.colsurfb.2018.02.036

Jiang, J., Lan, C., Li, L., Yang, D., Xia, X., Liao, Q., et al. (2018). A Novel Porcupine Inhibitor Blocks WNT Pathways and Attenuates Cardiac Hypertrophy. *Biochim. Biophys. Acta Mol. Basis Dis.* 1864 (10), 3459–3467. doi: 10.1016/j.bbadis.2018.07.035

Jochmans-Lemoine, A., Villalpando, G., Gonzales, M., Valverde, I., Soria, R., and Joseph, V. (2015). Divergent Physiological Responses in Laboratory Rats and Mice Raised at High Altitude. *J. Exp. Biol.* 218 (Pt 7), 1035–1043. doi: 10.1242/jeb.112862

Kaneto, C. M., Nascimento, J. S., Moreira, M. C. R., Ludovico, N. D., Santana, A. P., Silva, R. A. A., et al. (2017). MicroRNA Profiling Identifies MiR-7-5p and MiR-26b-5p as Differentially Expressed in Hypertensive Patients with Left Ventricular Hypertrophy. *Braz. J. Med. Biol. Res.* 50 (12), e6211. doi: 10.1590/1414-431X20176211

Leenen, F. H., White, R., and Yuan, B. (2001). Isoproterenol-Induced Cardiac Hypertrophy: Role of Circulatory versus Cardiac Renin-Angiotensin System. *Am. J. Physiol. Heart Circulatory Physiol.* 281 (6), H2410–H2416. doi: 10.1152/ajpheart.2001.281.6.H2410

Li, Y., Liang, Y., Zhu, Y., Zhang, Y., and Bei, Y. (2018). Noncoding RNAs in Cardiac Hypertrophy. *J. Cardiovasc. Trans. Res.* 11 (6), 439–449. doi: 10.1007/s12265-018-9797-x

Liu, Y., Wang, Z., and Xiao, W. (2016). MicroRNA-26a Protects against Cardiac Hypertrophy via Inhibiting GATA4 in Rat Model and Cultured Cardiomyocytes. *Mol. Med. Rep.* 14 (3), 2860–2866. doi: 10.3892/mmr.2016.5574

Loonat, A. A., Curtis, M.K., Richards, M. A., Nunez-Alonso, G., Michl, J., and Swietach, P. (2019). A High-Throughput Ratiometric Method for Imaging Hypertrophic Growth in Cultured Primary Cardiac Myocytes. *J. Mol. Cell. Cardiol.* 130, 184–196. doi: 10.1016/j.yjmcc.2019.04.001

Muthusamy, S., DeMartino, A. M., Watson, L. J., Brittian, K. R., Zafir, A., Dassanayaka, S., et al. (2014). MicroRNA-539 Is up-Regulated in Failing Heart, and Suppresses O-GlcNAcase Expression. *J. Biol. Chem.* 289 (43), 29665–29676. doi: 10.1074/jbc.M114.578682

Nakamura, M., and Sadoshima, J. (2018). Mechanisms of Physiological and Pathological Cardiac Hypertrophy. *Nat. Rev. Cardiol.* 15 (7), 387–407. doi: 10.1038/s41569-018-0007-y

Nugraha, B., Buono, M. F., von Boehmer, L., Hoerstrup, S. P., and Emmert, M. Y. (2019). Human Cardiac Organoids for Disease Modeling. *Clin. Pharmacol. Ther.* 105 (1), 79–85. doi: 10.1002/cpt.1286

O'Brien, J., Hayder, H., Zayed, Y., and Peng, C. (2018). Overview of MicroRNA Biogenesis, Mechanisms of Actions, and Circulation. *Front. Endocrinol.* 9, 402. doi: 10.3389/fendo.2018.00402

Ottaviani, L., and Martins, P. A. C. (2017). Non-Coding RNAs in Cardiac Hypertrophy. *J. Physiol.* 595 (12), 4037–4050. doi: 10.1113/JP273129

Porrello, E. R., Mahmoud, A.II, Simpson, E., Johnson, B. A., Grinsfelder, D., Canseco, D., et al. (2013). Regulation of Neonatal and Adult Mammalian Heart Regeneration by the MiR-15 Family. *Proc. Natl. Acad. Sci. U. S. A.* 110 (1), 187–192. doi: 10.1073/pnas.1208863110

Rysä, J., Tokola, H., and Ruskoaho, H. (2018). Mechanical Stretch Induced Transcriptomic Profiles in Cardiac Myocytes. *Sci. Rep.* 8 (1), 4733. doi: 10.1038/s41598-018-23042-w

Singh, G. B., Raut, S. K., Khanna, S., Kumar, A., Sharma, S., Prasad, R., et al. (2017). MicroRNA-200c Modulates DUSP-1 Expression in Diabetes-Induced Cardiac Hypertrophy. *Mol. Cell. Biochem.* 424 (1–2), 1–11. doi: 10.1007/s11010-016-2838-3

Spannbauer, A., Traxler, D., Zlabinger, K., Gugerell, A., Winkler, J., Mester-Tonczar, J., et al. (2019). Large Animal Models of Heart Failure With Reduced Ejection Fraction (HFrEF). *Front. Cardiovasc. Med.* 6, 117. doi: 10.3389/fcvm.2019.00117

Stansfield, W. E., Ranek, M., Pendse, A., Schisler, J. C., Wang, S., and Pulinilkunnil, T. (2014). "Chapter 4—The Pathophysiology of Cardiac Hypertrophy and Heart Failure," in *Cellular and Molecular Pathobiology of Cardiovascular Disease*. Eds. M. S. Willis, J. W. Homeister and J. R. Stone (San Diego, CA, USA: Academic Press), 51–78. doi: 10.1016/B978-0-12-405206-2.00004-1

Telgmann, R., Harb, B. A., Ozcelik, C., Perrot, A., Schönfelder, J., Nonnenmacher, A., et al. (2007). The G-231A Polymorphism in the Endothelin-A Receptor Gene Is Associated with Lower Aortic Pressure in Patients with Dilated Cardiomyopathy. *Am. J. Hypertension* 20 (1), 32–37. doi: 10.1016/j.amjhyper.2006.06.016

Tham, Y. K., Bernardo, B. C., Ooi, J. Y.Y., Weeks, K. L., and McMullen, J. R. (2015). Pathophysiology of Cardiac Hypertrophy and Heart Failure: Signaling Pathways and Novel Therapeutic Targets. *Arch. Toxicol.* 89 (9), 1401–1438. doi: 10.1007/s00204-015-1477-x

Thienpont, B., Aronsen, J. M., Robinson, E. L., Okkenhaug, H., Loche, E., Ferrini, A., et al. (2017). The H3K9 Dimethyltransferases EHMT1/2 Protect against Pathological Cardiac Hypertrophy. *J. Clin. Invest.* 127 (1), 335–348. doi: 10.1172/JCI88353

Travers, J. G., Kamal, F. A., Robbins, J., Yutzey, K. E., and Blaxall, B. C. (2016). Cardiac Fibrosis: The Fibroblast Awakens. *Circ. Res.* 118 (6), 1021–1040. doi: 10.1161/CIRCRESAHA.115.306565

Wang, K., Liu, F., Zhou, L.-Y., Long, B., Yuan, S.-M., Wang, Y., et al. (2014a). The Long Noncoding RNA CHRF Regulates Cardiac Hypertrophy by Targeting MiR-489. *Circ. Res.* 114 (9), 1377–1388. doi: 10.1161/CIRCRESAHA.114.302476

Wang, K., Long, B., Zhou, L.-Y., Liu, F., Zhou, Q.-Y., Liu, C.-Y., et al. (2014b). CARL LncRNA Inhibits Anoxia-Induced Mitochondrial Fission and Apoptosis in Cardiomyocytes by Impairing MiR-539-Dependent PHB2 Downregulation. *Nat. Commun.* 5, 3596. doi: 10.1038/ncomms4596

Wang, K., Long, B., Liu, F., Wang, J.-X., Liu, C.-Y., Zhao, B., et al. (2016). A Circular RNA Protects the Heart from Pathological Hypertrophy and Heart Failure by Targeting MiR-223. *Eur. Heart J.* 37 (33), 2602–2611. doi: 10.1093/eurheartj/ehv713

Wang, L., Kryshtal, D. O., Kim, K., Parikh, S., Cadar, A. G., Bersell, K. R., et al (2017). Myofilament Calcium-Buffering Dependent Action Potential Triangulation in Human-Induced Pluripotent Stem Cell Model of Hypertrophic Cardiomyopathy. *J. Am. Coll. Cardiol. U. S.* 70 (20), 2600–2602. doi: 10.1016/j.jacc.2017.09.033

Wehbe, N., Nasser, S. A., Pintus, G., Badran, A., Eid, A. H., and Baydoun, E. (2019). MicroRNAs in Cardiac Hypertrophy. *Int. J. Mol. Sci.* 20 (19), 4714. doi: 10.3390/ijms20194714

Wei, L., Yuan, M., Zhou, R., Bai, Q., Zhang, W., Zhang, M., et al. (2015). MicroRNA-101 Inhibits Rat Cardiac Hypertrophy by Targeting Rab1a. *J. Cardiovasc. Pharmacol.* 65 (4), 357–363. doi: 10.1097/FJC.0000000000000203

Xu, X.-D., Song, X.-W., Li, Q., Wang, G.-K., Jing, Q., and Qin, Y.-W. (2012). Attenuation of MicroRNA-22 Derepressed PTEN to Effectively Protect Rat Cardiomyocytes from Hypertrophy. *J. Cell. Physiol.* 227 (4), 1391–1398. doi: 10.1002/jcp.22852

Yu, C.-Y., and Kuo, H.-C. (2019). The Emerging Roles and Functions of Circular RNAs and Their Generation. *J. Biomed. Sci.* 26 (1):29. doi: 10.1186/s12929-019-0523-z

Zhang, Y., Xu, J., Long, Z., Wang, C., Wang, L., Sun, P., et al. (2016). Hydrogen (H (2)) Inhibits Isoproterenol-Induced Cardiac Hypertrophy via Antioxidative Pathways. *Front. Pharmacol.* 7:392:392. doi: 10.3389/fphar.2016.00392

Zhang, S.-J., Yun, C.-J., Liu, J., Yao, S.-Y., Li, Y., Wang, M., et al. (2020). MicroRNA-29a Attenuates Angiotensin-II Induced-Left Ventricular Remodeling by Inhibiting Collagen, TGF-β and SMAD2/3 Expression. *J. Geriatric Cardiol.* 17 (2), 96–104. doi: 10.11909/j.issn.1671-5411.2020.02.008

Zhao, D., Gao, Y., Wei, W., Pei, H., Xu, C., and Zhao, Z. (2020). PKD Deletion Promotes Autophagy and Inhibits Hypertrophy in Cardiomyocyte. *Exp. Cell Res.* 386 (2):111742. doi: 10.1016/j.yexcr.2019.111742

Zlabinger, K., Spannbauer, A., Traxler, D., Gugerell, A., Lukovic, D., Winkler, J., et al. (2019). MiR-21, MiR-29a, GATA4, and MEF2c Expression Changes in Endothelin-1 and Angiotensin II Cardiac Hypertrophy Stimulated Isl-1(+)Sca-1(+)c-Kit(+) Porcine Cardiac Progenitor Cells In Vitro. *Cells* 8 (11), 1416. doi: 10.3390/cells8111416

Zuppinger, C. (2016). 3D Culture for Cardiac Cells. *Biochim. Biophys. Acta (BBA)* 1863 (7, Part B), 1873–1881. doi: 10.1016/j.bbamcr.2015.11.036

Zuppinger, C. (2019). 3D Cardiac Cell Culture: A Critical Review of Current Technologies and Applications. *Front Cardiovasc. Med.* 6, 87. doi: 10.3389/fcvm.2019.00087

Conflict of Interest: The authors declare that the research was conducted in the absence of any commercial or financial relationships that could be construed as a potential conflict of interest.

frontiers in Pharmacology

ORIGINAL RESEARCH
published: 03 September 2020
doi: 10.3389/fphar.2020.01235

Endogenous CCN5 Participates in Angiotensin II/TGF-β_1 Networking of Cardiac Fibrosis in High Angiotensin II-Induced Hypertensive Heart Failure

Anan Huang[1,2], *Huihui Li*[3], *Chao Zeng*[2], *Wanli Chen*[3], *Liping Wei*[2], *Yue Liu*[2] *and Xin Qi*[1,2*]

[1] Nankai University School of Medicine, Tianjin, China, [2] Department of Cardiology, Tianjin Union Medical Center, Tianjin, China, [3] Graduate School, Tianjin University of Traditional Chinese Medicine, Tianjin, China

Aberrant activation of angiotensin II (Ang II) accelerates hypertensive heart failure (HF); this has drawn worldwide attention. The complex Ang II/transforming growth factor (TGF)-β_1 networking consists of central mechanisms underlying pro-fibrotic effects; however, this networking still remains unclear. Cellular communication network 5 (CCN5), known as secreted matricellular protein, mediates anti-fibrotic activity by inhibiting fibroblast-to-myofibroblast transition and the TGF-β_1 signaling pathway. We hypothesized that endogenous CCN5 plays an essential role in TGF-β_1/Ang II networking-induced cardiac fibrosis (CF), which accelerates the development of hypertensive HF. This study aimed to investigate the potential role of CCN5 in TGF-β_1/Ang II networking-induced CF. Our clinical retrospective study demonstrated that serum CCN5 decreased in hypertensive patients, but significantly increased in hypertensive patients taking oral angiotensin-converting enzyme inhibitor (ACEI). A negative association was observed between CCN5 and Ang II in grade 2and 3 hypertensive patients receiving ACEI treatment. We further created an experimental model of high Ang II-induced hypertensive HF. CCN5 was downregulated in the spontaneously hypertensive rats (SHRs) and increased *via* the inhibition of Ang II production by ACEI. This CCN5 downregulation may activate the TGF-β_1 signaling pathway, which promotes direct deposition of the extracellular matrix (ECM) and fibroblast-to-myofibroblast transition *via* activated Smad-3. Double immunofluorescence staining of CCN5 and cell markers of cardiac tissue cell types suggested that CCN5 was mainly expressed in the cardiac fibroblasts. Isolated cardiac fibroblasts were exposed to Ang II and transfected with small interfering RNA targeting CCN5. The expression of TGF-β_1 together with Col Ia and Col IIIa was further promoted, and alpha-smooth muscle actin (α-SMA) was strongly expressed in the cardiac fibroblasts stimulated with Ang II and siRNA. In our study, we confirmed the anti-fibrotic ability of endogenous CCN5 in high Ang II-induced hypertensive HF. Elevated Ang II levels may decrease CCN5 expression, which subsequently activates TGF-β_1 and finally promotes the direct deposition of the ECM and fibroblast-to-myofibroblast transition *via* Smad-3 activation. CCN5 may serve as a potential biomarker for estimating CF in hypertensive

OPEN ACCESS

Edited by:
Ya Liu,
Army Medical University, China
Reviewed by:
Nazareno Paolocci,
Johns Hopkins University, United States
Li Li,
Peking University Health Science Centre, China

***Correspondence:**
Xin Qi
qixinx2011@yeah.net

Specialty section:
This article was submitted to Cardiovascular and Smooth Muscle Pharmacology, a section of the journal Frontiers in Pharmacology

Received: *29 May 2020*
Accepted: *28 July 2020*
Published: *03 September 2020*

Citation:
Huang A, Li H, Zeng C, Chen W, Wei L, Liu Y and Qi X (2020) Endogenous CCN5 Participates in Angiotensin II/TGF-β_1 Networking of Cardiac Fibrosis in High Angiotensin II-Induced Hypertensive Heart Failure. Front. Pharmacol. 11:1235. doi: 10.3389/fphar.2020.01235

patients. A novel therapeutic target should be developed for stimulating endogenous CCN5 production.

Keywords: angiotensin II, CCN5, cardiac fibrosis, heart failure, hypertension

INTRODUCTION

Cardiovascular disease is the leading cause of deaths, accounting for 17.7 million deaths of 55 million deaths worldwide in 2017 (Yasin et al., 2019; Yasin et al., 2019). Hypertension is the main risk factor for cardiovascular disease and may lead to increased morbidity of coronary artery disease, heart failure (HF), and myocardial infarction. The worldwide prevalence of hypertension and the associated complication, especially HF secondary to hypertension, have drawn attention (Dagenais et al., 2019). Long-term high blood pressure (BP) may promote the development of pathological cardiac structural and functional deterioration, leading to left ventricular (LV) hypertrophy and cardiac fibrosis (CF). These irreversible cardiac remodeling responses always culminate into HF eventually (Lai et al., 2019).

Over-activation of the renin-angiotensin-aldosterone system (RAAS), as the major cause of juvenile hypertension, is often characterized by aberrant activation of angiotensin II (Ang II). Over-expression of Ang II affects regulation of high BP and CF, eventually leading to HF (Berk et al., 2007; Singh and Karnik, 2019). In this high Ang II-induced hypertensive HF, Ang II type 1 receptor, bound to Ang II, may activate transforming growth factor-β_1 (TGF-β_1), which subsequently promotes deposition of the extracellular matrix (ECM) and sensitize fibroblast-to-myofibroblast transition (Nagpal et al., 2016). Downregulation of Ang II expression by blocking the conversion of angiotensin I (Ang I) to Ang II using an angiotensin-converting enzyme inhibitor (ACEI) prevents cardiac function deterioration from HF in hypertensive patients (Zhang et al., 2019). In clinical practice, ACEI has high recommendation level in treatment of high Ang II-induced hypertensive HF (Yancy et al., 2017).

The cellular communication network (CCN) family, known as a group of matricellular proteins, has been described with variant cell functions in regulating fibrosis, angiogenesis, cell differentiation, and wound repair (Xu et al., 2015; Jeong et al., 2016). Several members of the CCN family play essential roles in the development of pressure overload-induced myocardial fibrosis. CCN2 (cellular communication network 2), also called as connective tissue growth factor, is a pro-fibrotic mediator in the development of CF, which can be induced by TGF-β_1 in cardiac fibroblasts and cardiomyocytes (Ye et al., 2019). Besides these pro-fibrotic effects of CCN2, the anti-fibrotic potential of cellular communication network 5 (CCN5, Wisp-2) (Grunberg et al., 2018). As secreted proteins, CCN2 and CCN5 play opposing roles in the development of CF. The possible mechanisms underlying anti-fibrotic effects involve in blocking fibroblast-to-myofibroblast transition, endothelial-mesenchymal transition, and the TGF-β_1 signaling pathway (Jeong et al., 2016). Although several studies have reported the anti-fibrotic effects of exogenous CCN5 in HF, the roles of endogenous CCN5 in high Ang II-induced hypertensive HF still remain unclear (Yoon et al., 2010; Jeong et al., 2016). We hypothesized that endogenous CCN5 plays an essential role in TGF-β_1/Ang II networking-induced CF which accelerates the development of hypertensive HF. We aimed to investigate the potential role of CCN5 in TGF-β_1/Ang II networking-induced CF.

Abbreviations: Ang II, angiotensin II; HF, heart failure; TGF, transforming growth factor; CCN5, cellular communication network 5; ACEI, angiotensin-converting enzyme inhibitor; SHR, spontaneously hypertensive rats; CCN2, cellular communication network 2; ECM, extracellular matrix; LV, left ventricular; RAAS, renin-angiotensin-aldosterone system; Ang I, angiotensin I; CF, cardiac fibrosis; WKY, Wistar-Kyoto rat; LVPW, left ventricle posterior wall; IVS, interventricular septum; LVEF, left ventricular ejection fraction; FS, fraction shortening; α-SMA, alpha-smooth muscle actin.

METHODS AND MATERIALS

For expanded and detailed information about the human study population, reagents, BP measurement, echocardiography, histopathology, ELISA estimation, reverse transcription and real-time quantitative polymerase chain reaction, protein extraction, Western blotting, neonatal rat cardiomyocytes, and cardiac fibroblasts culture, small interfering RNA transfection, and immunofluorescence assay, please refer to the **Supplementary Materials**.

Human Study Population

All protocols were approved by the Ethical Committee Board of Tianjin Union Medical Center, and all subjects provided informed consent.

Animals Model of Hypertensive Heart Failure

Spontaneously hypertensive rats (SHRs) obtained by selective inbreeding of the Wistar-Kyoto rats (WKYs; Vital River, Beijing, China) with a genetic basis for high BP were selected for mimicking hypertension. Normotensive WKY (Vital River, Beijing, China) were chosen as the negative controls. Twenty-four 13-week-old SHRs (weight 200 ± 20 g) were equally divided into the model group or enalapril group based on whether enalapril treatment [SFDA approval number H20170298, 5 mg/tablet, Merck Sharp & Dohme (Australia) Pty. Ltd] was given or not. Additionally, the control group comprised 13-week-old WKYs (n = 12). The animals were housed in a 12-h light/dark room and given free access to tap water and chow feed under laboratory conditions. This experiment proceeded after acclimatization in an on-site facility for 1 week. The enalapril group animals were administered with enalapril [1.05 mg. (Kg. day)$^{-1}$] orally in a 1 ml of distilled water; accordingly, animals in the control and model groups were administered with 1 ml of distilled water using a disposable plastic syringe.

Statistical Analysis

Data were analyzed using SPSS version 17.0 (SPSS Inc., Chicago, USA). Discrete variables were expressed as numbers and percentages. Mean ± SD or median with interquartile (IQ) 25% and 75% (Q25–Q75) were based on the normality for continuous variables. Normality for continuous variables was performed by the Kolmogorov-Smirnov tests. Categorical variables were analyzed using chi-square tests. To compare groups, we used the Mann-Whitney U-test followed by Tukey's multiple comparison tests or Kruskal-Wallis tests to analyze non-normally distributed continuous variables. Spearman correlation analysis was performed for non-conformity analysis. In all analyses, statistical significance was accepted at $P < 0.05$.

RESULTS

Demographic Characteristics

A total of 380 hypertensive patients and 39 normotensive subjects (control) were enrolled into this study. All characteristics of hypertensive patients across BP categories [grade 1 (n = 50), mean BP 149.76/87.84 mmHg; grade 2 (n = 110), mean BP 163.69/94.22 mmHg; grade 3 (n = 220), mean BP 190.21/104.03 mmHg] were demonstrated. There were no differences in age, nor history of hypertension between the hypertensive patients and the normotensive subjects ($P > 0.05$) (**Supplemental Table 1**). Compared to normotensive subjects, the heart rate levels of all hypertensive patients increased significantly ($P < 0.05$). The distribution of sex, drinking, and smoking was comparable between the hypertensive patients and normotensive subjects ($P > 0.05$). Additionally, no statistical difference was demonstrated in the lipid metabolism and renal function between hypertension and control groups ($P > 0.05$). Although the median body mass index (BMI) increased gradually with hypertension grade in patients, no significant difference was demonstrated among diverse sub-groups ($P > 0.05$). Cardiac structure deterioration was observed in the hypertensive patients, especially in patients with grade 3 hypertension [left atrium (LA), LV, left ventricle posterior wall (LVPW), interventricular septum (IVS), $P < 0.001$]. Cardiac systolic function [left ventricular ejection fraction (LVEF): $P > 0.05$] showed no difference among diverse sub-groups. However, the E/A ratio, an echocardiographic index for evaluating diastolic dysfunction, decreased significantly with increasing hypertension grade ($P < 0.05$). To indirectly evaluate the extension of CF, we calculated the left ventricular mass index (LVMI) value for each subject. The mean LVMI level were significantly increased with increasing hypertension grade ($P < 0.01$).

Elevation of Serum Ang II, CCN2, and CCN5

Serum Ang II, CCN2 concentrations were higher in the hypertensive patients, compared to normotensive subjects. grade 3 hypertension patients (CCN2: median 855.73 pg/ml, Ang II: median 209.72 ng/L) showed the highest CCN2 and Ang II concentrations compared with grade 1 (CCN2: median 404.13 pg/ml, Ang II: median 122.44 ng/L) and grade 2 patients (CCN2: median 653.43 pg/ml, Ang II: median 141.41 ng/L) ($P < 0.01$) (**Figures 1A, B**).

Contrarily, CCN5 levels decreased along with the increased BP (grade 1: median 344.17 pg/ml, grade 2: median 284.45 pg/ml, grade 3: median 224.01 pg/ml, $P < 0.05$) (**Figure 1C**). ACEI, which inhibits the conversion of Ang I to Ang II, could attenuate the expression of Ang II. CCN5 can be secreted into circulating blood from multiple vital organs including the heart, lung, and adipose tissue. To evaluate the effects of lung and adipose on serum CCN5 levels, the expression of CCN5 in the lung and adipose tissue was determined *via* Western blotting assay. No differences were showed in the expression of CCN5 between WKY and SHR in the lung and

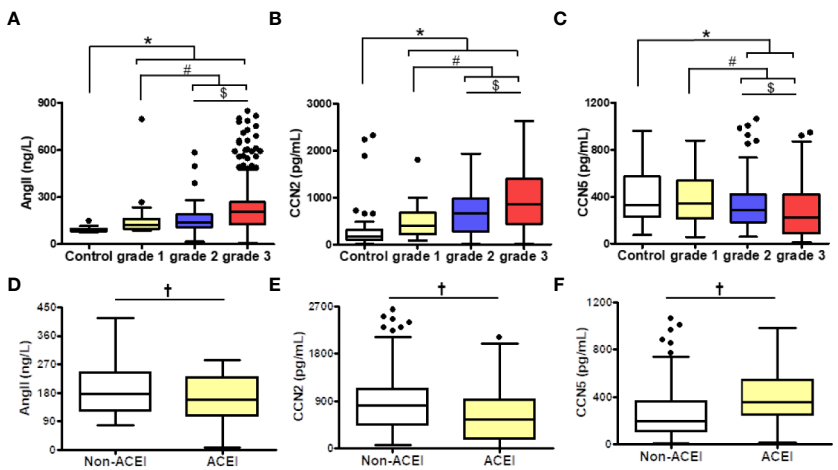

FIGURE 1 | Comparison of Ang II **(A, D)**, CCN2 **(B, E)**, and CCN5 **(C, F)** concentrations in different of blood pressure levels among hypertensive patients with or without ACEI. Data were expressed as median with interquartile range (IQR); whiskers represent ± 1.5 IQR (boxplots). $^{*}P < 0.05$ *vs*. control, $^{\#}P < 0.05$ *vs*. grade 1, $^{\$}P < 0.05$ *vs*. grade 2. $^{\dagger}P < 0.05$ *vs*. No ACEI. grade 1/2/3 were defined as the grade of blood pressure in hypertensive patients. Ang II, angiotensin II; CCN2, cellular communication network factor 2; CCN5, cellular communication network 5; ACEI, angiotensin converting enzyme inhibitor.

adipose tissue. However, the expression of CCN5 in adipose tissue was higher than that in the lung (WKY: $P < 0.05$, SHR: $P < 0.05$). This suggested that the change in serum CCN5 levels mainly be affected by production and secretions of the heart in normotensive and hypertensive subjects (**Figure S1**).

Moreover, we explored whether the downregulation of Ang II could affect the serum CCN2 or CCN5 levels in hypertensive patients (**Figures 1D–F**). We cataloged all hypertensive patients across ACEI usage rates. Serum Ang II levels were decreased after ACEI treatment in hypertensive patients ($P < 0.05$). Furthermore, we found that hypertensive patients using ACEI had elevated CCN2 and lower CCN5 levels ($P < 0.05$).

Association Between Ang II and CCN2/CCN5

Spearman analysis was performed to evaluate whether serum CCN2 and CCN5 are related to serum Ang II. To investigate whether downregulating Ang II had an influence on this association, all hypertensive patients were divided into two sub-groups according to the usage of ACEI (**Figures 2A–D**). Serum CCN2 levels (r = 0.286, $P < 0.01$) and serum CCN5 levels (r = −0.347, $P < 0.01$) correlated with serum Ang II levels in hypertensive patients without ACEI treatment. Coincidently, these Spearman rank relationships were further enhanced in hypertensive patients using ACEI (CCN2: r = 0.340, $P < 0.01$; CCN5: r = −0.406, $P < 0.01$). Afterward, we investigated this association between Ang II and CCN5 further from grade 1 to grade 3 hypertensive patients with ACEI or not. These results demonstrated that negative association between Ang II and CCN5 was found in grade 2, and 3 hypertensive patients with the treatment of ACEI respectively (grade 2: r = −0.544, $P < 0.01$; grade 3: r = −0.401, $P < 0.001$) (**Figures 2E, F**).

Characterization of High Ang II-Induced Hypertensive Heart Failure

After 14 weeks, the SHR model group exhibited a higher expression of Ang II in both serum and myocardial tissue than the WKYs of the control group. Moreover, the Ang II expression in the serum and myocardial tissue could be downregulated using enalapril (**Figures 3A–C**). Over the 14-week observation period, both SBP and DBP of the model group (SHR) were increased markedly compared to those of the control group (WKY) (**Figure 3D**). Enalapril decreased systolic blood pressure (SBP) and diastolic blood pressure (DBP) levels immediately. There was no difference in the ratio of the heart and body weight between the model and control groups until week 28 (**Figure 3E**).

Echocardiography was performed at distinct time points of 24- and 28-week to determine the success of the experimental model of hypertensive HF (**Figures 3F, G**). LV mass, as one of the essential cardiac hypertrophic indices, was increased in the model group with decreased LVEF and fraction shortening (FS) value at 24 weeks. The cardioprotective effects of enalapril from inhibiting Ang II, was not apparent until week 28. Enalapril protected LVEF, FS, and LV mass from deterioration. Enarapril could ameliorate cardiac dysfunction in the high Ang II-induced HF, but this protective effect depended on the persistent inhibition of Ang II. Subsequently, serum BNP and sST2 (soluble suppression of tumorigenicity-2) levels were detected, indicating that enalapril could attenuate high Ang II-induced hypertensive HF (**Figures 3H, I**).

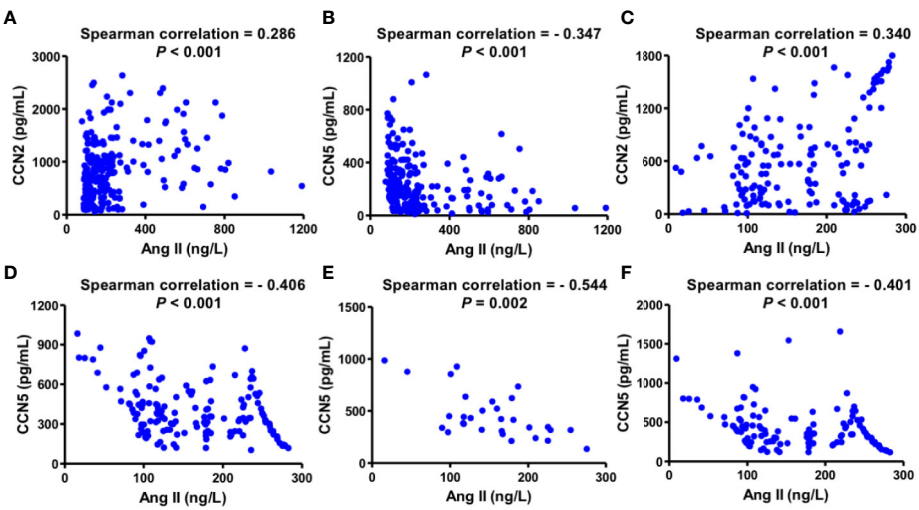

FIGURE 2 | Association between serum CCN2/CCN5 and serum Ang II in hypertensive patients. **(A)** Spearman analysis between serum CCN2 and serum Ang II in hypertensive patients without ACEI. **(B)** Spearman analysis between serum CCN5 and serum Ang II in hypertensive patients without ACEI. **(C)** Spearman analysis between serum CCN2 and serum Ang II in hypertensive patients with ACEI. **(D)** Spearman analysis between serum CCN5 and serum Ang II in hypertensive patients with ACEI. **(E)** Spearman analysis between serum CCN2 and serum Ang II in patients with grade 2 hypertension on treatment with ACEI treatment. **(F)** Spearman analysis between serum CCN2 and serum Ang II in patients with grade 3 hypertension on ACEI treatment. CCN2, cellular communication network factor 2; CCN5, cellular communication network 5; Ang II, angiotensin II; ACEI, angiotensin converting enzyme inhibitor.

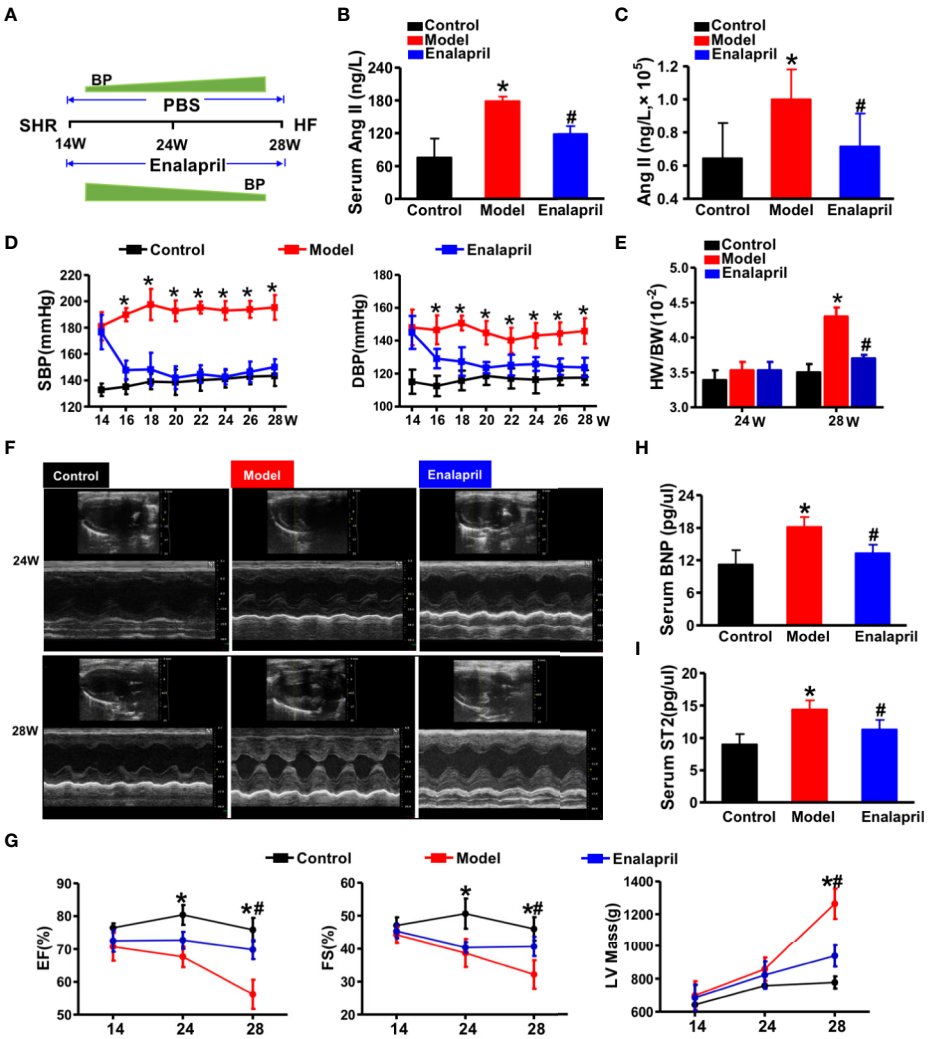

FIGURE 3 | High Ang II-induced hypertensive heart failure. **(A)** Illustration of the experimental strategy in this work. **(B, C)** Ang II concentrations in serum or myocardial tissue. *P < 0.05 vs. control, #P < 0.05 vs. model. **(D)** Blood pressure reduction in SHRs treated by enalapril for 14 weeks. *P < 0.05 vs. model. **(E)** Ratio of heart weight and body weight in SHR or treated by enalapril at 28 weeks. *P < 0.05 vs. control, #P < 0.05 vs. model. **(F)** Echocardiographic phenotype in SHRs or treated by enalapril at 24 and 28 weeks respectively. **(G)** Quantification of cardiac function at different time-points (EF, FS, LV mass). *P < 0.05 vs. control, #P < 0.05 vs. model. **(H, I)** Serum biomarker concentrations of myocardial injuries (BNP, and sST2) in SHRs at 28 weeks. *P < 0.05 vs. control, #P < 0.05 vs. model. Ang II, angiotensin II; SHRs, spontaneously hypertensive rats; EF, ejection fraction; FS, fractional shortening; LV mass, left ventricular mass; BNP, brain natriuretic peptide; sST2, soluble suppression of tumorigenicity-2.

Endogenous CCN5 and Ang II-TGF-β_1 Signaling Axis Networking in Hypertensive Heart Failure

After evaluation of cardiac structure, and function, our results indicated that long-term stimuli of high BP could induce CF, hypertrophy, and even severe HF. We evaluated the morphological changes of the heart tissue further. Myocyte hypertrophy occurred significantly in the model group from week 24; however, this kind of hypertrophy was reversed by enalapril at week 28 (**Figure S2**). Myocardial fibrosis participated in the entire cardiac hypertrophy process. Collagen deposition occurred in the model group at week 24 and further worsened at week 28. Enalapril could effectively attenuate this collagen deposition in SHRs at 24 and 28 weeks (**Figures 4A, B**). These results coincided with the expression of collagen Ia and collagen IIIa (**Figure 4C**).

A previous study demonstrated that CCN5 could block the TGF-β_1 signaling pathway and fibroblast-to-myofibroblast transition (Jeong et al., 2016). In our study, we found that TGF-β_1 and alpha-smooth muscle actin (α-SMA) were also elevated, which indicated that pro-fibrotic pathways and fibroblast-to-myofibroblast transition were activated in the model group (**Figures 4D**). These results demonstrated that endogenous CCN5 might create a link between Ang II and TGF-β_1 and α-SMA. Thereafter, we investigated the

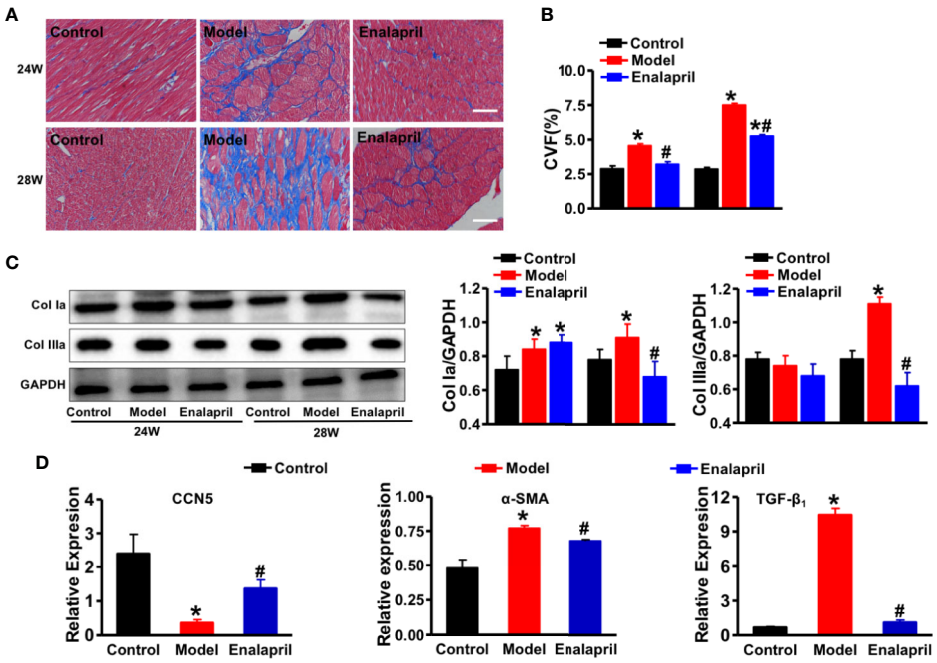

FIGURE 4 | Anti-fibrotic effects of CCN5 in high Ang II-induced hypertensive heart failure at 28 weeks. **(A)** Representative Masson staining of myocardial tissue from different groups at 24 and 28 weeks. Scale bar 100 μm. **(B)** Quantification of CVF from different groups at 24 and 28 weeks. *$P < 0.05$ vs. control, #$P < 0.05$ vs. model. **(C)** Western blot analysis of Col Ia and Col IIIa from different groups at 24 and 28 weeks. Quantification of Col Ia and Col IIIa in SHRs or treated by enalapril at 24 and 28 weeks. *$P < 0.05$ vs. control, #$P < 0.05$ vs. model. **(D)** Relative expression of CCN5, α-SMA, and TGF-β1 in SHRs or treated by enalapril at 24 and 28 weeks. *$P < 0.05$ vs. control, #$P < 0.05$ vs. model.

interaction of CCN5 and Ang II-TGF-β_1 signaling axis in fibrotic pathways. The expression of myocardial CCN5 was significantly reduced in the model group and in reverse increased after inhibition of Ang II by enalapril (**Figure 4D**). The results of Western blotting analysis also revealed decreased endogenous CCN5 and an activated TGF-β_1 signaling pathway and fibroblast-to-myofibroblast transition (**Figures 5A–H**).

To confirm the main resource of CCN5 in cardiac tissues, we isolated the rat neonatal cardiomyocytes (CMs) and cardiac fibroblasts from neonatal WKY. Then we performed double immunofluorescence staining of CCN5 and cell markers (TnI or vimentin) of CMs and cardiac fibroblasts. CCN5 was mainly expressed in cardiac fibroblasts ($P < 0.05$ *vs.* CMs) (**Figure 6A**). Additionally, we performed the double immunofluorescence staining of CCN5 and CD31 (cell marker of cardiac endothelial cells). No clear co-localization was found between CCN5 and CD31 in cardiac tissues, and this demonstrated that CCN5 may not be mainly expressed in cardiac endothelial cells (**Figure 6B**).

To evaluate the essential role of endogenous CCN5 in the Ang II induced profibrotic pathophysiology, the isolated cardiac fibroblasts were exposed to Ang II (0.1 μM). The siRNA targeting CCN5 was synthesized and transfected into cardiac fibroblasts to suppress the CCN5 expression. After stimulation with Ang II, CCN5 expression was significantly down-regulated in the cardiac fibroblasts, and this downregulation was further enhanced after on using siRNA (*$P < 0.05$ *vs.* control; #$P < 0.05$ *vs.* Ang II/scrambled siRNA) (**Figure 7A**). The expression of TGF-β_1, Col Ia, and Col IIIa was also upregulated on use of siRNA. These results confirmed that Ang II promoted the TGF-β_1 induced CF by down-regulating the expression of CCN5. We investigated the effects of downregulation of CCN5 on fibroblast-to-myofibroblast transition. siRNA could significantly promote expression of α-SMA in the cardiac fibroblasts, suggesting that fibroblast-to-myofibroblast transition was enhanced by downregulation of CCN5 expression (**Figure 7B**).

DISCUSSION

In this study, we demonstrated that CCN5 downregulation might be closely related to Ang II expression in hypertensive HF. CCN5 expression could be elevated by inhibiting Ang II, which provided a cardioprotective effect in hypertension-induced HF. Serum CCN5, CCN2, and Ang II concentrations were tested between hypertensive patients and healthy controls, and we further investigated on the association between Ang II and matricellular proteins of CCN5 and CCN2. Using our experimental model of high Ang II-induced hypertensive HF along with elevated expression of Ang II in both serum and myocardial tissue, we evaluated whether downregulation of CCN5 could affect the cardiac structure, function, and myocardial fibrosis.

Moreover, we elucidated the indispensable role of endogenous CCN5 in high Ang II-induced hypertensive HF. Our clinical results

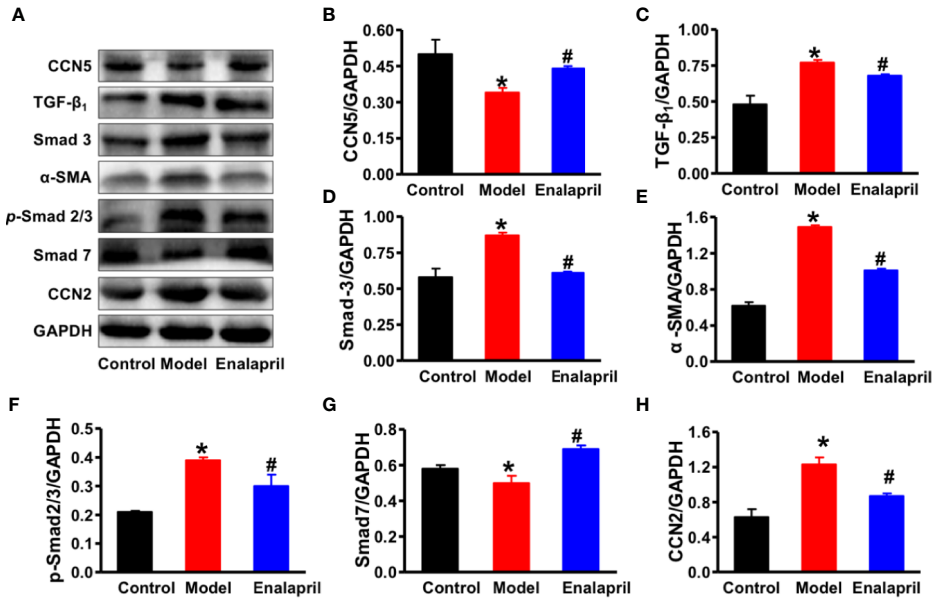

FIGURE 5 | (A) Representative Western blot analysis of CCN5, TGF-β_1, Smad-2, Smad-3, α-SMA, p-Smad-2/3, Smad-7, and CCN2 in myocardial tissue among different groups. **(B–H)** Quantification of CCN5, TGF-β_1, Smad-2, Smad-3, α-SMA, p-Smad-2/3, Smad-7, and CCN2 expression in myocardial tissue among different groups. *P < 0.05 vs. control, #P < 0.05 vs. model. CVF, collagen volume fraction; Col Ia, collagen Ia; Col IIIa, collagen IIIa; SHRs, spontaneously hypertensive rats; CCN5, cellular communication network 5; α-SMA, alpha smooth muscle actin; TGF-β1, transforming growth factor-β1; CCN2, cellular communication network 2.

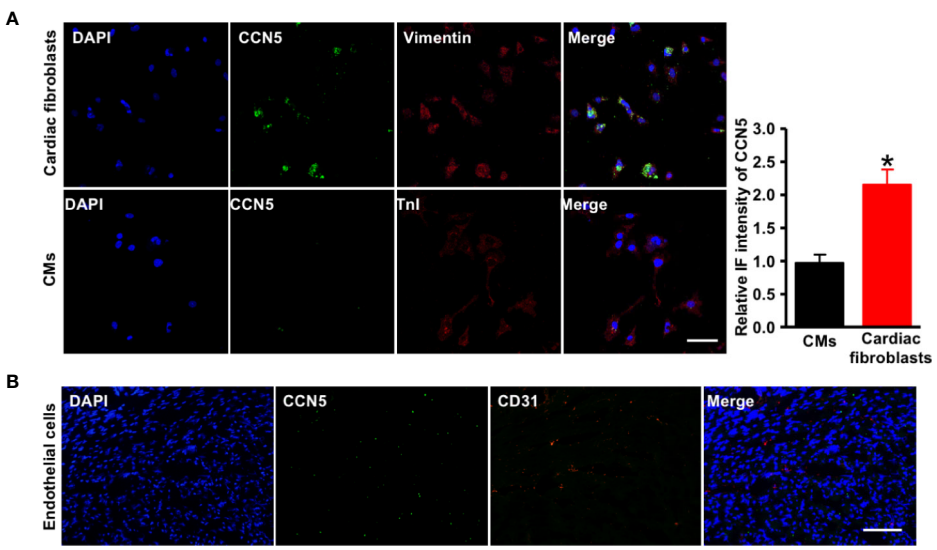

FIGURE 6 | CCN5 expression in major rat cardiac cell types. **(A)** Double immunofluorescence-staining of CCN5 and cell markers (vimentin/TnI) in CFs and CMs. Scale bar 30 μm. Quantitative analysis of intensive immunofluorescence density of CCN5. *P < 0.05 vs. CMs. **(B)** Double immunofluorescence-staining of CCN5 and CD31 (cell marker of cardiac ECs), scale bar 100 μm. CCN5, cellular communication network 5; CFs, cardiofibroblasts; CMs, cardiomyocytes; ECs, endothelial cells; IF, immunofluorescence.

demonstrated that serum CCN5 levels reduced significantly because of the increased severity and history of high BP in hypertensive patients. Additionally, this negative association was described between serum Ang II and CCN5, especially in grade 2 and 3 hypertensive patients using oral ACEI regularly. Our rat model of essential hypertensive HF revealed a significant decrease of CCN5 in high Ang II-induced hypertensive HF. Expression of CCN5 was upregulated after ACEI treatment, which further reversed

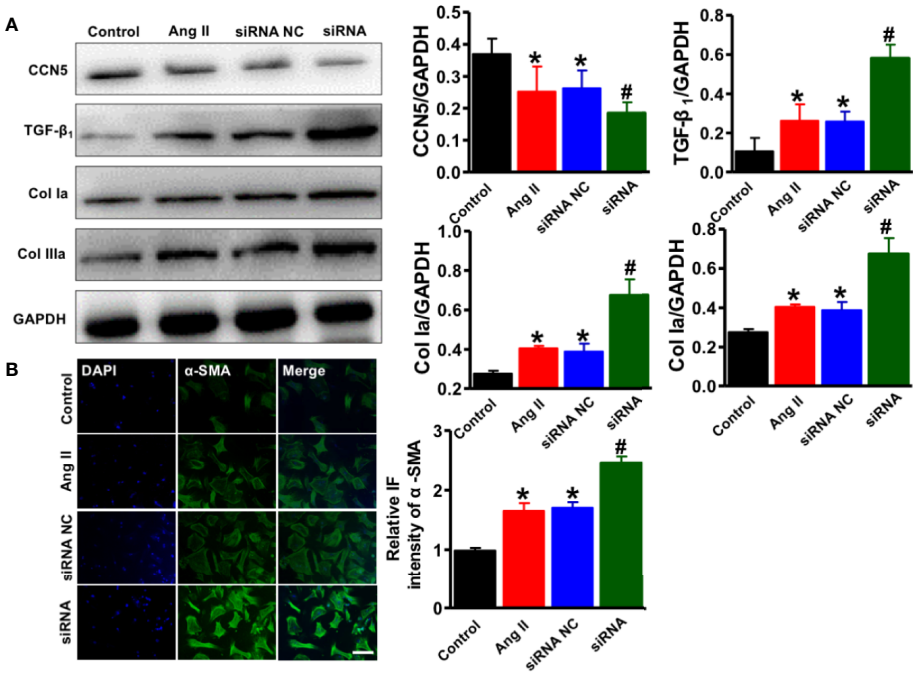

FIGURE 7 | Downregulation of CCN5 enhanced Ang II-induced activation of pro-fibrotic effects. **(A)** Representative Western blot analysis of CCN5, TGF- β_1, Col 1a, and Col IIIa. *$P < 0.05$ vs. control, #$P < 0.05$ vs. Ang II/siRNA NC. *$P < 0.05$ vs. control, #$P < 0.05$ vs. Ang II/siRNA NC. CCN, cellular communication network 5; TGF, transforming growth factor. **(B)** Representative image of immunofluorescent staining of myofibroblasts markers (α-SMA, Scale bar 50 μm. *$P < 0.05$ vs control, #$P < 0.05$ vs Ang II/siRNA NC.

myocardial fibrosis and protected heart function *via* inhibition of TGF-β_1 signaling and fibroblast-to-myofibroblast transition.

CCN5 has multiple biological functions (Bornstein and Sage, 2002). Unlike the other CCN family proteins, CCN5 specially lacks a cysteine-rich carboxyl-terminal repeat domain, suggesting that it may be an alternative regulator of other CCN family proteins. Comparison studies of CCN2 with prominent pro-fibrotic activity in cardiac remodeling, in which CCN5 is best characterized, reported anti-hypertrophic and anti-fibrotic effects in the heart (Jeong et al., 2016; Ye et al., 2019). Besides cardiac tissue, lung and adipose tissue show high CCN5 expression (Hammarstedt et al., 2013; Fiaturi et al., 2018; Grunberg et al., 2018). To exclude interference of serum CCN5 from secreted CCN5 from lung and adipose tissue, we compared the expression of CCN5 in lung and adipose tissue between WKY and SHR. The results suggested that CCN5 expression in lung and adipose tissue might not cause the differentiated expression of CCN5 in the serum. Therefore, we assessed the serum CCN5 levels to predict the expression of CCN5 in cardiac tissue. To the best of our knowledge, these protective effects of CCN5 in the heart were verified *via* supplementation of exogenous CCN5. However, whether expression of endogenous CCN5 could be modulated by exogenous stimuli and play an indispensable role in anti-hypertrophic and anti-fibrotic activity remained unclear.

Ang II is known as the primary regulatory factor in a series of RAAS-induced physiological and pathophysiological actions, which participates in homeostatic control of arterial pressure, tissue perfusion, and extracellular volume (Park et al., 2019). Active Ang II is converted from Ang I by ACE, which is cleaved by renin. High Ang II expression induced by RAAS over-activation contributes to the pathophysiology of diseases such as hypertension and hypertensive HF (Rosenkranz, 2004). Our results demonstrated that Ang II increased gradually in hypertensive patients with increasing BP levels. Additionally, we created an experimental model of hypertensive HF with increased Ang II in the serum and myocardial tissue. These results implied that our experimental model mimicked a high Ang II-induced hypertensive HF.

To verify the essential role of CCN5 in hypertension, firstly we detected decreased CCN5 levels, but elevated CCN2 levels in all hypertensive patients. A previous study indicates opposite effects of CCN2 and CCN5 on the regulation of CF, which is consistent with our results (Jeong et al., 2016). Through the comparison of CCN5 levels in hypertensive patients with and without ACEI treatment and further associated analysis, we found that patients with higher Ang II levels had lower concentrations of CCN5, which suggested that an interaction might exist between Ang II and CCN5. In our experimental model, we found that CCN5 was mainly expressed in cardiac fibroblasts, but not cardiomyocytes or cardiac endothelial cells. High Ang II expression could downregulate CCN5 expression to promote CF and deteriorate cardiac systolic and diastolic functions. Meanwhile, Ang II can be attenuated using ACEI, followed by ameliorateion of myocardial

fibrosis and cardiac function. During this process, we detected activated TGF-β_1, which both promoted direct deposition of ECM, and fibroblast-to-myofibroblast transition *via* activated Smad-3 (Nagpal et al., 2016).

Fibroblasts within a healthy working heart control the secretion and maintenance of ECM components and more importantly regulate the transmission of mechanical and electrical stimuli (Santiago et al., 2010). In hypertensive-induced cardiac hypertrophy and fibrosis, the phenotype conversion of cardiac fibroblast-to-myofibroblast is a critical event, this could precipitate HF (Czubryt, 2019). With elevation of BP, cardiac fibroblasts become overactivated and converted to myofibroblasts in response to pressure overload. During this process, several key phenotypic markers of myofibroblast are recognized including α-SMA and periostin (Bagchi et al., 2016). In this study, high α-SMA expression was found in the myocardial tissue of SHRs, opposed to the decreased expression after downregulation of Ang II using ACEI. After inhibiting the expression of CCN5 in the cardiac fibroblasts, we found a significant increase of α-SMA in the cardiac fibroblasts. These results demonstrated that Ang II might promote the phenotype conversion of cardiac fibroblast-to-myofibroblast by directly inhibiting the expression of CCN5.

Although the fibroblast-to-myofibroblast conversion has been described previously, the signaling mechanisms governing this conversion were not yet clearly elucidated. Phenotype fibroblast-to-myofibroblast conversion can be induced by mechanical tension, or TGF-β_1 stimuli, which aids in quick ECM pathological remodeling (Roche et al., 2015). The TGF-β_1-Smad signaling pathway, which is arguably one of the most potent inductive mechanisms, is involved in this process (Roche et al., 2015). Obviously, healthy myocardial tissue was devoid of myofibroblasts, but myofibroblasts became abundant after receiving several stimulating factors, which promoted hypersecretion of ECM components such as collagen type I, periostin, and fibronectin (Tomasek et al., 2002). Excessive ECM components produced by myofibroblast accelerate CF and even HF.

Taken together, the results of this study showed that serum CCN5 was reduced significantly in hypertensive patients and increased in hypertensive patients using ACEI. The negative association between CCN5 and Ang II in the serum indicated that Ang II interacted with CCN5. Our experimental model of high Ang II-induced hypertensive HF revealed that CCN5 was downregulated in the high Ang II SHR and increased *via* Ang II production inhibition by ACEI treatment. Thereafter, this downregulation of CCN5 activates TGF-β_1, which promotes direct deposition of ECM, and fibroblast-to-myofibroblast transition *via* activated Smad-3.

The current study highlights the essential role of endogenous CCN5 in CF. CCN5 participates in the Ang II/TGF-β_1 networking. However, this networking is a vastly and complicated process, endogenous CCN5 may interact with multiple signaling factors including matrix metalloproteases and metalloproteases within the Ang II/TGF-β_1 networking (Jeong et al., 2016). This study cannot cover all of biological functions of endogenous CCN5 within this networking. Further work will focus on the crucial role of endogenous CCN5 in degradation of the ECM.

In summary, we verifiy the essential role of endogenous CCN5 in high Ang II-induced hypertensive HF. Elevated Ang II inhibit CCN5 expression, which subsequently activates TGF-β_1 and finally promotes direct deposition of ECM and fibroblast-to-myofibroblast transition *via* Smad-3 activation. CCN5 can be used as a potential biomarker for estimating CF in hypertensive patients. A novel therapeutic target can be developed for stimulating endogenous CCN5 production.

DATA AVAILABILITY STATEMENT

The raw data supporting the conclusions of this article will be made available by the authors, without undue reservation, to any qualified researcher.

ETHICS STATEMENT

The studies involving human participants were reviewed and approved by Tianjin Union Medical Center. The patients/participants provided their written informed consent to participate in this study. The animal study was reviewed and approved by Tianjin Union Medical Center.

AUTHOR CONTRIBUTIONS

AH designed and completed the experiments, analyzed the data, and drafted the manuscript. HL analyzed the data, collected the clinical data, and analyzed the clinical data. CZ and WC completed the experiments and collected the clinical data. LW revised the draft. XQ conceived this study and finalized the manuscript. All authors contributed to the article and approved the submitted version.

FUNDING

The study was supported by the major projects of Science and Technology Committee of Tianjin (grant number 16ZXMJSY 00060); the Tianjin Health Bureau Key Project Fund (grant number 16KG155); and the Science and Technology Project of Tianjin Union Medical Center (grant number 2019YJZD001).

ACKNOWLEDGMENTS

We thank all the members of our laboratory for helpful discussion.

SUPPLEMENTARY MATERIAL

The Supplementary Material for this article can be found online at: https://www.frontiersin.org/articles/10.3389/fphar.2020.01235/full#supplementary-material

REFERENCES

Bagchi, R. A., Roche, P., Aroutiounova, N., Espira, L., Abrenica, B., Schweitzer, R., et al. (2016). The transcription factor scleraxis is a critical regulator of cardiac fibroblast phenotype. *BMC Biol.* 1714, 21. doi: 10.1186/s12915-016-0243-8

Berk, B. C., Fujiwara, K., and Lehoux, S. (2007). ECM remodeling in hypertensive heart disease. *J. Clin. Invest.* 117 (3), 568–575. doi: 10.1172/jci31044

Bornstein, P., and Sage, E. H. (2002). Matricellular proteins: extracellular modulators of cell function. *Curr. Opin. Cell Biol.* 14 (5), 608–616. doi: 10.1016/S0955-0674(02)00361-7

Czubryt, M. P. (2019). Cardiac Fibroblast to Myofibroblast Phenotype Conversion-An Unexploited Therapeutic Target. *J. Cardiovasc. Dev. Dis.* 6 (3), 28. doi: 10.3390/jcdd6030028

Dagenais, G. R., Leong, D. P., Rangarajan, S., Lanas, F., Lopez-Jaramillo, P., Gupta, R., et al. (2019). Variations in common diseases, hospital admissions, and deaths in middle-aged adults in 21 countries from five continents (PURE): a prospective cohort study. *Lancet* 785–794. doi: 10.1016/s0140-6736(19)32007-0

Fiaturi, N., Russo, J. W., Nielsen, H. C., and Castellot, J. J. Jr. (2018). CCN5 in alveolar epithelial proliferation and differentiation during neonatal lung oxygen injury. *J. Cell Commun. Signal.* 12 (1), 217–229. doi: 10.1007/s12079-017-0443-1

Grunberg, J. R., Elvin, J., Paul, A., Hedjazifar, S., Hammarstedt, A., and Smith, U. (2018). CCN5/WISP2 and metabolic diseases. *J. Cell Commun. Signal.* Mar12 (1), 309–318. doi: 10.1007/s12079-017-0437-z

Hammarstedt, A., Hedjazifar, S., Jenndahl, L., Gogg, S., Grunberg, J., Gustafson, B., et al. (2013). WISP2 regulates preadipocyte commitment and PPARgamma activation by BMP4. *Proc. Natl. Acad. Sci. U. S. A.* 12110 (7), 2563–2568. doi: 10.1073/pnas.1211255110

Jeong, D., Lee, M. A., Li, Y., Yang, D. K., Kho, C., Oh, J. G., et al. (2016). Matricellular Protein CCN5 Reverses Established Cardiac Fibrosis. *J. Am. Coll. Cardiol.* Apr 567 (13), 1556–1568. doi: 10.1016/j.jacc.2016.01.030

Lai, C.-H., Pandey, S., Day, C. H., Ho, T.-J., Chen, R.-J., Chang, R.-L., et al. (2019). β-catenin/LEF1/IGF-IIR Signaling Axis Galvanizes the Angiotensin-II-induced Cardiac Hypertrophy. *Int. J. Mol. Sci.* 20 (17), 4288. doi: 10.3390/ijms20174288

Nagpal, V., Rai, R., Place, A. T., Murphy, S. B., Verma, S. K., Ghosh, A. K., et al. (2016). MiR-125b Is Critical for Fibroblast-to-Myofibroblast Transition and Cardiac Fibrosis. *Circulation.* 133 (3), 291–301. doi: 10.1161/circulationaha.115.018174

Park, S., Nguyen, N. B., Pezhouman, A., and Ardehali, R. (2019). Cardiac fibrosis: potential therapeutic targets. *Transl. Res.* 209, 121–137. doi: 10.1016/j.trsl.2019.03.001

Roche, P. L., Filomeno, K. L., Bagchi, R. A., and Czubryt, M. P. (2015). Intracellular signaling of cardiac fibroblasts. *Compr. Physiol.* 5 (2), 721–760. doi: 10.1002/cphy.c140044

Rosenkranz, S. (2004). TGF-beta1 and angiotensin networking in cardiac remodeling. *Cardiovasc. Res.* 1563 (3), 423–432. doi: 10.1016/j.cardiores.2004.04.030

Santiago, J. J., Dangerfield, A. L., Rattan, S. G., Bathe, K. L., Cunnington, R. H., Raizman, J. E., et al. (2010). Cardiac fibroblast to myofibroblast differentiation *in vivo* and *in vitro*: expression of focal adhesion components in neonatal and adult rat ventricular myofibroblasts. *Dev. Dyn* 239 (6), 1573–1584. doi: 10.1002/dvdy.22280

Singh, K. D., and Karnik, S. S. (2019). Angiotensin Type 1 Receptor Blockers in Heart Failure. *Curr. Drug Targets*. 125–131. doi: 10.2174/1389450120666190821152000

Tomasek, J. J., Gabbiani, G., Hinz, B., Chaponnier, C., and Brown, R. A. (2002). Myofibroblasts and mechano-regulation of connective tissue remodelling. *Nat. Rev. Mol. Cell Biol.* 3 (5), 349–363. doi: 10.1038/nrm809

Xu, H., Li, P., Liu, M., Liu, C., Sun, Z., Guo, X., et al. (2015). CCN2 and CCN5 exerts opposing effect on fibroblast proliferation and transdifferentiation induced by TGF-beta. *Clin. Exp. Pharmacol. Physiol.* 42 (11), 1207–1219. doi: 10.1111/1440-1681.12470

Yancy, C. W., Jessup, M., Bozkurt, B., Butler, J., Casey, D. E.Jr., Colvin, M. M., et al. (2017). 2017 ACC/AHA/HFSA Focused Update of the 2013 ACCF/AHA Guideline for the Management of Heart Failure: A Report of the American College of Cardiology/American Heart Association Task Force on Clinical Practice Guidelines and the Heart Failure Society of America. *Circulation.* 136 (6), e137–e161. doi: 10.1161/CIR.0000000000000509

Yasin, Y. J., Banoub, J. A. M., Kanchan, T., GBD 2017 Risk Factor Collaborators (2019). Global, regional, and national comparative risk assessment of 84 behavioural, environmental and occupational, and metabolic risks or clusters of risks for 195 countries and territories, 1990-2017: a systematic analysis for the Global Burden of Disease Study 2017 (vol 392, pg 1923, 2017). *Lancet.* 393 (10190), E44–E44. doi: 10.1016/S0140-6736(18)32225-6

Yasin, Y. J., Banoub, J. A. M., Husseini, A., GBD 2017 Causes of Death Collaborators (2019). Global, regional, and national age- sex- specific mortality for 282 causes of death in 195 countries and territories, 1980-2017: a systematic analysis for the Global Burden of Disease Study 2017 (vol 392, pg 1736, 2017). *Lancet.* 22393 (10190), E44–E44. doi: 10.1016/S0140-6736(18)32203-7

Ye, S., Kwon, W. K., Bae, T., Kim, S., Lee, J. B., Cho, T. H., et al. (2019). CCN5 Reduces Ligamentum Flavum Hypertrophy by Modulating the TGF-beta Pathway. *J. Orthop Res.* 2634–2644. doi: 10.1002/jor.24425

Yoon, P. O., Lee, M.-A., Cha, H., Jeong, M. H., Kim, J., Jang, S. P., et al. (2010). The opposing effects of CCN2 and CCN5 on the development of cardiac hypertrophy and fibrosis. *J. Mol. Cell. Cardiol.* 49 (2), 294–303. doi: 10.1016/j.yjmcc.2010.04.010

Zhang, Y., Zhang, L., Fan, X., Yang, W., Yu, B., Kou, J., et al. (2019). Captopril attenuates TAC-induced heart failure *via* inhibiting Wnt3a/β-catenin and Jak2/Stat3 pathways. *Biomed. Pharmacother.* 113, 108780. doi: 10.1016/j.biopha.2019.108780

Conflict of Interest: The authors declare that the research was conducted in the absence of any commercial or financial relationships that could be construed as a potential conflict of interest.

frontiers in Pharmacology

ORIGINAL RESEARCH
published: 04 September 2020
doi: 10.3389/fphar.2020.566938

Effect of Triptolide on Temporal Expression of Cell Cycle Regulators During Cardiac Hypertrophy

Jing-Mei Li[1,2], Xi-Chun Pan[1], Yuan-Yuan Ding[1], Yang-Fei Tong[1,3], Xiao-Hong Chen[1], Ya Liu[1] and Hai-Gang Zhang[1]**

[1] Department of Pharmacology, College of Pharmacy, Army Medical University (Third Military Medical University), Chongqing, China, [2] Institute of Medical Biology, Chinese Academy of Medical Sciences & Peking Union Medical College, Kunming, China, [3] Department of Pharmacy, Chongqing Traditional Medicine Hospital, Chongqing, China

OPEN ACCESS

Edited by:
Liberato Berrino, University of Campania Luigi Vanvitelli, Italy

Reviewed by:
Wei Deng, Renmin Hospital of Wuhan University, China
Chengwen Sun, North Dakota State University, United States
Hongtao Xu, ShanghaiTech University, China
Gabriela Placona Diniz, University of São Paulo, Brazil

***Correspondence:**
Hai-Gang Zhang
hg2ster@gmail.com
Ya Liu
liuya1979@hotmail.com

Specialty section:
This article was submitted to Cardiovascular and Smooth Muscle Pharmacology, a section of the journal Frontiers in Pharmacology

Received: *29 May 2020*
Accepted: *19 August 2020*
Published: *04 September 2020*

Citation:
Li J-M, Pan X-C, Ding Y-Y, Tong Y-F, Chen X-H, Liu Y and Zhang H-G (2020) Effect of Triptolide on Temporal Expression of Cell Cycle Regulators During Cardiac Hypertrophy. Front. Pharmacol. 11:566938. doi: 10.3389/fphar.2020.566938

Adult mammalian cardiomyocytes may reenter the cell cycle and cause cardiac hypertrophy. Triptolide (TP) can regulate the expressions of various cell cycle regulators in cancer cells. However, its effects on cell cycle regulators during myocardial hypertrophy and mechanism are unclear. This study was designed to explore the profile of cell cycle of cardiomyocytes and the temporal expression of their regulators during cardiac hypertrophy, as well as the effects of TP. The hypertrophy models employed were neonatal rat ventricular myocytes (NRVMs) stimulated with angiotensin II (Ang II) for scheduled times (from 5 min to 48 h) *in vitro* and mice treated with isoprenaline (Iso) for from 1 to 21 days, respectively. TP was used *in vitro* at 1 μg/L and *in vivo* at 10 μg/kg. NRVMs were analyzed using flow cytometry to detect the cell cycle, and the expression levels of mRNA and protein of various cell cycle regulators were determined using real-time PCR and Western blot. It was found NRVM numbers in phases S and G_2 increased, while that in the G_1 phase decreased significantly after Ang II stimulation. The mRNA expression levels of p21 and p27 increased soon after stimulation, and thereafter, mRNA expression levels of all cell cycle factors showed a decreasing trend and reached their lowest levels in 1–3 h, except for cyclin-dependent kinase 1 (CDK1) and CDK4 mRNA. The mRNA expression levels of CDK1, p21, and p27 increased markedly after stimulation with Ang II for 24–48 h. In myocardium tissue, CDK and cyclin expression levels peaked in 3–7 days, followed by a decreasing trend, while those of p21 and p27 mRNA remained at a high level on day 21. Expression levels of all protein were consistent with the results of mRNA in NRVMs or mice. The influence of Ang II or Iso on protein expression was more obvious than that on mRNA. TP treatment effectively prevented the imbalance in the expression of cell cycle regulators in the hypertrophy model group. In Conclusion, an imbalance in the expression of cell cycle regulators occurs during cardiac hypertrophy, and triptolide corrects these abnormal expression levels and attenuates cardiac hypertrophy.

Keywords: cardiac hypertrophy, cardiomyocyte, cell cycle, cyclin, cyclin-dependent kinase, triptolide

INTRODUCTION

Cardiac hypertrophy is considered to be a compensatory adaptation in response to intrinsic and extrinsic stimuli and is characterized by the reactivation of fetal genes such as β-myosin heavy chain (β-MHC) and brain natriuretic peptide (BNP), enhanced protein synthesis, increased sarcomere organization, and an increase in heart mass with the enlargement of cardiomyocytes (Tan et al., 2011; Pillai et al., 2015; Martens et al., 2020). Although it initially occurs as a compensatory response, a sustained increase in hypertrophy eventually leads to ventricular dilatation and heart failure (Pillai et al., 2015), which increases the morbidity and mortality of various cardiovascular diseases. Therefore, reversing pathological myocardial hypertrophy has become an important strategy for the prevention and treatment of cardiovascular diseases.

Cardiomyocytes in mammals proliferate speedily during embryonic stage but withdraw from the cell cycle soon after birth and are considered terminally differentiated cells. Accumulated studies have revealed that adult cardiomyocytes are capable of cell cycle reentry (Li et al., 2013; Zebrowski and Engel, 2013; Estrella et al., 2015). The cell cycle is controlled by various regulators, including cyclins, cyclin-dependent kinases (CDK) and CDK inhibitors (CDKI). Cell cycle regulators in cardiomyocytes can be reactivated and expressed when stimulated by pathologic factors. Therefore, cardiomyocytes can undergo DNA and protein synthesis but cannot complete mitosis successfully, resulting in an increase in mass and volume, i.e., cardiac hypertrophy (Ahuja et al., 2007). Although the myocardial expression and activation of main cyclin/CDK complexes, such as cyclin A-CDK1/2, cyclin B-CDK1, cyclin D-CDK4/6, and cyclin E-CDK2, remain at high levels during early mammalian embryonic stages (Tane et al., 2014), the protein expression of cell cycle regulators is significantly downregulated in cardiomyocytes after birth (Ahuja et al., 2007). Various researchers have indicated that cell-cycle regulation plays an important role during the hypertrophic growth of cardiomyocytes (Hinrichsen et al., 2008). Di Stefano et al. reported that triple transfection with p21, p27, and p57 siRNAs induced both neonatal and adult cardiomyocytes to enter the S phase and increased the nuclei/cardiomyocyte ratio, which implies that CDKI expression plays an active role in maintaining cardiomyocyte withdrawal from the cell cycle (Di Stefano et al., 2011). Moreover, CDKI downmodulation increased both cyclin E and A levels. Hence, cell cycle activity is not only required for cell division but also involved in hypertrophic growth. Considering that all the cell cycle regulators vary dynamically and play roles synergistically with the progression of cardiac hypertrophy, it is necessary to elucidate the expression pattern of the cell cycle regulator family and explore the possible mechanisms of the hypertrophic response.

Triptolide (TP), the major active component of the Chinese medicinal herb *Tripterygium wilfordii* Hook F, has been used for the treatment of some inflammatory, autoimmune disorders, such as lupus, nephrotic syndrome, Behçet's disease, and rheumatoid arthritis, and a variety of cancers (Pan, 2010; Fan et al., 2016; Ziaei and Halaby, 2016; Hou et al., 2019; Noel et al., 2019). It has been suggested that TP could downregulate the expression of the retinoblastoma protein (Rb), cyclin A, cyclin B, CDK1, and CDK2; trigger cell cycle arrest in the S phase; and induce apoptosis in the cells involved in human renal cell carcinoma and multiple myeloma (Li et al., 2011; Noel et al., 2019). TP can also abrogate the growth of colon cancer and induce cell cycle arrest by inhibiting the transcriptional activation of early gene 2 promoter binding factor (E2F) (Oliveira et al., 2015). Besides the immunomodulatory and anti-cancer effects, It has been also reported that TP treatment can protect rat hearts against pressure overload-induced cardiac fibrosis, improve ventricular function (Wen et al., 2013; Zhang et al., 2013; Li et al., 2017) and attenuate cardiac hypertrophy (Ding et al., 2016), even though it may cause acute myocardial damage, such as myocardium denaturation, swelling, and necrosis when administered with high dose (Hou et al., 2019). However, the effects of TP on cell cycle regulators in myocardial hypertrophy and its mechanism are currently poorly understood. Therefore, the aims of the present study were to explore the temporal expression of cell cycle regulators in cardiac hypertrophy and the effects of TP *in vitro* and *in vivo*.

Abbreviations: Ang II, angiotensin II; CSA, cross-sectional area; CDK, cyclin-dependent kinase; CDKI, cyclin-dependent kinase inhibitor; HW, heart weight; Iso, isoprenaline; LVW, left ventricular weight; MHC, myosin heavy chain; NRVM, neonatal rat ventricular myocyte; TP, triptolide.

MATERIALS AND METHODS

Animals

Seventy-two male C57BL/6J mice (18–21 g) were provided by the Experimental Animals Center of the Third Military Medical University (Chongqing, China). Animals were kept in the facility for 1 week to become accustomed to the new environment. Mice were randomly divided into model groups and TP groups, injected subcutaneously with isoproterenol hydrochloride (Sigma, St. Louis, MO, USA) 10 mg/kg twice daily to induce ventricular hypertrophy referring to the method described by other researchers (Lin et al., 2008; Ma et al., 2011; Taglieri et al., 2011). Animals in the model groups (isoproterenol-treated group, Iso) and TP groups were respectively injected intraperitoneally with vehicle or TP (purity 99.69%; Beijing Medicass Biotechnol, Beijing, China) at doses of 10 μg/kg daily for 0, 1, 3, 7, 14, or 21 days ($n = 6$ in each group). TP was dissolved in DMSO and then diluted in normal saline. The final used concentration of TP and DMSO was 1 μg/ml and 0.1% (v/v), respectively. All animals were weighed every 3 days, and the doses were adjusted accordingly. The mice in all groups were housed in an animal room with a 12 h light/12 h dark conditions and fed freely standard chow and water. The temperature and relative humidity were kept constant. All protocols conform to the *Guide to the Care and Use of Laboratory Animals* published by the Canadian Council on Animal Care and were approved by the Ethical Committee for Animal Experimentation of the Third Military Medical University.

Sampling

At the end of the treatment, all animals were weighed. The mice were decapitated, and the hearts were carefully isolated, placed in a dish with normal saline, blotted slightly and then weighed. The tibial

length (TL) was measured to calculate the ratio of heart weight and left ventricular weight to tibial length (HW/TL and LVW/TL, respectively), and the degree of ventricular hypertrophy was assessed by measuring the HW/TL ratio. The ventricles were divided into multiple segments for histology, RNA extraction, and total cellular protein extraction. Middle ventricular slice was fixed with a formalin neutral buffer solution, and the apex of the ventricle was collected and stored in liquid nitrogen for further experiments.

Cell Culture and Treatment

Neonatal rat ventricular myocytes (NRVMs) from 1- to 3-day-old Sprague-Dawley rats were isolated and grown in DMEM containing 10% fetal bovine serum (FBS) and 1×10^{-7} mol/ml 5-Bromo-2-deoxyuridine under 5% CO_2 air at 37°C for 48 h. NRVMs were cultured in serum-free DMEM for 24 h and then incubated for 0, 5, 10, 30 min, and 1, 2, 3, 6, 12, 24, 48 h, respectively, in a serum-free medium containing 1.0 μmol/L Ang II, to which 1.0 μg/L TP was added to determine its effects. The cell size was determined with rhodamine-phalloidin staining and analyzed with ImageJ software (NIH Image, National Institutes of Health, Bethesda, MD, USA).

Cell Cycle Analysis

NRVM cells were cultured for 48 h in 6-well plates (5×10^6 cells per well) and then cultured in serum-free DMEM for 24 h. After incubation for a scheduled time (0, 5, 10, and 30 min, and 1, 2, 3, 6, 12, and 24 h) in a serum-free medium containing 1.0 μmol/L Ang II, the cells were trypsinized, centrifuged (4°C, 2500 × g, 5 min), fixed in ice-cold 70% ethanol for 24 h, washed with PBS and centrifuged (10 min, 2500 × g, 4°C). The cells were incubated with 50 μg/ml RNase at 37°C for 30 min, stained with 50 μg/ml propidium iodide (PI) at room temperature in the dark for 20 min, and analyzed with flow cytometry to detect the cell cycle, and progression of the cell cycle was assessed.

Real-Time PCR

Total RNA was extracted from NRVMs and left ventricular tissue using TRIzol reagent (TaKaRa, Japan) according to the manufacturer's instructions. RNA was reverse transcribed with a Prime Script RT reagent kit (TaKaRa, Japan) into complementary DNA (cDNA) in a total volume of 20 μl. Real-time PCR for β-MHC, cyclin A1, A2, B1, D1, E1, CDK1, 2, 4, 6, and CDK inhibitor p21 and p27 mRNA were performed using primers designed by Premier 5.0 (Premier Biosoft International, Palo Alto, CA, USA) (**Table 1**). The reaction was performed in a total volume of 10 μl with QPK-201 SYBR Green PCR Master Mix (Bio-Rad, USA), and the thermal cycling conditions were as follows: after an initial 3 min at 95°C, the samples were subjected to 44 cycles comprising 10 s at 95°C for denaturation, 30 s at 58°C for annealing, and 30 s at 72°C for elongation, and finally, 10 min at 72°C for ending the reaction. All results were repeated in six independent experiments. The Ct values were normalized to both the β-actin expression levels and the normal controls, and the relative quantification was calculated using the $2^{-\Delta\Delta Ct}$ method.

Western Blot Assay

NRVMs were stimulated with 1.0 μmol/L Ang II and 1.0 μg/L TP for 0.5, 2, 12, and 24 h, respectively. Total proteins were extracted from NRVMs or left ventricular tissue using RIPA lysis buffer (Beyotime, Shanghai, China) containing protease inhibitors. Equal amounts of denatured proteins were separated with 10% sodium dodecyl sulfate-polyacrylamide gels and then transferred to polyvinylidene difluoride membranes (Millipore, Bedford, MA,

TABLE 1 | Primers used for real-time RT-PCR.

Species	Gene	Forward (5'→3')	Reverse (5'→3')
Rat	CDK1	TCTTCGCTCGTTAAGAGTTAC	ATCTGCCAGTTTGATTGTTC
	CDK2	GTTGACGGGAGAAGTTGTGG	GCTTGACGATGTTAGGGTGAT
	CDK4	CTACGGACATACCTGGACAAA	AATCTAGGCCGCTTAGAAACT
	CDK6	GTGGAAGTTCAGACGTGGAT	CAAGCATTTCAGAAGGAGGT
	cyclin A1	TCTGACCGTTCCAACCAC	TGAATAGCCCGTAAATGC
	cyclin B1	CAGGCTTTCTCCGATGTGAT	TGCTCTTCCTCCAGTTGTCTG
	cyclin D1	GCCCTCCGTTTCTTACTTCA	CTCCTCTTCGCACTTCTGCT
	cyclin E1	GTCAACGACACGGGAGAAGT	AGCAGCGAGGACACCATAAG
	p21	GGTGATGTCCGACCTGTTCC	ACGCTCCCAGACGTAGTTGC
	p27	TTGGGTCTCAGGCAAACTCT	GCAGGTCGCTTCCTCATCC
	β-MHC	GACAACGCCTATCAGTACATG	CCAATGGCAGCAATAACA
	β-actin	CGTAAAGACCTCTATGCCAACA	TAGGAGCCAGGGCAGTAATC
Mouse	CDK1	GCTTTTCCACGGCGACTCAG	ATCCAAGCCGTTCTCGTCCA
	CDK2	GCATTCCTCTTCCCCTCATCA	TCCAAAGGCTCTTGCTAGTCCA
	CDK4	GCTGCTACTGGAAATGCTGACC	TCACTCTGCGTCGCTTTCCT
	CDK6	TTCCAAATCTGCTCAACCCATC	CTGGTTGGATGGCAGGTGAG
	cyclin A2	GAGGCAGCCAGACATCACTAACA	AACACAGACATGGAGGAGAGGAAT
	cyclin B1	TCTCCATGCTGGACTACGACAT	AGCAGGGAGTCTTCACTGTAGGAT
	cyclin D1	GTGAGGAGCAGAAGTGCGAAGA	CTCGGCAGTCAAGGGAATGGT
	cyclin E1	GAAGGCCCTTAAGTGGCGTCT	AGCACCTCACCCGTGTCGTT
	p21	TACTTCCTCTGCCCTGCTGC	TGGTCTGCCTCCGTTTTCG
	p27	GCGGTGCCTTTAATTGGGTC	AGCAGGTCGCTTCCTCATCC
	β-MHC	TGCCAATGACGACCTGAAAGA	CGCTCGCTGGTCTCAATCAG
	β-actin	CCGTAAAGACCTCTATGCCAACA	CTGCTGGAAGGTGGACAGTGAG

USA), which were blocked with 5% (w/v) nonfat milk powder in phosphate-buffered saline (PBS) containing 0.1% (v/v) Tween 20. Then, the membranes were incubated with primary antibodies for β-actin, β-MHC (1:500; Santa Cruz Biotechnology, USA), CDK4, CDK6, and cyclin D1 (1:500; Santa Cruz), and P21 and P27 (1:200; Santa Cruz) at 4°C overnight, followed by horseradish peroxidase (HRP)-conjugated secondary antibody. Antibody-reactive proteins were detected by means of chemiluminescence, and the intensity was captured using a ChemiDoc touch system (Bio-Rad, CA, USA).

Morphological Observation of Myocardium

Left ventricular tissue was fixed in 4% formalin for 48 h, embedded in paraffin and cut into 5 μm slices. The left ventricular tissue slices were stained with hematoxylin/eosin (HE) staining, Masson staining, and fluorescein isothiocyanate (FITC)-labeled lectin wheat germ agglutinin (Sigma, St. Louis, MO, USA). The cross-sectional areas (CSAs) were measured in a blinded fashion with the Image Pro Plus 5.1 Image analysis program (Media Cybernetics, Silver Spring, MD, USA). The fraction of myocardial volume occupied by fibrillar collagen was calculated as the ratio of the fibrotic area to the total LV area.

Statistical Analysis

The results are presented as the mean ± standard error of the mean (SEM), analyzed by one-way analysis of variance (ANOVA) with least significant difference (LSD) *post hoc* analyses with statistical software (SPSS, Chicago, IL, USA) and GraphPad Prism version 5.01 (GraphPad Software, La Jolla, CA, USA). *P* value of <0.05 was considered statistically significant.

RESULTS

Ang II Induces Cell Cycle Re-Entry in NRVMs

To further confirm that pathological stimuli could promote cardiomyocyte re-entry into the cell cycle during cardiac hypertrophy, cell cycle analysis by flow cytometry with PI staining revealed significant cell cycle alterations in NRVMs after stimulation with Ang II. After stimulation for 5 min, the number of treated cells in the G_1 phase increased more quickly than that of the controls (86.09% vs. 80.9%). Noticeably, the number of cells in the S phase showed a significantly increase after stimulation for 5 min. With the increase in stimulation time, the number of cells in the G_1 phase showed a decreasing trend, and simultaneously, the S +G_2 phase cell numbers increased. After Ang II stimulation for 24 h, we observed that 69.63% of NRVMs were found in the G_1 phase, and 28.33% were found in the S+G_2 phase. These results indicate that the NRVM cell cycle can be reinitiated by disease-related hypertrophic stimuli, which is represented by the increased cardiomyocyte number in the S+G_2 phase while the number of cells in the G_1 phase decreased significantly compared with that in the control group (**Figures 1A, B**).

Hypertrophic Response of NRVM

The NRVM size increased soon after stimulation with Ang II (1.0 μmol/L), and the surface area of the NRVMs was significantly increased after stimulation for 10 min. Then, the surface area continued to increase with the addition of stimulation time. After stimulation for 24–48 h, the cell area significantly increased by 2.7–3.1-fold compared to the control (Ang II vs. control: 6285~6870 ± 61~71 vs. 1682 ± 35 μm^2, respectively, $p < 0.01$). We observed that the TP treatment decreased cell size significantly compared with Ang II treatment (**Figures 2A, B**). Simultaneously, the number of binucleate cells elevated markedly after stimulated with Ang II, and TP treatment reduced it strikingly from 6 h (shown in **Figure 2C**).

Moreover, β-MHC mRNA and protein expressions, one of markers of cardiac hypertrophy and is induced by hypertrophic stimulation of NRVMs, was consistent with the results of cell size. The results showed that the mRNA and protein expressions of β-MHC did not alter significantly during the early stage of Ang II stimulation (within 3 and 12 h, respectively); however, during the late stage of cardiac hypertrophy, the mRNA and protein expression levels of β-MHC were the highest compared to those in the control group (0 min). Noticeably, TP significantly decreased the expression of β-MHC protein and mRNA compared to Ang II, as shown in **Figures 2D, E**.

Expression Levels of Cell Cycle Regulators in NRVMs

Cell cycle regulators have been implicated in cardiomyocyte proliferation and cell cycle processes. Herein, we detected the mRNA expression of the cell cycle regulators cyclin A1, B1, D1, and E1; CDK 1, 2, 4, and 6; p21 and p27 using real-time PCR. The results showed that the mRNA expression of cyclin A1, p21 and p27 increased soon after stimulation with Ang II (1.0 μmol/L) for 5 min, and p21 mRNA expression reached its maximum at 30 min. The mRNA expression of all cell cycle factors showed a decreasing trend. The mRNA expression levels of CDK1, 2, 4, and 6; cyclin B1 and D1; and p21 were lowest at 2 h, and the mRNA expression levels of cyclin A1 and p27 mRNA reached their lowest at 1 h. Cyclin E1 mRNA had minimum expression at 3 h, and a transient elevation of the cyclin A1 mRNA level was confirmed at 3 h (**Figure 3A**). Only the expression of CDK1, p21, and p27 mRNA increased significantly after stimulation with Ang II for 24–48 h ($P<0.01$ or 0.05). The results demonstrated that the mRNA expression levels of cell cycle regulators fluctuate in the hypertrophic progression of cardiomyocytes. The TP treatment not only significantly decreased NRVM size but also effectively prevented the abnormal expression of cell cycle regulators compared to the vehicle (Ang II) in NRVMs (**Figures 3A–J**). To further investigate the effect of TP on the protein expression of cell cycle regulators in NRVMs, we examined the expression of several cell cycle-specific proteins, cyclin D1, CDK4 and 6, and P21, on cardiac hypertrophy progression. The results demonstrated that all protein expression levels were upregulated in cells stimulated with Ang II for 12–24 h compared with the controls. In contrast, TP treatment dramatically inhibited Ang II-induced protein expression compared with the vehicle. The mRNA analysis results were consistent with the results obtained in the protein expression analyses. Taken together, these results suggested that cell cycle regulators were abnormally expressed in the process of cardiomyocyte hypertrophy and that TP could balance the expression of cell cycle regulators and attenuate cardiac hypertrophy (**Figures 3K–P**).

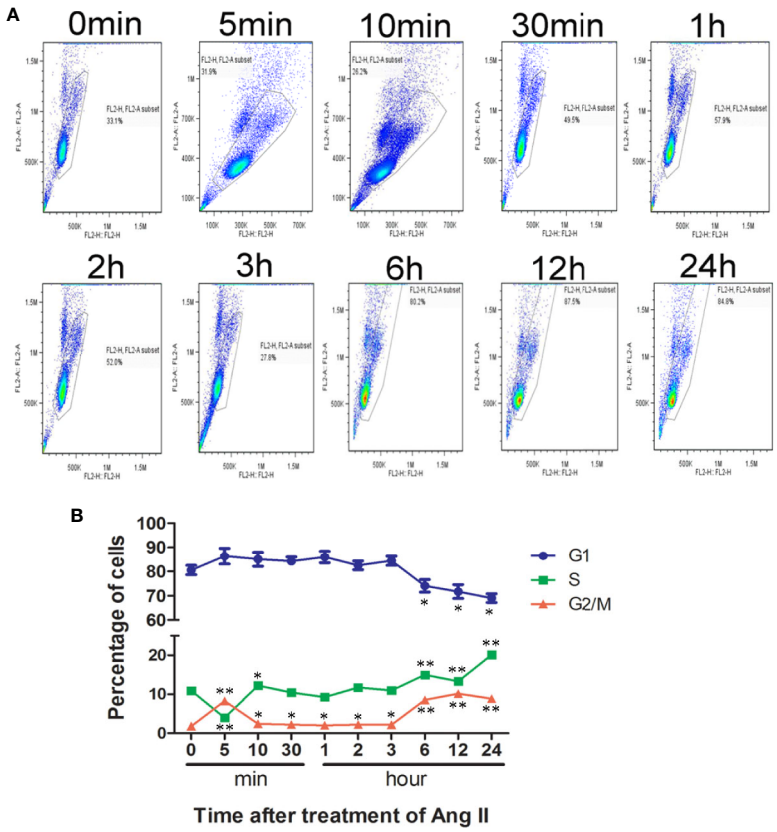

FIGURE 1 | Cell cycle analysis after stimulation with Ang II. Neonatal rat ventricular myocytes (NRVMs) were treated with Ang II (1.0 μmol/L) for the scheduled times (0, 5, 10, and 30 min, and 1, 2, 3, 6, 12, and 24 h). **(A)** Flow cytometry analysis of cardiomyocytes stained with propidium iodide (PI). All experiments were conducted in duplicate and repeated three times (n = 3). **(B)** Data are presented as the mean ± SEM, $^{*}P < 0.05$, $^{**}P < 0.01$ compared with the controls (0 min), (one-way ANOVA).

Survival of Mice

No animal died during the whole experimental period. All of the mice in the Iso groups showed waxy, lackluster fur, breathlessness and reduced activity, drumble, and lags in response with the stimulation time. Mice in the TP-treated groups were more active than those in the Iso group.

Myocardial Hypertrophy

First, the effects of TP on myocardial hypertrophy induced by Iso were observed. As shown in **Figure 4A**, mice showed a significant increase in heart weight (HW) to tibia length (TL) ratio compared with the normal control group after treatment with Iso for 3 days ($P < 0.01$). Then, the heart indexes (HW/TL) continued to increase with time. However, TP treatment could significantly decrease the heart index and inhibit the occurrence of myocardial hypertrophy compared with Iso groups, and the effect of inhibition was more obvious at day 14 ($P < 0.01$). Further studies showed that the mRNA expression of β-MHC was lowest at day 1, followed by an increasing trend (**Figure 4B**). Moreover, the protein level of β-MHC increased from day 0, and β-MHC expression levels of protein and mRNA reached a plateau at day 14, followed by a decreasing trend (**Figures 4B–D**). The results showed a compensatory response in mice. However, interestingly, the β-MHC protein displayed a more remarkable increase in myocardial tissue compared with mRNA during myocardial growth and hypertrophy. TP treatment downregulated β-MHC protein expression significantly (vs. Iso groups, $P < 0.05$). Collectively, these results indicate that TP treatment has the ability to inhibit the abnormal expression of β-MHC and attenuates the stimulation of pathologic factor-induced hypertrophy responses *in vivo*.

Histological Findings

We next tested whether TP treatment attenuated myocardial hypertrophy using HE, lectin, and Masson staining. As shown in **Figure 5**, the histology of mice was almost normal at day 1 after Iso induction. However, we found a hypertrophic myocardium, myocardial fiber disruption, focal necrosis and inflammatory cell infiltration at day 3 after Iso induction, and myocardial injury was aggravated with stimulation time. The Iso groups revealed extensive myocardium degeneration and inflammatory cell infiltration at day 21 (**Figure 5A**). Furthermore, Iso stimulation resulted in a significant increase in the CSA of the myocardium and LV interstitial fibrosis compared with the control group (**Figures 5B, C**). The Iso group showed wide areas of collagen deposition, and the CSA significantly increased, near 1-fold, compared to the control at day 21 ($P < 0.01$). TP-treated mice showed a marked decrease in the degenerated

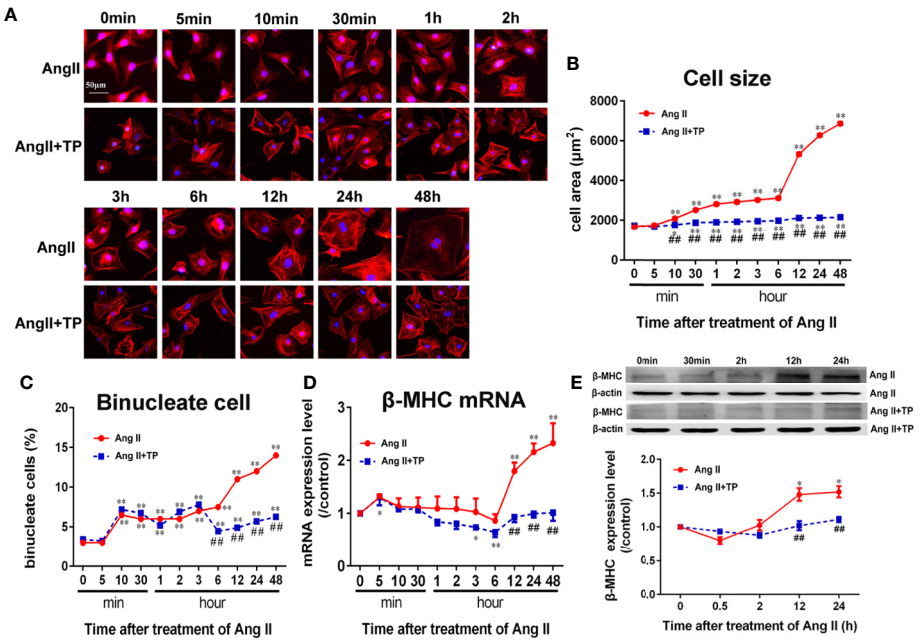

FIGURE 2 | Triptolide attenuated the hypertrophic response of neonatal rat ventricular myocytes. **(A)** NRVMs treated with Ang II (1.0 μmol/L) and 1.0 μg/L TP for the scheduled times and stained with rhodamine-phalloidin (bar = 50 μm). **(B)** Cell size (n = 50 cells in each group). **(C)** Binucleate cell percentage (n = 6 analysis and 150 cells for each analysis). **(D)** mRNA expression of β-MHC was determined using real-time PCR (n = 6). **(E)** β-MHC protein expression was determined using Western blotting (n = 4). The data are presented as the mean ± SEM, $^{*}P < 0.05$, $^{**}P < 0.01$ compared with the controls (0 min), $^{\#\#}P < 0.01$ compared with the Ang II-treated group at the same time point (one-way ANOVA).

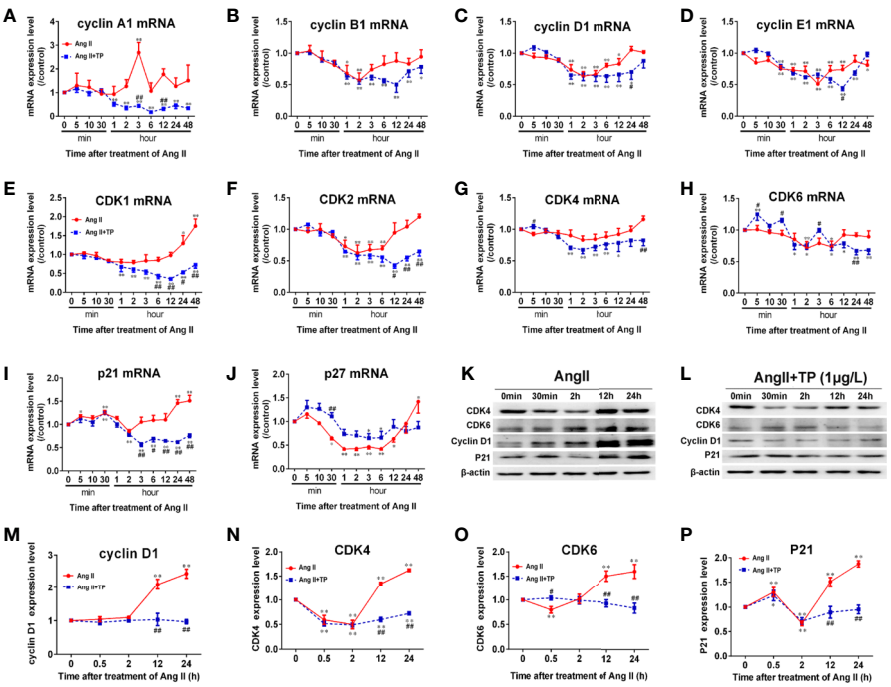

FIGURE 3 | Expression of cell cycle regulators at the mRNA and protein levels in NRVMs. **(A–J)** The mRNA expression levels of cyclin, CDK, and CDKI were measured with real-time PCR (n = 6) and normalized to β-actin and the control group, respectively. **(K, L)** Cyclin D1, CDK4 and 6, and P21 protein levels as shown by Western blot analysis (n = 4). **(M–P)** The intensity of each band was quantified by densitometry and normalized to the β-actin and control groups. Data are shown as the mean ± SEM, $^{*}P < 0.05$, $^{**}P < 0.01$ compared with the controls (0 min), $^{\#}P < 0.05$, $^{\#\#}P < 0.01$ compared with the Ang II-treated group at same time point (one-way ANOVA).

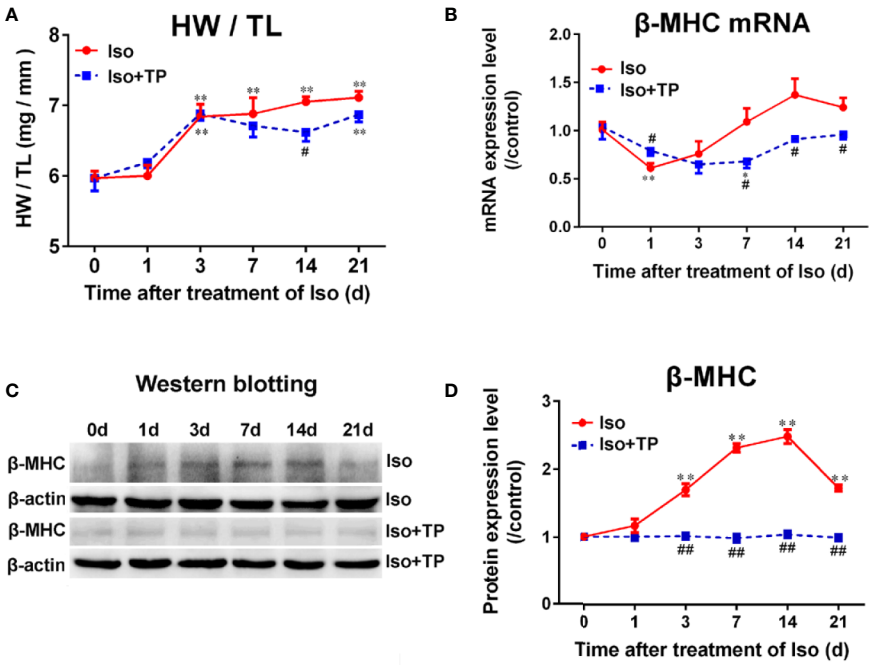

FIGURE 4 | Triptolide attenuated cardiac hypertrophy in mice. **(A)** Heart weight (HW) index to tibia length (TL). **(B)** β-MHC mRNA expression level (n = 6). **(C)** β-MHC protein level as assessed by Western blot analysis (n = 4). **(D)** The intensity of each band was quantified by densitometry and normalized to β-actin and the control group. Data are shown as the mean ± SEM, $^{*}P < 0.05$, $^{**}P < 0.01$ compared with the controls (0 day); $^{\#}P < 0.05$, $^{\#\#}P < 0.01$ compared with the Iso-treated group at the same time point (one-way ANOVA).

myocardium and cellular infiltrations. TP inhibits Iso-induced inflammatory factor activation and thereby contributes to the attenuation of the myocardial pathological injury response in mice. TP treatment significantly decreased myocardial tissue damage, CSA and the fibrosis score compared with the Iso group (**Figure 5**). Collectively, these results suggest that TP treatment attenuated the abnormal pathological features of myocardial hypertrophy.

Myocardial Expression of the Cell Cycle Regulators

Because the expression levels of cell cycle regulators in cardiomyocyte hypertrophy were abnormal, cell cycle regulators could play important roles in hypertrophy development. Therefore, we investigated whether pathological stimulation could induce abnormal expression of cell cycle regulators *in vivo*. The myocardial hypertrophic response of mice was induced by Iso. As shown in **Figure 6**, the Iso induced a gradual decrease in the myocardial mRNA expression of cyclin D1 and E1 and CDK2, 4, and 6 in mice. The mRNA expression of cyclin D1 and CDK6 reached a valley at day 1 and that of cyclin E1, CDK2 and CDK4 reached a valley at day 3. Following an increasing trend, the mRNA expression of cyclin A2, B1, and CDK1 increased dramatically on day 1, and cyclin B1 mRNA peaked on day 3. The expression levels of other factors all peaked at day 7, followed by a decreasing trend. After 21 days of treatment, the mRNA expression levels of cyclin B1 and E1 in the Iso groups were decreased markedly compared with those in the control group. Compared with the control, Iso upregulated the expression of p21 and decreased p27. The p27 mRNA expression level reached the lowest point on day 3 and increased to peak on day 14 with the expression of the p21 mRNA (**Figures 6A–J**). The protein expression levels of cell cycle regulators were determined using Western blotting. The results demonstrated that the expression levels of cyclin D1 and CDK6 increased dramatically post-Iso induction and reached a peak on day 3, followed by a decreasing trend. The protein expression levels of CDK4 and P21 were lowest on day 3, followed by a dramatic increase, and CDK4 reached a peak on day 14. P21 and P27 showed a significant, nearly 4-fold increase in the Iso group compared to the control group at day 21 ($P < 0.01$). However, TP treatment could effectively correct abnormal expression of the cell cycle regulators cyclin, CDK, and CDKI (**Figures 6K–Q**).

DISCUSSION

Cardiomyocyte death is a common end-point in many forms of cardiovascular disease, and a number of approaches have been explored to increase cardiomyocyte number in injured hearts, with the hope of promoting functional recovery after myocardial infarction (Hassink et al., 2008). It is believed that cardiomyocyte cell cycle activation is of great value (Pasumarthi and Field, 2002; Hassink et al., 2008; Eghbali et al., 2019). For decades, the common dogma was that the adult heart is incapable of regenerating lost myocardium after injury. The present knowledge suggests that

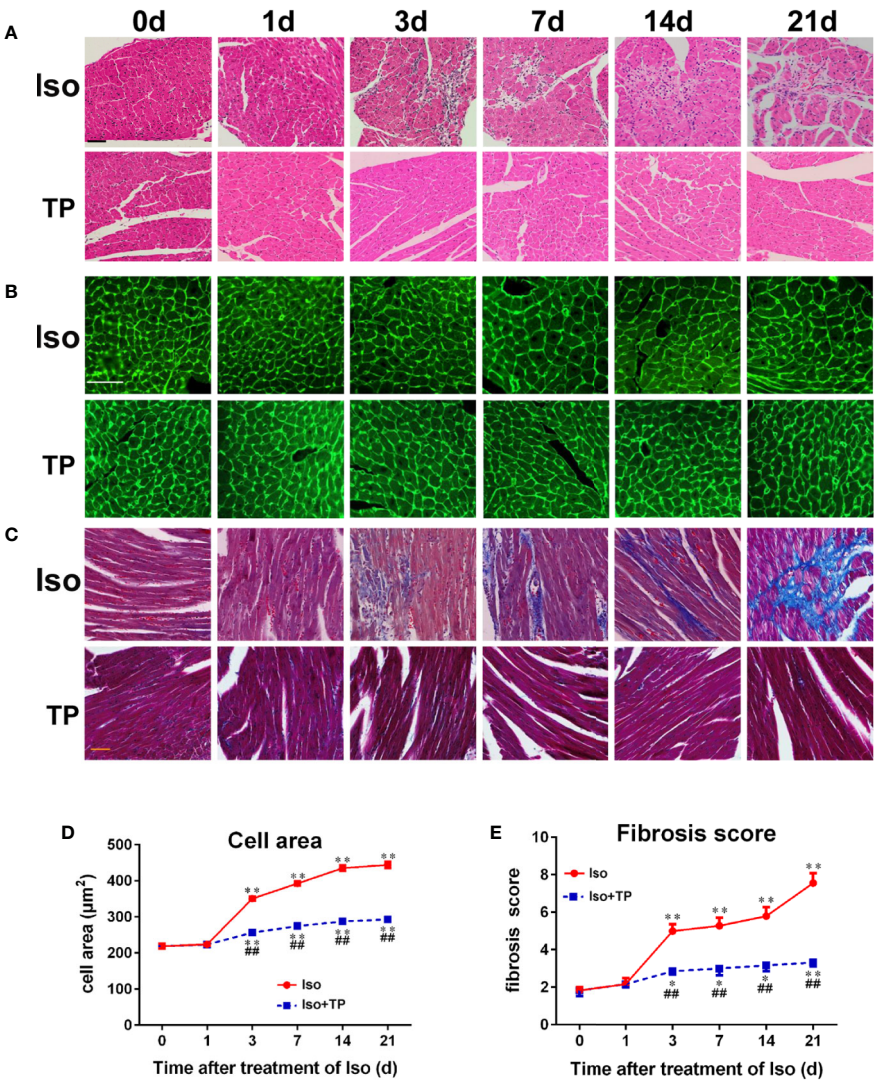

FIGURE 5 | Myocardial histological changes after TP treatment. **(A)** Hematoxylin and eosin (HE) staining of myocardial LV tissue (bar = 50 μm). **(B)** Wheat germ agglutinin lectin staining (bar = 50 μm). **(C)** Masson's trichome-stained left ventricular tissue (bar = 50 μm). **(D)** Cross-sectional area (n = 80). **(E)** Fibrosis score. Data are shown as the mean ± SEM (n = 6 in each group), $^{*}P < 0.05$, $^{**}P < 0.01$ compared with the controls (0 day); $^{\#\#}P < 0.01$ compared with the Iso-treated group at the same time point (one-way ANOVA).

cardiomyocytes in the adult mammalian heart exhibit some capacity to re-enter the cell cycle, but they cannot successfully complete mitosis, which results in cardiac hypertrophy (Ahuja et al., 2007). These issues, namely, that evidence of DNA and cell cycle protein synthesis, re-expression of embryonic genes or even nuclear division in cardiac myocytes does not necessarily represent true cardiac myocyte division, have been the major hurdles in the field when interpreting results (Beltrami et al., 2001). Cell cycle activity in adult cardiac myocytes can represent multinucleation and polyploidization (DNA replication without karyokinesis or cytokinesis) or DNA repair in addition to true proliferative activity. However, it is potentially even more problematic in patients with diseased hearts where cardiac myocyte ploidy increases dramatically with a patient's diastole and systole (Zhang et al., 2015). Cardiac hypertrophy has been regarded as an independent risk factor for cardiovascular morbidity and mortality (Cox and Marsh, 2014). Myocardial hypertrophy and fibrosis are the predominant pathological changes in myocardial remodeling, which results in both diastolic and systolic dysfunction (Li et al., 2017). In the present study, we found that NRVM size increased soon after stimulation with Ang II. Simultaneously, the number of binucleate cells increased with time. The overall change trends of cell size, binucleate cells percentage, and β-MHC are similar although the change of binucleate cells is not exactly the same as the expression of β-MHC mRNA. Flow cytometry analysis indicated that the number of myocytes in the S+G_2 phases increased and that in the G_1 phase decreased significantly compared with the control group. Significant cell cycle alterations were observed in

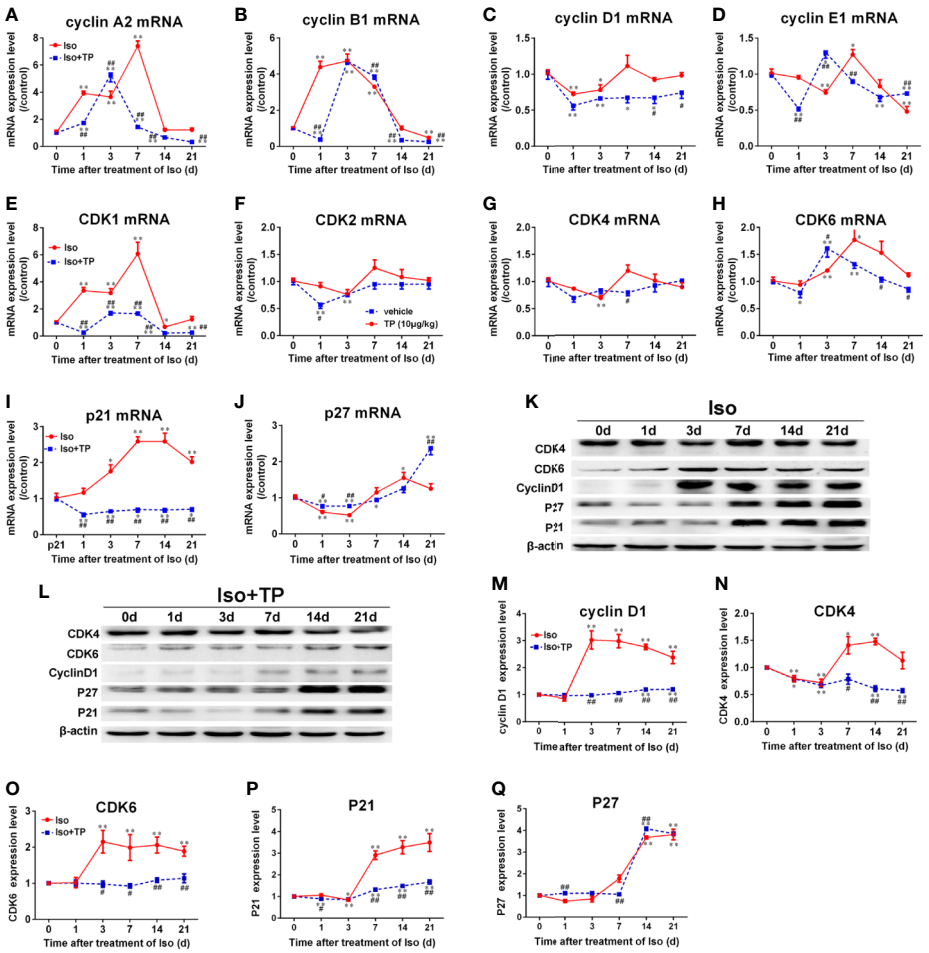

FIGURE 6 | The effects of TP on the myocardial expression of cell cycle regulators in mice. **(A–J)** The mRNA expression levels of all cell cycle regulators. **(K, L)** cyclin D1, CDK4 and 6, P21, and P27 protein levels as shown by Western blot analysis (n = 4 per group). **(M–Q)** The intensity of each band was quantified by densitometry and normalized to β-actin and control group. The data are shown as the mean ± SEM (n = 5), $^{*}P < 0.05$, $^{**}P < 0.01$ compared with the controls (0 day); $^{\#}P < 0.05$, $^{\#\#}P < 0.01$ compared with the Iso-treated group at the same time point (one-way ANOVA).

NRVMs during cardiac hypertrophy. The cariomyocytes response quickly to neurohumoral stimulators, such as Ang II and Iso. Ang II activates extracellular signal regulated kinase (ERK) and other MAPKs, as well as immediate-early gene, such as c-fos, which promote DNA synthesis. It has been reported that the increase of c-fos expression and ERK activation occur as quick as 2 min after Ang II stimulation (Sadoshima and Izumo, 1993; Aoki et al., 2000).

Cell cycle machinery driven by cyclin and CDK activity, is positively regulated by growth factors and negatively regulated by CDKI families. These CDKIs, which form complexes with cyclin–CDK, exert negative effects. The human genome encodes 21 CDKs, although only seven (CDK1-4, 6, 10, and 11) have been shown to have a direct role in cell cycle progression. Other CDKs play an indirect role *via* the activation of other CDKs, regulation of transcription or neuronal function (Malumbres et al., 2009; Sánchez-Martínez et al., 2015). In addition, it has been reported that the human genome contains 29 genes encoding cyclins (Malumbres and Barbacid, 2005). Of these, CDK1, 2, 4, and 6 and A, B, D, and E-type cyclins are identified as the major regulators of the cell cycle and are related to cell cycle progression (Bretones et al., 2015). Key regulators of G_1 progression are mainly cyclin D, which associates with and activates its catalytic partner CDK4, and CDK6 which phosphorylates the retinoblastoma protein (pRb), thereby activating E2F transcription factors. Cyclin E is mainly expressed at the G_1/S transition, and it binds to and activates CDK2 to accelerate the phosphorylation of the Rb proteins, which is required for entry into the S-phase and for DNA synthesis. Cyclin A/CDK2 plays a critical role in the control of the S phase and DNA replication and is also essential for G_2 progression. Cyclin A- and cyclin B-associated CDK1 regulates the G_2/M phases (Ahuja et al., 2007; Dai et al., 2013). Cell cycle activity is dependent on the balance between active and negative regulators (Zhang et al., 2015). The miR-16 inhibits the hypertrophic phenotype in cardiomyocytes through downregulation of CCND1, CCND2, and CCNE1 expression and inactivation of the cyclin/Rb pathway (Huang et al., 2015). Similar results were also seen in cyclin A2-overexpressing transgenic mice, including the induction

of cardiac regeneration, reduced scarring, improved LV function, and prevention of heart failure after myocardial infarction (Cheng et al., 2007). Cyclin A2 induces cardiac regeneration and improves cardiac function after myocardial injury (Shapiro et al., 2014). Cardiomyocyte cell cycle activation improves cardiac function after myocardial infarction (Hassink et al., 2008).

TP is an extract of the Chinese herb TwHF, which is widely used in China to treat autoimmune and inflammatory diseases due to its anti-inflammatory and immunosuppressive effects. TP attenuates pressure overload-induced myocardial remodeling in mice *via* the inhibition of NLRP3 inflammasome expression (Li et al., 2017). Additionally, in recent years, studies have suggested that TP could attenuate cardiac hypertrophy by upregulating FOXP3 expression and ameliorating cardiac fibrosis (Zhang et al., 2013; Ding et al., 2016). However, few studies have examined the regulatory role of TP in cardiomyocyte cycle regulator expression in cardiac hypertrophy.

Our results revealed that cyclin A1, p21, and p27 mRNA were highly expressed in NRVMs after stimulation with Ang II for 5 min. After 30 min, the mRNA expression levels of all cell cycle regulators showed a decreasing trend and reached their lowest levels at 1–3 h. Cell cycle analysis indicated that the number of myocytes in phases G_1 and G_2 was decreased compared with the 5 min group, which is related to the inhibition of the cell cycle. The expression of cell cycle regulators recovered later. Additionally, the number of myocytes in the S and G_2 phases increased and that in the G_1 phase decreased, demonstrating cell cycle reentry. However, only the expression of CDK1, p21, and p27 mRNA increased significantly after stimulation with Ang II for 24–48 h. The results showed the abnormal expression of cell cycle regulators with time during the process of hypertrophic response. Furthermore, a similar phenomenon occurs in adult myocytes; after treatment with Iso for 3–7 days, the expression levels of cell cycle regulators peaked, followed by a decreasing trend. After 21 days of Iso treatment, the mRNA expression levels of cyclin B1 and E1 were decreased markedly compared with those in the control group. In the present study, we found that the levels of the cell cycle inhibitors P21 and P27 were highest in the end stage of cardiac hypertrophy, whereas the cell cycle-promoting factors cyclins and CDK returned to the levels seen in normal adult myocytes. Interestingly, it has been shown that the effects of Ang II or Iso on protein expression were more obvious compared to effects on mRNA. Taken together, our results revealed abnormal expression of cell cycle regulators at both the mRNA and protein levels in NRVMs and adult mouse ventricles during cardiac hypertrophy. These findings indicate that cell cycle regulators are involved in cardiomyocyte hypertrophy. However, TP treatment attenuates the hypertrophy of cardiomyocytes through the effective correction of the abnormal expression of the cell cycle regulators cyclin, CDK, and CDKI. After treatment with Iso, from day 3 to day 21, heart index (HW/TL) and myocardial CSA increased significantly in the Iso group compared with the control group (0 day). Morphological analysis showed that myocardial injury, inflammatory cell infiltration and collagen deposition were markedly aggravated with increasing time in Iso-treated animals. Nevertheless, there was no significant between-group difference in the liver or kidney. The weights of the lung showed an increasing trend and were significantly increased in the Iso group compared with the control group after treatment with Iso for 21 days (data not shown). TP treatment could effectively prevent the abnormal expression of cell cycle regulators and markedly decrease the heart index, improve tissue injury and attenuate myocardial fibrosis compared with Iso groups.

The data in the current study indicate that the alteration of expression of cell cycle regulators is closely related with cardiac hypertrophy. Our study demonstrated that TP can mitigate pathological stimulation-induced cardiac hypertrophy and effectively alleviate the myocardial damage response *via* regulation of myocardial cell cycle regulators. In this study, we found that pathological cardiac hypertrophy in NRVMs and mice is associated with abnormal expression of β-MHC and the cell cycle regulators cyclin, CDK, and CDKI in cardiomyocytes and the myocardium. TP treatment significantly inhibits the occurrence of myocardial hypertrophy, reduces the left ventricular index, ameliorates pathological alterations by correcting the abnormal expression of various cell cycle regulators (**Figure 7**). Collectively, our results

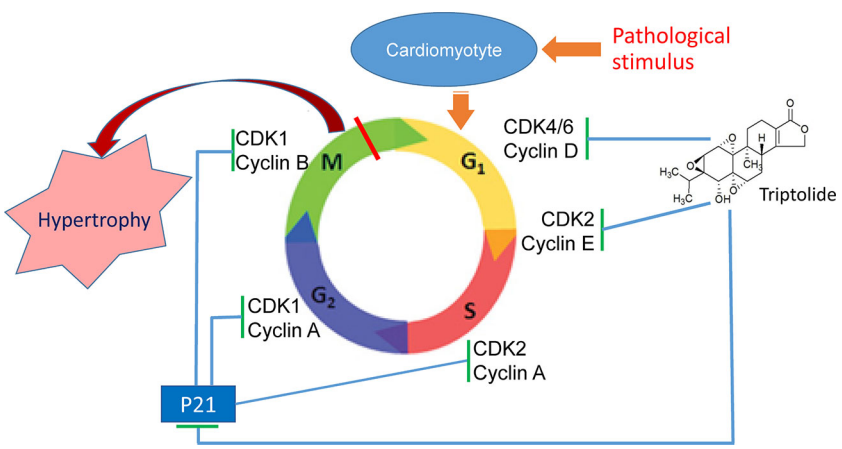

FIGURE 7 | Triptolide (TP) ameliorates cardiac hypertrophy *via* correcting the abnormal expression of cell cycle regulators in cardiomyocytes.

indicated that TP treatment had regulatory effects on cardiac hypertrophy induced by pathological stimulation and potentially acted through the inhibition of the abnormal expression of various cell cycle regulators, which is altogether indicative that the regulation of the cell cycle could become an important strategy for the prevention and treatment of cardiac hypertrophy.

Our study still has certain limitations. Although it has been found that the use of low dose of TP alone had no effects on the cell size of cariomyotytes *in vitro* and *in vivo* (Tong, 2015; Ding, 2017), its influence on the cell cycle of normal myocytes need to be explored. And the exact mechanism underlying the regulation of cell cycle regulators remains to be elucidated.

In summary, our results preliminarily revealed the temporal dynamic expression pattern of cell cycle regulators in cardiomyoctes during cardiac hypertrophy and demonstrated TP has the potential to attenuate cardiac hypertrophy *via* correction of the abnormal expression of various cell cycle regulators.

DATA AVAILABILITY STATEMENT

The raw data supporting the conclusions of this article will be made available by the authors, without undue reservation, to any qualified researcher.

ETHICS STATEMENT

The animal study was reviewed and approved by the Ethical Committee for Animal Experimentation of the Third Military Medical University.

AUTHOR CONTRIBUTIONS

H-GZ designed the experiments, drafted and revised the manuscript, and prepared the final version of the manuscript. X-HC and YL revised and prepared the final version of the manuscript. J-ML, Y-YD, YL, X-CP, and Y-FT performed the experiments and analyzed and interpreted the data. All authors contributed to the article and approved the submitted version.

FUNDING

This work was supported by grants from the Natural Science Foundation of Chongqing, China (No. cstc2018jcyjAX0504), and the Special project for promoting scientific and technological innovation capability: Frontier exploration project, Third Military Medical University (No. 2019XQY05).

REFERENCES

Ahuja, P., Sdek, P., and MacLellan, W. R. (2007). Cardiac myocyte cell cycle control in development, disease, and regeneration. *Physiol. Rev.* 87, 521–544. doi: 10.1152/physrev.00032.2006

Aoki, H., Richmond, M., Izumo, S., and Sadoshima, J. (2000). Specific role of the extracellular signal-regulated kinase pathway in angiotensin II-induced cardiac hypertrophy in vitro. *Biochem. J.* 347, 275–284. doi: 10.1042/bj3470275

Beltrami, A. P., Urbanek, K., Kajstura, J., Yan, S. M., Finato, N., Bussani, R., et al. (2001). Evidence that human cardiac myocytes divide after myocardial infarction. *N. Engl. J. Med.* 344, 1750–1757. doi: 10.1056/NEJM200106073442303

Bretones, G., Delgado, M. D., and León, J. (2015). Myc and cell cycle control. *Biochim. Biophys. Acta* 1849, 506–516. doi: 10.1016/j.bbagrm.2014.03.013

Cheng, R. K., Asai, T., Tang, H., Dashoush, N. H., Kara, R. J., Costa, K. D., et al. (2007). Cyclin A2 induces cardiac regeneration after myocardial infarction and prevents heart failure. *Circ. Res.* 100, 1741–1748. doi: 10.1161/CIRCRESAHA.107.153544

Cox, E. J., and Marsh, S. A. (2014). A systematic review of fetal genes as biomarkers of cardiac hypertrophy in rodent models of diabetes. *PloS One* 9, e92903. doi: 10.1371/journal.pone.0092903

Dai, L., Liu, Y., Liu, J., Wen, X., Xu, Z., Wang, Z., et al. (2013). A novel cyclinE/cyclinA-CDK inhibitor targets p27 (Kip1) degradation, cell cycle progression and cell survival: implications in cancer therapy. *Cancer Lett.* 333, 103–112. doi: 10.1016/j.canlet.2013.01.025

Di Stefano, V., Giacca, M., Capogrossi, M. C., Crescenzi, M., and Martelli, F. (2011). Knockdown of cyclin-dependent kinase inhibitors induces cardiomyocyte re-entry in the cell cycle. *J. Biol. Chem.* 286, 8644–8654. doi: 10.1074/jbc.M110.184549

Ding, Y. Y., Li, J. M., Guo, F. J., Liu, Y., Tong, Y. F., Pan, X. C., et al. (2016). Triptolide upregulates myocardial forkhead helix transcription factor p3 expression and attenuates cardiac hypertrophy. *Front. Pharmacol.* 7, 471. doi: 10.3389/fphar.2016.00471

Ding, Y. Y. (2017). *Role of p53-p21 signaling pathway in cardiac hypertrophy and effects of triptolide [dissertation/Master"s thesis]* (Chongqing, China: Third Military Medical University).

Eghbali, A., Dukes, A., Toischer, K., Hasenfuss, G., and Field, L. J. (2019). Cell cycle–mediated cardiac regeneration in the mouse heart. *Curr. Cardiol. Rep.* 21, 131. doi: 10.1007/s11886-019-1206-9

Estrella, N. L., Clark, A. L., Desjardins, C. A., Nocco, S. E., and Naya, F. J. (2015). MEF2D deficiency in neonatal cardiomyocytes triggers cell cycle re-entry and programmed cell death in vitro. *J. Biol. Chem.* 290, 24367–24380. doi: 10.1074/jbc.M115.666461

Fan, D., He, X., Bian, Y., Guo, Q., Zheng, K., Zhao, Y., et al. (2016). Triptolide modulates trem-1 signal pathway to inhibit the inflammatory response in rheumatoid arthritis. *Int. J. Mol. Sci.* 17, 498. doi: 10.3390/ijms17040498

Hassink, R. J., Pasumarthi, K. B., Nakajima, H., Rubart, M., Soonpaa, M. H., de la Rivière, A. B., et al. (2008). Cardiomyocyte cell cycle activation improves cardiac function after myocardial infarction. *Cardiovasc. Res.* 78, 18–25. doi: 10.1093/cvr/cvm101

Hinrichsen, R., Hansen, A. H., Haunsø, S., and Busk, P. K. (2008). Phosphorylation of pRb by cyclin D kinase is necessary for development of cardiac hypertrophy. *Cell Prolif.* 41, 813–829. doi: 10.1111/j.1365-2184.2008.00549.x

Hou, W., Liu, B., and Xu, H. (2019). Triptolide: medicinal chemistry, chemical biology and clinical progress. *Eur. J. Med. Chem.* 176, 378–392. doi: 10.1016/j.ejmech.2019.05.032

Huang, S., Zou, X., Zhu, J. N., Fu, Y. H., Lin, Q. X., Liang, Y. Y., et al. (2015). Attenuation of microRNA-16 derepresses the cyclins D1, D2 and E1 to provoke cardiomyocyte hypertrophy. *J. Cell Mol. Med.* 19, 608–619. doi: 10.1111/jcmm.12445

Li, J., Zhu, W., Leng, T., Shu, M., Huang, Y., Xu, D., et al. (2011). Triptolide-induced cell cycle arrest and apoptosis in human renal cell carcinoma cells. *Oncol. Rep.* 25, 979–987. doi: 10.3892/or.2011.1158

Li, Y., Hu, S., Ma, G., Yao, Y., Yan, G., Chen, J., et al. (2013). Acute myocardial infarction induced functional cardiomyocytes to re-enter the cell cycle. *Am. J. Transl. Res.* 5, 327–335.

Li, R., Lu, K., Wang, Y., Chen, M., Zhang, F., Shen, H., et al. (2017). Triptolide attenuates pressure overload-induced myocardial remodeling in mice via the inhibition of NLRP3 inflammasome expression. *Biochem. Biophys. Res. Commun.* 485, 69–75. doi: 10.1016/j.bbrc.2017.02.021

Lin, Y., Wang, L. N., Xi, Y. H., Li, H. Z., Xiao, F. G., Zhao, Y. J., et al. (2008). L-arginine inhibits isoproterenol-induced cardiac hypertrophy through nitric oxide and polyamine pathways. *Basic Clin. Pharmacol. Toxicol.* 103, 124–130. doi: 10.1111/j.1742-7843.2008.00261.x

Ma, X., Song, Y., Chen, C., Fu, Y., Shen, Q., Li, Z., et al. (2011). Distinct actions of intermittent and sustained β-adrenoceptor stimulation on cardiac remodeling. *Sci. China Life Sci.* 54, 493–501. doi: 10.1007/s11427-011-4183-9

Malumbres, M., and Barbacid, M. (2005). Mammalian cyclin-dependent kinases. *Trends Biochem. Sci.* 30, 630–641. doi: 10.1016/j.tibs.2005.09.005

Malumbres, M., Harlow, E., Hunt, T., Hunter, T., Lahti, J. M., Manning, G., et al. (2009). Cyclin-dependent kinases: a family portrait. *Nat. Cell Biol.* 11, 1275–1276. doi: 10.1038/ncb1109-1275

Martens, M. D., Field, J. T., Seshadri, N., Day, C., Chapman, D., Keijzer, R., et al. (2020). Misoprostol attenuates neonatal cardiomyocyte proliferation through Bnip3, perinuclear calcium signaling, and inhibition of glycolysis. *J. Mol. Cell. Cardiol.* 146, 19–31. doi: 10.1016/j.yjmcc.2020.06.010

Noel, P., Von Hoff, D. D., Saluja, A. K., Velagapudi, M., Borazanci, E., and Han, H. (2019). Triptolide and its derivatives as cancer therapies. *Trend. Pharmacol. Sci.* 40, 327–341. doi: 10.1016/j.tips.2019.03.002

Oliveira, A., Beyer, G., Chugh, R., Skube, S. J., Majumder, K., Banerjee, S., et al. (2015). Triptolide abrogates growth of colon cancer and induces cell cycle arrest by inhibiting transcriptional activation of E2F. *Lab. Invest.* 95, 648–659. doi: 10.1038/labinvest.2015.46

Pan, J. (2010). RNA polymerase - an important molecular target of triptolide in cancer cells. *Cancer Lett.* 292, 149–152. doi: 10.1016/j.canlet.2009.11.018

Pasumarthi, K. B., and Field, L. J. (2002). Cardiomyocyte cell cycle regulation. *Circ. Res.* 90, 1044–1054. doi: 10.1161/01.RES.0000020201.44772.67

Pillai, V. B., Samant, S., Sundaresan, N. R., Raghuraman, H., Kim, G., Bonner, M. Y., et al. (2015). Honokiol blocks and reverses cardiac hypertrophy in mice by activating mitochondrial Sirt3. *Nat. Commun.* 6, 6656. doi: 10.1038/ncomms7656

Sadoshima, J., and Izumo, S. (1993). Molecular characterization of angiotensin II–induced hypertrophy of cardiac myocytes and hyperplasia of cardiac fibroblasts. Critical role of the AT1 receptor subtype. *Cir. Res.* 73, 413–423. doi: 10.1161/01.res.73.3.413

Sánchez-Martínez, C., Gelbert, L. M., Lallena, M. J., and de Dios, A. (2015). Cyclin dependent kinase (CDK) inhibitors as anticancer drugs. *Bioorg. Med. Chem. Lett.* 25, 3420–3435. doi: 10.1016/j.bmcl.2015.05.100

Shapiro, S. D., Ranjan, A. K., Kawase, Y., Cheng, R. K., Kara, R. J., Bhattacharya, R., et al. (2014). Cyclin A2 induces cardiac regeneration after myocardial infarction through cytokinesis of adult cardiomyocytes. *Sci. Transl. Med.* 6, 224ra27. doi: 10.1126/scitranslmed.3007668

Taglieri, D. M., Monasky, M. M., Knezevic, I., Sheehan, K. A., Lei, M., Wang, X., et al. (2011). Ablation of p21-activated kinase-1 in mice promotes isoproterenol-induced cardiac hypertrophy in association with activation of Erk1/2 and inhibition of protein phosphatase 2A. *J. Mol. Cell. Cardiol.* 51, 988–996. doi: 10.1016/j.yjmcc.2011.09.016

Tan, X., Li, J., Wang, X., Chen, N., Cai, B., Wang, G., et al. (2011). Tanshinone IIA protects against cardiac hypertrophy via inhibiting calcineurin/NFATc3 pathway. *Int. J. Biol. Sci.* 7, 383–389. doi: 10.7150/ijbs.7.383

Tane, S., Ikenishi, A., Okayama, H., Iwamoto, N., Nakayama, K. I., and Takeuchi, T. (2014). CDK inhibitors, p21(Cip1) and p27(Kip1), participate in cell cycle exit of mammalian cardiomyocytes. *Biochem. Biophys. Res. Commun.* 443, 1105–1109. doi: 10.1016/j.bbrc.2013.12.109

Tong, Y. F. (2015). *Effects of triptolide on expression of cyclin-dependent kinase inhibitor 1a and cardiac hypertrophy in vitro and in vivo. [dissertation/master"s thesis]* (Chongqing, China: Third Military Medical University).

Wen, H. L., Liang, Z. S., Zhang, R., and Yang, K. (2013). Anti-inflammatory effects of triptolide improve left ventricular function in a rat model of diabetic cardiomyopathy. *Cardiovasc. Diabetol.* 12, 50. doi: 10.1186/1475-2840-12-50

Zebrowski, D. C., and Engel, F. B. (2013). The cardiomyocyte cell cycle in hypertrophy, tissue homeostasis, and regeneration. *Rev. Physiol. Biochem. Pharmacol.* 165, 67–96. doi: 10.1007/112_2013_12

Zhang, Z., Qu, X., Ni, Y., Zhang, K., Dong, Z., Yan, X., et al. (2013). Triptolide protects rat heart against pressure overload-induced cardiac fibrosis. *Int. J. Cardiol.* 168, 2498–2505. doi: 10.1016/j.ijcard.2013.03.001

Zhang, Y., Mignone, J., and MacLellan, W. R. (2015). Cardiac regeneration and stem cells. *Physiol. Rev.* 95, 1189–1204. doi: 10.1152/physrev.00021.2014

Ziaei, S., and Halaby, R. (2016). Immunosuppressive, anti-inflammatory and anti-cancer properties of triptolide: A mini review. *Avicenna. J. Phytomed.* 6, 149–164.

Conflict of Interest : The authors declare that the research was conducted in the absence of any commercial or financial relationships that could be construed as a potential conflict of interest.

frontiers in Pharmacology

REVIEW
published: 17 September 2020
doi: 10.3389/fphar.2020.572941

tRNA-Derived Small RNAs and Their Potential Roles in Cardiac Hypertrophy

*Jun Cao, Douglas B. Cowan and Da-Zhi Wang**

Department of Cardiology, Boston Children's Hospital, Harvard Medical School, Boston, MA, United States

Transfer RNAs (tRNAs) are abundantly expressed, small non-coding RNAs that have long been recognized as essential components of the protein translation machinery. The tRNA-derived small RNAs (tsRNAs), including tRNA halves (tiRNAs), and tRNA fragments (tRFs), were unexpectedly discovered and have been implicated in a variety of important biological functions such as cell proliferation, cell differentiation, and apoptosis. Mechanistically, tsRNAs regulate mRNA destabilization and translation, as well as retro-element reverse transcriptional and post-transcriptional processes. Emerging evidence has shown that tsRNAs are expressed in the heart, and their expression can be induced by pathological stress, such as hypertrophy. Interestingly, cardiac pathophysiological conditions, such as oxidative stress, aging, and metabolic disorders can be viewed as inducers of tsRNA biogenesis, which further highlights the potential involvement of tsRNAs in these conditions. There is increasing enthusiasm for investigating the molecular and biological functions of tsRNAs in the heart and their role in cardiovascular disease. It is anticipated that this new class of small non-coding RNAs will offer new perspectives in understanding disease mechanisms and may provide new therapeutic targets to treat cardiovascular disease.

Keywords: tRNA-derived small RNAs (tsRNAs), tRNA halves, tRNA fragments, heart, cardiac hypertrophy, mitochondria, non-coding RNAs, cardiovascular disease

OPEN ACCESS

Edited by:
Xiongwen Chen,
Temple University, United States

Reviewed by:
Qi Chen,
University of California, Riverside, United States
Aristeidis G. Telonis,
University of Miami, United States

***Correspondence:**
Da-Zhi Wang
Da-Zhi.Wang@childrens.harvard.edu

Specialty section:
This article was submitted to Cardiovascular and Smooth Muscle Pharmacology, a section of the journal Frontiers in Pharmacology

Received: *15 June 2020*
Accepted: *28 August 2020*
Published: *17 September 2020*

Citation:
Cao J, Cowan DB and Wang D-Z (2020) tRNA-Derived Small RNAs and Their Potential Roles in Cardiac Hypertrophy. Front. Pharmacol. 11:572941. doi: 10.3389/fphar.2020.572941

INTRODUCTION

Small noncoding RNA (sncRNA) usually refers to RNA molecules less than 200 nucleotides (nt) in length, which are transcribed from DNA, but not translated into protein. SncRNAs include but are not limited to microRNAs (miRNAs), endogenous short interfering RNAs (siRNAs), small nuclear RNAs (snRNAs), small nucleolar RNAs (snoRNAs), piwi interacting RNAs (piRNAs), ribosomal RNA derived fragments (rRFs), transfer RNAs (tRNAs), and their derived small RNAs (tsRNAs) (Mattick and Makunin, 2006; Kirchner and Ignatova, 2015; Wei et al., 2017; Lambert et al., 2019). With the advance of high-throughput RNA sequencing (Giraldez et al., 2018; Liu et al., 2019), new classes of sncRNAs are being discovered and studied.

Different sncRNAs exert diverse but specific functions in cells. For example, miRNAs and siRNAs regulate gene expression by tuning mRNA stability and translational efficiency (Valencia-Sanchez et al., 2006). In addition, snRNAs promote proteome diversity by regulating pre-mRNA splicing (Valadkhan,

2005), snoRNAs modify rRNAs, snRNAs, and even mRNAs with 2′-O-methylated nucleotides (Kiss, 2002), and piRNAs contribute to transposon silencing (Ozata et al., 2019). Studies have also uncovered multiple molecular pathways and functions related to a single type of sncRNAs (Kiss, 2002; Pillai, 2005; Rojas-Rios and Simonelig, 2018). Consequently, it is conceivable that new mechanisms and functions of sncRNAs remain to be discovered.

The important and various molecular functions of sncRNAs in cells make them vital regulators in both physiological and pathological conditions, such as during development (Mendell, 2008; Chen and Wang, 2012; Rojas-Rios and Simonelig, 2018), cancer progression (Ling et al., 2013; Peng and Croce, 2016; Romano et al., 2017), neurodegenerative disease (Rege et al., 2013; Watson et al., 2019), and cardiovascular disease (Romaine et al., 2015; Zhou et al., 2018). Among sncRNAs, tRNA-derived small RNAs (tsRNAs) have gained considerable attention as these molecules have various subtypes that are generated by different mechanisms and exert a variety of critical functions in cells. Moreover, they are also implicated in development and disease. As tsRNAs are expressed in the heart and participate in the function of this organ, we will focus on their biogenesis and function, and we will discuss potential research opportunities to study the role of tsRNAs in the heart.

BIOGENESIS AND EXPRESSION OF NUCLEAR AND MITOCHONDRIAL ENCODED TRANSFER RNAs

In eukaryotic cells, both the nucleus and mitochondria encode tRNA genes, producing two types of tRNAs—cytoplasmic tRNAs and mitochondrial tRNAs (mt-tRNAs). There are more than 500 tRNA genes either identified or predicted to exist in humans (Chan and Lowe, 2009; Chan and Lowe, 2016). About half of them are verified to be actively expressed genes (Schimmel, 2018), which are transcribed to 51 isoacceptor tRNA types and decode to 61 codons for translation (Mahlab et al., 2012; Chan and Lowe, 2016). Therefore, some codons are derived from multiple tRNA genes in the human genome. In contrast, mt-tRNAs are transcribed from only 22 mt-tRNA genes in the mitochondrial genome. These mt-tRNA genes play critical roles in assisting translation of mitochondrial proteins with less redundancy. Mutations in mt-tRNAs have also been implicated as important components in cardiovascular diseases such as coronary heart disease (Jia et al., 2013; Jia et al., 2019), cardiomyopathy (Taniike et al., 1992; Casali et al., 1995; Arbustini et al., 1998; Marin-Garcia et al., 2001; Hsu et al., 2008), and hypertension (Liu et al., 2009; Wang et al., 2011; Jiang

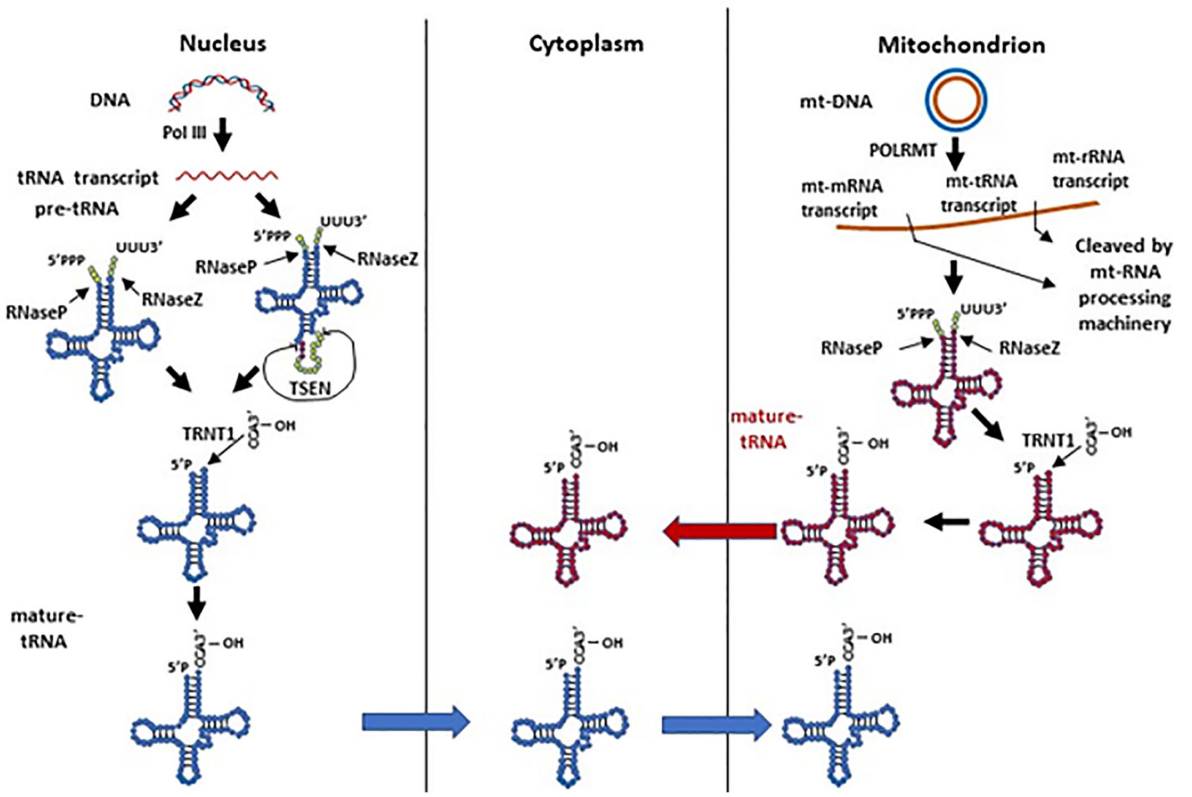

FIGURE 1 | The biogenesis of human nuclear and mitochondrial encoded tRNAs. Pre-tRNAs can be transcribed by Pol III in the nucleus or by POLRMT in mitochondria. The pre-tRNAs have 5'-leader and 3'-trailer sequences, which are trimmed by RNase P and RNase Z, respectively. A minority of nuclear pre-tRNAs have introns, which are spliced by the TSEN complex. A single "CCA" sequence is then added to all trailer trimmed 3'-ends of human tRNAs by the TRNT1 protein. Processed nuclear tRNAs are transported to the cytoplasm, while mitochondrial tRNAs predominantly remain in mitochondria.

et al., 2016). It is worth noting that cytoplasmic tRNAs can be imported to mitochondria, which suggests that they may also play essential roles in mitochondrial biology and disease (Rubio et al., 2008; Mercer et al., 2011).

Human nuclear tRNA genes are initially transcribed by RNA polymerase III (RNA Pol III) as pre-tRNAs, which contain 5'-leader and 3'-trailer sequences (Phizicky and Hopper, 2010). The 5'-leader and 3'-trailer are trimmed by RNase P (Frank and Pace, 1998) and RNase Z (Maraia and Lamichhane, 2011), respectively (**Figure 1**). Following that, a single "CCA" sequence is added to all trailer trimmed 3'-ends of human tRNAs by tRNA nucleotidyl transferase (TRNT1) (Anderson and Ivanov, 2014). A minority of human pre-tRNAs have intron sequences, which are spliced by a nuclear tRNA splicing endonuclease (TSEN) during tRNA processing (Anderson and Ivanov, 2014). TSEN cleaves a pre-tRNA containing intron into three parts: a 5'-exon with a 2'-3'-cyclic phosphate at its 3' end, a 3'-exon with a 5'-hydroxyl group (5'-OH) at its 5'-end, and the excised intron (Anderson and Ivanov, 2014). After the cleavage, the 5'-exon and 3'-exon are ligated to become a mature tRNA before being transported to the cytoplasm. In contrast, mitochondrial tRNA genes are transcribed by mitochondrial RNA polymerase (POLRMT) along with mitochondrial rRNA and mRNA genes in a long mitochondrial polycistronic DNA template (Suzuki et al., 2011). The mt-tRNA transcripts are then cleaved from rRNA and mRNA transcripts by mitochondrial RNA-processing enzymes according to the mt-tRNA "punctuation" model (Ojala et al., 1981; Rossmanith et al., 1995; Barchiesi and Vascotto, 2019). Similar to cytoplasmic pre-tRNAs, mitochondrial pre-tRNAs require RNase P and ELAC2 (mitochondrial RNase Z) to remove the 5'-leader and 3'-trailer, respectively (Rossmanith et al., 1995; Brzezniak et al., 2011; Suzuki et al., 2011; Haack et al., 2013; Siira et al., 2018). Finally, a "CCA" sequence is attached to the 3' terminus of mt-tRNA by a mitochondrial TRNT1 to complete mt-tRNA maturation (Suzuki et al., 2011). Mature human cytoplasmic tRNAs are usually 76 to 93 nts in size and form a cloverleaf-like secondary structure with stem and loop regions, and they are eventually compacted into an L-shape tertiary structure (Schimmel, 2018). Mature mt-tRNAs range from 59 to 75 nts in size with smaller stem and loop regions, and some of them lack entire domains (Schimmel, 2018). The mt-tRNAs form a non-canonical cloverleaf-like secondary structure (Helm et al., 1998; Suzuki et al., 2011; Schimmel, 2018) and L-shape tertiary structure (Messmer et al., 2009; Salinas-Giege et al., 2015). It is worth noting that mitochondrial tRNA-lookalikes have been detected in the nuclear genome in human and some other primates (Telonis et al., 2014; Telonis et al., 2015a), suggesting that mitochondria may not be the sole source of mitochondrial tRNAs. However, it remains elusive 1) whether these nuclear-encoded mitochondrial tRNA lookalikes are actively expressed; 2) if so, whether these tRNAs are transported to cytoplasm and/or mitochondria; and 3) what functions they may exert in different cellular compartments.

Although it seems that tRNA processing undergoes two parallel and separate systems in the nucleus and mitochondrion, we should not rule out the possibility of tRNA dynamics between these organelles (**Figure 1**). As mentioned above, nuclear-encoded tRNAs are able to shuttle between the cytoplasm and mitochondria (Rubio et al., 2008; Mercer et al., 2011); mitochondrial tRNA lookalikes exist in the nuclear genome (Telonis et al., 2014; Telonis et al., 2015a). On the other hand, though mature human mt-tRNAs mainly function in the mitochondria for mitochondrial gene translation, they have also been reported to be in the cytoplasm (Maniataki and Mourelatos, 2005). Moreover, the tRNA splicing endonuclease TSEN, which is expressed solely in the nucleus in humans, is located on the mitochondrial surface in yeast (Dhungel and Hopper, 2012; Hopper and Nostramo, 2019). In yeast, nuclear pre-tRNAs with introns have to be exported to the cytoplasm and spliced on the surface of mitochondria (Dhungel and Hopper, 2012; Hopper and Nostramo, 2019). These spliced tRNAs are subsequently modified in the cytoplasm, and imported back to the nucleus for additional modification before being again exported to the cytoplasm to carry out their intended function (Dhungel and Hopper, 2012; Hopper and Nostramo, 2019). Even though human cytoplasmic tRNA processing does not have this splicing step on mitochondria like yeast, it remains unclear whether these organelles play any other roles in cytoplasmic tRNA processing or modification, and whether mt-tRNAs have any function in the cytoplasm.

TRANSFER RNA-DERIVED SMALL RNAs (tsRNAs)

In general, tsRNAs can be grouped into two categories based on their size and biogenesis: tRNA halves (or tRNA-derived, stress-induced RNAs, also known as tiRNAs) and tRNA-derived fragments (also known as tRFs) (Anderson and Ivanov, 2014) (**Figure 2**). The tRNA halves or tiRNAs refer to the tsRNAs that are half the size of tRNAs. The tRFs usually refer to even smaller tsRNAs, which have a range of sizes based on their cleavage.

It is worth noting that "tRFs", "tRNA halves", and "tsRNAs" were sometimes used interchangeably because the nomenclature for them was not initially clear. For instance, some studies referred to "tRNA halves" as "tRFs" (Ivanov et al., 2011; Li et al., 2016; Sharma et al., 2016), while other studies referred to "tsRNAs" as "tRFs" (Anderson and Ivanov, 2014; Liapi et al., 2020). Therefore, we advise authors to scrutinize the literature carefully when reading and/or citing them so as to obtain extensive and precise information for each category of tsRNAs.

Transfer RNA Halves (tiRNAs)

The tRNA halves are generated by specific cleavage in or close to the anticodon region, which leads to 30-50 nt long 5' and 3' tRNA halves (Anderson and Ivanov, 2014). A number of studies showed that tRNA halves are expressed minimally in human cell lines, but are induced during stress conditions including oxidative stress (Thompson et al., 2008; Yamasaki et al., 2009), nutritional deficiency (Fu et al., 2009), hypoxia (Fu et al., 2009), heat shock (Fu et al., 2009; Yamasaki et al., 2009), UV irradiation (Yamasaki et al., 2009), and viral infection (Wang et al., 2013). Since tRNA halves are part of mature tRNAs, there is a question

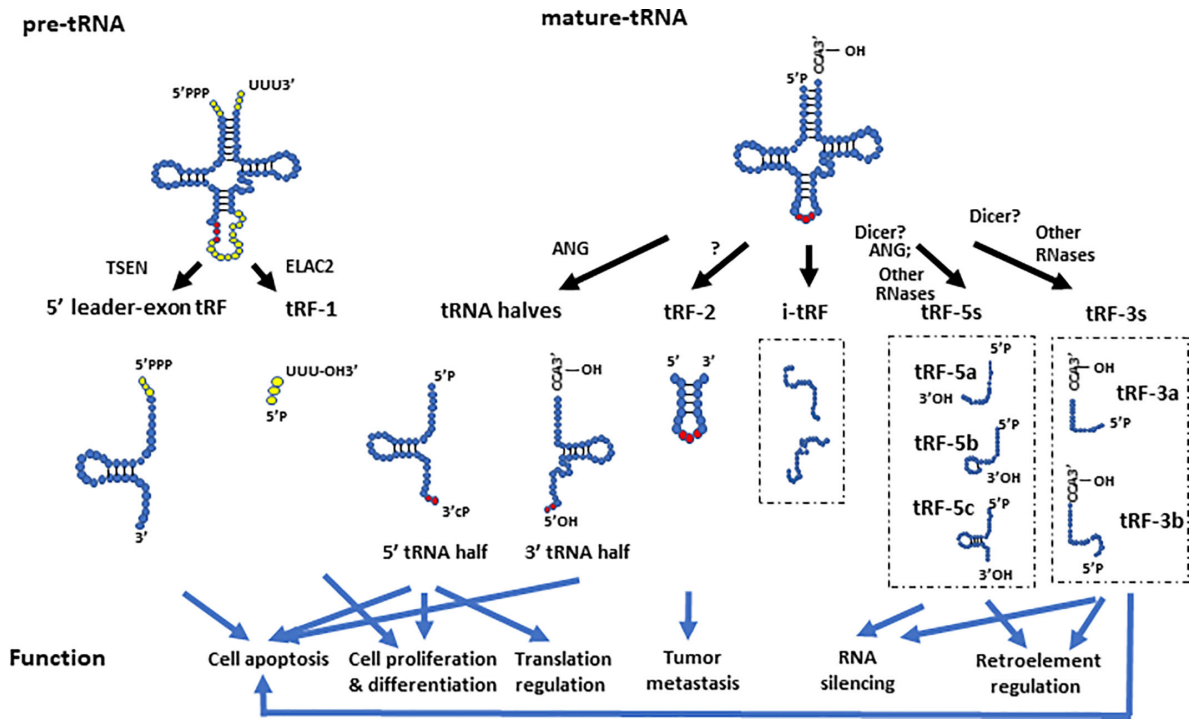

FIGURE 2 | The biogenesis and function of different tsRNAs derived from pre- and mature- tRNAs. The 5' leader-exon tRFs and tRF-1s are generated from cleavage of pre-tRNAs by TSEN and ELAC2, respectively. The 5'- and 3'- tRNA halves are generated by cleavage of mature tRNAs at the anticodon region by ANG. tRF-2s contain anticodon stem and loop regions of mature tRNAs. The tRF-5 group includes tRF-5a, tRF-5b, and tRF-5c, which are generated by endonucleolytic cleavage of mature tRNAs at D loop, D stem, and the stem regions between the D stem and anticodon loop, respectively. The tRF-3 group includes the tRF-3a and tRF-3b subgroups, which are generated by endonucleolytic cleavage of mature tRNAs at different locations of their T arms. The i-tRFs are generated from internal parts of tRNAs, whose 5' termini start from the second or subsequent nucleotide of mature tRNAs. They are usually about 36 nts in size, and have various subtypes. This figure only showed two examples of i-tRFs. The different tsRNAs contribute to a variety of molecular processes such as translational regulation, RNA silencing, and retro-element regulation. They are also involved in tumor metastasis, apoptosis, cell proliferation, and differentiation.

whether these tRNA halves are artificial degradation by-products derived from tRNAs that have real functions in cells and tissues. Multiple pieces of evidence have demonstrated the specificity of tiRNA biogenesis, implying that they may actually possess unique functions in the cell. First, several studies have shown the level of tRNA halves do not always correlate with the levels of their cognate mature tRNAs (Gebetsberger and Polacek, 2013; Honda et al., 2015; Krishna et al., 2019). For instance, arsenite stress induced Met-tRNA halves without affecting their parental mature Met-tRNA levels (Yamasaki et al., 2009). Second, tRNA halves were enriched in fetal mouse liver, while expressed at low levels in the heart (Fu et al., 2009), which suggests that tRNA halves have specific expression patterns in different tissues. In addition, Gly-, Val-, Met-, and Arg- tRNA halves were dramatically increased upon nutritional starvation, while Tyr-tRNA halves were not induced (Fu et al., 2009); thereby, reinforcing the idea of specific biogenesis of tRNA halves in different conditions. In line with this work, a recent study identified tRNA halves in mouse serum by RNA-Seq, and revealed that Gly- and Val- tRNA halves together account for ~90% of circulating tRNA halves, whereas the majority of these molecules are below detectable limits (Dhahbi et al., 2013). Interestingly, 5' tRNA halves were found to be much more enriched than 3' tRNA halves in serum (Dhahbi et al., 2013), which indicates a specific role for 5' tRNA halves compared with 3' tRNA halves in mouse serum (Dhahbi et al., 2013). However, we would like to point out that we could not rule out the possibility that 3' tRNA halves may be underestimated. 3'-tRNA halves were found to be charged with amino acids at their 3'-end in cancer cells, which may prevent their detection in small RNA sequencing or PCR amplification based methods involving adaptor ligations (Honda et al., 2015). In addition, some of the 3'-tRNA halves, such as 3'-His-tRNA halves, cannot be detected by RACE due to the presence of guanine at their 5' end, as that residue is often modified to 1-methyl-guanosine (m^1G), which inhibits reverse-transcription (Honda et al., 2015). In summary, the expression levels of tRNA halves vary across different conditions, tissues, species, and 5' vs 3' origins, and they do not always correlate with their cognate mature tRNA expression levels, which together demonstrate a specificity in their biogenesis. Although individual tRNA halves have been characterized in different cells or tissues, how genome wide tRNA halves are expressed in various tissues and conditions remains an open question.

tRNA halves are recognized to be generated by angiogenin cleavage during stress (Fu et al., 2009; Yamasaki et al., 2009).

Angiogenin (ANG), also known as ribonuclease 5, is a secreted ribonuclease that cleaves tRNAs into tRNA halves both *in vitro* and *in vivo* (Fu et al., 2009; Yamasaki et al., 2009; Su et al., 2019). Exogenous expression of ANG (Fu et al., 2009) or the knockdown of an ANG inhibitor (RNH1) (Yamasaki et al., 2009) promotes the generation of tRNA halves, while knock down of ANG itself reduces the levels of stress-induced tRNA halves (Yamasaki et al., 2009). After ANG cleaves tRNAs at the anticodon region, it leaves 2'- 3'- cyclic phosphates at the 3' ends and hydroxyl groups at 5' ends of tRNA halves (Yamasaki et al., 2009). It is worth noting that since these 2'-3'-cyclic phosphates may inhibit detection by small RNA sequencing or PCR amplification based methods involving adaptor ligations, there might be an underestimation of existing tRNA halves when performing the above quantification methods. The 2'- 3'- cyclic phosphates at the 3' ends and hydroxyl groups at 5' ends of tRNA halves differentiate tRNA halves from other small RNAs cleaved by Dicer or RNase III type enzymes, which usually have a 5' phosphate rather than a 5' hydroxyl group (Kumar et al., 2016). Although ANG is a major contributor for tRNA halves, it is not clear what other nucleases may also contribute to the generation of tRNA halves. Additional research would provide a greater understanding of the biogenesis of tRNA halves.

Transfer RNA-Derived Fragments (tRFs)

tRFs are even smaller fragments derived from mature tRNAs or pre-tRNAs—usually 14–32 nt in length. Similar to tRNA halves, various tRFs have distinct expression patterns in different tissues (Kawaji et al., 2008), and there is no correlation between parental tRNA levels and their derived tRF levels (Kim et al., 2017). In addition, certain parental tRNAs only produce certain subtypes of tRFs (Su et al., 2019). Even when derived from the same parental tRNAs, some tRFs are differentially expressed (Li et al., 2012; Kumar et al., 2014; Telonis et al., 2015b), which is referred to as asymmetric processing of tRFs from mature tRNAs (Li et al., 2012). For instance, a recent research study examined the abundance of tRFs in transcriptomic data from 452 healthy people and 311 breast cancer patients, and found that different tRFs form the same parental tRNAs do not have correlated abundance (Telonis et al., 2015b). In addition, it identified specific genomic loci clusters that may be responsible for generation of particular types of tRFs (Telonis et al., 2015b), which suggests that the abundance of particular tRFs, at least partially, depends on their genomic location. Collectively, these studies indicate that tRFs are likely not random degradation by-products of tRNAs, but seem to have their own specific biogenesis and function independent of their parental tRNAs in different biological conditions.

Depending on their cleavage sites and origin, tRFs can be divided into several groups such as tRF-1s (also known as 3'U tRFs), tRF-2s, tRF-3s (also known as 3'CCA tRFs), tRF-5s, i-tRFs (Telonis et al., 2015b), and 5' leader-exon tRFs (Gebetsberger and Polacek, 2013; Goodarzi et al., 2015; Shen Y. et al., 2018). The tRF-2s, tRF-3s, tRF-5s, and i-tRFs are derived from mature tRNAs, whereas tRF-1s and 5' leader-exon tRFs are generated from pre-tRNAs (Shen Y. et al., 2018). As discussed above, a mature tRNA forms a cloverleaf secondary structure. Cloverleaf-like tRNAs have four arms, which are designated as the acceptor stem, dihydrouridine (D) stem-loop (D arm), anticodon stem-loop, and TψC stem-loop (T arm) (Schimmel, 2018). tRF-2s are a newly discovered type of tRF identified in breast cancer cells, and they primarily contain anticodon stem and loop regions of tRNAs (Goodarzi et al., 2015; Kumar et al., 2016). This type of tRF is stress sensitive, and is significantly increased under hypoxic conditions (Goodarzi et al., 2015). The tRF-3s and tRF-5s are generated by endonucleolytic cleavage of mature tRNAs at the T arm and D arm, respectively (Anderson and Ivanov, 2014). A recent study sequenced tRFs in HEK293 cells and divided tRF-5s to three subtypes: tRF-5a (~15 nt in size), tRF-5b (~22 nt in size) and tRF-5c (~32 nt in size), which are generated by endonucleolytic cleavage of mature tRNAs at D loop, D stem, and the stem region between the D stem and anticodon loop, respectively (Kumar et al., 2014). The tRF-5cs may straddle the categories of tRF-5s and tRNA halves, as it is known that ANG can cleave tRNAs before the anticodon region which could potentially generate tRNA halves shorter than the typical 35 nts (Honda et al., 2015; Shigematsu and Kirino, 2017). The tRF-3s were classified into two sub-classes based on their tRF sequencing in HEK293 cells: tRF-3a (~18 nt in size) and tRF-3b (~22 nts in size), which are generated by endonucleolytic cleavage of mature tRNAs at different areas of their T arms (Kumar et al., 2014). It is worth noting that the subgroups of tRFs are not strictly defined by length, as tRF size may vary in different tissues or biological conditions. For example, additional tRF-5s with lengths of 20, 26, 33, and 36 nts as well as tRF-3s with lengths of 33 and 36 nts, were identified in a dataset from lymphoblastoid cell lines (Telonis et al., 2015b). The i-tRFs (internal fragments) were newly identified tRFs in breast cancer samples and breast cancer cell lines (Telonis et al., 2015b). This type of tRFs correspond to an internal part of mature tRNAs, which means that they neither start from the exact 5' terminus (the first nucleotide of 5' terminus) nor end at the 3' terminus (any base in 3' terminal "CCA" sequence) of mature tRNAs (Telonis et al., 2015b). Instead, the 5' terminus of i-tRFs starts from the second or subsequent nucleotide of mature tRNAs, and they are usually about 36 nts in size (Telonis et al., 2015b). This differentiates this type of tRFs from tRF-3s and tRF-5s.

Aside from tRNA halves, small tRFs usually possess both a 5'-phosphate and 3'-hydroxyl group (Haussecker et al., 2010). Since Dicer recognizes the 5'-phosphate group of small RNAs (Park et al., 2011), it was initially considered to be required for the processing of tRF-3s and tRF-5s. However, there are studies that indicate the existence of both Dicer-dependent and Dicer-independent biogenesis of tRFs. Therefore, it remains unknown if Dicer is indispensable for generation of tRFs or whether it is required for some types of tRFs under certain conditions. Some tRF-3s were detected by high-throughput sequencing in wild-type mouse embryonic stem cells (mESCs), but not in mESCs with a Dicer 1 deletion, which suggests that the generation of tRF-3s requires Dicer 1 (Babiarz et al., 2008). In line with this work, depletion of Dicer significantly reduced the abundance of tRF-5s derived from Gln-tRNAs in HeLa cells (Cole et al., 2009), which reinforces the importance of Dicer for

the generation of tRFs. On the other hand, there are a number of studies that show Dicer is dispensable for tRF biogenesis. For instance, knockout of Dicer or DGCR8 (a microprocessor complex subunit) did not exert any effect on tsRNA expression in mESCs (Li et al., 2012). Consistently, mutation of DICER1/DGCR8 did not decrease tRF expression in mouse ESCs (Kumar et al., 2014). In addition, ANG, which has been identified as an endonuclease contributing to the biogenesis of tRNA halves, was found to contribute to the generation of tRFs (Li et al., 2012). RNase A, RNase I, and RNase T1 were also found to be able to cleave tRNAs to tRFs, and the tRFs derived from RNase T1 cleavage were different from the ones digested by ANG and RNase A/I (Li et al., 2012).

tRF-1s derived from the 3' end of pre-tRNAs contain a stretch of U residues that are usually produced by RNA polymerase III (Lee et al., 2009). Since the tRF-1s are generated from pre-tRNAs, they would be assumed to reside in the nucleus; however, tRF-1s can also be located in the cytoplasm (Lee et al., 2009; Kumar et al., 2014). The tRF-1s were found to be cleaved by ELAC2 in the cytoplasm, and tRF-1 expression levels are regulated by ELAC2 in prostate cancer cell lines (Lee et al., 2009). On the other hand, Dicer was found not to be a regulator for tRF-1 in HEK293 cells (Haussecker et al., 2010). Another type of tRFs derived from pre-tRNAs are the 5' leader-exon tRFs, which were discovered in mouse embryonic fibroblasts (MEFs) with RNA sequencing (Hanada et al., 2013). This type of tRFs contain a complete 5' leader triphosphate group followed by the 5' exon tRNA sequence, and their expression decreases upon TSEN depletion (**Figure 2**) (Hanada et al., 2013). The 5' leader-exon tRFs are stress sensitive, as they were induced by H_2O_2, but not ANG in MEFs (Hanada et al., 2013).

MOLECULAR AND BIOLOGICAL FUNCTIONS OF tsRNAs

The tRNA halves and different tRFs have specific molecular functions that allow them to play distinct roles in different conditions. The tsRNAs regulate a variety of biological processes including translation (Emara et al., 2010; Ivanov et al., 2011) (Kim et al., 2017), RNA stability (Haussecker et al., 2010; Kumar et al., 2014; Kuscu et al., 2018), retro-element reverse transcription and post-transcription (Schorn et al., 2017; Boskovic et al., 2020), apoptosis (Saikia et al., 2014), cell proliferation and differentiation (Honda et al., 2015; Krishna et al., 2019). These characteristics involve them in many physiological and pathological conditions, including development (Krishna et al., 2019), aging (Dhahbi et al., 2013), neurodegenerative diseases (Hanada et al., 2013), cancer (Honda et al., 2015), and cardiovascular diseases (Shen L. et al., 2018) (**Table 1**) (**Figure 2**).

tRNA Halves (tiRNAs)

The most well-characterized function of tRNA halves is their inhibitory effect on protein translation (Ivanov et al., 2011; Sobala and Hutvagner, 2013; Krishna et al., 2019). Exogenous expression of 5'-tRNA halves but not 3'-tRNA halves have been found to induce phospho-eIF2α independent assembly of stress granules and inhibit protein translation in cultured U2OS cells (Emara et al., 2010; Ivanov et al., 2011). In particular, the 5'-Ala tRNA halves were found to bind with translation inhibitor YB-1, and cooperate with YB-1 to displace eIF4G/A from uncapped and capped mRNAs as well as dissociate eIF4F from the m^7G cap, which leads to repression of protein translation (Ivanov et al., 2011).

Despite it being accepted that ANG induces tRNA halves *vivo* (Fu et al., 2009; Yamasaki et al., 2009; Su et al., 2019), there are many outstanding questions about the relationship between stress, ANG, enriched tRNA halves, and translational arrest that have yet to be answered. For instance, is ANG the only stress-induced enzyme responsible for tRNA halves? Is there any difference in the species of tRNA halves derived from different sources of stress? Is YB-1 indispensable for the translational inhibition by tRNA halves? A recent study showed that there are both ANG-dependent and ANG-independent tRNA halves induced by high concentration arsenite, which suggests that ANG may be not the only RNase responsible for generation of tRNA-halves under this particular stress condition (Su et al., 2019). Moreover, high concentrations of arsenite resulted in translational arrest in both wild-type and ANG depleted U2OS cells, suggesting that ANG regulated translational repression does not account for all of the translational control caused by stress (Su et al., 2019). To comprehensively answer these questions, more research needs to be done.

At cellular level, a variety of tRNA halves have been shown to exert divergent functions such as cell apoptosis, proliferation, and differentiation. ANG-induced tRNA halves were fund to interact with cytochrome c (Cyt c) to protect cells from chronic hyperosmotic stress-induced apoptosis (Saikia et al., 2014). Cyt c is a peripheral protein located at the mitochondrial inner membrane, where it functions to transport electrons between complex III and complex IV of the respiratory chain (Garrido et al., 2006). During apoptosis, the mitochondrial membrane is permeabilized, allowing Cyt c to be released into the cytoplasm (Reubold and Eschenburg, 2012). Cytosolic Cyt c binds apoptotic protease activating factor 1 (Apaf-1) (Zou et al., 1999) to activate caspase pathways, which leads to the morphological changes observed in apoptosis (Zou et al., 1999; Wang, 2001). A recent study detected 20 enriched tRNA halves in the Cyt c ribonucleoprotein complex, and showed that ANG treatment mitigated stress-induced apoptosis in primary neurons (Saikia et al., 2014). As a result, it proposed that ANG-induced tRNA halves bind to Cyt c and prevent it from activating caspases and apoptosis (Saikia et al., 2014).

Sex hormone-dependent tRNA halves were found to be enriched in estrogen receptor-positive breast cancer and androgen receptor-positive prostate cancer, where they enhanced cell proliferation (Honda et al., 2015). In addition, stable tRNA halves were found to be in extracellular exosomes and transferred between breast cancer cell cells (Gambaro et al., 2019). Proliferative cancer cells are prone to migration, escaping the immune response to form a metastatic niche that undergoes

TABLE 1 | Summary of transfer RNA-derived small RNAs (tsRNAs) and their biological functions.

Tissue/Cell line	Inducers	tsRNA type	Examples of tsRNAs	Biological functions	Molecular mechanisms	Reference
U2OS	ANG	5'-tRNA halves	5'-Ala-tRNA halves; 5'-Cys-tRNA halves	Repress translation	The 5'-tRNA halves cooperate with YB-1 to displace eIF4G/A from uncapped and capped mRNAs, thus inhibit translation.	(Ivanov et al., 2011)
Mouse Embryonic Fibroblasts	ANG	5'-tRNA halves; 3'-tRNA halves	5'-Asp-tRNA halves; 3'-Arg-tRNA halves; 3'-Gly-tRNA halves; 3'-Ala-tRNA halves	Inhibit cell apoptosis	The tRNA halves bind to Cyt c and prevent Cyt c from binding to Apaf-1 and activating caspase pathways.	(Saikia et al., 2014)
Breast cancer and prostate cancer cells	ANG and sex hormone	5'-tRNA halves	5'-Asp-tRNA halves; 5'-His-tRNA halves	Promote cell proliferation	Unknown	(Honda et al., 2015)
Mouse embryonic stem cells	Endogenously detected	5'-tRNA halves	5'-Gln-tRNA halves; 5'-Gly-tRNA halves; 5'-Glu- tRNA halves; 5'-Val- tRNA halves	Facilitate cell differentiation	The 5'- tRNA halves interact with IGF2BP1, and prevent IGF2BP1 from binding to and stabilizing the transcripts of c-*myc*, which is a pluripotency-promoting factor.	(Krishna et al., 2019)
Mouse sperms	High-fat diet	5'-tRNA halves	5'-Gly-tRNA halves; 5'-Glu-tRNA halves; 5'-Val- tRNA halves	Promote intergenerational inheritance of metabolic disorder	May affect expression of genes involving apoptosis, autophagy, oxidative stress, glucose input etc.	(Chen et al., 2016)
Breast cancer cells	Endogenously detected	tRF-2s	tRF-Gly; tRF-Asp; tRF-Glu; tRF-Tyr	Suppress cancer progression and metastasis	The tRF-2s displace 3'UTR of oncogenic transcripts from protein YBX1, which reduces stability of oncogenic transcripts.	(Goodarzi et al., 2015)
Hela, HCT-116 cells	Endogenously detected	tRF-3s	tRF-Leu	Promote cell viability	The tRF-3s interact with ribosomal protein mRNAs *RPS28* and *RPS15* to enhance their translation, which results in fine-tuning of gene expression in cells.	(Kim et al., 2017)
HEK293T	Endogenously detected	tRF-3s	tRF-Leu; tRF-Cys	RNA silencing	The tRFs target RNAs by base pairing, and associate Argonaute-GW182 containing RISC to mediate gene silencing.	(Kuscu et al., 2018)
Mouse stem cells	Endogenously detected	tRF-3s	tRF-Lys	Inhibit retrotransposition	22nt tRF-3s mediate post-transcriptional gene silencing; 18nt tRF-3s inhibit reverse transcription of retrotransposons.	(Schorn et al., 2017)
Human and mouse embryonic stem cells	Endogenously detected	tRF-5s	tRF-Gly	Inhibit retroelement transcription; regulate Cajal body biogenesis	The tRFs positively regulate histone genes, which repress retroelement transcription; the RNA binding proteins hnRNPF and hnRNPH bind to the tRFs, which are required for generation of Cajal body.	(Boskovic et al., 2020)
HEK293; A549; MCF7, mouse tissue etc.	Endogenously detected	tRF-5s	tRF-Tyr; tRF-Asp; tRF-Lys; tRF-Gly; tRF-Arg etc.	May regulate RNA silencing	The tRF-5s are associated with Argonaute proteins.	(Kumar et al., 2014)
Breast cancer samples and breast cancer cell lines	Endogenously detected	i-tRFs	tRF-Asp, tRF-Gly, mitochondrial tRF-Glu	unknown	unknown	(Telonis et al., 2015b)
HEK293, HCT-116 cells	Endogenously detected	tRF-1s	tRF-Ser	The antisense sequence of the tRFs enhances RNA silencing	The antisense sequence of tRFs enhances Ago2 loading to duplexed double-stranded RNA.	(Haussecker et al., 2010)
Prostate cancer cell lines	Endogenously detected	tRF-1s	tRF-Ser	Promote cell proliferation	Unknown	(Lee et al., 2009)
Mouse embryonic stem cells; spinal cord	CLP1 depletion; H_2O_2	5' leader-exon tRFs	tRF-Tyr	Promote motor neuron loss	The tRFs may contribute to neuron loss in CLP1 knockout mice by coupling to p53 dependent cell death.	(Hanada et al., 2013)

angiogenesis (Osaki and Okada, 2019). Therefore, tRNA halves seemingly participate in both intracellular and extracellular signal transduction in cancer.

Besides their role in cancer, tRNA halves also define the cellular state of mESCs (Krishna et al., 2019). Sequencing of small RNAs in mESCs under several differentiation regimens revealed that tsRNAs such as 5'-Gln-, Glu-, Val-, and Gly-tRNA halves were enriched in differentiated cells compared with isogenic stem-like cells (Krishna et al., 2019). Transfection of mimics of these 5'-tRNA halves inhibited pluripotency, whereas blocking these 5'-tRNA halves using antisense oligonucleotides enhanced cell pluripotency (Krishna et al., 2019). This study also identified tsRNA associated proteins such as IGF2BP1, YBX1, and RPL10 by pulldown assays flowed with mass spectrometry, and showed that binding of 5'-tRNA halves with IGF2BP1 prevented it from binding to c-*myc* mRNA; thereby, facilitating differentiation of mESCs (Krishna et al., 2019).

Transfer RNA Fragments

At molecular level, tRFs have been demonstrated to be involved in regulating mRNA stability (Haussecker et al., 2010; Kumar et al., 2014; Kuscu et al., 2018), translation (Kim et al., 2017), and retro-element regulation (Boskovic et al., 2020). The tRF-5s and tRF-3s were found to be associated with the human Argonaute proteins AGO1, 3, and 4 by photoactivatable ribonucleoside-enhanced crosslinking and immunoprecipitation (PAR-CLIP) in HEK293 cells (Kumar et al., 2014), which raised the question of whether tRFs are involved in gene silencing pathways like miRNAs. miRNAs usually harbor 7–8 nucleotide long seeding sequences at their 5' end to base pair with the 3'UTR of mRNAs (Bartel, 2009) at the same time nucleotide positions 8–13 interact with AGO (Hafner et al., 2010; Kumar et al., 2014). Interestingly, tRF-5s and tRF-3s were found to be associated with AGO in a miRNA like pattern (*i.e.* tRF-3s interact with AGO at nucleotide positions 8–12 and tRF-5s binds to AGO at nucleotide position 7 (Kumar et al., 2014). Additionally, thousands of RNAs were found to interact with tRF-3s and tRF-5s *via* AGO1 by human AGO1 cross-linking, ligation, and sequencing of hybrids (CLASH) (Kumar et al., 2014).

A recent study revealed that tRF-3s regulate mRNA expression *via* AGO-dependent and Dicer-independent pathways (Kuscu et al., 2018). The tRF-3s were demonstrated to be associated with Argonaute by immunoprecipitation followed by northern blotting (Kuscu et al., 2018). Transfection of tRF-3s decreased luciferase activity of mRNAs containing the complementary sequence of tRF-3s (Kuscu et al., 2018). This regulation of luciferase activity by tRF-3s was abolished by depletion of Argonaute proteins but not Dicer (Kuscu et al., 2018). In addition, the tRF-3s were also found to be associated with GW182/TNRC6 proteins (Kuscu et al., 2018), which are critical players in assisting mRNA degradation processes with RNA-induced silencing complexes (RISCs) (Eulalio et al., 2009). Collectively, these findings illustrated the mechanism by which tRFs base-pair match with target RNAs, and slice RNAs by associating with Argonaute and GW182/TNRC6 proteins (Eulalio et al., 2009). Not only have tRFs been found to be loaded on Argonaute proteins, but also the loading itself is cell-type-specific (Telonis et al., 2015b).

Apart from regulation of mRNA degradation, tRF-3s were also determined to be able to influence proteomics by affecting ribosomal biogenesis (Kim et al., 2017). The tRF-3s from LeuCAG tRNAs were found to bind to ribosomal protein mRNAs *RPS28* and *RPS15* by base-pairing (Kim et al., 2017). Inhibition of LeuCAG tRF-3s resulted in reduced translation of *RPS28* and *RPS15* mRNAs, which decreased abundance of 40S ribosomal subunits and eventually led to cell apoptosis (Kim et al., 2017). Furthermore, tRFs have also been shown to be associated with RNA binding proteins to affect gene expression. The tRF-2s derived from tRNA-Glu in breast cancer cells were shown to harbor YBX1 binding motifs and able to bind YBX1 protein, thus displacing the 3'UTR of oncogenic transcripts from YBX1 and suppressing the stability of oncogenic transcripts (Goodarzi et al., 2015). Similarly, several tRFs from nuclear tRNA-His, tRNA-Ala, and mitochondrial tRNA-Glu were found to harbor HuR binding motifs in breast cancer datasets (Telonis and Rigoutsos, 2018). Since HuR is involved in multiple biological functions including alternative splicing (Zhu et al., 2006; Izquierdo, 2008; Zhou et al., 2011; Akaike et al., 2014), alternative polyadenylation (Zhu et al., 2007; Dai W. et al., 2012), stabilizing mRNA transcripts (Fan and Steitz, 1998; Peng et al., 1998; Wang et al., 2000a; Wang et al., 2000b; Sengupta et al., 2003), destabilizing transcripts (Kim et al., 2009; Chang et al., 2010; Cammas et al., 2014), and mediating translation efficiency (Kullmann et al., 2002; Gorospe, 2003; Mazan-Mamczarz et al., 2003; Glorian et al., 2011), it is conceivable that tRFs may interact with HuR similar to YBX1. The molecular functions of tRFs associated with RNA binding proteins such as HuR remain to be fully understood. Besides these effects on mRNA stability and translation, particular tRFs were found to modulate histone expression and mediate reverse transcriptional and post-transcriptional regulation of endogenous retro-elements (Schorn et al., 2017; Boskovic et al., 2020). The regulation of tRFs on retro-elements not only helped to protect genome integrity, but could also regulate the expression of protein-coding genes through these embedded retro-elements in their introns and/or exons (Sharma et al., 2016; Boskovic et al., 2020).

The multiple functions of tsRNAs in various pathways demonstrates their critical role in biological processes such as apoptosis, proliferation, and differentiation as well as (Lee et al., 2009; Hanada et al., 2013; Kim et al., 2017) in pathological

TABLE 2 | Summary of transfer RNA-derived small RNAs (tsRNAs) expressed in cardiac tissue.

tsRNA types	Examples of tsRNA	References
5' tRNA halves	5'-Val-tRNA halves	(Fu et al., 2009; Dhahbi et al., 2013)
5' tRNA halves	5'-Gly-tRNA halves	(Dhahbi et al., 2013; Dhahbi, 2015)
5' leader-exon tRFs	tRF-Tyr	(Hanada et al., 2013)
tRF-3s	tRF-Arg; tRF-Gln	(Torres et al., 2019)
tRF-5s	tRF-Gly; tRF-Cys	(Torres et al., 2019)
tRF-5s	tRF-Gly	(Shen L. et al., 2018)

conditions such as neurodegenerative diseases (Hanada et al., 2013) and cancer (Goodarzi et al., 2015).

TRANSFER RNA-DERIVED SMALL RNAs IN THE HEART

Investigation of the expression and function of tsRNAs in the heart has just started, which opens up both opportunities and challenges. Previous studies have shown the existence of tsRNAs in the heart (**Table 2**). 5' tRNA halves from Val- (Fu et al., 2009; Dhahbi et al., 2013) and Gly-tRNAs (Dhahbi, 2015) (Dhahbi et al., 2013) were detected in mouse hearts by northern blot analysis. The 5' leader-exon tRFs from Tyr-tRNAs are also expressed in mouse hearts, and their levels were augmented upon CLP1 deletion (Hanada et al., 2013). CLP1 is a component of the mRNA 3' end processing complex, and it has been found to be associated with the TSEN complex and, potentially, contributes to pre-tRNA splicing (Hanada et al., 2013). Depletion of CLP1 led to accumulation of Tyr-5' leader-exon tRFs in multiple tissues including the cortex, spinal cord, heart, and kidney, and eventually results in progressive motor neuron loss (Hanada et al., 2013). Transgenic expression of CLP1 in motor neurons can rescue impaired neuronal function in CLIP1 knockout mice (Hanada et al., 2013), but it remains elusive how these Tyr- 5' leader-exon tRFs in cardiac tissue may affect heart function. Specific tRF-3s and tRF-5s were also detected human heart tissues. For example, tRF-3s from Arg- and Gln-tRNA, as well as tRF-5s from Gly- and Cys- tRNAs were detected in human heart tissues (Torres et al., 2019).

ROLE OF TRANSFER RNA-DERIVED SMALL RNAs IN CARDIAC HYPERTROPHY

A very recent study identified tRF-5s enriched in isoproterenol (ISO)-induced hypertrophic rat hearts by small RNA transcriptome sequencing, and indicated that these tRF-5s may contribute to intergenerational inheritance of cardiac hypertrophy (Shen L. et al., 2018). These tRF-5s were demonstrated to bind to the 3'UTR of the hypertrophic regulator *Timp3* mRNA to inhibit its expression, leading to hypertrophy of cardiomyocytes (Shen L. et al., 2018). Importantly, these tRFs were found enriched in sperm from ISO-induced hypertrophic mice compared to healthy male mice (Shen L. et al., 2018). In addition, the F1 offspring derived from ISO-treated mice exhibited increased cardiac muscle fiber breakage, hypertrophic marker gene expression, cell apoptosis, and fibrosis in their hearts when compared to the F1 from healthy controls (Shen L. et al., 2018). Therefore, the study raised a very intriguing question of whether tsRNAs induced by cardiac hypertrophy could be inherited by the next generation and lead to pathogenesis. In fact, there are several lines of evidence consistently indicating that tsRNAs are enriched in sperm (Chen et al., 2016; Sharma et al., 2016; Natt et al., 2019; Sarker et al., 2019; Zhang et al., 2019). Some studies demonstrated the intergenerational inheritance of tsRNAs by injecting tsRNAs from the sperm of males fed a high fat diet into normal zygotes, and showed the offspring had altered expression of metabolic pathway components in addition to developing a metabolic disorder (Chen et al., 2016; Sarker et al., 2019). Therefore, it would be interesting to investigate more thoroughly whether tsRNAs-induced cardiac hypertrophy could also be inherited, which may identify novel therapeutic targets.

At the molecular level, the tRF-5s may not be the only functional tsRNAs involved in cardiac hypertrophy. Deep small RNA sequencing with advanced bioinformatic tools could help to identify or verify extensive tsRNAs in cardiac hypertrophy. High-throughput sequencing combined with immunoprecipitation (*i.e.* RNA immunoprecipitation (RIP)-seq) could be employed to detect Argonaute protein associated tsRNAs involved in cardiac hypertrophy. It would be also important to test whether neutralization of tsRNAs by antisense oligonucleotides could rescue the heart from fibrosis and the hypertrophic response. Moreover, because tRF-5s can inhibit retro-element transcription and regulate Cajal body biogenesis (Boskovic et al., 2020), it would be interesting to test whether these functions are all or partly associated with tRF-5-mediated cardiac hypertrophy. Furthermore, upon having defined specific tsRNAs involved in cardiac hypertrophy, the mRNA networks which are associated with tsRNAs in cardiac hypertrophy could be explored by pulling down mRNAs in hypertrophic hearts with *in vitro* transcribed tsRNAs that are labeled with digoxigenin or biotin. Alternatively, CLASH-seq experiments could be employed to directly crosslink endogenous tsRNA-mRNA hybrids in hypertrophic hearts for detection. On the other hand, tsRNA-associated protein networks could be determined through tsRNA pull down assays followed by mass-spectrometry or western blotting. It is anticipated that identification of cardiac hypertrophy associated tsRNAs and further defining their function in the heart will shed light onto novel therapeutic targets and approaches to treat cardiac disease.

ROLE OF TRANSFER RNA-DERIVED SMALL RNA INDUCERS AND REGULATORS IN CARDIAC HYPERTROPHY

While increasing evidence supports the direct involvement of tsRNAs in the heart, we may also learn how tsRNA biogenesis-related "inducers" and "regulators" participate in governing cardiac function and hypertrophy. The inducers and regulators mentioned here refer to currently known factors that control expression of tsRNAs.

Oxidative Stress in Cardiac Hypertrophy

Cardiac cells undergo pathological hypertrophy in response to mechanical stress. Although it is an adaptive process to increase contractility (*i.e.* compensated hypertrophy), it eventually leads

to a high risk for heart failure through pathological remodeling (*i.e.* decompensated hypertrophy) (Frey and Olson, 2003; Diwan and Dorn, 2007; Nakamura and Sadoshima, 2018). Oxidative stress is an important inducer of this response (Takimoto and Kass, 2007; Maulik and Kumar, 2012). It occurs when excessive reactive oxygen species (ROS) are produced that cannot be offset by the intrinsic antioxidant defenses (Takimoto and Kass, 2007). ROS include superoxide and hydroxyl radicals as well as hydrogen peroxide (Takimoto and Kass, 2007). Because these molecules are inducers of tRNA halves (Thompson et al., 2008; Yamasaki et al., 2009) it would be interesting to study their role in oxidative stress-induced cardiac hypertrophy. Specifically, ROS induces mitochondrial DNA mutations, damages mitochondrial membrane permeability, as well as the respiratory chain and anti-oxidant defenses (Guo et al., 2013), which can further trigger cell apoptosis through mitochondrial stress and downstream signaling pathways (Chen et al., 2018). Mitochondrial dynamics and metabolism have been found to play a pivotal role in regulating differentiation of stem cells to cardiomyocytes (Chung et al., 2007; Porter et al., 2011); maintaining cardiomyocyte function (Piquereau et al., 2013; Eisner et al., 2017; Zhao et al., 2019), and mediating hypertrophy of cardiomyocytes (Rosca et al., 2013; Pennanen et al., 2014). The intrinsic links between ROS, mitochondria biology, and cardiac hypertrophy/cardiac function makes it an intriguing area to explore how tsRNAs might be functionally involved in any of these processes. Although not much research has been done, there are several lines of evidence indicating the existence of mitochondrial-derived tsRNAs in humans (Telonis et al., 2015b; Natt et al., 2019). Moreover, mitochondrial-derived tsRNAs were found to be enriched in sperms from people eating a high-sugar diet for a week compared to sperms from the same people eating a normal diet (Natt et al., 2019). These findings imply a potentially significant role for mitochondrial tsRNAs in intergenerational inheritance. As mentioned above, cardiac hypertrophy has been shown to affect offspring through sperm tsRNAs, it would therefore be extremely interesting to unveil the potential role of mitochondrial tsRNAs in cardiac function, and decipher whether these small ncRNAs could lead to intergenerational inheritance of cardiac hypertrophy. On the other hand, a very recent study showed that a paternal low-protein diet promoted ROS production in the testicular germ cells, which led to ATF7 activation and further reduced H3K9me2 expression (Abel and Doenst, 2011; Zhang and Chen, 2020). The altered epigenetic status affected tsRNA biogenesis and their expression profile in the spermatozoa, which resulted in intergenerational effects (Abel and Doenst, 2011; Zhang and Chen, 2020). This not only reinforced the tsRNA function in intergenerational inheritance but also revealed the link between oxidative stress, tsRNA generation, and epigenetic regulation. These studies also raised questions about whether oxidative stress-induced cardiac hypertrophy could transmit intergenerationally, and if so, whether ATF7 and/or epigenetic alterations could be considered as therapeutic targets for inherited cardiac hypertrophy.

Aging and Caloric Intake in Cardiac Hypertrophy

Aging and excessive caloric intake are highly associated with cardiac hypertrophy (Dong et al., 2007; Dai D. F. et al., 2012; Chiao and Rabinovitch, 2015; Wang et al., 2015). Elevated ROS released by mitochondria has been proposed to be the primary driving force of aging and a major determinant of lifespan (Harman, 1972; Miquel et al., 1980; Dai et al., 2014). Consistent with this, ROS production by mitochondria, as well as disrupted mitochondrial function, have been shown in the aging brain, heart, and skeletal muscle tissues (Sawada and Carlson, 1987; Capel et al., 2005; Retta et al., 2012; Tocchi et al., 2015; Lesnefsky et al., 2016; Boengler et al., 2017; Grimm and Eckert, 2017). Aging intertwines with ROS related mitochondrial DNA mutation, respiratory chain deterioration, and mitochondrial metabolism impairment (Fleming et al., 1982; Wallace, 1992). The disrupted mitochondrial function along with aging increases production of ROS, which, in turn (as introduced above), could affect mitochondria by damaging mitochondrial DNA and causing functional deterioration, which is referred to as the "vicious cycle" concept (Alexeyev et al., 2004; Dai et al., 2014). Therefore, age-related cardiac hypertrophy is a complex syndrome from a mitochondrial function and oxidative stress perspective. On the other hand, 3'-tRFs and 5'-tRFs were detected in rat brain, and the 3'-tRFs were found to be increased with rat age (Karaiskos and Grigoriev, 2016). Thus it is conceivable that tsRNAs might be enriched in aging hearts, and age-related hypertrophic hearts. Moreover, there is also an interesting link between calorie restriction and aging retardation as well as cardiac functional improvement. A number of studies suggest that caloric restriction can prevent or reduce cardiac hypertrophy, improve cardiac function, and even retard aging (Yu, 1994; Cruzen and Colman, 2009; Dolinsky et al., 2010; de Lucia et al., 2018; An et al., 2020). Although the mechanisms are still unclear, there is evidence showed that aging and caloric restriction can modulate specific 5' tRNA halves (Dhahbi et al., 2013). Val- and Gly-5'-tRNA halves were found to be enriched in aged mouse serum when compared to young mice and that caloric restriction mitigated these differences (Dhahbi et al., 2013). In addition, as introduced above, several studies have shown that high sugar or high fat diets affect mitochondrial and other tsRNA expression profiles in sperm (Chen et al., 2016; Natt et al., 2019; Sarker et al., 2019). So, it would be interesting to determine the role of tsRNAs in the dynamics of aging, oxidative stress, and metabolism during development of cardiac hypertrophy.

ANG in Cardiac Hypertrophy and Heart Failure

ANG is a major inducer of tRNA halves (Thompson et al., 2008; Fu et al., 2009; Yamasaki et al., 2009; Su et al., 2019), and several studies suggest ANG is involved in cardiac hypertrophy and heart failure (Patel et al., 2008; Jiang et al., 2014; Yu et al., 2018; Oldfield et al., 2020). ANG not only functions as an RNase, but is also a potent stimulus for angiogenesis (Tello-Montoliu et al.,

2006). Pro-angiogenic factors such as vascular endothelial growth factor (VEGF), basic fibroblast growth factor, and ANG, are involved in the development of cardiac hypertrophy (Oldfield et al., 2020). Cardiomyocytes secret pro-angiogenic molecules to support vascular growth to increase blood flow in the hypertrophic heart (Oldfield et al., 2020). Interestingly, ANG has been proposed to be a biomarker for left ventricular systolic dysfunction and heart failure (Patel et al., 2009; Jiang et al., 2014; Yu et al., 2018). A clinical study collected serum from 16 patients with heart failure with preserved ejection fraction (HFpEF) and 16 healthy individuals, and found that ANG differed the most among 507 proteins between the two groups (Jiang et al., 2014). Particularly, the average serum ANG level was 374 ng/ml (%95 CI 348–400 ng/ml) in healthy controls and 477 ng/ml (95% CI 438–515 ng/ml) in HFpEF patients ($P<0.001$) (Jiang et al., 2014). A follow-up study were performed in 203 patients with coronary heart failure (CHF), 413 coronary heart disease patients without chronic heart failure (also called CHD disease controls), and 53 healthy controls to explore the potential utility of ANG as a biomarker (Yu et al., 2018). The CHF group were further subgrouped into heart failure with reduced ejection fraction (HFrEF) and heart failure with preserved ejection fraction (HFpEF). It was found that the CHF group had higher ANG plasma levels compared with either healthy controls or CHD disease controls. The HFrEF patients had higher ANG plasma levels compared with HFpEF patients or CHD disease control patients.

Besides cardiac hypertrophy and heart failure, ANG has been linked to other diseases such as diabetes (Altara et al., 2018) and hypertension (Marek-Trzonkowska et al., 2015). Therefore, it is likely that dysregulation of ANG in cardiac hypertrophy, heart failure, and other cardiovascular diseases may lead to tsRNA dysregulation in the heart, and it is worth further investigating the potential biological function of ANG-induced tsRNAs in these instances.

ELAC2 in Cardiac Hypertrophy

Cytosolic ELAC2 contributes to the generation of tRF-1 (Lee et al., 2009), while mitochondrial ELAC2 is responsible for mt-tRNA processing (Brzezniak et al., 2011; Siira et al., 2018). A few studies suggest that ELAC2 is implicated in mitochondrial disorders and cardiac hypertrophy (Haack et al., 2013; Siira et al., 2018). Cardiac-specific ELAC2 deletion in mice leads to reduced mitochondrial protein synthesis, OXPHOS biogenesis, mitochondrial oxygen consumption, and disruption of regulatory non-coding RNAs (Siira et al., 2018). The combined disruptive effects causes early-onset dilated cardiomyopathy and premature death by 4 weeks (Siira et al., 2018). Furthermore, mutations in the human *ELAC2* gene is associated with mt-tRNA processing defects associated with cardiac hypertrophy (Haack et al., 2013). Unfortunately, the underling mechanisms remain unclear and the role of mitochondria in cardiac hypertrophy and heart failure is dynamic and complicated.

During the development of cardiac hypertrophy, mitochondria compensate by increasing oxidative phosphorylation and ATP synthesis (Rabinowitz and Zak, 1975); however, this can result in mitochondrial dysfunction (Zhou and Tian, 2018). This complication can disrupt the electron transport chain and APT production, as well as affecting the modification of proteins, calcium homeostasis, and inflammation, which are important contributors to cardiac hypertrophy and heart failure (Abel and Doenst, 2011; Rosca et al., 2013; Zhou and Tian, 2018). Consequently, it would be interesting to determine the following: 1) ELAC2 function in mitochondria during compensation and decompensation, 2) ELAC2 levels in hypertrophic hearts, and 3) the functional role of these tsRNAs in cardiac hypertrophy.

Hypoxia in Cardiac Hypertrophy

Though hypoxia can generate tRNA halves (Fu et al., 2009), it is also associated with cardiac hypertrophy due to increases in oxygen consumption and reductions in the blood supply to the enlarged heart (Kumar et al., 2018). Sustained hypoxia leads to reprogramming of gene expression and metabolism, which further aggravate decompensated cardiac hypertrophy and, ultimately, lead to heart failure (Giordano, 2005; Chu et al., 2012; Mirtschink and Krek, 2016). So, it is not surprising that an ischemic injury causes up-regulation of Val-and Gly-tRNA derived tRF-5s in the rat brain as determined using deep sequencing (Li et al., 2016). Consistent with this observation, these tRF-5s were also enriched in a hind limb ischemia model and in hypoxic endothelial cells (Li et al., 2016). Moreover, exogenously expressed Val- and Gly-tRF-5s repress cell proliferation, migration, and tube formation in hypoxic endothelial cells (Li et al., 2016). Coincidently, tsRNAs from Val- (Fu et al., 2009) (Dhahbi et al., 2013) and Gly-tRNAs (Dhahbi, 2015) (Dhahbi et al., 2013) were documented to be detectable in mouse hearts by northern blot. Therefore, it would be worthwhile to test whether these tsRNAs are regulated by hypoxia during cardiac hypertrophy.

CONCLUSION AND PERSPECTIVES OF TRANSFER RNA-DERIVED SMALL RNAs IN CARDIOVASCULAR BIOLOGY AND MEDICINE

The tsRNAs are newly-identified sncRNAs derived from endonucleolytic cleavage of pre-tRNAs or mature tRNAs. Based on differences in cleavage sites and the size of cleavage products, tsRNAs are divided into tRNA halves and tRFs. tRNA halves can regulate stress granule assembly and protein translation (Emara et al., 2010; Ivanov et al., 2011), and affect cell apoptosis (Saikia et al., 2014), proliferation (Honda et al., 2015) and differentiation (Krishna et al., 2019). tRFs are also involved in mRNA stability regulation (Haussecker et al., 2010; Kumar et al., 2014; Kuscu et al., 2018), translation regulation (Kim et al., 2017), and retro-element transcriptional regulation (Boskovic et al., 2020). These tsRNAs play important roles in physiological and pathological conditions such as development (Krishna et al., 2019), aging (Dhahbi et al., 2013), neurogenerative diseases (Hanada et al., 2013), cancer (Honda et al., 2015), and cardiovascular diseases (Shen L. et al., 2018).

As tsRNAs are relatively new, limited studies have been performed on their role in cardiac function. However, several studies suggest that tsRNAs exist in cardiac tissues (Fu et al., 2009; Dhahbi et al., 2013; Dhahbi, 2015). There is also a study that shows tsRNAs are implicated in the inheritance of cardiac hypertrophy (Shen L. et al., 2018). Furthermore, there appears to be a relationship between cardiac hypertrophy and tsRNA inducers or regulators such as oxidative stress (Takimoto and Kass, 2007; Maulik and Kumar, 2012), hypoxia (Kumar et al., 2018) (Giordano, 2005; Chu et al., 2012; Mirtschink and Krek, 2016), ANG (Patel et al., 2009; Jiang et al., 2014; Yu et al., 2018), ELAC2 (Haack et al., 2013; Siira et al., 2018), aging, and caloric intake, (Dong et al., 2007; Dai D. F. et al., 2012; Chiao and Rabinovitch, 2015; Wang et al., 2015), which indicates an important role for tsRNAs in cardiac hypertrophy.

Therefore, there are a number of research opportunities to examine the role of tsRNAs in cardiac hypertrophy and other cardiac diseases. While it is not clear how global tsRNAs are changed during the development of cardiac hypertrophy, although tRF-5s were identified in ISO-induced hypertrophy (Shen L. et al., 2018). Whether other inducers modulate tsRNA in different cardiac hypertrophy models remains unknown. If this happens to be the case, it would be interesting to see if different hypertrophy inducers generate different tsRNAs and understand their biological function. As we discussed, cardiac hypertrophy can be categorized into compensation and decompensation stages (Frey and Olson, 2003; Diwan and Dorn, 2007; Nakamura and Sadoshima, 2018). Dissecting the role of tsRNAs in these stages may provide new perspectives or therapeutic targets. Since there is very limited research that has investigated the role mitochondrial tsRNAs, most of the molecular and biological functions of tsRNAs described here are cytoplasmic tsRNAs generated from nuclear-encoded tRNAs. So, mitochondrial-encoded tRNAs (Suzuki et al., 2011) and those that can shuttle between the cytoplasm and mitochondria (Rubio et al., 2008; Mercer et al., 2011) represent an opportunity for further investigation.

Several lines of evidence demonstrate that mitochondrial tsRNAs differ from nuclear tsRNAs in terms of their sequence and size (Hirose et al., 2015; Telonis et al., 2015b; Loher et al., 2017). Mitochondrial tsRNAs may also contribute to miRNA biogenesis in these organelles (Venkatesh et al., 2017). As mitochondria are heavily involved in hypertrophic responses (Ballinger, 2005; Abel and Doenst, 2011; Rosca et al., 2013) and mt-tRNA mutations are associated with cardiovascular disease (Jia, Wang et al., 2013; Scheibye-Knudsen et al., 2015), there is a pressing need to uncover the role of tsRNAs in the heart. Lastly, tRNAs (especially mt-tRNAs) undergo extensive post-transcriptional regulation that may affect their function (Suzuki and Suzuki, 2014; Lyons et al., 2018; Richter et al.,

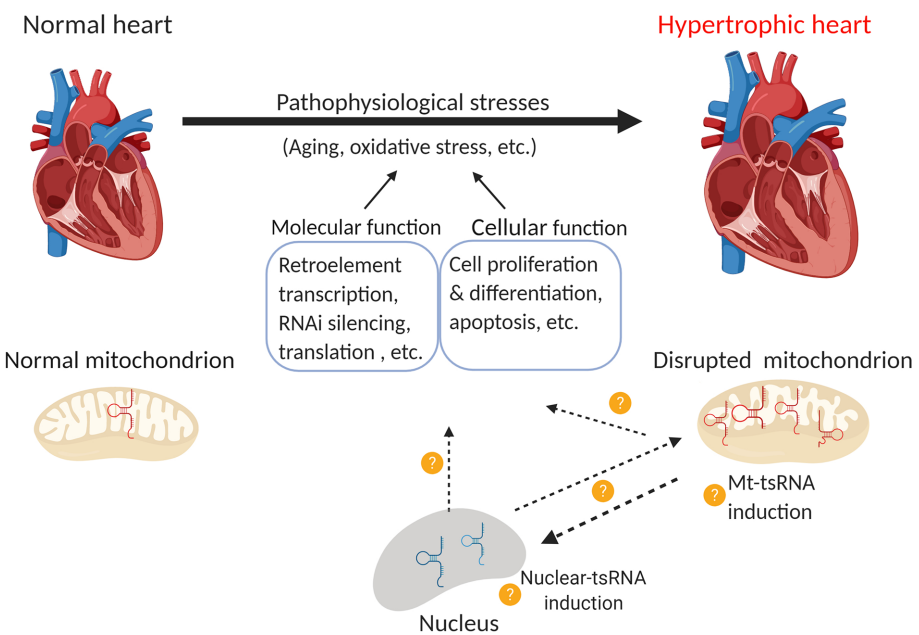

FIGURE 3 | Function of nuclear and mitochondrial tsRNAs in cardiac hypertrophy. Pathological stress (*e.g.* oxidative stress) leads to the development of cardiac hypertrophy. Emerging evidence indicates that the disruption of mitochondrial tsRNAs plays a role in this process. Consequently, it would be interesting to investigate the following questions: 1) Whether nuclear-tsRNAs or mt-tsRNAs are induced or dysregulated during cardiac hypertrophy, 2) Whether any of these tsRNAs exert molecular functions such as the regulation of retro-element transcription, RNAi silencing, and translation, or cellular functions such as cell proliferation, differentiation, and apoptosis, and 3) Whether nuclear-tsRNAs and mt-tsRNAs shuttle between the nucleus and mitochondria, and if their function in different organelles affects cardiac hypertrophy (Created with BioRender.com).

2018). For instance, cytosin-C5 tRNA methylation by DNMT2 and NSUN2 promoted tRNA stability (Tuorto et al., 2012). Deletion of DNMT2 caused upregulation of tsRNA-Gly in mouse sperm (Zhang et al., 2018), whereas loss of NSUN2 promoted tsRNA generation in tumors (Blanco et al., 2016). PUS7 is a pseudouridylation epigenetic "writer" of tRNAs, the deletion of which leads to altered expression of tsRNAs in embryonic stem cells, which further impairs tRF-mediated translation regulation and results in defective germ layer specification (Guzzi et al., 2018). Understanding these modifications may provide insights into tsRNA biology and their role in cardiac disorders and diseases (**Figure 3**).

tsRNAs have also been linked to the gene translational program in embryonic stem cells (Blanco et al., 2016; Krishna et al., 2019), thus it would be interesting to define the role of tsRNAs in cardiac development as well as differentiation of stem cells into mature cardiomyocytes. In addition, retro-elements are highly expressed in stem cells (Boroviak et al., 2018), whose regulation helps to determine cell differentiation and development (Schoorlemmer et al., 2014; Robbez-Masson and Rowe, 2015). As introduced above, tsRNAs are implicated in the regulation of retro-element expression (Schorn et al., 2017; Boskovic et al., 2020); therefore, it would be interesting to decipher whether tsRNAs are implicated in determining these developmental stages by regulating retro-element expression.

AUTHOR CONTRIBUTIONS

JC and D-ZW conceived the idea for this review. JC, D-ZW, and DC wrote and edited the review.

FUNDING

Research in the Wang laboratory is supported by the NIH (HL138757, HL125925, and HL093242). JC is supported by an American Heart Association Postdoctoral Fellowship (18POST33990181).

ACKNOWLEDGMENTS

We thank members of the Wang laboratory for helpful discussions and their support.

REFERENCES

Abel, E. D., and Doenst, T. (2011). Mitochondrial adaptations to physiological vs. pathological cardiac hypertrophy. *Cardiovasc. Res.* 90 (2), 234–242. doi: 10.1093/cvr/cvr015

Akaike, Y., Masuda, K., Kuwano, Y., Nishida, K., Kajita, K., Kurokawa, K., et al. (2014). HuR regulates alternative splicing of the TRA2beta gene in human colon cancer cells under oxidative stress. *Mol. Cell Biol.* 34 (15), 2857–2873. doi: 10.1128/MCB.00333-14

Alexeyev, M. F., Ledoux, S. P., and Wilson, G. L. (2004). Mitochondrial DNA and aging. *Clin. Sci. (Lond.)* 107 (4), 355–364. doi: 10.1042/CS20040148

Altara, R., Zouein, F. A., Brandao, R. D., Bajestani, S. N., Cataliotti, A., and Booz, G. W. (2018). In Silico Analysis of Differential Gene Expression in Three Common Rat Models of Diastolic Dysfunction. *Front. Cardiovasc. Med.* 5, 11. doi: 10.3389/fcvm.2018.00011

An, H. S., Lee, J. Y., Choi, E. B., Jeong, E. A., Shin, H. J., Kim, K. E., et al. (2020). Caloric restriction reverses left ventricular hypertrophy through the regulation of cardiac iron homeostasis in impaired leptin signaling mice. *Sci. Rep.* 10 (1), 7176. doi: 10.1038/s41598-020-64201-2

Anderson, P., and Ivanov, P. (2014). tRNA fragments in human health and disease. *FEBS Lett.* 588 (23), 4297–4304. doi: 10.1016/j.febslet.2014.09.001

Arbustini, E., Diegoli, M., Fasani, R., Grasso, M., Morbini, P., Banchieri, N., et al. (1998). Mitochondrial DNA mutations and mitochondrial abnormalities in dilated cardiomyopathy. *Am. J. Pathol.* 153 (5), 1501–1510. doi: 10.1016/S0002-9440(10)65738-0

Babiarz, J. E., Ruby, J. G., Wang, Y., Bartel, D. P., and Blelloch, R. (2008). Mouse ES cells express endogenous shRNAs, siRNAs, and other Microprocessor-independent, Dicer-dependent small RNAs. *Genes Dev.* 22 (20), 2773–2785. doi: 10.1101/gad.1705308

Ballinger, S. W. (2005). Mitochondrial dysfunction in cardiovascular disease. *Free Radic. Biol. Med.* 38 (10), 1278–1295. doi: 10.1016/j.freeradbiomed.2005.02.014

Barchiesi, A., and Vascotto, C. (2019). Transcription, Processing, and Decay of Mitochondrial RNA in Health and Disease. *Int. J. Mol. Sci.* 20 (9), 2221. doi: 10.3390/ijms20092221

Bartel, D. P. (2009). MicroRNAs: target recognition and regulatory functions. *Cell* 136 (2), 215–233. doi: 10.1016/j.cell.2009.01.002

Blanco, S., Bandiera, R., Popis, M., Hussain, S., Lombard, P., Aleksic, J., et al. (2016). Stem cell function and stress response are controlled by protein synthesis. *Nature* 534 (7607), 335–340. doi: 10.1038/nature18282

Boengler, K., Kosiol, M., Mayr, M., Schulz, R., and Rohrbach, S. (2017). Mitochondria and ageing: role in heart, skeletal muscle and adipose tissue. *J. Cachexia Sarcopenia Muscle* 8 (3), 349–369. doi: 10.1002/jcsm.12178

Boroviak, T., Stirparo, G. G., Dietmann, S., Hernando-Herraez, I., Mohammed, H., Reik, W., et al. (2018). Single cell transcriptome analysis of human, marmoset and mouse embryos reveals common and divergent features of preimplantation development. *Development* 145 (21), dev167833. doi: 10.1242/dev.167833

Boskovic, A., Bing, X. Y., Kaymak, E., and Rando, O. J. (2020). Control of noncoding RNA production and histone levels by a 5' tRNA fragment. *Genes Dev.* 34 (1-2), 118–131. doi: 10.1101/gad.332783.119

Brzezniak, L. K., Bijata, M., Szczesny, R. J., and Stepien, P. P. (2011). Involvement of human ELAC2 gene product in 3' end processing of mitochondrial tRNAs. *RNA Biol.* 8 (4), 616–626. doi: 10.4161/rna.8.4.15393

Cammas, A., Sanchez, B. J., Lian, X. J., Dormoy-Raclet, V., van der Giessen, K., de Silanes, I. L., et al. (2014). Destabilization of nucleophosmin mRNA by the HuR/KSRP complex is required for muscle fibre formation. *Nat. Commun.* 5, 4190. doi: 10.1038/ncomms5190

Capel, F., Rimbert, V., Lioger, D., Diot, A., Rousset, P., Mirand, P. P., et al. (2005). Due to reverse electron transfer, mitochondrial H2O2 release increases with age in human vastus lateralis muscle although oxidative capacity is preserved. *Mech. Ageing Dev.* 126 (4), 505–511. doi: 10.1016/j.mad.2004.11.001

Casali, C., Santorelli, F. M., D'Amati, G., Bernucci, P., DeBiase, L., and DiMauro, S. (1995). A novel mtDNA point mutation in maternally inherited cardiomyopathy. *Biochem. Biophys. Res. Commun.* 213 (2), 588–593. doi: 10.1006/bbrc.1995.2172

Chan, P. P., and Lowe, T. M. (2009). GtRNAdb: a database of transfer RNA genes detected in genomic sequence. *Nucleic Acids Res.* 37, D93–D97. doi: 10.1093/nar/gkn787

Chan, P. P., and Lowe, T. M. (2016). GtRNAdb 2.0: an expanded database of transfer RNA genes identified in complete and draft genomes. *Nucleic Acids Res.* 44 (D1), D184–D189. doi: 10.1093/nar/gkv1309

Chang, N., Yi, J., Guo, G. E., Liu, X. W., Shang, Y. F., Tong, T. J., et al. (2010). HuR Uses AUF1 as a Cofactor To Promote p16(INK4) mRNA Decay. *Mol. Cell. Biol.* 30 (15), 3875–3886. doi: 10.1128/Mcb.00169-10

Chen, J., and Wang, D. Z. (2012). microRNAs in cardiovascular development. *J. Mol. Cell Cardiol.* 52 (5), 949–957. doi: 10.1016/j.yjmcc.2012.01.012

Chen, Q., Yan, M., Cao, Z., Li, X., Zhang, Y., Shi, J., et al. (2016). Sperm tsRNAs contribute to intergenerational inheritance of an acquired metabolic disorder. *Science* 351 (6271), 397–400. doi: 10.1126/science.aad7977

Chen, Y., Zhou, Z., and Min, W. (2018). Mitochondria, Oxidative Stress and Innate Immunity. *Front. Physiol.* 9, 1487. doi: 10.3389/fphys.2018.01487

Chiao, Y. A., and Rabinovitch, P. S. (2015). The Aging Heart. *Cold Spring Harb. Perspect. Med.* 5 (9), a025148. doi: 10.1101/cshperspect.a025148

Chu, W., Wan, L., Zhao, D., Qu, X., Cai, F., Huo, R., et al. (2012). Mild hypoxia-induced cardiomyocyte hypertrophy via up-regulation of HIF-1alpha-mediated TRPC signalling. *J. Cell Mol. Med.* 16 (9), 2022–2034. doi: 10.1111/j.1582-4934.2011.01497.x

Chung, S., Dzeja, P. P., Faustino, R. S., Perez-Terzic, C., Behfar, A., and Terzic, A. (2007). Mitochondrial oxidative metabolism is required for the cardiac differentiation of stem cells. *Nat. Clin. Pract. Cardiovasc. Med.* 4 (Suppl 1), S60–S67. doi: 10.1038/ncpcardio0766

Cole, C., Sobala, A., Lu, C., Thatcher, S. R., Bowman, A., Brown, J. W., et al. (2009). Filtering of deep sequencing data reveals the existence of abundant Dicer-dependent small RNAs derived from tRNAs. *RNA* 15 (12), 2147–2160. doi: 10.1261/rna.1738409

Cruzen, C., and Colman, R. J. (2009). Effects of caloric restriction on cardiovascular aging in non-human primates and humans. *Clin. Geriatr. Med.* 25 (4), 733–743, ix-x. doi: 10.1016/j.cger.2009.07.001

Dai, D. F., Chen, T., Johnson, S. C., Szeto, H., and Rabinovitch, P. S. (2012). Cardiac aging: from molecular mechanisms to significance in human health and disease. *Antioxid. Redox Signal* 16 (12), 1492–1526. doi: 10.1089/ars.2011.4179

Dai, W., Zhang, G., and Makeyev, E. V. (2012). RNA-binding protein HuR autoregulates its expression by promoting alternative polyadenylation site usage. *Nucleic Acids Res.* 40 (2), 787–800. doi: 10.1093/nar/gkr783

Dai, D. F., Chiao, Y. A., Marcinek, D. J., Szeto, H. H., and Rabinovitch, P. S. (2014). Mitochondrial oxidative stress in aging and healthspan. *Longev. Healthspan* 3, 6. doi: 10.1186/2046-2395-3-6

de Lucia, C., Gambino, G., Petraglia, L., Elia, A., Komici, K., Femminella, G. D., et al. (2018). Long-Term Caloric Restriction Improves Cardiac Function, Remodeling, Adrenergic Responsiveness, and Sympathetic Innervation in a Model of Postischemic Heart Failure. *Circ. Heart Fail* 11 (3), e004153. doi: 10.1161/CIRCHEARTFAILURE.117.004153

Dhahbi, J. M., Spindler, S. R., Atamna, H., Yamakawa, A., Boffelli, D., Mote, P., et al. (2013). 5' tRNA halves are present as abundant complexes in serum, concentrated in blood cells, and modulated by aging and calorie restriction. *BMC Genomics* 14, 298. doi: 10.1186/1471-2164-14-298

Dhahbi, J. M. (2015). 5' tRNA Halves: The Next Generation of Immune Signaling Molecules. *Front. Immunol.* 6, 74. doi: 10.3389/fimmu.2015.00074

Dhungel, N., and Hopper, A. K. (2012). Beyond tRNA cleavage: novel essential function for yeast tRNA splicing endonuclease unrelated to tRNA processing. *Genes Dev.* 26 (5), 503–514. doi: 10.1101/gad.183004.111

Diwan, A., and Dorn, 2. G.W. (2007). Decompensation of cardiac hypertrophy: cellular mechanisms and novel therapeutic targets. *Physiol. (Bethesda)* 22, 56–64. doi: 10.1152/physiol.00033.2006

Dolinsky, V. W., Morton, J. S., Oka, T., Robillard-Frayne, I., Bagdan, M., Lopaschuk, G. D., et al. (2010). Calorie restriction prevents hypertension and cardiac hypertrophy in the spontaneously hypertensive rat. *Hypertension* 56 (3), 412–421. doi: 10.1161/HYPERTENSIONAHA.110.154732

Dong, F., Li, Q., Sreejayan, N., Nunn, J. M., and Ren, J. (2007). Metallothionein prevents high-fat diet induced cardiac contractile dysfunction: role of peroxisome proliferator activated receptor gamma coactivator 1alpha and mitochondrial biogenesis. *Diabetes* 56 (9), 2201–2212. doi: 10.2337/db06-1596

Eisner, V., Cupo, R. R., Gao, E., Csordas, G., Slovinsky, W. S., Paillard, M., et al. (2017). Mitochondrial fusion dynamics is robust in the heart and depends on calcium oscillations and contractile activity. *Proc. Natl. Acad. Sci. U. S. A.* 114 (5), E859–E868. doi: 10.1073/pnas.1617288114

Emara, M. M., Ivanov, P., Hickman, T., Dawra, N., Tisdale, S., Kedersha, N., et al. (2010). Angiogenin-induced tRNA-derived stress-induced RNAs promote stress-induced stress granule assembly. *J. Biol. Chem.* 285 (14), 10959–10968. doi: 10.1074/jbc.M109.077560

Eulalio, A., Tritschler, F., and Izaurralde, E. (2009). The GW182 protein family in animal cells: new insights into domains required for miRNA-mediated gene silencing. *RNA* 15 (8), 1433–1442. doi: 10.1261/rna.1703809

Fan, X. H. C., and Steitz, J. A. (1998). Overexpression of HuR, a nuclear-cytoplasmic shuttling protein, increases the in vivo stability of ARE-containing mRNAs. *EMBO J.* 17 (12), 3448–3460. doi: 10.1093/emboj/17.12.3448

Fleming, J. E., Miquel, J., Cottrell, S. F., Yengoyan, L. S., and Economos, A. C. (1982). Is cell aging caused by respiration-dependent injury to the mitochondrial genome. *Gerontology* 28 (1), 44–53. doi: 10.1159/000212510

Frank, D. N., and Pace, N. R. (1998). Ribonuclease P: unity and diversity in a tRNA processing ribozyme. *Annu. Rev. Biochem.* 67, 153–180. doi: 10.1146/annurev.biochem.67.1.153

Frey, N., and Olson, E. N. (2003). Cardiac hypertrophy: the good, the bad, and the ugly. *Annu. Rev. Physiol.* 65, 45–79. doi: 10.1146/annurev.physiol.65.092101.142243

Fu, H., Feng, J., Liu, Q., Sun, F., Tie, Y., Zhu, J., et al. (2009). Stress induces tRNA cleavage by angiogenin in mammalian cells. *FEBS Lett.* 583 (2), 437–442. doi: 10.1016/j.febslet.2008.12.043

Gambaro, F., Li Calzi, M., Fagundez, P., Costa, B., Greif, G., Mallick, E., et al. (2019). Stable tRNA halves can be sorted into extracellular vesicles and delivered to recipient cells in a concentration-dependent manner. *RNA Biol.* 7, 1168–1182. doi: 10.1080/15476286.2019.1708548

Garrido, C., Galluzzi, L., Brunet, M., Puig, P. E., Didelot, C., and Kroemer, G. (2006). Mechanisms of cytochrome c release from mitochondria. *Cell Death Differ.* 13 (9), 1423–1433. doi: 10.1038/sj.cdd.4401950

Gebetsberger, J., and Polacek, N. (2013). Slicing tRNAs to boost functional ncRNA diversity. *RNA Biol.* 10 (12), 1798–1806. doi: 10.4161/rna.27177

Giordano, F. J. (2005). Oxygen, oxidative stress, hypoxia, and heart failure. *J. Clin. Invest.* 115 (3), 500–508. doi: 10.1172/JCI200524408

Giraldez, M. D., Spengler, R. M., Etheridge, A., Godoy, P. M., Barczak, A. J., Srinivasan, S., et al. (2018). Comprehensive multi-center assessment of small RNA-seq methods for quantitative miRNA profiling. *Nat. Biotechnol.* 36 (8), 746–757. doi: 10.1038/nbt.4183

Glorian, V., Maillot, G., Poles, S., Iacovoni, J. S., Favre, G., and Vagner, S. (2011). HuR-dependent loading of miRNA RISC to the mRNA encoding the Ras-related small GTPase RhoB controls its translation during UV-induced apoptosis. *Cell Death Differ.* 18 (11), 1692–1701. doi: 10.1038/cdd.2011.35

Goodarzi, H., Liu, X., Nguyen, H. C., Zhang, S., Fish, L., and Tavazoie, S. F. (2015). Endogenous tRNA-Derived Fragments Suppress Breast Cancer Progression via YBX1 Displacement. *Cell* 161 (4), 790–802. doi: 10.1016/j.cell.2015.02.053

Gorospe, M. (2003). HuR in the mammalian genotoxic response: post-transcriptional multitasking. *Cell Cycle* 2 (5), 412–414. doi: 10.4161/cc.2.5.491

Grimm, A., and Eckert, A. (2017). Brain aging and neurodegeneration: from a mitochondrial point of view. *J. Neurochem.* 143 (4), 418–431. doi: 10.1111/jnc.14037

Guo, C., Sun, L., Chen, X., and Zhang, D. (2013). Oxidative stress, mitochondrial damage and neurodegenerative diseases. *Neural Regener. Res.* 8 (21), 2003–2014. doi: 10.3969/j.issn.1673-5374.2013.21.009

Guzzi, N., Ciesla, M., Ngoc, P. C. T., Lang, S., Arora, S., Dimitriou, M., et al. (2018). Pseudouridylation of tRNA-Derived Fragments Steers Translational Control in Stem Cells. *Cell* 173 (5), 1204–1216 e1226. doi: 10.1016/j.cell.2018.03.008

Haack, T. B., Kopajtich, R., Freisinger, P., Wieland, T., Rorbach, J., Nicholls, T. J., et al. (2013). ELAC2 mutations cause a mitochondrial RNA processing defect associated with hypertrophic cardiomyopathy. *Am. J. Hum. Genet.* 93 (2), 211–223. doi: 10.1016/j.ajhg.2013.06.006

Hafner, M., Landthaler, M., Burger, L., Khorshid, M., Hausser, J., Berninger, P., et al. (2010). Transcriptome-wide identification of RNA-binding protein and microRNA target sites by PAR-CLIP. *Cell* 141 (1), 129–141. doi: 10.1016/j.cell.2010.03.009

Hanada, T., Weitzer, S., Mair, B., Bernreuther, C., Wainger, B. J., Ichida, J., et al. (2013). CLP1 links tRNA metabolism to progressive motor-neuron loss. *Nature* 495 (7442), 474–480. doi: 10.1038/nature11923

Harman, D. (1972). The biologic clock: the mitochondria. *J. Am. Geriatr. Soc.* 20 (4), 145–147. doi: 10.1111/j.1532-5415.1972.tb00787.x

Haussecker, D., Huang, Y., Lau, A., Parameswaran, P., Fire, A. Z., and Kay, M. A. (2010). Human tRNA-derived small RNAs in the global regulation of RNA silencing. *RNA* 16 (4), 673–695. doi: 10.1261/rna.2000810

Helm, M., Brule, H., Degoul, F., Cepanec, C., Leroux, J. P., Giege, R., et al. (1998). The presence of modified nucleotides is required for cloverleaf folding of a human mitochondrial tRNA. *Nucleic Acids Res.* 26 (7), 1636–1643. doi: 10.1093/nar/26.7.1636

Hirose, Y., Ikeda, K. T., Noro, E., Hiraoka, K., Tomita, M., and Kanai, A. (2015). Precise mapping and dynamics of tRNA-derived fragments (tRFs) in the development of Triops cancriformis (tadpole shrimp). *BMC Genet.* 16, 83. doi: 10.1186/s12863-015-0245-5

Honda, S., Loher, P., Shigematsu, M., Palazzo, J. P., Suzuki, R., Imoto, I., et al. (2015). Sex hormone-dependent tRNA halves enhance cell proliferation in breast and prostate cancers. *Proc. Natl. Acad. Sci. U. S. A.* 112 (29), E3816–E3825. doi: 10.1073/pnas.1510077112

Hopper, A. K., and Nostramo, R. T. (2019). tRNA Processing and Subcellular Trafficking Proteins Multitask in Pathways for Other RNAs. *Front. Genet.* 10, 96. doi: 10.3389/fgene.2019.00096

Hsu, P. C., Chu, C. S., Lin, T. H., Lu, Y. H., Lee, C. S., Lai, W. T., et al. (2008). Adult-onset hypertrophic cardiomyopathy manifested as initial major presentation of mitochondrial disease with A-to-G 3243 tRNA (Leu(UUR)) point mutation. *Int. J. Cardiol.* 129 (3), 441–443. doi: 10.1016/j.ijcard.2007.06.098

Ivanov, P., Emara, M. M., Villen, J., Gygi, S. P., and Anderson, P. (2011). Angiogenin-induced tRNA fragments inhibit translation initiation. *Mol. Cell* 43 (4), 613–623. doi: 10.1016/j.molcel.2011.06.022

Izquierdo, J. M. (2008). Hu antigen R (HuR) functions as an alternative pre-mRNA splicing regulator of Fas apoptosis-promoting receptor on exon definition. *J. Biol. Chem.* 283 (27), 19077–19084. doi: 10.1074/jbc.M800017200

Jia, Z., Wang, X., Qin, Y., Xue, L., Jiang, P., Meng, Y., et al. (2013). Coronary heart disease is associated with a mutation in mitochondrial tRNA. *Hum. Mol. Genet.* 22 (20), 4064–4073. doi: 10.1093/hmg/ddt256

Jia, Z., Zhang, Y., Li, Q., Ye, Z., Liu, Y., Fu, C., et al. (2019). A coronary artery disease-associated tRNAThr mutation altered mitochondrial function, apoptosis and angiogenesis. *Nucleic Acids Res.* 47 (4), 2056–2074. doi: 10.1093/nar/gky1241

Jiang, H., Zhang, L., Yu, Y., Liu, M., Jin, X., Zhang, P., et al. (2014). A pilot study of angiogenin in heart failure with preserved ejection fraction: a novel potential biomarker for diagnosis and prognosis. *J. Cell Mol. Med.* 18 (11), 2189–2197. doi: 10.1111/jcmm.12344

Jiang, P., Wang, M., Xue, L., Xiao, Y., Yu, J., Wang, H., et al. (2016). A Hypertension-Associated tRNAAla Mutation Alters tRNA Metabolism and Mitochondrial Function. *Mol. Cell Biol.* 36 (14), 1920–1930. doi: 10.1128/MCB.00199-16

Karaiskos, S., and Grigoriev, A. (2016). Dynamics of tRNA fragments and their targets in aging mammalian brain. *F1000Res* 5, ISCB Comm J-2758. doi: 10.12688/f1000research.10116.1

Kawaji, H., Nakamura, M., Takahashi, Y., Sandelin, A., Katayama, S., Fukuda, S., et al. (2008). Hidden layers of human small RNAs. *BMC Genomics* 9, 157. doi: 10.1186/1471-2164-9-157

Kim, H. H., Kuwano, Y., Srikantan, S., Lee, E. K., Martindale, J. L., and Gorospe, M. (2009). HuR recruits let-7/RISC to repress c-Myc expression. *Genes Dev.* 23 (15), 1743–1748. doi: 10.1101/gad.1812509

Kim, H. K., Fuchs, G., Wang, S., Wei, W., Zhang, Y., Park, H., et al. (2017). A transfer-RNA-derived small RNA regulates ribosome biogenesis. *Nature* 552 (7683), 57–62. doi: 10.1038/nature25005

Kirchner, S., and Ignatova, Z. (2015). Emerging roles of tRNA in adaptive translation, signalling dynamics and disease. *Nat. Rev. Genet.* 16 (2), 98–112. doi: 10.1038/nrg3861

Kiss, T. (2002). Small nucleolar RNAs: an abundant group of noncoding RNAs with diverse cellular functions. *Cell* 109 (2), 145–148. doi: 10.1016/S0092-8674(02)00718-3

Krishna, S., Yim, D. G., Lakshmanan, V., Tirumalai, V., Koh, J. L., Park, J. E., et al. (2019). Dynamic expression of tRNA-derived small RNAs define cellular states. *EMBO Rep.* 20 (7), e47789. doi: 10.15252/embr.201947789

Kullmann, M., Gopfert, U., Siewe, B., and Hengst, L. (2002). ELAV/Hu proteins inhibit p27 translation via an IRES element in the p27 5 ' UTR. *Genes Dev.* 16 (23), 3087–3099. doi: 10.1101/gad.248902

Kumar, P., Anaya, J., Mudunuri, S. B., and Dutta, A. (2014). Meta-analysis of tRNA derived RNA fragments reveals that they are evolutionarily conserved and associate with AGO proteins to recognize specific RNA targets. *BMC Biol.* 12, 78. doi: 10.1186/s12915-014-0078-0

Kumar, P., Kuscu, C., and Dutta, A. (2016). Biogenesis and Function of Transfer RNA-Related Fragments (tRFs). *Trends Biochem. Sci.* 41 (8), 679–689. doi: 10.1016/j.tibs.2016.05.004

Kumar, S., Wang, G., Liu, W., Ding, W., Dong, M., Zheng, N., et al. (2018). Hypoxia-Induced Mitogenic Factor Promotes Cardiac Hypertrophy via Calcium-Dependent and Hypoxia-Inducible Factor-1alpha Mechanisms. *Hypertension* 72 (2), 331–342. doi: 10.1161/HYPERTENSIONAHA.118.10845

Kuscu, C., Kumar, P., Kiran, M., Su, Z., Malik, A., and Dutta, A. (2018). tRNA fragments (tRFs) guide Ago to regulate gene expression post-transcriptionally in a Dicer-independent manner. *RNA* 24 (8), 1093–1105. doi: 10.1261/rna.066126.118

Lambert, M., Benmoussa, A., and Provost, P. (2019). Small Non-Coding RNAs Derived From Eukaryotic Ribosomal RNA. *Noncoding RNA* 5 (1), 16. doi: 10.3390/ncrna5010016

Lee, Y. S., Shibata, Y., Malhotra, A., and Dutta, A. (2009). A novel class of small RNAs: tRNA-derived RNA fragments (tRFs). *Genes Dev.* 23 (22), 2639–2649. doi: 10.1101/gad.1837609

Lesnefsky, E. J., Chen, Q., and Hoppel, C. L. (2016). Mitochondrial Metabolism in Aging Heart. *Circ. Res.* 118 (10), 1593–1611. doi: 10.1161/CIRCRESAHA.116.307505

Li, Z., Ender, C., Meister, G., Moore, P. S., Chang, Y., and John, B. (2012). Extensive terminal and asymmetric processing of small RNAs from rRNAs, snoRNAs, snRNAs, and tRNAs. *Nucleic Acids Res.* 40 (14), 6787–6799. doi: 10.1093/nar/gks307

Li, Q., Hu, B., Hu, G. W., Chen, C. Y., Niu, X., Liu, J., et al. (2016). tRNA-Derived Small Non-Coding RNAs in Response to Ischemia Inhibit Angiogenesis. *Sci. Rep.* 6, 20850. doi: 10.1038/srep20850

Liapi, E., van Bilsen, M., Verjans, R., and Schroen, B. (2020). tRNAs and tRNA fragments as modulators of cardiac and skeletal muscle function. *Biochim. Biophys. Acta Mol. Cell Res.* 1867 (3), 118465. doi: 10.1016/j.bbamcr.2019.03.012

Ling, H., Fabbri, M., and Calin, G. A. (2013). MicroRNAs and other non-coding RNAs as targets for anticancer drug development. *Nat. Rev. Drug Discov.* 12 (11), 847–865. doi: 10.1038/nrd4140

Liu, Y., Li, R., Li, Z., Wang, X. J., Yang, L., Wang, S., et al. (2009). Mitochondrial transfer RNAMet 4435A>G mutation is associated with maternally inherited hypertension in a Chinese pedigree. *Hypertension* 53 (6), 1083–1090. doi: 10.1161/HYPERTENSIONAHA.109.128702

Liu, Q., Ding, C., Lang, X., Guo, G., Chen, J., and Su, X. (2019). Small noncoding RNA discovery and profiling with sRNAtools based on high-throughput sequencing. *Brief Bioinform* 00 (00), 2011–2011. doi: 10.1093/bib/bbz151

Loher, P., Telonis, A. G., and Rigoutsos, I. (2017). MINTmap: fast and exhaustive profiling of nuclear and mitochondrial tRNA fragments from short RNA-seq data. *Sci. Rep.* 7, 41184. doi: 10.1038/srep41184

Lyons, S. M., Fay, M. M., and Ivanov, P. (2018). The role of RNA modifications in the regulation of tRNA cleavage. *FEBS Lett.* 592 (17), 2828–2844. doi: 10.1002/1873-3468.13205

Mahlab, S., Tuller, T., and Linial, M. (2012). Conservation of the relative tRNA composition in healthy and cancerous tissues. *RNA* 18 (4), 640–652. doi: 10.1261/rna.030775.111

Maniataki, E., and Mourelatos, Z. (2005). Human mitochondrial tRNAMet is exported to the cytoplasm and associates with the Argonaute 2 protein. *RNA* 11 (6), 849–852. doi: 10.1261/rna.2210805

Maraia, R. J., and Lamichhane, T. N. (2011). 3' processing of eukaryotic precursor tRNAs. *Wiley Interdiscip. Rev. RNA* 2 (3), 362–375. doi: 10.1002/wrna.64

Marek-Trzonkowska, N., Kwieczynska, A., Reiwer-Gostomska, M., Kolinski, T., Molisz, A., and Siebert, J. (2015). Arterial Hypertension Is Characterized by Imbalance of Pro-Angiogenic versus Anti-Angiogenic Factors. *PLoS One* 10 (5), e0126190. doi: 10.1371/journal.pone.0126190

Marin-Garcia, J., Goldenthal, M. J., and Moe, G. W. (2001). Mitochondrial pathology in cardiac failure. *Cardiovasc. Res.* 49 (1), 17–26. doi: 10.1016/s0008-6363(00)00241-8

Mattick, J. S., and Makunin, I. V. (2006). Non-coding RNA. *Hum. Mol. Genet.* 15 (Spec No 1), R17–R29. doi: 10.1093/hmg/ddl046

Maulik, S. K., and Kumar, S. (2012). Oxidative stress and cardiac hypertrophy: a review. *Toxicol. Mech. Methods* 22 (5), 359–366. doi: 10.3109/15376516.2012.666650

Mazan-Mamczarz, K., Galban, S., Lopez de Silanes, I., Martindale, J. L., Atasoy, U., Keene, J. D., et al. (2003). RNA-binding protein HuR enhances p53 translation in response to ultraviolet light irradiation. *Proc. Natl. Acad. Sci. U. S. A.* 100 (14), 8354–8359. doi: 10.1073/pnas.1432104100

Mendell, J. T. (2008). miRiad roles for the miR-17-92 cluster in development and disease. *Cell* 133 (2), 217–222. doi: 10.1016/j.cell.2008.04.001

Mercer, T. R., Neph, S., Dinger, M. E., Crawford, J., Smith, M. A., Shearwood, A. M., et al. (2011). The human mitochondrial transcriptome. *Cell* 146 (4), 645–658. doi: 10.1016/j.cell.2011.06.051

Messmer, M., Putz, J., Suzuki, T., Suzuki, T., Sauter, C., Sissler, M., et al. (2009). Tertiary network in mammalian mitochondrial tRNAAsp revealed by solution probing and phylogeny. *Nucleic Acids Res.* 37 (20), 6881–6895. doi: 10.1093/nar/gkp697

Miquel, J., Economos, A. C., Fleming, J., and Johnson, J. E.Jr (1980). Mitochondrial role in cell aging. *Exp. Gerontol.* 15 (6), 575–591. doi: 10.1016/0531-5565(80)90010-8

Mirtschink, P., and Krek, W. (2016). Hypoxia-driven glycolytic and fructolytic metabolic programs: Pivotal to hypertrophic heart disease. *Biochim. Biophys. Acta* 1863 (7 Pt B), 1822–1828. doi: 10.1016/j.bbamcr.2016.02.011

Nakamura, M., and Sadoshima, J. (2018). Mechanisms of physiological and pathological cardiac hypertrophy. *Nat. Rev. Cardiol.* 15 (7), 387–407. doi: 10.1038/s41569-018-0007-y

Natt, D., Kugelberg, U., Casas, E., Nedstrand, E., Zalavary, S., Henriksson, P., et al. (2019). Human sperm displays rapid responses to diet. *PLoS Biol.* 17 (12), e3000559. doi: 10.1371/journal.pbio.3000559

Ojala, D., Montoya, J., and Attardi, G. (1981). tRNA punctuation model of RNA processing in human mitochondria. *Nature* 290 (5806), 470–474. doi: 10.1038/290470a0

Oldfield, C. J., Duhamel, T. A., and Dhalla, N. S. (2020). Mechanisms for the transition from physiological to pathological cardiac hypertrophy. *Can. J. Physiol. Pharmacol.* 98 (2), 74–84. doi: 10.1139/cjpp-2019-0566

Osaki, M., and Okada, F. (2019). Exosomes and Their Role in Cancer Progression. *Yonago Acta Med.* 62 (2), 182–190. doi: 10.33160/yam.2019.06.002

Ozata, D. M., Gainetdinov, I., Zoch, A., O'Carroll, D., and Zamore, P. D. (2019). PIWI-interacting RNAs: small RNAs with big functions. *Nat. Rev. Genet.* 20 (2), 89–108. doi: 10.1038/s41576-018-0073-3

Park, J. E., Heo, I., Tian, Y., Simanshu, D. K., Chang, H., Jee, D., et al. (2011). Dicer recognizes the 5' end of RNA for efficient and accurate processing. *Nature* 475 (7355), 201–205. doi: 10.1038/nature10198

Patel, J. V., Sosin, M., Gunarathne, A., Hussain, I., Davis, R. C., Hughes, E. A., et al. (2008). Elevated angiogenin levels in chronic heart failure. *Ann. Med.* 40 (6), 474–479. doi: 10.1080/07853890802001419

Patel, J. V., Abraheem, A., Chackathayil, J., Gunning, M., Creamer, J., Hughes, E. A., et al. (2009). Circulating biomarkers of angiogenesis as indicators of left ventricular systolic dysfunction amongst patients with coronary artery disease. *J. Intern. Med.* 265 (5), 562–567. doi: 10.1111/j.1365-2796.2008.02057.x

Peng, Y., and Croce, C. M. (2016). The role of MicroRNAs in human cancer. *Signal Transduct. Target Ther.* 1, 15004. doi: 10.1038/sigtrans.2015.4

Peng, S. S. Y., Chen, C. Y. A., Xu, N. H., and Shyu, A. B. (1998). RNA stabilization by the AU-rich element binding protein, HuR, an ELAV protein. *EMBO J.* 17 (12), 3461–3470. doi: 10.1093/emboj/17.12.3461

Pennanen, C., Parra, V., Lopez-Crisosto, C., Morales, P. E., Del Campo, A., Gutierrez, T., et al. (2014). Mitochondrial fission is required for cardiomyocyte hypertrophy mediated by a Ca2+-calcineurin signaling pathway. *J. Cell Sci.* 127 (Pt 12), 2659–2671. doi: 10.1242/jcs.139394

Phizicky, E. M., and Hopper, A. K. (2010). tRNA biology charges to the front. *Genes Dev.* 24 (17), 1832–1860. doi: 10.1101/gad.1956510

Pillai, R. S. (2005). MicroRNA function: multiple mechanisms for a tiny RNA. *RNA* 11 (12), 1753–1761. doi: 10.1261/rna.2248605

Piquereau, J., Caffin, F., Novotova, M., Lemaire, C., Veksler, V., Garnier, A., et al. (2013). Mitochondrial dynamics in the adult cardiomyocytes: which roles for a highly specialized cell. *Front. Physiol.* 4, 102. doi: 10.3389/fphys.2013.00102

Porter, G. A.Jr., Hom, J., Hoffman, D., Quintanilla, R., de Mesy Bentley, K., and Sheu, S. S. (2011). Bioenergetics, mitochondria, and cardiac myocyte differentiation. *Prog. Pediatr. Cardiol.* 31 (2), 75–81. doi: 10.1016/j.ppedcard.2011.02.002

Rabinowitz, M., and Zak, R. (1975). Mitochondria and cardiac hypertrophy. *Circ. Res.* 36 (3), 367–376. doi: 10.1161/01.res.36.3.367

Rege, S. D., Geetha, T., Pondugula, S. R., Zizza, C. A., Wernette, C. M., and Babu, J. R. (2013). Noncoding RNAs in Neurodegenerative Diseases. *ISRN Neurol.* 2013, 375852. doi: 10.1155/2013/375852

Retta, S. F., Chiarugi, P., Trabalzini, L., Pinton, P., and Belkin, A. M. (2012). Reactive oxygen species: friends and foes of signal transduction. *J. Signal Transduct.* 2012, 534029. doi: 10.1155/2012/534029

Reubold, T. F., and Eschenburg, S. (2012). A molecular view on signal transduction by the apoptosome. *Cell Signal* 24 (7), 1420–1425. doi: 10.1016/j.cellsig.2012.03.007

Richter, U., Evans, M. E., Clark, W. C., Marttinen, P., Shoubridge, E. A., Suomalainen, A., et al. (2018). RNA modification landscape of the human mitochondrial tRNA(Lys) regulates protein synthesis. *Nat. Commun.* 9 (1), 3966. doi: 10.1038/s41467-018-06471-z

Robbez-Masson, L., and Rowe, H. M. (2015). Retrotransposons shape species-specific embryonic stem cell gene expression. *Retrovirology* 12, 45. doi: 10.1186/s12977-015-0173-5

Rojas-Rios, P., and Simonelig, M. (2018). piRNAs and PIWI proteins: regulators of gene expression in development and stem cells. *Development* 145 (17), dev161786. doi: 10.1242/dev.161786

Romaine, S. P., Tomaszewski, M., Condorelli, G., and Samani, N. J. (2015). MicroRNAs in cardiovascular disease: an introduction for clinicians. *Heart* 101 (12), 921–928. doi: 10.1136/heartjnl-2013-305402

Romano, G., Veneziano, D., Acunzo, M., and Croce, C. M. (2017). Small non-coding RNA and cancer. *Carcinogenesis* 38 (5), 485–491. doi: 10.1093/carcin/bgx026

Rosca, M. G., Tandler, B., and Hoppel, C. L. (2013). Mitochondria in cardiac hypertrophy and heart failure. *J. Mol. Cell Cardiol.* 55, 31–41. doi: 10.1016/j.yjmcc.2012.09.002

Rossmanith, W., Tullo, A., Potuschak, T., Karwan, R., and Sbisa, E. (1995). Human mitochondrial tRNA processing. *J. Biol. Chem.* 270 (21), 12885–12891. doi: 10.1074/jbc.270.21.12885

Rubio, M. A., Rinehart, J. J., Krett, B., Duvezin-Caubet, S., Reichert, A. S., Soll, D., et al. (2008). Mammalian mitochondria have the innate ability to import tRNAs by a mechanism distinct from protein import. *Proc. Natl. Acad. Sci. U. S. A.* 105 (27), 9186–9191. doi: 10.1073/pnas.0804283105

Saikia, M., Jobava, R., Parisien, M., Putnam, A., Krokowski, D., Gao, X. H., et al. (2014). Angiogenin-cleaved tRNA halves interact with cytochrome c, protecting cells from apoptosis during osmotic stress. *Mol. Cell Biol.* 34 (13), 2450–2463. doi: 10.1128/MCB.00136-14

Salinas-Giege, T., Giege, R., and Giege, P. (2015). tRNA biology in mitochondria. *Int. J. Mol. Sci.* 16 (3), 4518–4559. doi: 10.3390/ijms16034518

Sarker, G., Sun, W., Rosenkranz, D., Pelczar, P., Opitz, L., Efthymiou, V., et al. (2019). Maternal overnutrition programs hedonic and metabolic phenotypes across generations through sperm tsRNAs. *Proc. Natl. Acad. Sci. U. S. A.* 116 (21), 10547–10556. doi: 10.1073/pnas.1820810116

Sawada, M., and Carlson, J. C. (1987). Changes in superoxide radical and lipid peroxide formation in the brain, heart and liver during the lifetime of the rat. *Mech. Ageing Dev.* 41 (1-2), 125–137. doi: 10.1016/0047-6374(87)90057-1

Scheibye-Knudsen, M., Fang, E. F., Croteau, D. L., Wilson, 3. D.M., and Bohr, V. A. (2015). Protecting the mitochondrial powerhouse. *Trends Cell Biol.* 25 (3), 158–170. doi: 10.1016/j.tcb.2014.11.002

Schimmel, P. (2018). The emerging complexity of the tRNA world: mammalian tRNAs beyond protein synthesis. *Nat. Rev. Mol. Cell Biol.* 19 (1), 45–58. doi: 10.1038/nrm.2017.77

Schoorlemmer, J., Perez-Palacios, R., Climent, M., Guallar, D., and Muniesa, P. (2014). Regulation of Mouse Retroelement MuERV-L/MERVL Expression by REX1 and Epigenetic Control of Stem Cell Potency. *Front. Oncol.* 4, 14. doi: 10.3389/fonc.2014.00014

Schorn, A. J., Gutbrod, M. J., LeBlanc, C., and Martienssen, R. (2017). LTR-Retrotransposon Control by tRNA-Derived Small RNAs. *Cell* 170 (1), 61–71 e11. doi: 10.1016/j.cell.2017.06.013

Sengupta, S., Jang, B. C., Wu, M. T., Paik, J. H., Furneaux, H., and Hla, T. (2003). The RNA-binding protein HuR regulates the expression of cyclooxygenase-2. *J. Biol. Chem.* 278 (27), 25227–25233. doi: 10.1074/jbc.M301813200

Sharma, U., Conine, C. C., Shea, J. M., Boskovic, A., Derr, A. G., Bing, X. Y., et al. (2016). Biogenesis and function of tRNA fragments during sperm maturation and fertilization in mammals. *Science* 351 (6271), 391–396. doi: 10.1126/science.aad6780

Shen, L., Gan, M., Tan, Z., Jiang, D., Jiang, Y., Li, M., et al. (2018). A Novel Class of tRNA-Derived Small Non-Coding RNAs Respond to Myocardial Hypertrophy and Contribute to Intergenerational Inheritance. *Biomolecules* 8 (3), 54. doi: 10.3390/biom8030054

Shen, Y., Yu, X., Zhu, L., Li, T., Yan, Z., and Guo, J. (2018). Transfer RNA-derived fragments and tRNA halves: biogenesis, biological functions and their roles in diseases. *J. Mol. Med. (Berl.)* 96 (11), 1167–1176. doi: 10.1007/s00109-018-1693-y

Shigematsu, M., and Kirino, Y. (2017). 5'-Terminal nucleotide variations in human cytoplasmic tRNAHisGUG and its 5'-halves. *RNA* 23 (2), 161–168. doi: 10.1261/rna.058024.116

Siira, S. J., Rossetti, G., Richman, T. R., Perks, K., Ermer, J. A., Kuznetsova, I., et al. (2018). Concerted regulation of mitochondrial and nuclear non-coding RNAs by a dual-targeted RNase Z. *EMBO Rep.* 19 (10), e46198. doi: 10.15252/embr.201846198

Sobala, A., and Hutvagner, G. (2013). Small RNAs derived from the 5' end of tRNA can inhibit protein translation in human cells. *RNA Biol.* 10 (4), 553–563. doi: 10.4161/rna.24285

Su, Z., Kuscu, C., Malik, A., Shibata, E., and Dutta, A. (2019). Angiogenin generates specific stress-induced tRNA halves and is not involved in tRF-3-mediated gene silencing. *J. Biol. Chem.* 294 (45), 16930–16941. doi: 10.1074/jbc.RA119.009272

Suzuki, T., and Suzuki, T. (2014). A complete landscape of post-transcriptional modifications in mammalian mitochondrial tRNAs. *Nucleic Acids Res.* 42 (11), 7346–7357. doi: 10.1093/nar/gku390

Suzuki, T., Nagao, A., and Suzuki, T. (2011). Human mitochondrial tRNAs: biogenesis, function, structural aspects, and diseases. *Annu. Rev. Genet.* 45, 299–329. doi: 10.1146/annurev-genet-110410-132531

Takimoto, E., and Kass, D. A. (2007). Role of oxidative stress in cardiac hypertrophy and remodeling. *Hypertension* 49 (2), 241–248. doi: 10.1161/01.HYP.0000254415.31362.a7

Taniike, M., Fukushima, H., Yanagihara, I., Tsukamoto, H., Tanaka, J., Fujimura, H., et al. (1992). Mitochondrial tRNA(Ile) mutation in fatal cardiomyopathy. *Biochem. Biophys. Res. Commun.* 186 (1), 47–53. doi: 10.1016/S0006-291X(05)80773-9

Tello-Montoliu, A., Patel, J. V., and Lip, G. Y. (2006). Angiogenin: a review of the pathophysiology and potential clinical applications. *J. Thromb. Haemost.* 4 (9), 1864–1874. doi: 10.1111/j.1538-7836.2006.01995.x

Telonis, A. G., and Rigoutsos, I. (2018). Race Disparities in the Contribution of miRNA Isoforms and tRNA-Derived Fragments to Triple-Negative Breast Cancer. *Cancer Res.* 78 (5), 1140–1154. doi: 10.1158/0008-5472.CAN-17-1947

Telonis, A. G., Loher, P., Kirino, Y., and Rigoutsos, I. (2014). Nuclear and mitochondrial tRNA-lookalikes in the human genome. *Front. Genet.* 5, 344. doi: 10.3389/fgene.2014.00344

Telonis, A. G., Kirino, Y., and Rigoutsos, I. (2015a). Mitochondrial tRNA-lookalikes in nuclear chromosomes: could they be functional. *RNA Biol.* 12 (4), 375–380. doi: 10.1080/15476286.2015.1017239

Telonis, A. G., Loher, P., Honda, S., Jing, Y., Palazzo, J., Kirino, Y., et al. (2015b). Dissecting tRNA-derived fragment complexities using personalized transcriptomes reveals novel fragment classes and unexpected dependencies. *Oncotarget* 6 (28), 24797–24822. doi: 10.18632/oncotarget.4695

Thompson, D. M., Lu, C., Green, P. J., and Parker, R. (2008). tRNA cleavage is a conserved response to oxidative stress in eukaryotes. *RNA* 14 (10), 2095–2103. doi: 10.1261/rna.1232808

Tocchi, A., Quarles, E. K., Basisty, N., Gitari, L., and Rabinovitch, P. S. (2015). Mitochondrial dysfunction in cardiac aging. *Biochim. Biophys. Acta* 1847 (11), 1424–1433. doi: 10.1016/j.bbabio.2015.07.009

Torres, A. G., Reina, O., Stephan-Otto Attolini, C., and Ribas de Pouplana, L. (2019). Differential expression of human tRNA genes drives the abundance of tRNA-derived fragments. *Proc. Natl. Acad. Sci. U. S. A.* 116 (17), 8451–8456. doi: 10.1073/pnas.1821120116

Tuorto, F., Liebers, R., Musch, T., Schaefer, M., Hofmann, S., Kellner, S., et al. (2012). RNA cytosine methylation by Dnmt2 and NSun2 promotes tRNA stability and protein synthesis. *Nat. Struct. Mol. Biol.* 19 (9), 900–905. doi: 10.1038/nsmb.2357

Valadkhan, S. (2005). snRNAs as the catalysts of pre-mRNA splicing. *Curr. Opin. Chem. Biol.* 9 (6), 603–608. doi: 10.1016/j.cbpa.2005.10.008

Valencia-Sanchez, M. A., Liu, J., Hannon, G. J., and Parker, R. (2006). Control of translation and mRNA degradation by miRNAs and siRNAs. *Genes Dev.* 20 (5), 515–524. doi: 10.1101/gad.1399806

Venkatesh, T., Hussain, S. A., and Suresh, P. S. (2017). A tale of three RNAs in mitochondria: tRNA, tRNA derived fragments and mitomiRs. *J. Theor. Biol.* 435, 42–49. doi: 10.1016/j.jtbi.2017.09.002

Wallace, D. C. (1992). Mitochondrial genetics: a paradigm for aging and degenerative diseases. *Science* 256 (5057), 628–632. doi: 10.1126/science.1533953

Wang, W., Caldwell, M. C., Lin, S., Furneaux, H., and Gorospe, M. (2000a). HuR regulates cyclin A and cyclin B1 mRNA stability during cell proliferation. *EMBO J.* 19 (10), 2340–2350. doi: 10.1093/emboj/19.10.2340

Wang, W., Furneaux, H., Cheng, H., Caldwell, M. C., Hutter, D., Liu, Y., et al. (2000b). HuR regulates p21 mRNA stabilization by UV light. *Mol. Cell Biol.* 20 (3), 760–769. doi: 10.1128/MCB.20.3.760-769.2000

Wang, S., Li, R., Fettermann, A., Li, Z., Qian, Y., Liu, Y., et al. (2011). Maternally inherited essential hypertension is associated with the novel 4263A>G mutation in the mitochondrial tRNAIle gene in a large Han Chinese family. *Circ. Res.* 108 (7), 862–870. doi: 10.1161/CIRCRESAHA.110.231811

Wang, Q., Lee, I., Ren, J., Ajay, S. S., Lee, Y. S., and Bao, X. (2013). Identification and functional characterization of tRNA-derived RNA fragments (tRFs) in respiratory syncytial virus infection. *Mol. Ther.* 21 (2), 368–379. doi: 10.1038/mt.2012.237

Wang, Z., Li, L., Zhao, H., Peng, S., and Zuo, Z. (2015). Chronic high fat diet induces cardiac hypertrophy and fibrosis in mice. *Metabolism* 64 (8), 917–925. doi: 10.1016/j.metabol.2015.04.010

Wang, X. (2001). The expanding role of mitochondria in apoptosis. *Genes Dev.* 15 (22), 2922–2933.

Watson, C. N., Belli, A., and Di Pietro, V. (2019). Small Non-coding RNAs: New Class of Biomarkers and Potential Therapeutic Targets in Neurodegenerative Disease. *Front. Genet.* 10, 364. doi: 10.3389/fgene.2019.00364

Wei, J. W., Huang, K., Yang, C., and Kang, C. S. (2017). Non-coding RNAs as regulators in epigenetics (Review). *Oncol. Rep.* 37 (1), 3–9. doi: 10.3892/or.2016.5236

Yamasaki, S., Ivanov, P., Hu, G. F., and Anderson, P. (2009). Angiogenin cleaves tRNA and promotes stress-induced translational repression. *J. Cell Biol.* 185 (1), 35–42. doi: 10.1083/jcb.200811106

Yu, D., Cai, Y., Zhou, W., Sheng, J., and Xu, Z. (2018). The Potential of Angiogenin as a Serum Biomarker for Diseases: Systematic Review and Meta-Analysis. *Dis. Markers* 2018, 1984718. doi: 10.1155/2018/1984718

Yu, B. P. (1994). How diet influences the aging process of the rat. *Proc. Soc. Exp. Biol. Med.* 205 (2), 97–105. doi: 10.3181/00379727-205-43684

Zhang, X., and Chen, Q. (2020). A Twist between ROS and Sperm-Mediated Intergenerational Epigenetic Inheritance. *Mol. Cell* 78 (3), 371–373. doi: 10.1016/j.molcel.2020.04.003

Zhang, Y., Zhang, X., Shi, J., Tuorto, F., Li, X., Liu, Y., et al. (2018). Dnmt2 mediates intergenerational transmission of paternally acquired metabolic disorders through sperm small non-coding RNAs. *Nat. Cell Biol.* 20 (5), 535–540. doi: 10.1038/s41556-018-0087-2

Zhang, Y., Shi, J., Rassoulzadegan, M., Tuorto, F., and Chen, Q. (2019). Sperm RNA code programmes the metabolic health of offspring. *Nat. Rev. Endocrinol.* 15 (8), 489–498. doi: 10.1038/s41574-019-0226-2

Zhao, Q., Sun, Q., Zhou, L., Liu, K., and Jiao, K. (2019). Complex Regulation of Mitochondrial Function During Cardiac Development. *J. Am. Heart Assoc.* 8 (13), e012731. doi: 10.1161/JAHA.119.012731

Zhou, B., and Tian, R. (2018). Mitochondrial dysfunction in pathophysiology of heart failure. *J. Clin. Invest.* 128 (9), 3716–3726. doi: 10.1172/JCI120849

Zhou, H. L., Hinman, M. N., Barron, V. A., Geng, C., Zhou, G., Luo, G., et al. (2011). Hu proteins regulate alternative splicing by inducing localized histone hyperacetylation in an RNA-dependent manner. *Proc. Natl. Acad. Sci. U. S. A.* 108 (36), E627–E635. doi: 10.1073/pnas.1103344108

Zhou, S. S., Jin, J. P., Wang, J. Q., Zhang, Z. G., Freedman, J. H., Zheng, Y., et al. (2018). miRNAS in cardiovascular diseases: potential biomarkers, therapeutic targets and challenges. *Acta Pharmacol. Sin.* 39 (7), 1073–1084. doi: 10.1038/aps.2018.30

Zhu, H., Hasman, R. A., Barron, V. A., Luo, G. B., and Lou, H. (2006). A nuclear function of Hu proteins as neuron-specific alternative RNA processing regulators. *Mol. Biol. Cell* 17 (12), 5105–5114. doi: 10.1091/mbc.E06-02-0099

Zhu, H., Zhou, H. L., Hasman, R. A., and Lou, H. (2007). Hu proteins regulate polyadenylation by blocking sites containing U-rich sequences. *J. Biol. Chem.* 282 (4), 2203–2210. doi: 10.1074/jbc.M609349200

Zou, H., Li, Y., Liu, X., and Wang, X. (1999). An APAF-1.cytochrome c multimeric complex is a functional apoptosome that activates procaspase-9. *J. Biol. Chem.* 274 (17), 11549–11556. doi: 10.1074/jbc.274.17.11549

Conflict of Interest: The authors declare that the research was conducted in the absence of any commercial or financial relationships that could be construed as a potential conflict of interest.

frontiers in Pharmacology

CASE REPORT
published: 25 September 2020
doi: 10.3389/fphar.2020.579450

Mixed Hypertrophic and Dilated Phenotype of Cardiomyopathy in a Patient With Homozygous In-Frame Deletion in the *MyBPC3* Gene Treated as Myocarditis for a Long Time

*Olga Blagova[1], Indira Alieva[1], Eugenia Kogan[1], Alexander Zaytsev[1], Vsevolod Sedov[1], S. Chernyavskiy[1], Yulia Surikova[2], Ilya Kotov[3] and Elena V. Zaklyazminskaya[2]**

[1] Sechenov First Moscow State Medical University, Sechenov University, Moscow, Russia, [2] Medical Genetics Laboratory, Petrovsky National Research Centre of Surgery, Moscow, Russia, [3] Department of Bioinformatics, Centre of Genetics and Reproductive Medicine "Genetico", Moscow, Russia

OPEN ACCESS

Edited by:
Ya Liu,
Army Medical University, China

Reviewed by:
Tamer M. A. Mohamed,
University of Louisville, United States
Thomas Seidel,
University of Erlangen Nuremberg, Germany

***Correspondence:**
Elena V. Zaklyazminskaya
zhelene@mail.ru

Specialty section:
This article was submitted to Cardiovascular and Smooth Muscle Pharmacology, a section of the journal Frontiers in Pharmacology

Received: *02 July 2020*
Accepted: *09 September 2020*
Published: *25 September 2020*

Citation:
Blagova O, Alieva I, Kogan E, Zaytsev A, Sedov V, Chernyavskiy S, Surikova Y, Kotov I and Zaklyazminskaya EV (2020) Mixed Hypertrophic and Dilated Phenotype of Cardiomyopathy in a Patient With Homozygous In-Frame Deletion in the MyBPC3 Gene Treated as Myocarditis for a Long Time. Front. Pharmacol. 11:579450. doi: 10.3389/fphar.2020.579450

Hypertrophic cardiomyopathy (HCM) is the most common inherited disease, with a prevalence of 1:200 worldwide. The cause of HCM usually presents with an autosomal dominant mutation in the genes encoding one of more than 20 sarcomeric proteins, incomplete penetrance, and variable expressivity. HCM classically manifests as an unexplained thickness of the interventricular septum (IVS) and left ventricular (LV) walls, with or without the obstruction of the LV outflow tract (LVOT), and variable cardiac arrhythmias. Here, we present a rare case of mixed cardiomyopathy (cardiac hypertrophy and dilation) and erythrocytosis in a young patient. A 27-year-old man was admitted to the clinic due to biventricular heart failure (HF) NYHA class III. Personal medical records included a diagnosis of dilated cardiomyopathy (DCM) since the age of 4 years and were, at the time, considered an outcome of myocarditis. Severe respiratory infection led to circulatory decompensation and acute femoral thrombosis. The combination of non-obstructive LV hypertrophy (LV walls up to 15 mm), LV dilatation, decreased contractility (LV EF 24%), and LV apical thrombosis were seen. Cardiac MRI showed a complex pattern of late gadolinium enhancement (LGE). Endomyocardial biopsy (EMB) revealed primary cardiomyopathy with intravascular coagulation and an inflammatory response. No viral genome was detected in the plasma or EMB samples. Whole exome sequencing (WES) revealed a homozygous in-frame deletion p.2711_2737del in the *MyBPC3* gene. The clinically unaffected mother was a heterozygous carrier of this deletion, and the father was unavailable for clinical and genetic testing. Essential erythrocytosis remains unexplained. No significant improvement was achieved by conventional treatment, including prednisolone 40 mg therapy. ICD was implanted due to sustained VT and high risk of SCD. Orthotopic heart transplantation (HTx) was considered optimal. Early manifestation combined hypertrophic and dilated phenotype, and progression may reflect a complex genotype with more than one pathogenic allele and/or a combination of genetic diseases in one patient.

Keywords: hypertrophic cardiomyopathy, dilated cardiomyopathy, *MyBPC3* gene, heart failure progression, bi-allelic mutations, myocarditis, endomyocardial biopsy

INTRODUCTION

Primary myocardial diseases are one of the most difficult to diagnose and treat in cardiology. The most common inherited disease of the myocardium is hypertrophic cardiomyopathy (HCM), with an overall prevalence of approximately 1:200 worldwide (Maron et al., 2018). The disease is characterized by cardiac hypertrophy unexplained by pressure or volume overload, non-dilated left ventricle, and preserved or increased ejection fraction (Marian and Braunwald, 2017). HCM classically manifests as an unexplained thickness of the interventricular septum (IVS) and left ventricular (LV) walls with or without obstruction of the left ventricular outflow tract (LVOT), and variable arrhythmias (Marian and Braunwald, 2017). The cause of HCM is usually an autosomal dominant mutation in the genes encoding one of more than 20 sarcomeric proteins, incomplete penetrance, and variable expressivity (Kuusisto, 2020). The most common findings are causative variants of the *MYH7* and *MyBPC3* genes (Marian and Braunwald, 2017; Maron et al., 2018; Kuusisto, 2020). Generally, 5% to 7% of HCM index cases have two or more presumably damaging variants in the genes of interest; such patients have earlier manifestations, more pronounced cardiac hypertrophy, higher risk of sudden cardiac death, and increased risk of heart failure (Wang et al., 2014; Marian and Braunwald, 2017).

Multi-systemic disorders, which can mimic "sarcomeric" HCM and progress to heart failure, account for up to 40% of all unexplained myocardial hypertrophy (Authors/Task Force members et al., 2014). These phenocopies have rather different genetic origins, molecular pathogenesis, and natural course of disease. Precise etiological diagnosis is significant because the short-term and long-term prognosis may widely differ, and some of these phenocopies have gene-specific targets available for therapy (Fabry disease, TTR-amyloidosis, etc.). Various epigenetic factors and mechanisms may also significantly modulate the clinical course of the disease and prognosis; an important factor being inflammation. The driving role of inflammation is widely discussed in dilated cardiomyopathy, but there are few studies discussing the role of myocarditis in the progression and de-compensation in patients with HCM (Frustaci et al., 2007). We suggest that myocarditis should always be taken into consideration in cases of unexplained deterioration of cardiomyopathy. The mixed phenotype of cardiomyopathy makes the search for more than one cause, especially relevant.

Here, we present a case of progressive mixed hypertrophic and dilated cardiomyopathy in a young patient with a rare genetic cause: bi-allelic mutations in the *MyBPC3* gene.

CASE DESCRIPTION

A 27-year-old man was admitted to the cardiology department with symptoms of biventricular heart failure (NYHA class III), excessive sweating, and pain in the postoperative wound area at the site of thrombectomy 6 months prior to hospitalization.

His family history was unremarkable. Parents were not consanguineous. The father died at the age of 35, in a traumatic accident, and to the best of the patient's knowledge, had no cardiac complaints. At the time of the first hospitalization, the mother was 56 years old and had no complaints. The proband had a sister who died at 15 days of age due to a congenital heart disease (transposition of the great arteries). No other relative was diagnosed with cardiomyopathy of other cardiac disease before 50 years of age. External risk factors: smoking average of three cigarettes/day for 7 years. No alcohol abuse or other toxic factors were mentioned.

Personal medical history with main milestones and medications taken (when possible) was reconstructed from the available medical records (**Figure 1**).

The patient had an average height (174 cm) and weight of 79 kg for his age, BMI 26.1 kg/m^2, and normal arterial blood pressure (120/80 mmHg). Edema of the leg and slight serous discharge from the wound in the right groin area were found on the initial physical examination.

DIAGNOSTIC ASSESSMENT

Headings Instrumental Investigations (ECG, EchoCG, Cardiac CT, and MRI With Gadolinium Enhancement)

Resting ECG showed HR 98 bpm, sinus tachycardia, signs of hypertrophy of both atria and ventricles, and low R waves in standard leads (**Figure 2**). Holter 24-h ECG monitoring revealed 289 PVBs of two morphologies and two episodes of non-sustained ventricular tachycardia of 4–7 beats 104–227 bpm. Echocardiography had shown (**Figure 3**) enlarged LA (110 ml) and RA (69 ml), dilated LV (end-diastolic diameter 6.4 cm, end-diastolic volume 236 ml, end-systolic volume 192 ml) with decreased contractility (LV EF 20%), and an enlarged RV (end-diastolic diameter 3.1 cm). LV diastolic function was significantly impaired (E, 35 cm/s; A, 23 cm/s; E/A, 1.5; DecT, 70 ms; Emed, 2.2 cm/s; E/Emed 15.8, 5 cm/s). Diffuse cardiac hypertrophy was revealed (IVS 14–16 mm, LV posterior wall 15–16 mm, RV walls 7–11 mm), with LV myocardial mass at 554.84 g. In the region of the apex, a fixed parietal thrombus was detected. Mild mitral, tricuspid, and pulmonary regurgitation were noted. The systolic pressure in the pulmonary artery was 36 mmHg.

Cardiac CT revealed dilation of the LV chamber (69 mm) with a parietal clot spreading from the middle segment of the anterior wall to the apex (5 mm × 19 mm × 90 mm), and LV myocardial hypertrophy (up to 16 mm). In the delayed phase of LV myocardial contrast, it was diffusely heterogeneous. No definite late contrast enhancement or significant coronary stenosis was detected.

On cardiac MRI, the LV was spherical and severely dilated (EDD 71 mm, EDV 120 ml/m^2) (**Supplementary Figure 1**). The wall thickness of the LV was 14 mm. Increased trabeculation of the LV was found but did not meet the criteria of the LVNC. A decrease in LV contractility with LV EF of 21% was confirmed.

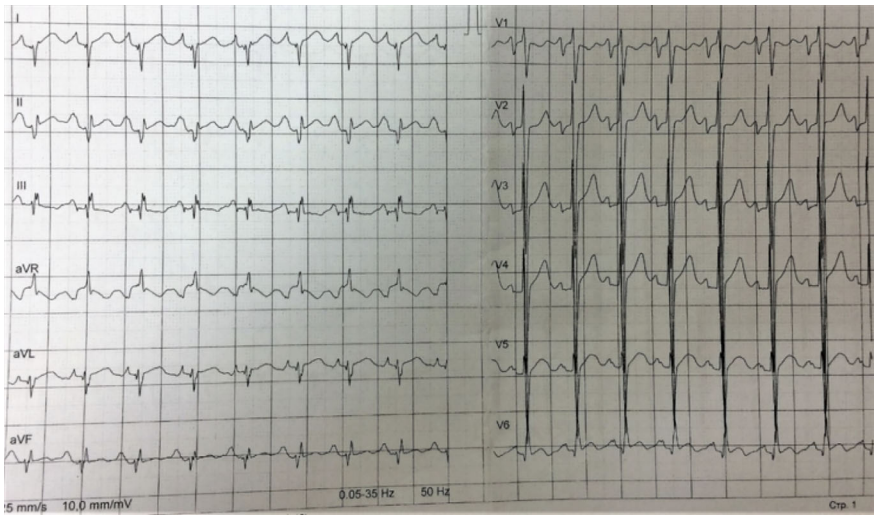

FIGURE 1 | The main milestones of the proband's medical history. Reconstructed by the patient's reports and medical records.

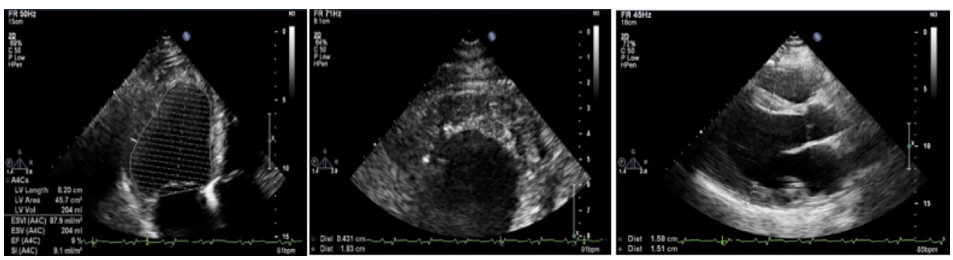

FIGURE 2 | Resting ECG. HR 98 bpm, sinus tachycardia, signs of hypertrophy of both atria and ventricles, and decreased votage of the R waves in standard leads.

Several LGE sites were identified: transmural along the lower wall, subendocardial (up to 60%) in the apex of LV and apical segment of the anterior septum, and extended intra-ventricular LGE ("strip") in the middle and apical segments of the septum. The apex of the LV was lined with a flat linear thrombus of 3.5 mm across it.

Laboratory Blood Tests

Initial blood tests revealed erythrocytosis (RBC, 6.85 mcL) and high white blood cell count (WBC, 27.8 × 10U3/ul). Platelet count was normal. Clinical chemistry showed a high hemoglobin level (193 g/L), increased hematocrit (65.8%), elevated erythropoietin (81.3 U/ml), slightly elevated creatinine (119.5 μmol/L), fibrinogen 4.67 g/L, and INR 5.85.

High levels of anti-heart antibodies against cardiomyocytes' nuclear antigens, endothelial antigens, cardiomyocyte antigens, conduction system fibers, and smooth muscle antigens were detected. No viral genome was detected by virus-specific PCR in the blood.

Endomyocardial and Bone Marrow Biopsy

A right ventricular endomyocardial biopsy was performed to verify the diagnosis of myocarditis. A combination of pathologically altered cardiomyocytes, productive vasculitis with thrombosis of individual vessels, and small perivascular lymphocytic-macrophage infiltrates (less than 14 cells) was detected (**Figure 4**). Morphological changes were specific for primary cardiomyopathies in combination with disseminated intravascular coagulation and secondary inflammatory reactions. The genomes of herpes virus, adenovirus, and parvovirus B19 were not detected by PCR in the myocardial biopsy sample.

A bone marrow trepanobiopsy was performed to clarify the origin of erythrocytosis, but no evidence of myeloproliferative disease was found.

Genetic Analysis

Whole exome sequencing (WES) for the proband's DNA was performed using a TruSeq Exome library preparation kit (IDT-Illumina) followed by next-generation sequencing on an Illumina

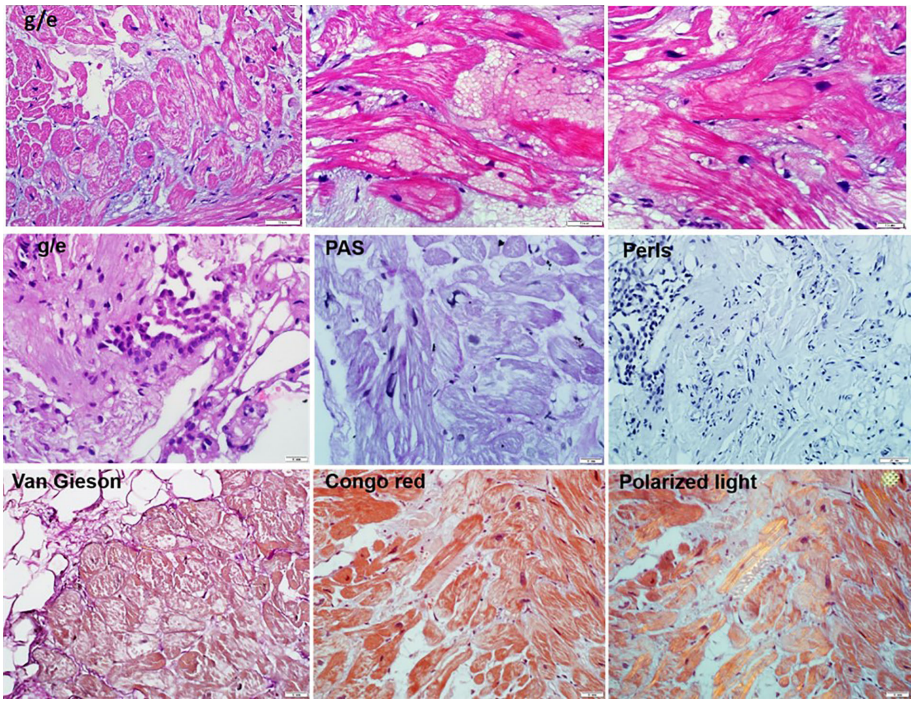

FIGURE 3 | Echocardiography. On the left—a severe decrease in left ventricular EF (at this measurement of 9%); in the center—a lining clot in the apex of the left ventricle with dimensions of 4 mm × 18 mm; on the right—hypertrophy of the left ventricular wall to 15–16 mm.

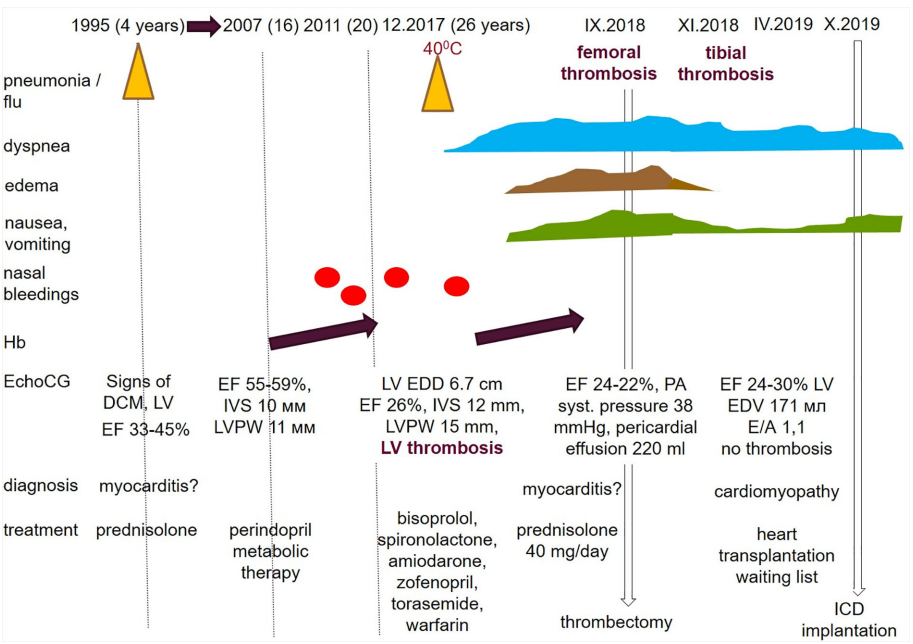

FIGURE 4 | The endomyocardial biopsy of the right ventricle (10–50 micron scale). Hematoxylin eosin staining showed: the endocardium is thin. Cardiomyocytes with foci of enlightenment in the perinuclear zone, disarray, with homogenization of the cytoplasm. In individual cardiomyocytes, there are foci of myolysis with the formation of voids in the cytoplasm. Microvessels with red blood cell sludge phenomenon, sclerosed walls, proliferation of endothelial cells, stenosis of the lumen and single perivascular lymphohistiocytic cells. There are minor hemorrhages, mild sclerosis. Staining of congo red (in non-polarized and polarized light), Perls reaction, the PAS reaction are a negative.

system. Reads were aligned to the human genome build GRCh37/UCSC hg19 and analyzed for sequence variants using a custom-developed bioinformatics pipeline. The proband's WES identified the homozygous deletion chr11:g.47357432_47357458del (ENST00000545968.1: c.2711_2737del) in the *MyBPC3* gene p.2711_2737del. This variant was confirmed in the proband's DNA in the homozygous state, and in his mother's DNA in a heterozygous state. In-frame 27 bp deletion leads to the shortening of cardiac myosin binding protein for nine amino acids in the fibronectin III 2 (C7) domain (**Supplementary Figure 2**). This variant was classified as likely pathogenic (Class IV) based on the ACMG (2015) criteria (Richards et al., 2015). No additional pathogenic, likely pathogenic variants nor unique variant of unknown clinical significance was found in the genes responsible for cardiomyopathies or any other storage disorders. Thus, we suggest that bi-allelic deletion in the MyBPC3 gene might be sufficient explanation of the progressive cardiomyopathy in this patient. But, presence of additional variant in the less studied genomic area cannot be completely excluded. Strictly speaking there is an alternative explanation of the NGS and Sanger results for this patient. In theory, it might be a combination of hemizygous deletion due to the whole/partial deletion of the paternal allele (inherited or *de novo*). But, we have no any prove for it and for the best of our knowledge proband's father had no complaints until he died in car accident at his 35.

No known pathogenic mutations or rare variants were found in the *EPOR* or other genes responsible for the familial erythrocytosis. No unique or known variants with proven clinical significance were found in the genes associated with inherited thrombophilia.

The combination of data from complex evaluation results in the following diagnosis: 1. Familial sarcomeric cardiomyopathy (homozygous deletion p.2711_2737del in the MyBPC3 gene), mixed phenotype (diffuse hypertrophic, dilated). 2. Ischemic cardiomyopathy due to impaired microcirculation with secondary inflammation. 3. Erythrocytosis of unknown origin

Supportive therapy was prescribed: prednisolone 5 mg, bisoprolol 2.5 mg, amiodarone 200 mg, perindopril 2.5 mg, furosemide 40 mg, spironolactone 50 mg, warfarin, acetylsalicylic acid 100 mg, and omeprazole 20 mg. The patient's condition remains relatively stable for 6 months of follow-up but transient edema, palpitations, sweating, dyspnea at the level of NYHA class 2–3 persisted. Hemoglobin levels returned to normal, but LV dysfunction (LV EF 19%) remained after a temporary improvement (LV EF 28%).

Six months later, the patient experienced another acute thrombosis of the right posterior tibial artery without flotation, and conservative treatment was administered. Due to the development of thyrotoxicosis, amiodarone was replaced with sotalol. Therapy with prednisolone 5 mg per day was continued. In the next 6 months, ICD was implanted. No appropriate shocks were noted. The patient was included in the waiting list for heart transplantation. Unfortunately, despite the normalization of erythrocyte levels and two-component antithrombotic therapy, no improvement in myocardial contractility was noted. Prolonged therapy with prednisolone (at an initial dose of 40 mg per day) and standard cardiotropic therapy had no effect. Heart transplantation appears to be the optimal treatment option.

DISCUSSION

This clinical case was unusual and challenging in many respects. The combination of severe systolic dysfunction with dilatation of all heart chambers and evident diffuse myocardial hypertrophy is a rare clinical observation. Dilatation of the spherical changed LV with a markedly reduced EF can be a manifestation of both primary DCM and severe myocarditis. At the same time, dilated cardiomyopathy might represent the decompensating stage of any cardiomyopathy.

The wall thickness of the LV met the criteria for HCM. Typical cardiomyocyte disarray found in myocardial biopsy samples was a particular feature of the primary HCM, and the patient had no obvious reason for pressure overload. However, the anatomical variant of cardiac remodeling with diffused, generalized LV walls and right ventricular involvement is more typical for phenocopies of HCM, especially for storage disorders. Among the storage diseases, the earliest decompensation is typical of Danon disease. Therefore, in one of the last studies, unfavorable outcomes (death/transplantation) were noted in one-third of men, with an average age of 21 years (Brambatti et al., 2019). However, the degree of myocardial hypertrophy in our patient was unusually low for Danon disease in men. In addition, he had no typical systemic manifestations of Danon disease, as well as other storage diseases involving the heart (Fabry's disease, for example). No data was obtained for storage disease in myocardial biopsy after special staining (periodic Acid-Schiff and Congo red in polarized light). Finally, no pathogenic/likely pathogenic genetic variant was found in the genes responsible for the known storage disorders after whole-exome sequencing.

Prolonged undulating course of the disease from 4 years with periods of persistent improvement, possible effects of steroid therapy in the past, the association of rapid deterioration at 26 years with influenza, LV apex thrombosis, preservation of elevated titers of anti-heart antibodies, and mild signs of inflammation in myocardial biopsy despite steroid therapy, might provide evidence of myocarditis. Steroid therapy was started before the patient came to the clinic, which made it difficult to interpret the biopsy data. However, no clinical effect of the steroid prescription was observed despite the absence of viruses in the myocardium.

Inefficiency of steroids and early debut of the disease may have been evidence of primary DCM. However, there was no explanation for diffuse myocardial hypertrophy. The presence of increased trabeculation of the myocardium according to MRI is more typical for sarcomeric cardiomyopathy. Mixed and severe phenotypes have also been reported. Some authors have even proposed the concept of a continuum of sarcomeric cardiomyopathies (Baldi et al., 2010). The cause of rapid decompensation in a previously stable course (myocardial embolic infarct? myocarditis)? was unclear in this case. The pattern of LGE according to MRI could reflect both inflammation and myocardial necrosis. In addition, there were signs of fibrosis, typical of primary myocardial hypertrophy. The diagnosis of isolated sarcomeric

HCM was inconsistent with the early manifestation of the DCM phenotype.

According to a large multicenter cohort study, the average age of decompensation for patients with sarcomeric HCM was 45 years (Biagini et al., 2014). The earliest (41 years on average) appearance of final stage of HCM developed in patients with mutations in gene MYH7 and multiple mutations. However, only adult patients were included in the study. According to the data from the Mayo Clinic, out of 2,073 patients with HCM, only eight had EF below 50%, (Killu et al., 2018). Their average age was 44 years. Only five patients underwent LVAD implantation and cardiac heart transplantation 15 years prior to HCM diagnosis. All this data indicated that our case was atypical for an isolated sarcomeric HCM.

The most likely, therefore, was the primary (genetically determined) nature of cardiomyopathy in our patient. One could think of a combination of two or more mutations in the genes of interest for HCM, and we found a bi-allelic mutation in the *MyBPC3* gene. Deletion of nine amino acids raised in the highly conservative C7 FnIII domain (**Supplementary Figure 2**) framed with amino acids from 872 to 967 (Karsai et al., 2011). Several missense mutations (for example, p.Pro873Leu, p. Pro873His, p.Asn948Thr, p. Thr957Ser, p.Thr958Ile) leading to HCM, DCM and LV non-compaction were described in this region (Daehmlow et al., 2002; Nanni et al., 2003; Lekanne Deprez et al., 2006; Ehlermann et al., 2008; Probst et al., 2011). It's remarkable that most of them were discussed in patients with rapid progression of HCM to a dilated phase even in mono-allelic state (Daehmlow et al., 2002; Nanni et al., 2003; Lekanne Deprez et al., 2006; Ehlermann et al., 2008; Probst et al., 2011). There is no large randomized study regarding the natural course of HCM in patients carrying more than one pathogenic or likely pathogenic allele. However, many particular clinical cases, case-control and observational studies have pointed out that the role of a second genetic hit can be crucial in the age of HCM manifestation (Wessels et al., 2015; Dzemeshkevich et al., 2018; Kissopoulou et al., 2018). Prospective genetic counseling was also challenging. Despite well-accepted autosomal dominant nature of HCM and severe phenotype in our patient, the prognosis for off-springs seems to be favorable. We based it on the fact that his parents were asymptomatic (mother, confirmed carrier, is asymptomatic at 57 y.o.; and father, presumed carrier, was asymptomatic at 35 y.o. when died in accident). Thus, we hypothesize that this deletion p.2711_2737del in mono-allelic state is highly tolerated. But, in the absence of direct confirmation of the health status and genotype of the father, we cannot claim it confidently.

The role of associated myocarditis in the development of rapid decompensation cannot be excluded. However, a mild inflammatory reaction detected in the biopsy may have developed secondary to primary myocardial damage. In any case, there were no indications for aggressive treatment of inflammation.

Finally, it was necessary to exclude *polycythemia vera* as a cause of erythrocytosis, which can aggravate myocardial dysfunction due to microcirculation disorders. Even cases of massive myocardial infarcts in patients with polycythemia and normal coronary arteries are described (Nahler et al., 2017). Myocardial biopsy data confirmed this mechanism to be dysfunctional. There were no strong data to support primary erythrocytosis. No mutations in the genes of interest were identified based on wide genetic screening, and no signs of myeloproliferative disease in bone marrow biopsy were found. Elevated erythropoietin levels could indicate a compensatory mechanism of erythrocytosis due to hypoxia.

Among epigenetic mechanisms, decompensation may influence a lot of the clinical appearance and disease progression. However, we believe chronic microcirculation disorder (sludge, microthrombosis, hemorrhage with cardiomyocyte death) and secondary inflammatory response are responsible for the myocardial damage. It is also impossible to rule out embolic infarction of the lower wall of the left ventricle or necrosis due to intravascular clogging.

Correct diagnosis influence a lot the treatment strategy, long-term prognosis, life style modifications, and reproductive strategy. Information about primary nature of disease is usually stressful what raises many questions regarding risk of transmission and health perspectives and may affect quality of life. Communicating the genetic risk information to maximize understanding and promote health is increasingly important given the rapidly expanding availability and capabilities of genomic and reproductive technologies (Lautenbach et al., 2013). In this clinical case, the prognosis for offspring is favorable provided that second partner in the couple has no HCM. This information was very important for our patient. Currently, there are no options of intervention in primary genetic cardiomyopathy. But, currently, several gene therapy approaches have been developed to rescue genetic defects in "sarcomeric" genes, and, especially, in the *MyBPC3* (Prondzynski et al., 2019). We believe that accumulation of information about natural course of HCM caused by particular mutations and their combinations may provide important insights of new treatment strategies.

CONCLUSION

Here, we present a rare case of mixed hypertrophic and dilated cardiomyopathy in a young patient complicated by myocarditis, erythrocytosis, and recurrent thrombi. Disease progression was more severe than usual in classic HCM patients, but relatively long lasting for pediatric DCM first diagnosed at 4 years. Etiological diagnosis was challenging. It required a differential diagnosis between primary, inflammatory, and ischemic myocardial damage. Whole exome sequencing revealed bi-allelic deletion in the *MyBPC3* gene, but erythrocytosis remained unexplained. This observation supports the hypothesis that the co-existence of the genetic causes and additional external factors (thrombosis, inflammation, etc.) contribute significantly to the phenotype and HF progression, and it is important to reveal all of them. Successful diagnostic search and optimal management is only possible with a multidisciplinary team and a whole spectrum of investigations from cardiac imaging and myocardial biopsy to deep genotyping. Experimental research including iPS-CMs studies are needed for the detailed evaluation of the effect of the p.2711_2737del variant in hetero- and homozygous state on myosin-binding protein C3 functioning, and for further insight on molecular mechanisms of cardiomyopathy.

Patient Perspective

"I have many concerns regarding my future. I've thought about heart transplantation and came to the referred Centre. I need to live close to this Centre but I don't have any opportunity to live in Moscow continiously. I would get on the waiting list but have many concerns about risks related to the operation by itself and subsequent immunosupression. So the question is still open. Well, how to say, I will live as long as I can, and how long it left. I think it will get worse, and I sometimes feel it, but I'm not telling anyone in my city what the condition is now, not to relatives nor my doctor from my city. I don't think it makes sense if no one can really change the course of genetic disease, right?"

DATA AVAILABILITY STATEMENT

The raw clinical and genetic data supporting this article cannot be placed in public repository due to ethical reason (personal data protection) but it will be available by the corresponding author (ZE, zhelene@mail.ru) upon reasonable request.

ETHICS STATEMENT

Informed written consent was obtained from the patient for this clinical case publication, and all data and figures included in this article.

AUTHOR CONTRIBUTIONS

OB, IA, AZ, and SC participated in the diagnosis and treatment of the patient. EK and VS performed histopathological and instrumental investigations. YS and IK performed wet and bioinformatic genetic investigation. EZ performed genetic counseling of the family. OB and ZE prepared the draft of the manuscript. All authors contributed to the article and approved the submitted version.

FUNDING

This work was funded by Russian Science Foundation (Grant № 16-15-10421).

ACKNOWLEDGMENTS

We thank our patient for his kind permission to present this clinical case and sharing his personal perception of disease and its genetic nature.

SUPPLEMENTARY MATERIAL

The Supplementary Material for this article can be found online at: https://www.frontiersin.org/articles/10.3389/fphar.2020.579450/full#supplementary-material

SUPPLEMENTARY FIGURE 1 | Cardiac MRI with gadolinium enchamcement. LV was spherical, severely dilated (EDD 71 mm, EDV 120 ml/m^2), with increased thickness (14 mm) and trabeculae. LV EF of 21%. Several LGE sites: transmural along the lower wall, subendocardial (up to 60%) in the apex of LV and apical segment of the anterior septum, and extended intra-ventricular LGE ("strip") in the middle and apical segments of the septum. The apex of the LV was lined with a flat linear thrombus of 3.5 mm across it.

SUPPLEMENTARY FIGURE 2 | Schematic representation of deletion of the 27 bp (chr11:g.47357432_47357458del (ENST00000545968.1: c.2711_2737del) in the *MyBPC3* gene found in proband in homozygous state at the DNA, mRNA, and protein level.

REFERENCES

Authors/Task Force members, Elliott, P. M., Anastasakis, A., Borger, M. A., Borggrefe, M., Cecchi, F., et al. (2014). ESC Guidelines on diagnosis and management of hypertrophic cardiomyopathy: the Task Force for the Diagnosis and Management of Hypertrophic Cardiomyopathy of the European Society of Cardiology (ESC). *Eur. Heart J.* 35 (39), 2733–2779. doi: 10.1093/eurheartj/ehu284

Baldi, M., Sgalambro, A., Nistri, S., Girolami, F., Baldini, K., Fantini, S., et al. (2010). Clinica e genetica del ventricolo sinistro non compatto: conferma di un continuum nelle cardiomiopatie [Clinical and genetic features of left ventricular noncompaction: a continuum in cardiomyopathies]. *G. Ital. Cardiol. (Rome)* 11 (5), 377–385.

Biagini, E., Olivotto, I., Iascone, M., Parodi, M. I., Girolami, F., Frisso, G., et al. (2014). Significance of sarcomere gene mutations analysis in the end-stage phase of hypertrophic cardiomyopathy. *Am. J. Cardiol.* 114 (5), 769–776. doi: 10.1016/j.amjcard.2014.05.065

Brambatti, M., Caspi, O., Maolo, A., Koshi, E., Greenberg, B., Taylor, M., et al. (2019). Danon disease: Gender differences in presentation and outcomes. *Int. J. Cardiol.* 286, 92–98. doi: 10.1016/j.ijcard.2019.01.020

Daehmlow, S., Erdmann, J., Knueppel, T., Gille, C., Froemmel, C., Hummel, M., et al (2002). Novel mutations in sarcomeric protein genes in dilated cardiomyopathy. *Biochem. Biophys. Res. Commun.* 298 (1), 116–120. doi: 10.1016/s0006-291x(02)02374-4

Dzemeshkevich, S., Motreva, A., Nechepurenko, A., Korzh, D., Tarasov, D., Frolova, Y., et al. (2018). [Sudden cardiac death prevention in a patient with diffised generalyzed hypertrophic cardiomyopathy in a patient with two mutations in the MYH7 and MyBPC3 genes]. *Clin. Exp. Surg.* 3 (6), 78–84. doi: 10.24411/2308-1198-2018-13008

Ehlermann, P., Weichenhan, D., Zehelein, J., Steen, H., Pribe, R., and Zeller, R. (2008). et al. Adverse events in families with hypertrophic or dilated cardiomyopathy and mutations in the MYBPC3 gene. *BMC Med. Genet.* 9:95. doi: 10.1186/1471-2350-9-95

Frustaci, A., Verardo, R., Caldarulo, M., Acconcia, M. C., Russo, M. A., and Chimeni, C. (2007). Myocarditis in hypertrophic cardiomyopathy patients presenting acute clinical deterioration. *Eur. Heart J.* 28 (6), 733–740. doi: 10.1093/eurheartj/ehl525

Karsai, A., Kellermayer, M. S., and Harris, S. P. (2011). Mechanical unfolding of cardiac myosin binding protein-C by atomic force microscopy. *Biophys. J.* 101 (8), 1968–1977. doi: 10.1016/j.bpj.2011.08.030

Killu, A. M., Park, J. Y., Sara, J. D., Hodge, D. O., Gersh, B. J., Nishimura, R. A., et al. (2018). Cardiac resynchronization therapy in patients with end-stage hypertrophic cardiomyopathy. *Europace* 20 (1), 82–88. doi: 10.1093/europace/euw327

Kissopoulou, A., Trinks, C., Green, A., Karlsson, J.-E., Jonasson, J., and Gunnarsson, C. (2018). Homozygous missense MYBPC3 Pro873His mutation associated with increased risk for heart failure development in

hypertrophic cardiomyopathy. *ESC. Heart Fail.* 5 (4), 716–723. doi: 10.1002/ehf2.12288

Kuusisto, J. (2020). Genetics of hypertrophic cardiomyopathy: what is the next step? *Heart* 106 (17), 1291–1292. doi: 10.1136/heartjnl-2020-317043 heartjnl-2020-317043.

Lautenbach, D. M., Christensen, K. D., Sparks, J. A., and Green, R. C. (2013). Communicating genetic risk information for common disorders in the era of genomic medicine. *Annu. Rev. Genomics Hum. Genet.* 14, 491–513. doi: 10.1146/annurev-genom-092010-110722

Lekanne Deprez, R. H., Muurling-Vlietman, J. J., Hruda, J., Baars, M. J. H., Wijnaendts, L. C. D., Stolte-Dijkstra, I., et al. (2006). Two cases of severe neonatal hypertrophic cardiomyopathy caused by compound heterozygous mutations in the MYBPC3 gene. *J. Med. Genet.* 43 (10), 829–832. doi: 10.1136/jmg.2005.040329

Marian, A. J., and Braunwald, E. (2017). Hypertrophic Cardiomyopathy: Genetics, Pathogenesis, Clinical Manifestations, Diagnosis, and Therapy. *Circ. Res.* 121 (7), 749–770. doi: 10.1161/CIRCRESAHA.117.311059

Maron, B. J., Rowin, E. J., and Maron, M. S. (2018). Global Burden of Hypertrophic Cardiomyopathy. *JACC Heart Fail.* 6 (5), 376–378. doi: 10.1016/j.jchf.2018.03.004

Nahler, A., Fuchs, D., Reiter, C., Kiblböck, D., Steinwender, C., and Lambert, T. (2017). Myocardial infarction with proximal occlusion of the left anterior descending coronary artery in a 22-year-old patient with polycythaemia vera. *Clin. Med. (Lond).* 17 (1), 46–47. doi: 10.7861/clinmedicine.17-1-46

Nanni, L., Pieroni, M., Chimenti, C., Simionati, B., and Zimbello, R. (2003). Hypertrophic cardiomyopathy: two homozygous cases with "typical" hypertrophic cardiomyopathy and three new mutations in cases with progression to dilated cardiomyopathy. *Biochem. Biophys. Res. Commun.* 309 (2), 391–398. doi: 10.1016/j.bbrc.2003.08.014

Probst, S., Oechslin, E., Schuler, P., Greutmann, M., Boyé, P., Knirsch, W., et al. (2011). Sarcomere gene mutations in isolated left ventricular noncompaction cardiomyopathy do not predict clinical phenotype. *Circ. Cardiovasc. Genet.* 4 (4), 367–374. doi: 10.1161/CIRCGENETICS.110.959270

Prondzynski, M., Mearini, G., and Carrier, L. (2019). Gene therapy strategies in the treatment of hypertrophic cardiomyopathy. *Pflugers Arch.* 471 (5), 807–815. doi: 10.1007/s00424-018-2173-5

Richards, S., Aziz, N., Bale, S., Bick, D., Das, S., Gastier-Foster, J., et al. (2015). Standards and guidelines for the interpretation of sequence variants: a joint consensus recommendation of the American College of Medical Genetics and Genomics and the Association for Molecular Pathology. *Genet. Med.* 17 (5), 405–424. doi: 10.1038/gim.2015.30

Wang, J., Wang, Y., Zou, Y., Sun, K., Wang, Z., Ding, H., et al. (2014). Malignant effects of multiple rare variants in sarcomere genes on the prognosis of patients with hypertrophic cardiomyopathy. *Eur. J. Heart Fail.* 16 (9), 950–957. doi: 10.1002/ejhf.144

Wessels, M. W., Herkert, J. C., Frohn-Mulder, I. M., Dalinghaus, M., van den Wijngaard, A., de Krijger, R. R., et al. (2015). Compound heterozygous or homozygous truncating MYBPC3 mutations cause lethal cardiomyopathy with features of noncompaction and septal defects. *Eur. J. Hum. Genet.* 23 (7), 922–928. doi: 10.1038/ejhg.2014.21116

Conflict of Interest: The authors declare that the research was conducted in the absence of any commercial or financial relationships that could be construed as a potential conflict of interest.

frontiers in Pharmacology

ORIGINAL RESEARCH
published: 30 October 2020
doi: 10.3389/fphar.2020.559220

Signaling via the Interleukin-10 Receptor Attenuates Cardiac Hypertrophy in Mice During Pressure Overload, but not Isoproterenol Infusion

Nicholas Stafford[1,2†], *Farryah Assrafally*[1,2†], *Sukhpal Prehar*[1,2], *Min Zi*[1,2], *Ana M. De Morais*[1,2], *Arfa Maqsood*[1,2], *Elizabeth J. Cartwright*[1,2], *Werner Mueller*[3] *and Delvac Oceandy*[1,2*]

[1]Division of Cardiovascular Sciences, Faculty of Biology, Medicine and Health, The University of Manchester, Manchester, United Kingdom, [2]Manchester Academic Health Science Centre, The University of Manchester, Manchester, United Kingdom, [3]School of Biological Sciences, The University of Manchester, Manchester, United Kingdom

OPEN ACCESS

Edited by:
Ya Liu,
Army Medical University, China

Reviewed by:
InKyeom Kim,
Kyungpook National University, South Korea
Zhongbing Lu,
Chinese Academy of Sciences (CAS), China

***Correspondence:**
Delvac Oceandy
delvac.oceandy@manchester.ac.uk

[†]These authors have contributed equally to this work

Specialty section:
This article was submitted to Cardiovascular and Smooth Muscle Pharmacology, a section of the journal Frontiers in Pharmacology

Received: 05 May 2020
Accepted: 06 October 2020
Published: 30 October 2020

Citation:
Stafford N, Assrafally F, Prehar S, Zi M, De Morais AM, Maqsood A, Cartwright EJ, Mueller W and Oceandy D (2020) Signaling via the Interleukin-10 Receptor Attenuates Cardiac Hypertrophy in Mice During Pressure Overload, but not Isoproterenol Infusion. Front. Pharmacol. 11:559220. doi: 10.3389/fphar.2020.559220

Inflammation plays a key role during cardiac hypertrophy and the development of heart failure. Interleukin-10 (IL-10) is a major anti-inflammatory cytokine that is expressed in the heart and may play a crucial role in cardiac remodeling. Based on the evidence that IL-10 potentially reduces pathological hypertrophy, it was hypothesized that signaling via the IL-10 receptor (IL10R) in the heart produces a protective role in reducing cardiac hypertrophy. The aim of this study was to investigate the effects of the ablation of *Il-10-r1* gene during pathological cardiac hypertrophy in mice. We found that IL-10R1 gene silencing in cultured cardiomyocytes diminished the anti-hypertrophic effect of Il-10 in TNF-α induced hypertrophy model. We then analyzed mice deficient in the *Il-10-r1* gene (IL-10R1$^{-/-}$ mice) and subjected them to transverse aortic constriction or isoproterenol infusion to induce pathological hypertrophy. In response to transverse aortic constriction for 2 weeks, IL-10R1$^{-/-}$ mice displayed a significant increase in the hypertrophic response as indicated by heart weight/body weight ratio, which was accompanied by significant increases in cardiomyocyte surface area and interstitial fibrosis. In contrast, there was no difference in hypertrophic response to isoproterenol infusion (10 days) between the knockout and control groups. Analysis of cardiac function using echocardiography and invasive hemodynamic studies did not show any difference between the WT and IL-10R1$^{-/-}$ groups, most likely due to the short term nature of the models. In conclusion, our data shows that signaling via the IL-10 receptor may produce protective effects against pressure overload-induced hypertrophy but not against β-adrenergic stimuli in the heart. Our data supports previous evidence that signaling modulated by IL-10 and its receptor may become a potential target to control pathological cardiac hypertrophy.

Keywords: interleukin-10, cardiac hypertrophy, signaling pathway, inflammation, heart failure

INTRODUCTION

Heart failure remains one of the primary causes of morbidity and mortality across the global spectrum of cardiovascular disease. Despite current advances in the therapeutic approach, prognosis of this disease remains poor and its prevalence is rising (Mozaffarian et al., 2015; Taylor et al., 2017). Understanding the pathophysiology of heart failure is essential for the development of effective and efficient new therapeutic approaches.

The involvement of pro-inflammatory cytokines in HF was first reported three decades ago, when elevated TNF-α was found in the serum of HF patients (Levine et al., 1990). Since then, growing bodies of evidence have indicated the key roles of inflammatory mediators in the development of HF (reviewed in (Adamo et al., 2020)). Almost all primary myocardial injuries such as pressure overload and ischemia can trigger activation of the immune response. In addition, molecules that are released by damaged myocytes, for example heat shock proteins, fibronectins and reactive oxygen species, may activate residential macrophages and other immune cells, which eventually triggers the release of inflammatory cytokines (Mann, 2015).

It is widely accepted that cytokines are involved in the pathogenesis of heart failure, not only by affecting the inflammatory response but also by directly affecting cardiomyocytes and other cells in the heart such as fibroblasts and vascular cells. This is underlined by the fact that cardiomyocytes and other non-inflammatory cells in the heart are also producing cytokines and expressing their receptors under stress (Yoshida et al., 2005). Evidence has shown that pro-inflammatory cytokines contribute significantly to the pathogenesis of heart failure, in particular in modulating left ventricular remodeling and myocardial contractility. For example, cardiac overexpression of TNF-α in mice induces cardiac hypertrophy and reduces contractility (Kubota et al., 1997), whereas ablation of TNF-α attenuates cardiac hypertrophy, inflammation, apoptosis and fibrosis following aortic constriction (Sun et al., 2007).

In contrast to the knowledge on the role of pro-inflammatory cytokines in the heart, less is known about the roles of anti-inflammatory molecules in the context of cardiac hypertrophy and heart failure. One of the best characterized anti-inflammatory cytokines in the heart is the interleukin-10 (IL-10). IL-10 is mainly produced by T-cells and is able to modulate both acute and chronic inflammation (reviewed in (Ouyang and O'Garra, 2019)). The main targets of IL-10's actions are inflammatory cells expressing the IL-10 receptor (IL-10R) such as macrophages/monocytes, dendritic cells, T and B cells (Ouyang and O'Garra, 2019). However, expression of the IL-10 receptor in cardiomyocytes is also reported (Yoshida et al., 2005), suggesting that IL-10 may have a direct effect on these cells.

Several prior studies have shown beneficial effects of IL-10 treatment in pathological conditions. Observations in isolated cardiomyocytes have shown beneficial effects of IL-10 in inhibiting TNF-α induced apoptosis and oxidative stress (Dhingra et al., 2007; Dhingra et al., 2009). Likewise, treatment with IL-10 produces beneficial effects in animal models of myocardial infarction and pressure overload hypertrophy (Krishnamurthy et al., 2009; Verma et al., 2012; Jung et al., 2017). In addition, involvement of IL-10 in the clinical setting has been underlined by the finding that serum IL-10 is elevated in HF patients (Lindberg et al., 2008). However, the precise characterization of IL-10's effects in the cardiomyocytes and in the heart, and whether it exerts these effects via activation of its receptor are not fully understood. Therefore, we will address this question in the present project by investigating the effects of IL-10R1 gene ablation in the setting of pathological cardiac hypertrophy.

MATERIALS AND METHODS

Isolation of Neonatal Rat Cardiomyocytes

Primary neonatal rat cardiomyocytes (NRCM) were derived from 1- to 3- days old Sprague Dawley rat neonates. The neonates were sacrificed by cervical dislocation and the hearts were removed and put into filter-sterilized ADS solution pH 7.35 (116 mM NaCl, 20 mM HEPES, 1 mM NaH2PO4, 5.5 mM glucose, 5.5 mM KCl and 1 mM MgSO4). The hearts were sliced into small pieces and then digested in ADS solution containing 0.6 mg/ml collagenase A (Roche) and 0.6 mg/ml pancreatin (Sigma) in a shaking 37°C water bath for 7 min. Digested cells were collected and the process was repeated a further seven times. Cells were pooled and centrifuged at 1,200 r.p.m. for 5 min. The pellet was then resuspended in 40 ml of pre-plating medium (68% DMEM, 17% M199, 10% horse serum, 5% FBS and 2.5 mg/ml amphotericin B). The cardiac fibroblasts were removed by plating cells in 10 mm culture dishes for 1 h to allow them to adhere, and then retrieving cardiomyocytes from the media supernatant. NRCM were then plated into 6-well BD Falcon Primaria tissue culture plates (for expression analysis) or on laminin coated coverslips in 24-well plates (for cellular hypertrophy analysis). Plating medium was similar to pre-plating medium, with the addition of 1 mM BrdU (5-bromo-2-deoxyuridine). From the second day onward, cardiomyocytes were cultured in maintenance medium (80% DMEM and 20% Medium 199, 1% FBS, 2.5 mg/mlamphotericin B and 1 mM BrdU).

In vitro Experiments

For expression analysis, NRCM were plated in 6 well plates at a density of 1×10^6 cells per well. After 24 h, cells were infected with adenovirus expressing either control or IL-10R shRNA driven by the U6 promoter. The shRNA constructs were obtained from SABiosciences (Qiagen). The U6-shRNA fragments were cloned into the pENTR11 and then recombined to pAd-PL-DEST (Gateway system, Invitrogen) to obtain the adenovirus construct. Adenovirus were generated in HEK293 cells using a standard protocol.

For the cellular hypertrophy models, cells were plated in 24-well plates onto laminin coated coverslips (Sigma, 10 μg/ml) at a density of 5×10^4 cells per well. After 24 h, cells were infected with Ad-shRNA control or Ad-shIL-10R in serum-free maintenance medium. To induce hypertrophy, 10 ng/ml TNF-α (Sigma) or

1 μM isoproterenol (Sigma) were added for 48 h, while the IL-10 treatment group received 20 ng/ml recombinant IL-10 (Peprotech) for the same time period. After 48 h cells were fixed and permeabilised with 4% PFA and 0.1% Triton-X solution, respectively. Cells were stained with anti-α-actinin antibody (Sigma) and DAPI to visualize the cardiomyocytes and nuclei, respectively, and imaged using an Olympus BX51 fluorescent microscope at 20× magnification. A minimum of 100 cells per treatment group were measured per independent experiment using ImageJ software (NIH).

Animal Model

We used mice with ubiquitous ablation of the IL-10R1 gene. Generation of these mice has been described in a previous publication (Pils et al., 2010). In brief, the IL-10R1 allele was mutated by the insertion of two loxP sites flanking exon 1 and the promotor region of IL-10R1. To generate mice with systemic deletion of the IL-10R1 gene, the IL-10R1flox/flox mice were crossed with transgenic mice expressing Cre recombinase in early development (the (K14-Cre,B6.D2-Tg(KRT14-cre)1Cgn) strain)(Hafner et al., 2004). The human keratin 14 promoter is active in driving transgene expression in the epidermal tissues. When female mice carry this K14-Cre transgene the promoter is active in their oocytes (Hafner et al., 2004). Consequently, breeding of IL-10R1flox/flox mice with female K14-Cre mice will result in systemic deletion of the IL-10R1 gene (Pils et al., 2010).

All experiments using animals were performed in accordance with the United Kingdom Animals (Scientific Procedures) Act 1986 and were approved by the University of Manchester Ethics Committee.

Transverse Aortic Banding

Pressure overload was induced by constricting the transverse aorta using a method as previously described (Mohamed et al., 2016). Briefly, 8–12 weeks old mice were induced with 5% isoflurane and intubated orally, and thereafter maintained at 3% isoflurane during surgery with mechanical ventilation. The chest was opened via minithoracotomy and the aortic arch exposed. Constriction was performed by tying a 7–0 silk suture around a 27-gauge needle overlying the arch, between the origin of the brachiocephalic trunk and left common carotid artery. Sham surgery followed the same procedure, but the suture was passed around the aorta and withdrawn without tying. The chest was then sutured shut and mice administered with 0.1 mg/kg BW buprenorphine as analgesia before recovery at 30°C and return to normal housing. After 14 days final analyses were performed, and mice were sacrificed via an approved schedule one method before heart excision and storage at −80°C.

Isoproterenol-Induced Hypertrophy

To generate a model of isoproterenol-induced hypertrophy, mice received a dose of 10 mg/kg BW per day isoproterenol (Sigma) or saline control for 10 days via a subcutaneously implanted osmotic minipump (Alzet). For minipump implantation, mice were anesthetized with 3% isoflurane. A small horizontal incision was made through the dermal layers on the dorsal surface of the mouse to create a small pocket into which minipumps were implanted. The skin was sutured shut, following which mice received analgesia (0.1 mg/kg BW buprenorphine) and were allowed to recover at 30°C before return to normal housing.

Echocardiography Analysis

For transthoracic echocardiography, mice were anesthetized by IP injection of tribromoethanol (250 mg/kg BW, Sigma), following which hearts were imaged in the two-dimensional short-axis view with an Acuson Sequoia C256 ultrasound system fitted with a 14-MHz transducer (Siemens). Chamber dimensions and wall thicknesses were measured in systole and diastole from M-mode images taken in the short-axis view at the level of the papillary muscle using the leading-edge method over a minimum period of three cardiac cycles.

Invasive Hemodynamic Analysis

Hemodynamic analysis was performed as described in our previous publication (Mohamed et al., 2016). Following administration of anesthetic (tribromoethanol, 250 mg/kg BW by IP injection), a midline cervical incision was made and the sternohyoid muscles retracted. The exposed right carotid artery was tied at its bifurcation and occluded proximally, allowing an incision to be made with minimal blood loss. Through this incision, a 1.4 F pressure–volume catheter (SPR-839, Millar Instruments) was inserted and fed through the ascending aorta into the left ventricle. A PowerLab system (Millar Instruments) was used to record LV pressure–volume changes once traces had stabilized. The maximum and minimum rates of left ventricular pressure change, dP/dtmax and dP/dtmin, respectively, were used to assess cardiac function in systole and diastole using Millar's PVAN software.

Histology

A transverse section through the ventricles of approximately 1mm in thickness, was cut from excised hearts and fixed in 4% PFA overnight. Sections were then dehydrated overnight in a Leica automated tissue processor and embedded in paraffin wax, before sectioning at 5 μM using a rotary microtome (Leica 2255). Masson's trichrome and H and E staining were performed to quantify interstitial fibrosis and cell size, respectively, using standard protocols. Whole sections were imaged using a 3D Histech Panoramic slide scanner in the University of Manchester bioimaging facility. Cell size measurements were acquired from a minimum of 100 cells per heart, and total LV interstitial fibrosis was recorded.

Western Blot

NRCM were lyzed in 100 μl RIPA buffer (containing 1% IGEPAL CA-630, 0.5% sodium deoxycholate, 0.1% SDS, 0.5 mM phenylmethylsulphonyl fluoride, 500 ng/ml Leupeptin, 1 mg/ml Aprotinin and 2.5 mg/ml Pepstatin A). Western blot analysis was conducted using standard protocols. Proteins were separated by SDS-PAGE and transferred to PVDF membranes (Millipore). Membranes were blocked in 3% BSA and incubated with primary antibodies against IL-10R1 (Santa Cruz), phosphorylated STAT3 or total STAT3 (Cell Signaling) overnight, followed by HRP-

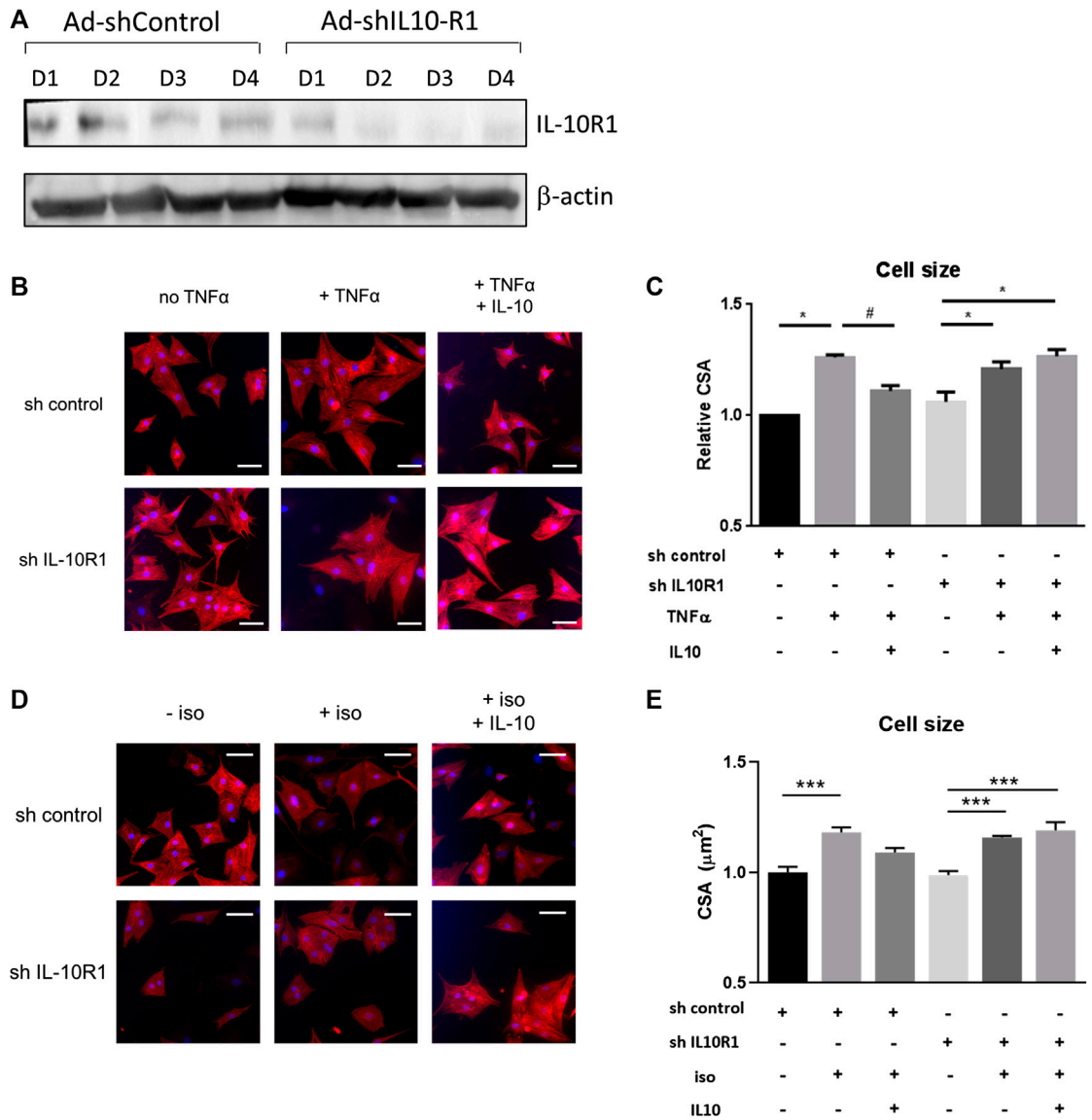

FIGURE 1 | Effects of IL-10 treatment and IL-10R1 gene silencing in TNF-α-induced cardiomyocyte hypertrophy. **(A)** Western blot analysis showing the expression of IL-10R1 in NRCM treated with adenovirus expressing either control shRNA or shRNA for IL-10R1 for 1–4 days. **(B)** Representative images of NRCM stained with α-actinin (red) and DAPI (blue) expressing either shRNA control or shRNA IL-10R1 after treatment with TNF-α (10 ng/ml) or with or without addition of IL-10 (20 ng/ml) for 48 h. Scale bar = 25 μM **(C)** Quantification of cell surface area (N = 3 independent experiments, with a minimum of n = 100 cells per experiment,*$p < 0.05$ vs. no TNF, #$p < 0.05$ vs. TNF without IL-10 **(D)** NRCM treated with 1 μM isoproterenol for 48 h ± IL-10. Scale bar = 25 μM and **(E)** quantification of myocyte cross-sectional area (N = 4 independent experiments, minimum 50 cells each, ***$p < 0.001$).

linked anti-rabbit secondary antibody (Cell Signaling) for 2 h. Proteins were visualized using enhanced chemiluminescence (GE Healthcare) on a ChemiDoc XRS Imaging System (Biorad). Membranes were then incubated with β-actin or GAPDH antibody (abcam) as loading control.

Statistical Analysis

Data was analyzed using Microsoft Excel and GraphPad Prism. Data is expressed as mean ± s.e.m. Student's t-test or one-way ANOVA followed by post-hoc adjustment for multiple comparisons were used where appropriate. The probability level for statistical significance was set at $p < 0.05$.

RESULTS

Interleukin-10R1 Gene Silencing in Cardiomyocytes

It has been reported that IL-10 treatment produces beneficial effects in controlling adverse cardiac remodeling following

pressure overload or acute myocardial infarction in rodents(Krishnamurthy et al., 2009; Verma et al., 2012; Jung et al., 2017). However, the signaling pathways modulated by IL-10 in the cardiomyocytes are not fully understood. To investigate whether IL-10 exerts its function through activation of the IL-10 receptor (IL-10R), we generated adenovirus expressing shRNA to inhibit the expression of the IL-10R1 gene encoding the main sub-unit of the receptor, in isolated neonatal rat cardiomyocytes (NRCM). Marked reduction of IL-10R1 expression was observed at day 2–3 following adenovirus treatment (**Figure 1A**) providing evidence of successful silencing of this gene.

Signaling via Interleukin-10R1 Is Necessary to Inhibit Hypertrophy in Isolated Cardiomyocytes

In immune cells, IL-10 mediated-signalling represses the pro-inflammatory signals of cytokines such as TNF-α and IL-6 by inducing the STAT3-mediated expression of anti-inflammatory gene SOCS3 (Cassatella et al., 1999; Williams et al., 2004). In cardiomyocytes the pro-inflammatory cytokines including TNF-α and IL-6 are known to induce hypertrophy (Kubota et al., 1997; Melendez et al., 2010). Based on this knowledge we performed experiments to investigate whether IL-10 and its receptor are involved in mediating TNF-α induced hypertrophy. We tested this hypothesis in primary rat neonatal cardiomyocytes (NRCM). In these cells TNF-α treatment induced cardiomyocyte hypertrophy by 26% as indicated by cell size measurement. As expected, co-treatment with IL-10 abolished the pro-hypertrophic effect of TNF-α (**Figures 1B,C**). Interestingly in IL-10R1 deficient cardiomyocytes, although TNF-α on its own was able to induce hypertrophy, treatment with IL-10 failed to reduce the hypertrophic effect (**Figures 1B,C**). This finding suggests that IL-10 mediated signaling in cardiomyocytes is important in repressing the hypertrophic effect of TNF-α, and sufficient expression of the IL-10R1 gene is required for this effect.

We then examined whether signaling via the IL-10R1 also affected hypertrophy induced by the β-adrenergic agonist isoproterenol. NRCM displayed significantly increased cell size following 48 h of isoproterenol treatment, while co-treatment with IL-10 reduced the hypertrophic response (**Figures 1D,E**). As with TNF-α treatment, isoproterenol also induced hypertrophy in IL-10R1 deficient cardiomyocytes, which was not affected upon co-treatment with IL-10 (**Figures 1D,E**). These findings suggest that signaling via the IL-10 receptor may modulate cardiac hypertrophy induced by multiple agonists.

Genetic Ablation of the Interleukin-10R1 Gene Exaggerates Pathological Hypertrophy in Mice

Results from the *in vitro* model prompted us to question if IL-10R1 plays a key role in mediating cardiac hypertrophy in an *in vivo* model. To address this question we analyzed mice with global ablation of the IL-10R1 gene (IL-10R1$^{-/-}$). The generation of this strain was described previously (Pils et al., 2010). To confirm deletion of IL-10R1 in the heart, Western blot analysis was performed. Expression of IL-10R1 was completely ablated in total heart extracts of IL-10R1$^{-/-}$ mice (**Figure 2A**). To investigate the pathologic hypertrophic response we subjected the IL-10R1$^{-/-}$ and wild type (WT) littermates to transverse aortic constriction (TAC) for 2 weeks. Global ablation of IL-10R1 significantly enhanced the hypertrophic response to pressure overload as indicated by heart weight/body weight (HW/BW) ratio. We observed a 48% increase in HW/BW ratio in IL-10$^{-/-}$ mice compared to 29% increase in WT littermates (**Figure 2b**). Consistently, measurement of cardiomyocyte cross-sectional area from histological sections showed a marked increase in cardiomyocyte size in the IL-10R1$^{-/-}$ TAC group compared to WT TAC (**Figures 2C,D**).

Interleukin-10R1$^{-/-}$ Mice Display More Fibrosis in the Heart After Transverse Aortic Constriction

Cardiac fibrosis is an important detrimental feature of the heart's response to pathological stimuli. To assess the level of fibrosis in the heart we stained heart tissue sections with Masson's trichrome staining. Analysis of fibrotic area as depicted in **Figures 2E,F** revealed a significantly higher fibrosis level in IL-10R1$^{-/-}$ mice after TAC compared to the WT-TAC group.

Echocardiography Analysis to Assess Cardiac Morphology and Function

To further analyze cardiac morphology and function of IL-10R1$^{-/-}$ mice following pressure overload we carried out echocardiography analysis at 2 weeks after TAC. We found that there was no difference in the left ventricular chamber dimension at both diastole and systole (LVEDD and LVESD, **Figures 3A,B**). As expected, the ventricular wall thickness was significantly elevated in both groups after TAC. However, we found that the IL-10R1$^{-/-}$ mice exhibited significantly greater septal wall thickness. Also, although there was no statistically significant difference in the posterior wall thickness between WT vs. IL-10R1$^{-/-}$ mice, the increase in posterior wall thickness seemed to be more apparent in the knockout mice compared to WT (**Figures 3C,D**).

We also analyzed ejection fraction from the echocardiography data to assess if the pathological damage affected cardiac function. We found that there was no difference in ejection fraction between IL-10R1$^{-/-}$ vs. WT mice after TAC (**Figure 3E**).

Invasive Hemodynamic Analysis to Assess Heart Function

Following echocardiography measurement, we conducted analysis to evaluate cardiac hemodynamic functions by inserting a pressure-volume catheter into the left ventricle. As shown in **Figure 4A**, the end-systolic pressure was markedly elevated in both WT and IL-10R1 knockout mice after TAC, indicating successful induction of pressure-overload in both groups. The fact that there was no difference in cardiac end-systolic pressure between these groups confirmed that a

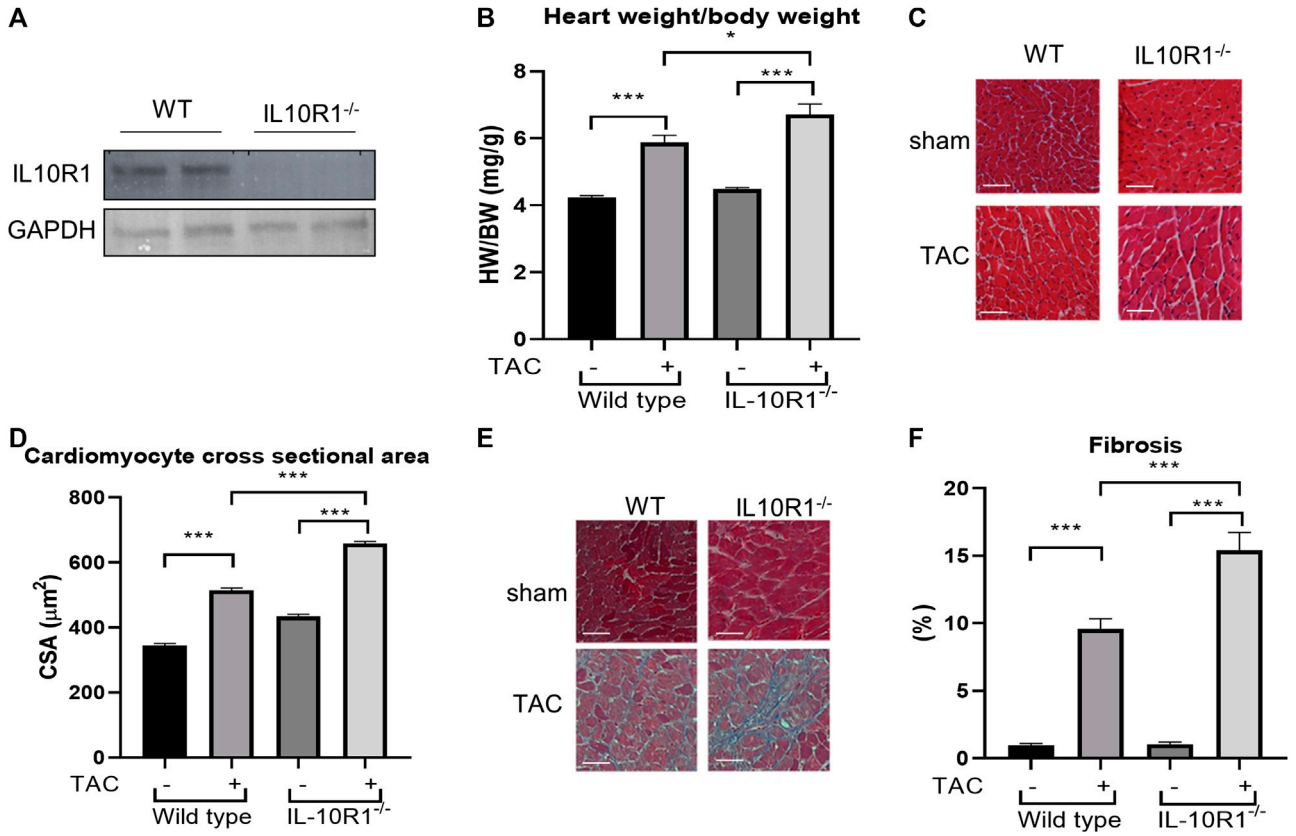

FIGURE 2 | Pressure overload-induced hypertrophy model in IL-10R1$^{-/-}$ mice. **(A)** Representative Western blot of total heart extracts from IL-10R1$^{-/-}$ mice and WT littermates showing complete ablation of IL-10R1 expression in the knockout mice. **(B)** Analysis of heart weight/body weight ratio (HW/BW) of WT and IL-10R1$^{-/-}$ mice following transverse aortic constriction (TAC) for 2 weeks. IL-10R1$^{-/-}$ mice showed a significant increase in hypertrophic response compared to WT littermates (WT-sham, n = 13; WT-TAC, n = 19; KO-sham, n = 11; KO-TAC, n = 12, $^{*}p < 0.05$, $^{***}p < 0.001$). **(C)** Histological sections of heart tissues stained with hematoxylin and eosin and **(D)** quantification of cardiomyocyte cross-sectional area showed enhanced cardiomyocyte size in IL-10R1$^{-/-}$ mice after TAC. **(E)** Masson's trichrome staining and **(F)** quantification of fibrotic area indicated significantly higher fibrosis in IL-10R1$^{-/-}$ mice (WT-sham, n = 7; WT-TAC, n = 8; KO-sham, n = 8; KO-TAC, n = 7) Scale bars = 50 μM.

comparable degree of overload was applied to each genotype. The end-diastolic pressure was not different between the groups (**Figure 4B**).

We then measured the rate of developed pressure during systole (dP/dt max) and the rate of reduced pressure during diastole (dP/dt min). We found no difference of dP/dt max and dP/dt min in all groups tested (**Figures 4C,D**). This data was consistent with the ejection fraction analysis showing that there was no change in contractility after 2 weeks of pressure overload.

Isoproterenol-Induced Hypertrophy Model in Interleukin-10R1$^{-/-}$ Mice

To investigate whether the effects of IL-10R1 genetic ablation also occur in a different model of cardiac hypertrophy, we established β-adrenergic mediated hypertrophy by stimulation with isoproterenol. We implanted osmotic minipumps subcutaneously in mice to enable continuous infusion of isoproterenol (10 mg/kg BW/day) for 10 days. As expected, isoproterenol infusion markedly increased heart rate and systolic pressure compared to vehicle-treated groups (**Figures 5A,B**). As a consequence, the rate of developed pressure (dP/dt max) and relaxation (dP/dt min) were dramatically enhanced following isoproterenol treatment (**Figures 5C,D**). However, we did not observe an altered hemodynamic response to isoproterenol stimulation between IL-10R1$^{-/-}$ and WT mice as indicated by these parameters.

Furthermore, we found a significant enlargement of heart size following isoproterenol in both groups; interestingly however, there was no significant difference in HW/BW ratio between IL-10R1$^{-/-}$ vs. WT mice suggesting a comparable hypertrophic response to beta adrenergic stimulation (**Figure 6A**). These results were corroborated by histological measurement of cardiomyocyte cross sectional area, which was increased significantly by isoproterenol, but did not differ when comparing IL-10R1$^{-/-}$ and WT hearts (**Figures 6B,C**). We also assessed levels of fibrosis in Masson's trichrome stained sections following β-adrenergic stimulation, but did not find that isoproterenol induced significant levels of interstitial fibrosis in either group (**Figures 6D,E**).

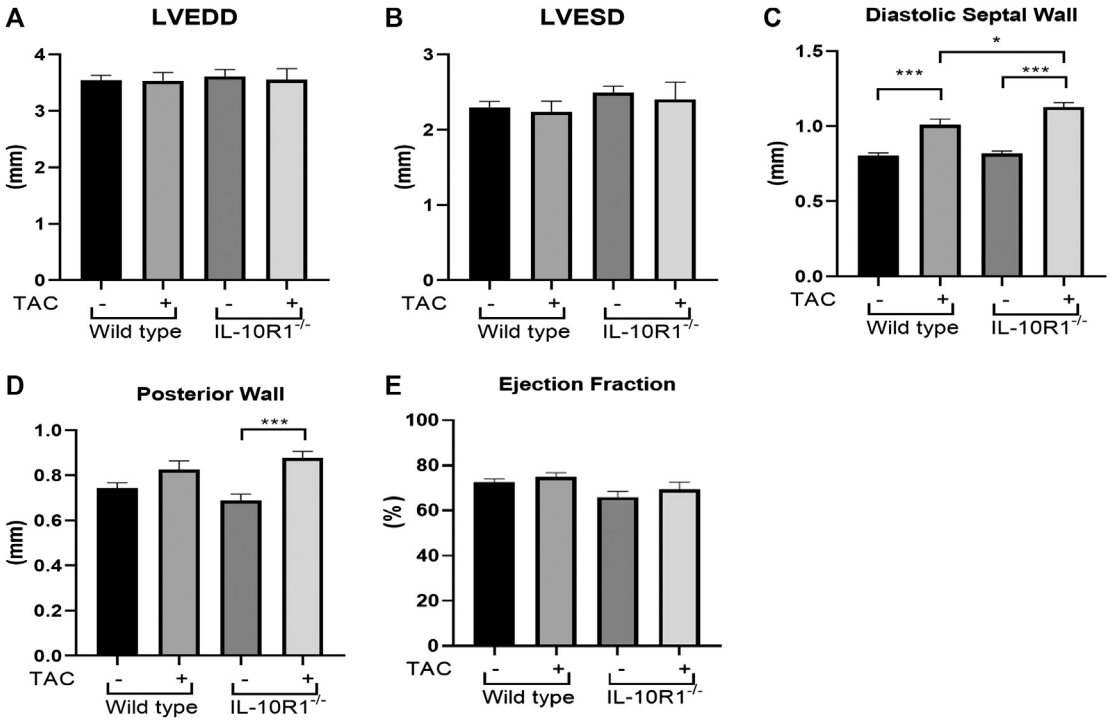

FIGURE 3 | Echocardiography analysis of IL-10R1$^{-/-}$ mice following TAC. **(A)** Left ventricular end diastolic dimension (LVEDD) and **(B)** Left ventricular end systolic dimension (LVESD) were not different between IL-10R1$^{-/-}$ mice and WT controls basally and after TAC. **(C)** Ventricular septal wall thickness at diastole was bigger in IL-10R1$^{-/-}$ mice after TAC, while **(D)** posterior wall thickness did not differ between these genotypes. **(E)** There was no significant difference in ejection fraction between all experimental groups (WT-sham, n = 13; WT-TAC, n = 15; KO-sham, n = 11; KO-TAC, n = 12,*$p < 0.05$,***$p < 0.001$).

Detailed echocardiographic analysis revealed that isoproterenol did not alter left ventricular dimensions but increased ventricular wall thickness in both genotypes. However, consistent with the HW/BW data there was no significant difference between WT and IL-10R1$^{-/-}$ groups (**Figures 7A–D**). Similarly, we did not find any difference in posterior wall thickness or ejection fraction between IL-10R1$^{-/-}$ vs. WT group after induction with isoproterenol (**Figure 7E**). Together, the data showed that there was no difference in the hypertrophic and hemodynamic response to beta-adrenergic stimulation between IL-10R1$^{-/-}$ mice compared to WT controls.

The Inflammatory Response in Transverse Aortic Constriction and Isoproterenol Treated Mice

In order to examine whether the different responses to TAC and isoproterenol treatment in IL-10R1$^{-/-}$ mice could be due to altered levels of inflammation, we examined the level of pro-inflammatory cytokine TNF-α in each model. Performing ELISA on extracts from pressure-overloaded heart tissue revealed no significant difference in TNF-α concentration among sham and TAC hearts, nor IL-10R1$^{-/-}$ and WT hearts 2 weeks post-TAC (**Figure 8A**). We also examined expression of TNF-α in isoproterenol-infused heart tissue by qPCR. In contrast to the TAC model, we found isoproterenol to increase TNF-α expression compared to water controls, although we did not see a difference in levels between IL-10R1$^{-/-}$ and WT mice (**Figure 8B**). This indicates that the inflammatory response may have been different in the two models used in this study.

Interleukin-10R1 Deficiency Prevents IL-10-Induced STAT3 Activation

Previous studies have shown IL-10 to exert protective effects in response to TAC and isoproterenol via activation of STAT3, and subsequent suppression of p38 and NF-kB signaling (Verma et al., 2012). We therefore examined activation of STAT3 in IL-10R1 deficient NRCM. Upon stimulation with IL-10, control myocytes displayed significantly increased phosphorylation, and hence activation, of STAT3 after 4 h (**Figures 9A,B**). This effect was abolished in IL-10R1 deficient NRCM. We then examined whether isoproterenol treatment affected IL-10 induced STAT3 activation. Interestingly, we found that isoproterenol treated NRCM did not exhibit activation of STAT3 upon addition of IL-10 (**Figures 9C,D**). These results indicate that IL-10 induced activation of STAT3 is dependent upon intact signaling via the IL-10 receptor, while other pathways may also be involved during β-adrenergic stimulation.

DISCUSSION

Our findings suggest that intact IL-10 receptor mediated signaling in the heart is required to control the extent of

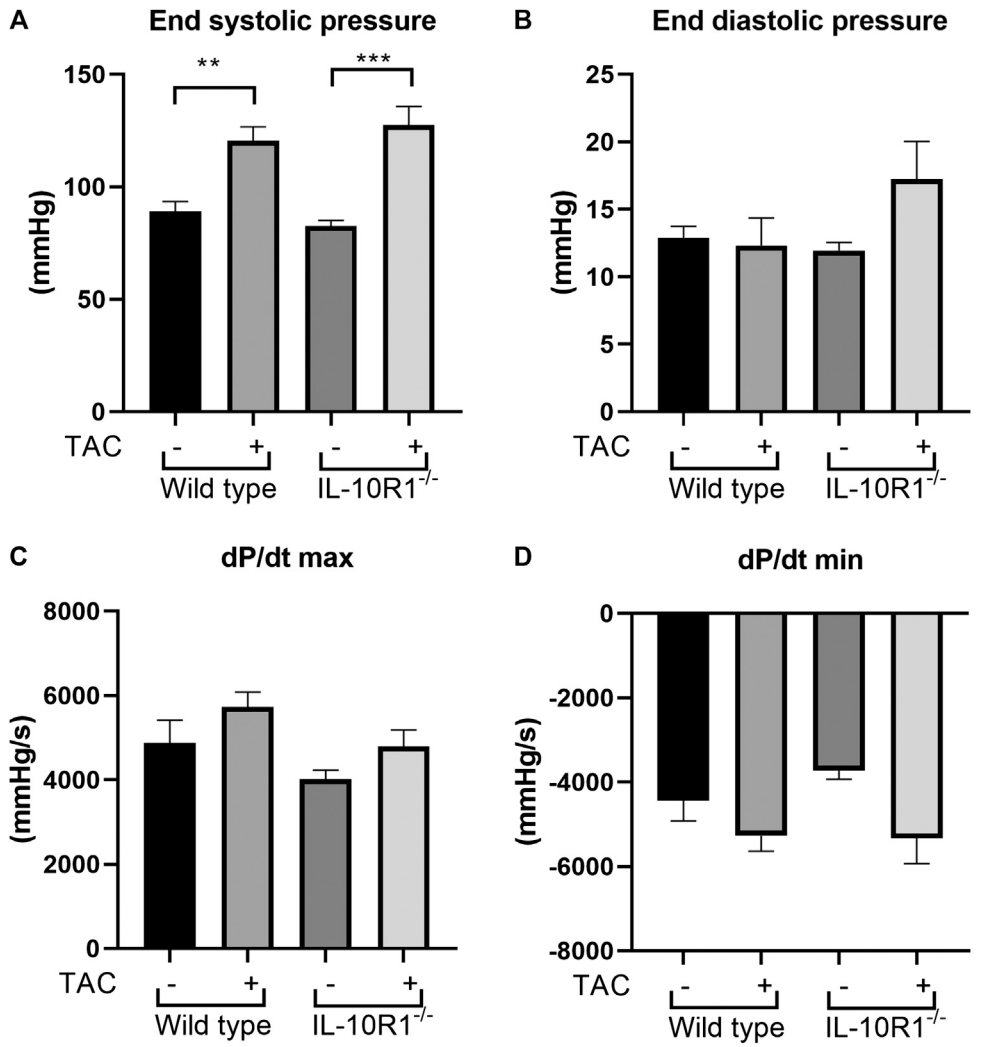

FIGURE 4 | Invasive hemodynamics assessment using micro-catheter. **(A)** End systolic ventricular pressure was significantly increased in both genotypes following TAC, however there was no difference between IL-10R1$^{-/-}$ mice vs. WT. **(B)** There was no statistically significant difference in end systolic pressure **(C)** dP/dt max and **(D)** dP/dt min in all experimental groups(WT-sham, n = 13; WT-TAC, n = 15; KO-sham, n = 11; KO-TAC, n = 12, $^{**}p < 0.01$, $^{***}p < 0.001$).

myocardial hypertrophy following pressure overload stimulation. Interestingly, our data demonstrate that ablation of the IL-10 receptor did not alter hypertrophy in response to β-adrenergic stimulation. IL-10 is known as a powerful negative regulator of the inflammatory response (Mosser and Zhang, 2008). Thus, our results confirm previous findings that an uncontrolled inflammatory response in the heart might cause an excessive hypertrophic response to pathological stimuli.

Cardiac hypertrophy is known as an initial adaptive compensatory response to pathological stimuli (Burchfield et al., 2013). The myocardial tissue produces numerous proteins in response to stress mainly to limit the extent of tissue damage, to induce tissue repair and to preserve function (Doroudgar and Glembotski, 2011). Among the molecules increased in pathologic hearts, inflammatory mediators appear to have essential roles since they may modulate cardiac function and contractile remodeling as well as altering endothelial function (Prabhu and Frangogiannis, 2016). For example, pro-inflammatory cytokines which are known to be elevated in human failing hearts, such as TNF-α, IL-1β and IL-6, negatively regulate cardiac contractility (Pagani et al., 1992; Janssen et al., 2005; Van Tassell et al., 2013). In addition, these cytokines are also involved in mediating cardiac remodeling as evidenced by the finding that genetic deletion of the TNF-α gene leads to a reduction in TAC-induced hypertrophy (Sun et al., 2007), whereas infusion of IL-6 in rat induces cardiac hypertrophy (Melendez et al., 2010). These findings support the idea that excessive release of pro-inflammatory cytokines is detrimental to the heart.

Conversely, evidence has indicated protective roles of anti-inflammatory cytokines in the heart. IL-10, which is a powerful anti-inflammatory cytokine, reduces the extent of hypertrophy

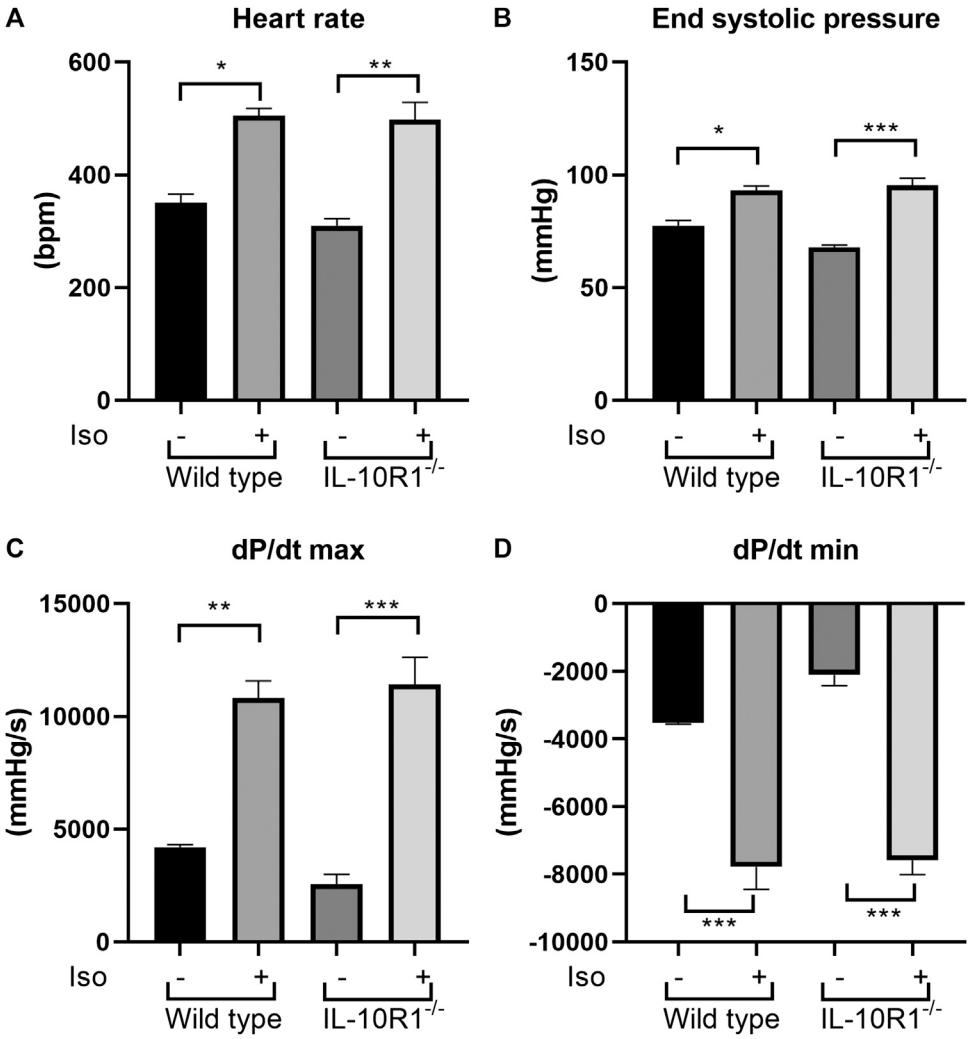

FIGURE 5 | Effects of isoproterenol infusion in IL-10R1$^{-/-}$ mice and WT littermates. **(A)** Heart rate and **(B)** end systolic pressure were significantly increased in both genotypes following isoproterenol infusion (10 mg/kg BW/day) for 10 days. Consistently, **(C)** the rate of developed ventricular pressure (dP/dt max) and **(D)** the rate of ventricular relaxation (dP/dt max) were increased following isoproterenol treatment. However, there was no significant difference between IL-10R1$^{-/-}$ mice vs. WT controls (WT-vehicle, n = 3; WT-Iso, n = 6; KO-vehicle, n = 3; KO-Iso, n = 7, $^{*}p < 0.05$,$^{**}p < 0.01$,$^{***}p < 0.001$).

in response to pressure overload and angiotensin II (Verma et al., 2012; Kishore et al., 2015), improves cardiac function and inhibits adverse remodeling post-myocardial infarction (Stumpf et al., 2008; Krishnamurthy et al., 2009; Jung et al., 2017). Importantly, in patients with severe heart failure the level of serum IL-10 is significantly reduced (Stumpf et al., 2003). Furthermore, survivors of acute myocardial infarction with higher serum IL-10 levels are less likely to develop heart failure (Domínguez Rodríguez et al., 2005).

It is believed that IL-10 exerts its protective role by suppressing the production of inflammatory mediators through activation of the STAT3 signaling pathway (Williams et al., 2004). Components of the innate immune system such as monocytes, macrophages and neutrophils are thought to be the main target of IL-10 (Pils et al., 2010). Following binding and activation of the IL-10 receptor in these cells, STAT3 will be recruited and phosphorylated, triggering expression of STAT3 target genes, notably the suppressor of cytokine signaling 3 (SOCS3) (Niemand et al., 2003). The latter is a strong inhibitor of IL-6 activity by interfering with gp130 signaling (Babon et al., 2014).

In this study we sought to address an important question as to how IL-10 reduced cardiac hypertrophy. Our *in vitro* model demonstrated that signaling through the IL-10 receptor in cardiomyocytes was required to exert the anti-hypertrophic response of IL-10 treatment, since deficiency of the major subunit of the receptor IL-10R1, abolished the anti-hypertrophic effect of IL-10 upon TNF-α and isoproterenol treatment. Indeed, it remains to be elucidated if this process is also important in the regulation of the cardiomyocyte response to other stimuli, such as α-adrenergic agonists or angiotensin. Nevertheless, the data prompted us to question if ablation of the Il-10R1 gene *in*

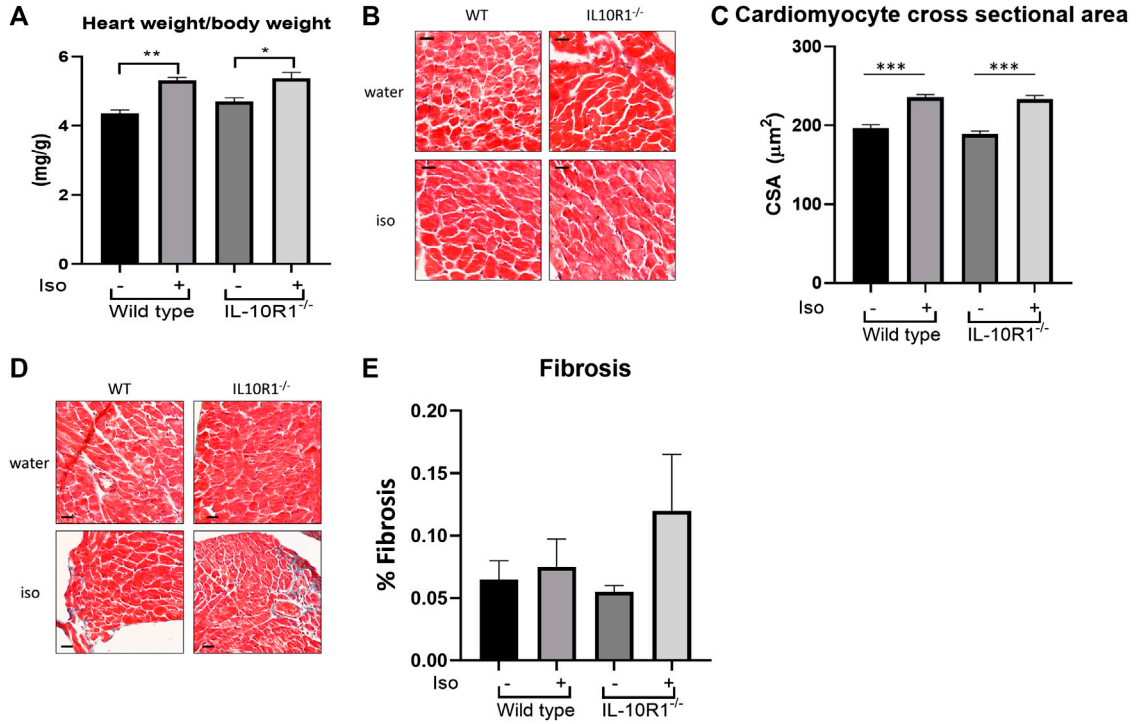

FIGURE 6 | Hypertrophic and fibrotic response in isoproterenol model. **(A)** Although there was significantly increased HW/BW ratio following isoproterenol infusion, there was no significant difference between IL-10R1$^{-/-}$ and WT mice (WT-vehicle,n = 3; WT-Iso, n = 6; KO-vehicle, n = 3; KO-Iso, n = 7,$^{*}p < 0.05$,$^{**}p < 0.01$). **(B)** Histological sections of heart tissues stained with hematoxylin and eosin and **(C)** quantification of cardiomyocyte cross-sectional area **(D)** Masson's trichrome staining and **(E)** quantification of fibrotic area following isoproterenol infusion (WT-vehicle, n = 3; WT-Iso, n = 4; KO-vehicle, n = 3; KO-Iso, n = 3,$^{***}p < 0.001$) Scale bars = 25 μM.

vivo would alter the cardiac hypertrophic response. We generated two models of hypertrophy, i.e. TAC-induced and isoproterenol-induced hypertrophy. In our hands we found that the receptor deficiency only affected the TAC-induced hypertrophic response, but not the response to isoproterenol stimulation. This is not to say that IL-10 signaling is not capable of protecting the heart from chronic β-adrenergic stimulation. A previous study has shown that IL-10 knockout mice exhibit a slightly worse phenotype to isoproterenol stimulation, albeit at a higher dose and for a longer period than the one used in our study, and that IL-10 treatment was protective in this model (Verma et al., 2012). Since IL-10 likely works by reducing the effects of pro-inflammatory factors, it is possible that in the TAC-model and at higher doses of isoproterenol, a different inflammatory response occurs compared to the one in our isoproterenol model. In this study we examined TNF-α levels in heart tissue following 2 weeks TAC and 10 days isoproterenol, and in fact found little evidence of inflammation in the TAC model at this time point. Further analysis is needed to understand the exact role that inflammatory cytokines are playing in each model. For example, it is thought that inflammation is more active in the first days of TAC-induced hypertrophy, which also coincides with the greatest extent of hypertrophic growth (Bacmeister et al., 2019).

While we show here that signaling via IL-10R1 is important in regulating cardiac hypertrophy and fibrosis after TAC, we did not find that ablation of the receptor translated to any functional deterioration after 14 days pressure overload. It would be interesting to see if left ventricular function declined in IL-10R1 ablated mice in a more chronic TAC model. Indeed, IL-10 knockout mice have been shown to exhibit reduced fractional shortening and ejection fraction 28 days post TAC, which was not apparent at 14 days (Verma et al., 2017).

It would also be interesting to further investigate the cellular and molecular mechanisms through which signaling via the IL-10 receptor acts during pressure overload. Our *in vitro* data suggests that activation of IL-10 signaling directly in cardiomyocytes can negatively regulate hypertrophy; however our *in vivo* TAC model utilized mice with global ablation of IL10R1 and therefore cannot rule out further involvement of IL-10 signaling in other cell types such as macrophages or lymphocytes. In order to investigate the precise actions of IL-10 signaling in each cell type tissue specific knockouts would be required.

Furthermore, it will be important to further explore the molecular mechanisms involved in the regulation of pressure overload and isoproterenol induced-hypertrophy and fibrosis downstream of the receptor. Previous studies have shown IL-10 signaling to exert protective effects during pressure overload via activation of STAT3 signaling, and subsequent suppression of p38, NF-κB and TGF-β-Smad2/3 signaling (Verma et al.,

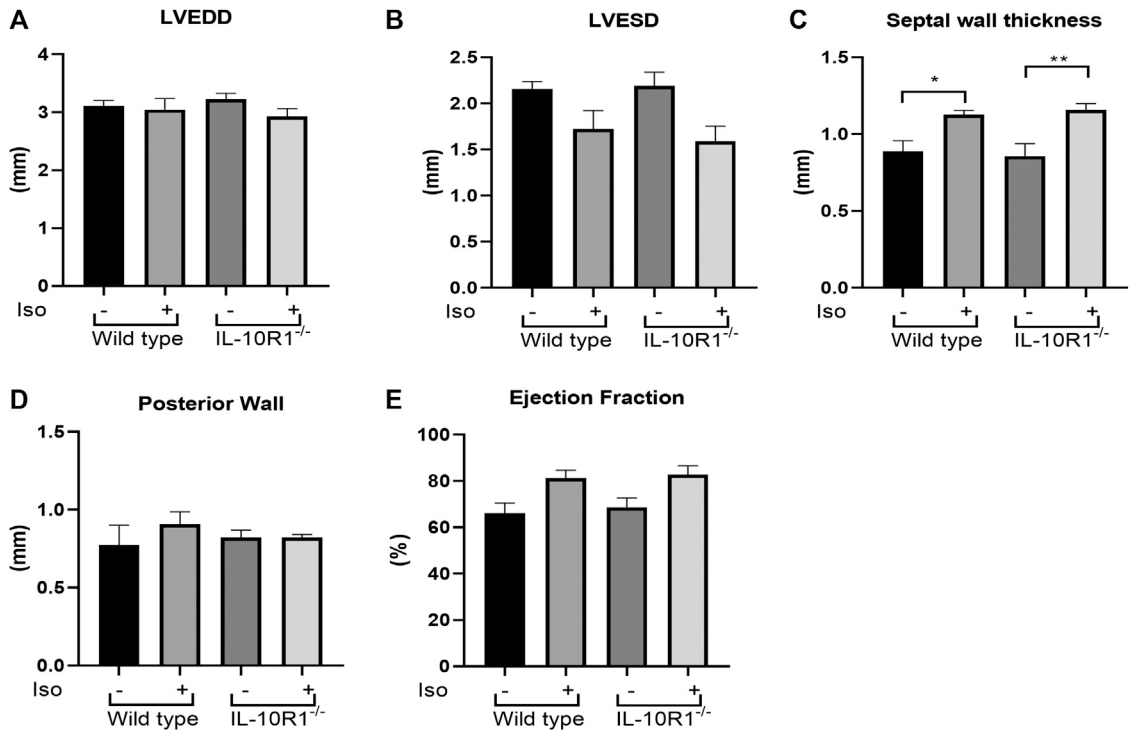

FIGURE 7 | Echocardiography analysis of IL-10R1$^{-/-}$ mice in isoproterenol model. **(A)** Echocardiography assessment revealed that there was no difference in LVEDD and **(B)** LVESD among experimental groups. **(C)** Septal wall thickness was augmented in both groups after isoproterenol treatment but there was no difference between genotypes. **(D)** No difference in posterior wall thickness and **(E)** Ejection fraction among experimental groups at the end of isoproterenol treatment (WT-vehicle, n = 3; WT-Iso, n = 6; KO-vehicle, n = 3; KO-Iso, n = 7,*$p < 0.05$,**$p < 0.01$).

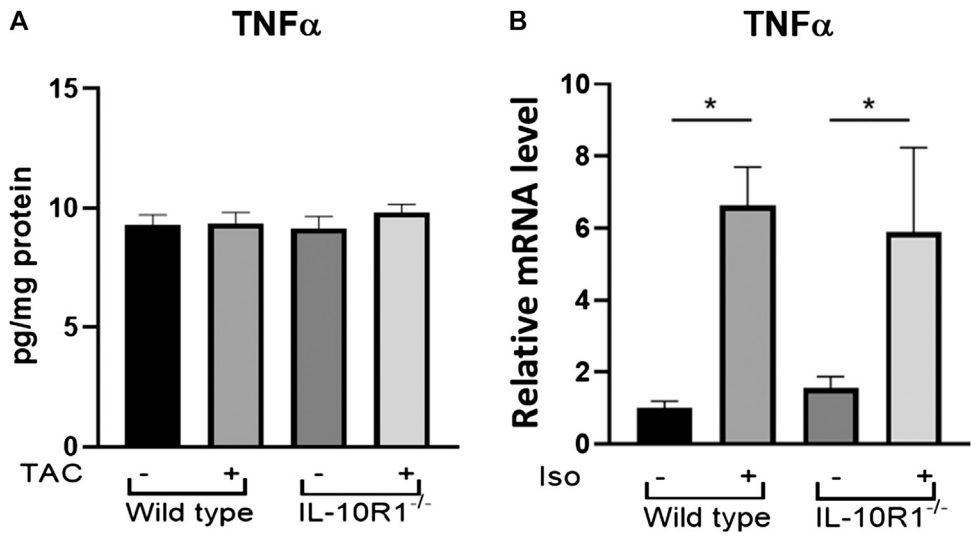

FIGURE 8 | TNF-α levels in TAC and isoproterenol models. **(A)** Analysis of TNF-α levels in heart tissue extracts from WT and IL-10R1$^{-/-}$ mice following TAC as measured by ELISA (n = 5) **(B)** Cardiac TNF-α mRNA expression relative to β-actin as loading control did not differ between isoproterenol treated WT and IL-10R1$^{-/-}$ mice (WT-vehicle, n = 3; WT-Iso, n = 4; KO-vehicle, n = 3; KO-Iso, n = 3,*$p < 0.05$).

2012; Verma et al., 2017). On the other hand chronic angiotensin II infusion has been shown to also activate Akt, p38 and NF-κB pathways in IL-10 knockout mice (Kwon et al., 2016). Here we confirm that IL-10 can activate STAT3 in cardiomyocytes, and that the IL-10R1 is required for this. We also found that isoproterenol treatment prevented this

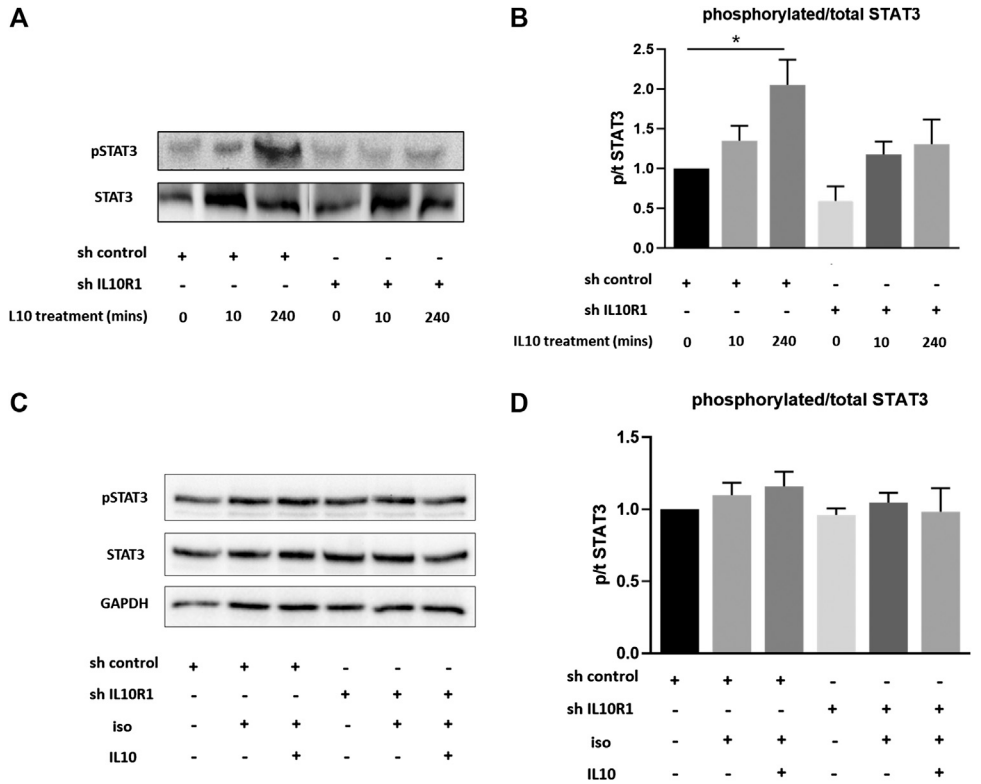

FIGURE 9 | IL-10 induced activation of STAT3. **(A)** Representative western blot showing STAT3 phosphorylation in shRNA control or shRNA IL-10R1 NRCM basally, and following the addition of 20 ng/ml IL-10 for 10 min or 4 h **(B)** Ratio of phosphorylated:total STAT3 (N = 5,*$p < 0.05$) **(C)** Representative western blot showing STAT3 phosphorylation in shRNA control or shRNA IL-10R1 NRCM following the addition of 1 μM isoproterenol with or without 20 ng/ml IL-10, along with loading control GAPDH **(D)** Ratio of phosphorylated:total STAT3 (N = 3).

IL-10 induced activation. Further studies will be needed to elucidate the full signaling pathways downstream of the receptor involved in regulating the hypertrophic response to each stimuli.

Overall, this study adds to the growing body of evidence suggesting that IL-10 based therapy may be a promising avenue to develop treatments for a number of cardiac pathologies associated with heart failure, including those induced by pressure overload (Verma et al., 2012; Verma et al., 2017), myocardial infarction (Krishnamurthy et al., 2009), high fat diet (Kondo et al., 2018) and angiotensin (Kishore et al., 2015). Anti-inflammatory based-therapies may offer a more attractive target compared to pro-inflammatory cytokine antagonists such as anti-TNF-α treatment, which have failed to show benefits in clinical trials in heart failure patients, likely due to TNF-α's pleiotropic nature (Chung et al., 2003; Mann et al., 2004). However, while IL-10 based therapy is attractive, further work will be required in order to perfect the stability and delivery of the peptide to the heart, as trials for its use in diseases such as rheumatoid arthritis and Crohn's disease have found only modest improvements (Mosser and Zhang, 2008). The development of stable recombinant IL-10 will be the key to future therapeutic advances.

DATA AVAILABILITY STATEMENT

The raw data supporting the conclusions of this article will be made available by the authors, without undue reservation.

AUTHOR CONTRIBUTIONS

NS, performed experiments, analyzed data, wrote manuscript; FA, performed experiments, analyzed data; SP and MZ, performed *in vivo* experiments; AMDM and AM, performed *in vitro* experiments; EJC, designed and supervised *in vivo* experiments; WM conceived scientific idea; DO, conceived scientific idea, designed experiments, analyzed data, supervised the whole project, wrote manuscript.

FUNDING

This study was supported by British Heart Foundation (BHF) Project Grants (PG/16/77/32400, PG/17/78/33304, PG/18/40/33767), Medical Research Council (MRC) Research Grant (MR/P015816/1) to DO and a BHF Project Grant PG/11/23/28801 jointly held by DO and WM

REFERENCES

Adamo, L., Rocha-Resende, C., Prabhu, S. D., and Mann, D. L. (2020). Reappraising the role of inflammation in heart failure. *Nat. Rev. Cardiol.* 17, 269–285. doi:10.1038/s41569-019-0315-x.

Babon, J. J., Varghese, L. N., and Nicola, N. A. (2014). Inhibition of IL-6 family cytokines by SOCS3. *Semin. Immunol.* 26, 13–19. doi:10.1016/j.smim.2013.12.004.

Bacmeister, L., Schwarzl, M., Warnke, S., Stoffers, B., Blankenberg, S., Westermann, D., et al. (2019). Inflammation and fibrosis in murine models of heart failure. *Basic Res. Cardiol.* 114, 19. doi:10.1007/s00395-019-0722-5.

Burchfield, J. S., Xie, M., and Hill, J. A. (2013). Pathological Ventricular Remodeling. *Circulation* 128, 388–400. doi:10.1161/circulationaha.113.001878.

Cassatella, M. A., Gasperini, S., Bovolenta, C., Calzetti, F., Vollebregt, M., Scapini, P., et al. (1999). Interleukin-10 (IL-10) selectively enhances CIS3/SOCS3 mRNA expression in human neutrophils: evidence for an IL-10-induced pathway that is independent of STAT protein activation. *Blood* 94, 2880–2889. doi:10.1182/blood.v94.8.2880.420k31_2880_2889.

Chung, E. S., Packer, M., Lo, K. H., Fasanmade, A. A., and Willerson, J. T.; Anti-TNF Therapy Against Congestive Heart Failure Investigators (2003). Randomized, double-blind, placebo-controlled, pilot trial of infliximab, a chimeric monoclonal antibody to tumor necrosis factor-α, in patients with moderate-to-severe heart failure. *Circulation* 107, 3133–3140. doi:10.1161/01.cir.0000077913.60364.d2.

Dhingra, S., Sharma, A. K., Arora, R. C., Slezak, J., and Singal, P. K. (2009). IL-10 attenuates TNF- -induced NF B pathway activation and cardiomyocyte apoptosis. *Cardiovasc. Res.* 82, 59–66. doi:10.1093/cvr/cvp040.

Dhingra, S., Sharma, A. K., Singla, D. K., and Singal, P. K. (2007). p38 and ERK1/2 MAPKs mediate the interplay of TNF-α and IL-10 in regulating oxidative stress and cardiac myocyte apoptosis. *Am. J. Physiol. Heart Circ. Physiol.* 293, H3524–H3531. doi:10.1152/ajpheart.00919.2007.

Domínguez Rodríguez, A., Abreu González, P., García González, M., and Ferrer Hita, J. (2005). Association between serum interleukin 10 level and development of heart failure in acute myocardial infarction patients treated by primary angioplasty. *Rev. Esp. Cardiol.* 58, 626–630. doi:10.1016/s1885-5857(06)60248-x.

Doroudgar, S., and Glembotski, C. C. (2011). The cardiokine story unfolds: ischemic stress-induced protein secretion in the heart. *Trends Mol. Med.* 17, 207–214. doi:10.1016/j.molmed.2010.12.003.

Hafner, M., Wenk, J., Nenci, A., Pasparakis, M., Scharffetter-Kochanek, K., Smyth, N., et al. (2004). Keratin 14 Cre transgenic mice authenticate keratin 14 as an oocyte-expressed protein. *Genesis* 38, 176–181. doi:10.1002/gene.20016.

Janssen, S. P. M., Gayan-Ramirez, G., Van Den Bergh, A., Herijgers, P., Maes, K., Verbeken, E., et al. (2005). Interleukin-6 causes myocardial failure and skeletal muscle atrophy in rats. *Circulation* 111, 996–1005. doi:10.1161/01.cir.0000156469.96135.0d.

Jung, M., Ma, Y., Iyer, R. P., Deleon-Pennell, K. Y., Yabluchanskiy, A., Garrett, M. R., et al. (2017). IL-10 improves cardiac remodeling after myocardial infarction by stimulating M2 macrophage polarization and fibroblast activation. *Basic Res. Cardiol.* 112, 33. doi:10.1007/s00395-017-0622-5.

Kishore, R., Krishnamurthy, P., Garikipati, V. N. S., Benedict, C., Nickoloff, E., Khan, M., et al. (2015). Interleukin-10 inhibits chronic angiotensin II-induced pathological autophagy. *J. Mol. Cell. Cardiol.* 89, 203–213. doi:10.1016/j.yjmcc.2015.11.004.

Kondo, H., Abe, I., Gotoh, K., Fukui, A., Takanari, H., Ishii, Y., et al. (2018). Interleukin 10 treatment ameliorates high-fat diet-induced inflammatory atrial remodeling and fibrillation. *Circ. Arrhythm. Electrophysiol.* 11, e006040. doi:10.1161/circep.117.006040.

Krishnamurthy, P., Rajasingh, J., Lambers, E., Qin, G., Losordo, D. W., and Kishore, R. (2009). IL-10 inhibits inflammation and attenuates left ventricular remodeling after myocardial infarction via activation of STAT3 and suppression of HuR. *Circ. Res.* 104, e9–e18. doi:10.1161/circresaha.108.188243.

Kubota, T., Mctiernan, C. F., Frye, C. S., Slawson, S. E., Lemster, B. H., Koretsky, A. P., et al. (1997). Dilated cardiomyopathy in transgenic mice with cardiac-specific overexpression of tumor necrosis factor-α. *Circ. Res.* 81, 627–635. doi:10.1161/01.res.81.4.627.

Kwon, W.-Y., Cha, H.-N., Heo, J.-Y., Choi, J.-H., Jang, B. I., Lee, I.-K., et al. (2016). Interleukin-10 deficiency aggravates angiotensin II-induced cardiac remodeling in mice. *Life Sci.* 146, 214–221. doi:10.1016/j.lfs.2016.01.022.

Levine, B., Kalman, J., Mayer, L., Fillit, H. M., and Packer, M. (1990). Elevated circulating levels of tumor necrosis factor in severe chronic heart failure. *N. Engl. J. Med.* 323, 236–241. doi:10.1056/nejm199007263230405.

Lindberg, E., Magnusson, Y., Karason, K., and Andersson, B. (2008). Lower levels of the host protective IL-10 in DCM-a feature of autoimmune pathogenesis? *Autoimmunity* 41, 478–483. doi:10.1080/08916930802031645.

Mann, D. L. (2015). Innate Immunity and the Failing Heart. *Circ. Res.* 116, 1254–1268. doi:10.1161/circresaha.116.302317.

Mann, D. L., Mcmurray, J. J. V., Packer, M., Swedberg, K., Borer, J. S., Colucci, W. S., et al. (2004). Targeted anticytokine therapy in patients with chronic heart failure. *Circulation* 109, 1594–1602. doi:10.1161/01.cir.0000124490.27666.b2.

Meléndez, G. C., Mclarty, J. L., Levick, S. P., Du, Y., Janicki, J. S., and Brower, G. L. (2010). Interleukin 6 mediates myocardial fibrosis, concentric hypertrophy, and diastolic dysfunction in rats. *Hypertension* 56, 225–31. doi:10.1161/HYPERTENSIONAHA.109.148635.

Mohamed, T. M., Abou-Leisa, R., Stafford, N., Maqsood, A., Zi, M., Prehar, S., et al. (2016). The plasma membrane calcium ATPase 4 signalling in cardiac fibroblasts mediates cardiomyocyte hypertrophy. *Nat. Commun.* 7, 11074. doi:10.1038/ncomms11074.

Mosser, D. M., and Zhang, X. (2008). Interleukin-10: new perspectives on an old cytokine. *Immunol. Rev.* 226, 205–218. doi:10.1111/j.1600-065x.2008.00706.x.

Mozaffarian, D., Benjamin, E. J., Go, A. S., Arnett, D. K., Blaha, M. J., Cushman, M., et al.; American Heart Association Statistics Committee and Stroke Statistics Subcommittee (2015). Heart disease and stroke statistics–2015 update: a report from the American Heart Association. *Circulation* 131, e29–e322. doi:10.1161/cir.0000000000000152.

Niemand, C., Nimmesgern, A., Haan, S., Fischer, P., Schaper, F., Rossaint, R., et al. (2003). Activation of STAT3 by IL-6 and IL-10 in primary human macrophages is differentially modulated by suppressor of cytokine signaling 3. *J. Immunol.* 170, 3263–3272. doi:10.4049/jimmunol.170.6.3263.

Ouyang, W., and O'Garra, A. (2019). IL-10 family cytokines IL-10 and IL-22: from basic science to clinical translation. *Immunity* 50, 871–891. doi:10.1016/j.immuni.2019.03.020.

Pagani, F. D., Baker, L. S., Hsi, C., Knox, M., Fink, M. P., and Visner, M. S. (1992). Left ventricular systolic and diastolic dysfunction after infusion of tumor necrosis factor-alpha in conscious dogs. *J. Clin. Invest.* 90, 389–398. doi:10.1172/jci115873.

Pils, M. C., Pisano, F., Fasnacht, N., Heinrich, J.-M., Groebe, L., Schippers, A., et al. (2010). Monocytes/macrophages and/or neutrophils are the target of IL-10 in the LPS endotoxemia model. *Eur. J. Immunol.* 40, 443–448. doi:10.1002/eji.200939592.

Prabhu, S. D., and Frangogiannis, N. G. (2016). The biological basis for cardiac repair after myocardial infarction. *Circ. Res.* 119, 91–112. doi:10.1161/circresaha.116.303577.

Stumpf, C., Lehner, C., Yilmaz, A., Daniel, W. G., and Garlichs, C. D. (2003). Decrease of serum levels of the anti-inflammatory cytokine interleukin-10 in patients with advanced chronic heart failure. *Clin. Sci. (Lond.)* 105, 45–50. doi:10.1042/cs20020359.

Stumpf, C., Seybold, K., Petzi, S., Wasmeier, G., Raaz, D., Yilmaz, A., et al. (2008). Interleukin-10 improves left ventricular function in rats with heart failure subsequent to myocardial infarction. *Eur. J. Heart Fail.* 10, 733–739. doi:10.1016/j.ejheart.2008.06.007.

Sun, M., Chen, M., Dawood, F., Zurawska, U., Li, J. Y., Parker, T., et al. (2007). Tumor necrosis factor-α mediates cardiac remodeling and ventricular dysfunction after pressure overload state. *Circulation* 115, 1398–1407. doi:10.1161/circulationaha.106.643585.

Taylor, C. J., Ryan, R., Nichols, L., Gale, N., Hobbs, F. R., and Marshall, T. (2017). Survival following a diagnosis of heart failure in primary care. *Fam. Pract.* 34, 161–168. doi:10.1093/fampra/cmx040.

Van Tassell, B. W., Seropian, I. M., Toldo, S., Mezzaroma, E., and Abbate, A. (2013). Interleukin-1β induces a reversible cardiomyopathy in the mouse. *Inflamm. Res.* 62, 637–640. doi:10.1007/s00011-013-0625-0.

Verma, S. K., Garikipati, V. N. S., Krishnamurthy, P., Schumacher, S. M., Grisanti, L. A., Cimini, M., et al. (2017). Interleukin-10 inhibits bone marrow fibroblast progenitor cell-mediated cardiac fibrosis in pressure-overloaded myocardium. *Circulation* 136, 940–953. doi:10.1161/circulationaha.117.027889.

Verma, S. K., Krishnamurthy, P., Barefield, D., Singh, N., Gupta, R., Lambers, E., et al. (2012). Interleukin-10 treatment attenuates pressure overload-induced hypertrophic remodeling and improves heart function via signal transducers and activators of transcription 3-dependent inhibition of nuclear factor-κB. *Circulation* 126, 418–429. doi:10.1161/circulationaha.112.112185.

Williams, L. M., Ricchetti, G., Sarma, U., Smallie, T., and Foxwell, B. M. J. (2004). Interleukin-10 suppression of myeloid cell activation–a continuing puzzle. *Immunology* 113, 281–292. doi:10.1111/j.1365-2567.2004.01988.x.

Yoshida, T., Hanawa, H., Toba, K., Watanabe, H., Watanabe, R., Yoshida, K., et al. (2005). Expression of immunological molecules by cardiomyocytes and inflammatory and interstitial cells in rat autoimmune myocarditis. *Cardiovasc. Res.* 68, 278–288. doi:10.1016/j.cardiores.2005.06.006.

Conflict of Interest: The authors declare that the research was conducted in the absence of any commercial or financial relationships that could be construed as a potential conflict of interest.

frontiers in Pharmacology

ORIGINAL RESEARCH
published: 16 February 2021
doi: 10.3389/fphar.2021.608523

Role of PI3-Kinase in Angiotensin II-Induced Cardiac Hypertrophy: Class I Versus Class III

Tiecheng Zhong[1,3†], Zonggui Wang[2†], Sayeman Islam Niloy[1], Yue Shen[1], Stephen T. O'Rourke[1] and Chengwen Sun[1*]*

[1]Department of Pharmaceutical Sciences, North Dakota State University, Fargo, ND, United States, [2]Department of Otolaryngology, The Second Hospital, Jilin University, Changchun, China, [3]Institute of Pharmacology and Toxicology, Zhejiang Province Key Laboratory of Anti-Cancer Drug Research, College of Pharmaceutical Sciences, Zhejiang University, Hangzhou, China

Cardiac hypertrophy is an adaptive response to cardiac overload initially but turns into a decompensated condition chronically, leading to heart failure and sudden cardiac death. The molecular mechanisms involved in cardiac hypertrophy and the signaling pathways that contribute to the switch from compensation to decompensation are not fully clear. The aim of the current study was to examine the role of PI3-kinases Class I (PI3KC1) and Class III (PI3KC3) in angiotensin (Ang) II-induced cardiac hypertrophy. The results demonstrate that treatment of cardiomyocytes with Ang II caused dose-dependent increases in autophagy, with an increasing phase followed by a decreasing phase. Ang II-induced autophagic increases were potentiated by inhibition of PI3KC1 with LY294002, but were impaired by inhibition of PI3KC3 with 3-methyladenine (3-MA). In addition, blockade of PI3KC1 significantly attenuated Ang II-induced ROS production and cardiomyocyte hypertrophy. In contrast, blockade of PI3KC3 potentiated Ang II-induced ROS production and cardiac hypertrophy. Moreover, blockade of PI3KC1 by overexpression of dominant negative p85 subunit of PI3KC1 significantly attenuated Ang II-induced cardiac hypertrophy in normotensive rats. Taken together, these results demonstrate that both PI3KC1 and PI3KC3 are involved in Ang II-induced cardiac hypertrophy by different mechanisms. Activation of PI3KC1 impairs autophagy activity, leading to accumulation of mitochondrial ROS, and, hence, cardiac hypertrophy. In contrast, activation of PI3KC3 improves autophagy activity, thereby reducing mitochondrial ROS and leads to a protective effect on Ang II-induced cardiac hypertrophy.

Keywords: PI3-kinases, cardiac hypertrophy, heart failure, angiotensin II, autophagy

OPEN ACCESS

Edited by:
Ya Liu,
Army Medical University, China

Reviewed by:
Linxi Chen,
University of South China, China
Jue Wang,
The University of Texas Health Science Center at Tyler, United States

***Correspondence:**
Zonggui Wang
zgw1965@hotmail.com
Chengwen Sun
Chengwen.Sun@ndsu.edu

†These authors have contributed equally to this work

Specialty section:
This article was submitted to Cardiovascular and Smooth Muscle Pharmacology, a section of the journal Frontiers in Pharmacology

Received: *21 September 2020*
Accepted: *13 January 2021*
Published: *16 February 2021*

Citation:
Zhong T, Wang Z, Niloy SI, Shen Y, O'Rourke ST and Sun C (2021) Role of PI3-Kinase in Angiotensin II-Induced Cardiac Hypertrophy: Class I Versus Class III. Front. Pharmacol. 12:608523. doi: 10.3389/fphar.2021.608523

INTRODUCTION

Cardiac hypertrophy refers to the enlargement of cardiomyocytes with a series of physiological and pathological modifications such as heart expansion, altered gene expression, enhanced protein synthesis, and contractile machinery reorganization (Harvey and Leinwand, 2011). Cardiac hypertrophy is initially adaptive to compensate for the increasing physiological oxygen and nutrient demands during exercise or pregnancy (Hill and Olson, 2008). Pathological state-related stresses such as hypertension, obesity, and myocardial infarction elicit maladaptive cardiac hypertrophy that is associated with unusual cardiac structures and metabolism, as well as abnormal cardiac functions (Hill and Olson, 2008). If improperly

treated, cardiac hypertrophy is a detrimental factor that would ultimately result in heart failure and sudden cardiac death, threatening the well-being of individuals and creating a tremendous burden on society as a whole.

Among those physiological and pathological factors that cause cardiac hypertrophy, Angiotensin II (Ang II) stimulation plays a pivotal role (Sadoshima et al., 1993). Ang II acts as a vasoconstrictor, thus increasing blood pressure and cardiac load; it also stimulates cardiomyocytes directly via activation of angiotensin receptor type I receptors (AT1R) (Hunyady and Catt, 2006). PI3-kinases are involved in the intracellular downstream signal-transduction pathways of AT1 receptors in cardiomyocytes (Wenzel et al., 2006). Two classes of PI3-kinase, Class I (PI3KC1) and Class III (PI3KC3), have been identified in the heart (Misawa et al., 1998). Targeted over-expression of PI3KC1 increased heart size and manifested cardiac hypertrophy. Conversely, dominant negative (DN) treatment-induced inactivation of certain essential signal-transduction components, such as the p110 subunit of PI3KC1 in the heart, attenuated cardiac hypertrophy in transgenic mice (Shioi et al., 2000). However, the role of PI3KC1 vs. PI3KC3 in Ang II-induced cardiac hypertrophy is still unknown.

Previous studies demonstrate that reactive oxygen species (ROS) derived from NADPH oxidases are involved in Ang II-induced cardiac hypertrophy through a PI3-kinase-dependent pathway (Yao et al., 2008). However, genetic modification resulting in inactivation of the gp91phox subunit, a vital component within NADPH oxidase, in transgenic mice did not show significant benefits to alleviate Ang II-induced hypertension or cardiac hypertrophy (Touyz et al., 2005). These findings suggest there might be an alternative intracellular pathway to generate ROS in cardiomyocytes under conditions of prolonged Ang II exposure. Recent studies demonstrate that damaged mitochondria may also generate ROS in cardiomyocytes (Pei et al., 2016). However, the intracellular mechanisms involved in accumulation of damaged mitochondria-derived ROS in Ang II-induced cardiac hypertrophy are still unclear.

It is well known that autophagy is a very important intracellular process to protect cells from hazardous material accumulation by scavenging damaged mitochondria or proteins that produce reactive oxygen species (ROS). Accumulating evidence indicates the possible involvement of autophagy in the pathophysiology of Ang II-induced cardiac hypertrophy (Zhou et al., 2016). Thus, the major aim of the current study was to test the hypothesis that activation of PI3-kinases is involved in Ang II-induced cardiac hypertrophy by regulating autophagy activity and mitochondrial ROS generation.

METHODS

Animals

Twelve-week-old male Sprague-Dawley (SD) rats were used in this study (purchased from Charles River Laboratories International, Wilmington, MA). Rats were housed at 25 ± 2°C on a 12:12-h light-dark cycle and provided with food and water *ad libitum*. All animal protocols were approved by the North Dakota State University Institutional Animal Care and Use Committee and the Jilin University Institutional Animal Care and Use Committee (IACUC). All experiments were carried out in accordance with guidelines and regulations approved by the IACUCs.

In vivo Myocardial Gene Delivery

Construction and titration of lentiviral vectors of Lv-GFP (negative control) and Lv-DNp85 (the dominant negative p85α subunit of PI3KC1) were performed as described in our previous publication (Sun et al., 2009). The lentiviral vectors were transferred into the myocardium by injection into the root of the aorta, as published previously (Iwanaga et al., 2004; Yan et al., 2015). Briefly, male adult SD rats were anesthetized with an O_2 (1 L/min) and isoflurane (3%) mixture administrated through a nose cone. Left anterior thoracotomy was carried out in the left second intercostal space. For arterial occlusion, ligatures were loosely looped around the main pulmonary arteries and the ascending aorta. To inject viral particles into the coronary arteries, a vascular catheter was inserted through the right carotid artery into the aortic root between the aortic valve and the occlusion ligature loop. Ice packs were used to create a general hypothermic environment for the rats in order to cool their body temperatures below 26°C. Then, a protective cardioplegic solution (2 μL/g body weight) was injected, containing (in mM): NaCl 110, KCl 20, $MgCl_2$ 16, $NaHCO_3$ 10, and $CaCl_2$ 1.2 via the arterial catheter, followed by injection of Lv-GFP or Lv-DNp85 viral particles (200 μL 2×10^{10} TU/mL). Substance P was also added to the cardioplegic solution, at a final concentration of 25 μg/ml, to enhance permeability of the coronary artery wall and guarantee access of viral vectors into the myocardium. After injection, both occlusions were loosened and rat body temperature was heated back to normal using a heating pad. To enhance the gene transfection, Lv-DNp85 or Lv-GFP were also injected directly into the anterior ventricular well. The chest was then closed; intrathoracic air was evacuated by suction with a syringe.

Evaluation of Heart Morphology

The morphology of hearts was evaluated after the hearts were transversely sectioned. Heart sections were fixed in 10% formalin/PBS solution. The cardiomyocyte morphology and cellular dimension were examined by hematoxylin and eosin (H&E) staining in cardiac sections (4~5 μm thickness). The stained cardiac sections were visualized under light microscopy (Olympus). The cross-sectional diameter of single myocytes was measured by the cellular diameter crossing the nuclei, using Infinity Capture and Analyze Software under a microscope (Olympus). The outline of 100–200 cardiomyocytes was traced from each rat.

Preparation of Primary Cardiomyocyte Culture

Primary cardiomyocyte cultures were prepared as described previously (Yao et al., 2010; Zhao et al., 2015). Briefly, 1-day-old neonatal SD rats were euthanized by overdose with sodium pentobarbital (200 mg/kg, *i. p.*, Sigma, St. Louis, MO). Ventricles of the heart were quickly excised, minced into small pieces in cold HBSS, and washed several additional times. The minced tissue was digested with 0.1% trypsin in a 37 °C water bath with shaking

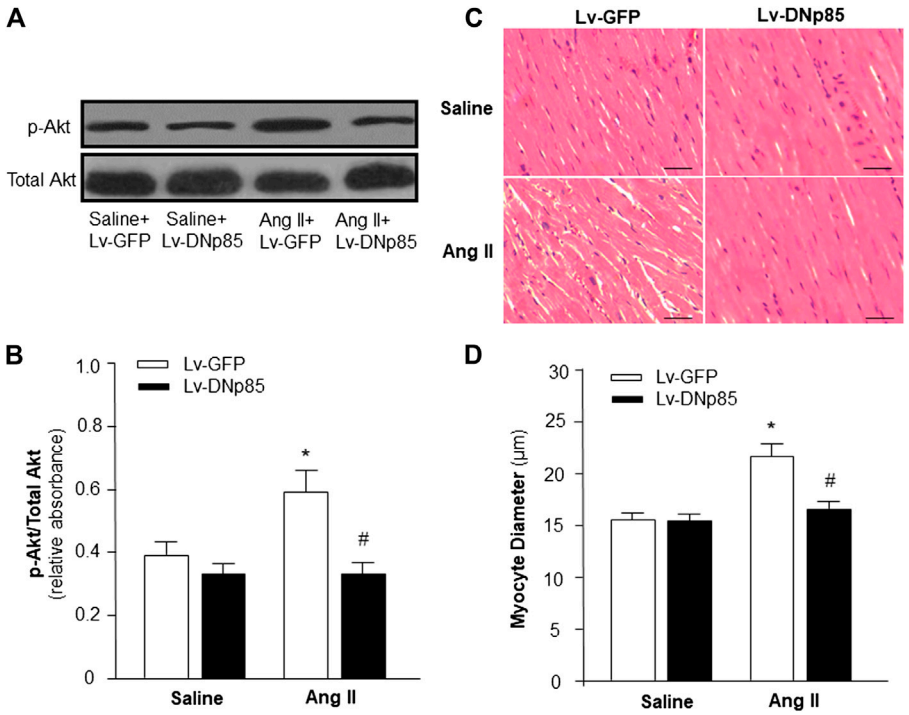

FIGURE 1 | Effect of blockade of PI3KC1 on Ang II-induced cardiac hypertrophy in rat hearts. Cardiomyocyte diameter and Akt phosphorylation were examined in SD rats that received subcutaneous infusion of Ang II or saline control with cardiac transduction of Lv-DNp85 or Lv-GFP. **(A)** Representative western blots of phosphorylated Akt (p-Akt) and total Akt in the heart of each group of rats. **(B)** Bar graphs summarizing the ratio of phosphorylated Akt vs. total Akt. Data are presented as means ± SE (n = 6 rats). *$p < 0.05$ as compared with the group of saline + Lv-GFP. #$p < 0.05$ as compared with the group of Ang II + Lv-GFP. **(C)** Micrographs showing representative heart sections stained with hematoxylin/eosin in each group of rats. **(D)** Bar graphs summarizing diameter of cardiac myocytes from transverse cardiac sections of each group of rats. 100 cells per rat were observed randomly and averaged. Scale bar: 50 μm. Data are means ± SE (n = 6 rats in each group). *$p <$ 0.05 vs. rats that received saline + Lv-GFP. #$p < 0.05$ vs. rats that received Ang II + Lv-GFP.

for 5-min rounds of tissue digestion (10–12 times). The supernatants from each incubation were pooled and added into an equal volume of DMEM containing 10% FBS. Isolated cells were then filtered with a 70 μm cell sieve and centrifuged (1,000 rpm) for 10 min. After centrifuge, supernatants were discarded and cell pellets were re-suspended in DMEM composed of 10% FBS and 1% penicillin-streptomycin. The cells were placed in an incubator for 1.5 h to allow non-myocyte cells, such as fibroblasts, to attach on the plate bottom. The cell suspension (final cellular density 5×10^5 cells/cm^2) was then transferred to a 24-well plate. In the first three days, 5-Bromodeoxyuridine (10^{-4} M) was added to suppress fibroblast growth. All of the manipulations were performed in a culture hood to ensure an aseptic environment. After the cell cultures reached confluence (5 days on average) in an incubator filled with a humidified atmosphere of 5% CO_2 at 37°C, cardiomyocytes were used for *in vitro* experiments.

Cardiomyocyte Morphology Examination and Autophagy Detection

Cultured cardiomyocytes were treated with the HBSS control, vehicle (0.1% DMSO) control, Ang II, LY-294002 (a PI3KC1 inhibitor), 3-MA (a PI3KC3 inhibitor), LY-294002 + Ang II, or 3-MA + Ang II for 24 h. Cardiomyocyte autophagy was determined using immunofluorescent staining with anti-MAP-LC3 antibodies as described in our previous publication (Yao et al., 2010). In brief, cells were fixed with 4% paraformaldehyde for 30 min. The cells were washed with fresh PBS containing 0.1% Triton X-100 three times. After pre-incubation with 3% bovine serum albumin (BSA) for 20 min, the cells were incubated with a mixture of primary antibodies against α-actin and LC3 (1:100 dilution) overnight at 4°C. After washing with PBS-Triton X-100 solution, cells were incubated with fluorescence-conjugated secondary antibodies (1:1,000 dilution) for 2 h at room temperature in the dark. The images were taken under a fluorescence microscope (Olympus). The cardiomyocytes were identified by α-actin positive cells. The puncta were counted inside of the cardiomyocytes that were identified with α-actin. The average number of puncta in each cell was calculated as described in previous literature (Hou et al., 2014). At least 10 different cells in each dish were randomly chosen to measure autophagy. A higher average number of puncta in each cell indicates a larger degree of autophagy occurence. The results are expressed as fold changes vs. HBSS control.

In addition, photographic images of cardiomyocytes taken with the fluorescence microscope were analyzed using computer

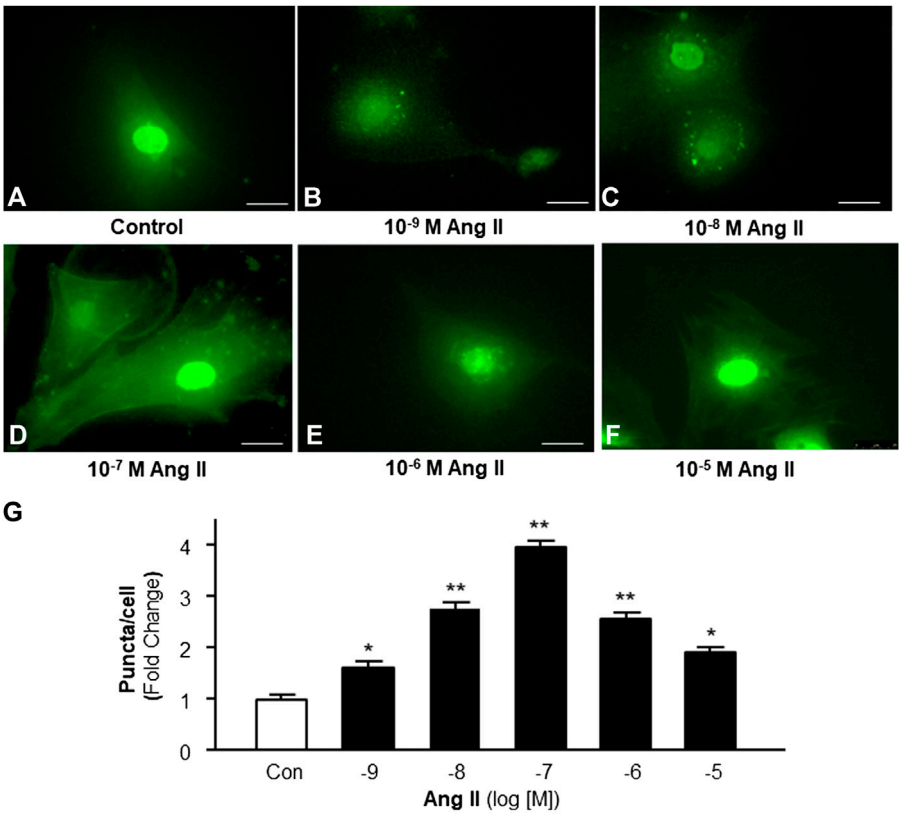

FIGURE 2 | Effect of Ang II on autophagy in cardiomyocytes. Autophagy was detected with MAP-LC3 antibody immunofluorescence by counting intracellular puncta as formation of autophagosomes. **(A–F)** Representative fluorescence micrographs of cultured cardiomyocytes stained with anti-LC3 antibodies after treatments with HBSS control **(A)**, and Ang II at different concentrations (from 10^{-9} to 10^{-5} M, B-F). **(G)** Bar graphs showing the effect on autophagy under Ang II exposure at different concentrations. Data are mean ± SE, n = 10 in each group. *$p < 0.05$ vs. Control. **$p < 0.01$ vs. Control.

software (Image Pro plus 6.0, Media Cybernetics, Bethesda, MD). The cell surface area of cardiomyocytes that were positively stained for sarcomeric actin was measured. At least 50 cells in each dish were randomly selected for surface area analysis.

Measurement of ROS Production in Cardiomyocytes

Mitochondrial ROS production was determined using the superoxide-sensitive ($O_2^{\cdot-}$) fluorogenic probe MitoSox (Thermo Fisher, M-36008, Rockford, IL) as detailed in our previous publication (Guo et al., 2017). MitoSOX has a dihydroethidium (DHE) part linked to a triphenylphosphoninum (TPP) component and yields red fluorescence when oxidized (excitation/emission wavelength: 510/580 nm). This compound is more concentrated in the mitochondria than in the cytosol since the former has more positively charged TPP. Cultured cardiomyocytes were pretreated with the vehicle (DMSO, 0.1%) control, LY-294002, or 3-MA for 30 min. Then the cardiomyocytes were treated with Ang II (10^{-6} M) or HBSS control. Intracellular mitochondrial ROS levels were measured immediately after the addition of Ang II or HBSS control by incubation with MitoSOX (5×10^{-6} M, 15 min). The fluorescence resulting from intracellular probe oxidation was measured with a fluorescence microscope (Olympus) and analyzed with computer software (Image Pro plus 6.0).

Western Blot Analysis

The protein levels of p-Akt and total Akt in heart tissue were assessed by Western Blots, as described in our previous publication (Yao et al., 2008). Briefly, antibodies against p-Akt or total Akt (Santa Cruz, Dallas, TX) were used as primary antibodies (1:500 dilution). Peroxidase-conjugated antibodies against rabbit IgG and mouse IgG (Bio-Rad, Hercules, CA) were used as secondary antibodies (1:15,000 dilution). Immunoreactivity was detected by enhanced chemiluminescence autoradiography. Films were analyzed using Image J.

Data Analysis

All data are presented as means ± SE. Data were statistically analyzed using computer software (GraphPad Prism 5.0). Statistical significance was determined using one- or two-way ANOVA, as appropriate; and confirmed by either a Newman–Keuls or Bonferroni's *post hoc* analysis. *p* values

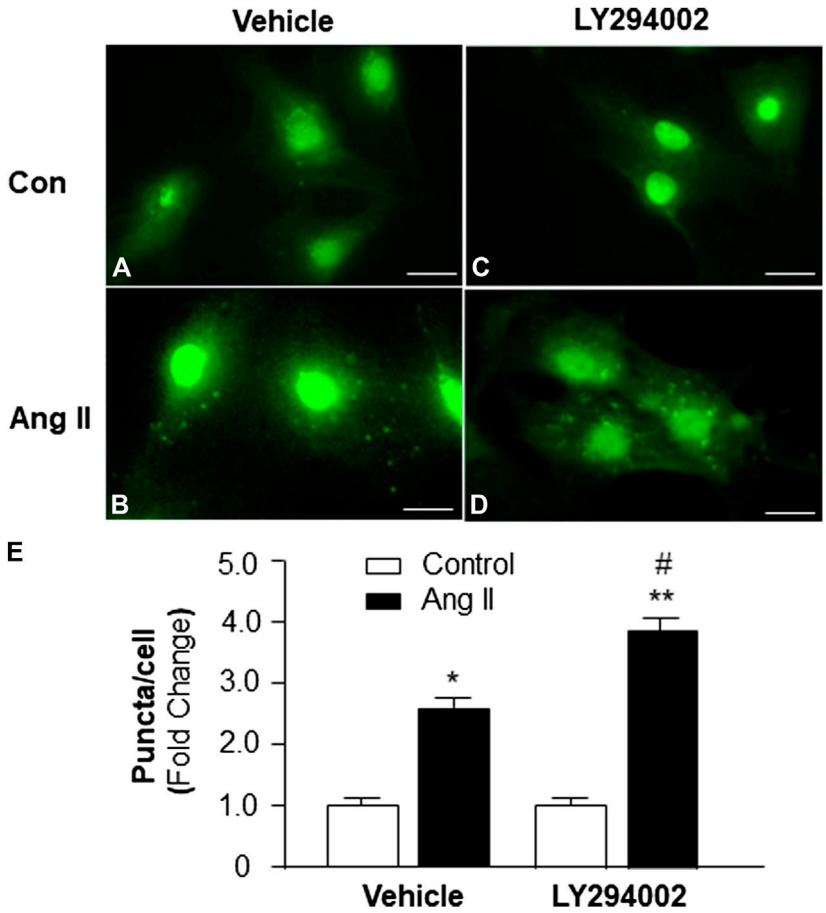

FIGURE 3 | Effect of Ang II and blockade of PI3KC1 on autophagy in cardiomyocytes. Autophagy was examined in cardiomyocytes by immunostaining fluorescence with MAP-LC3 antibodies in cardiomyocytes treated with vehicle control, Ang II (10^{-6} M) with or without the PI3KC1 inhibitor, LY-294002 (10^{-6} M) for 24 h **(A–D)** Representative fluorescence micrographs of cultured cardiomyocytes stained with MAP-LC3 antibodies after treatments. **(E)** Bar graphs summarizing quantitative analysis of autophagic alterations in cardiomyocytes treated under the conditions described in the above. The scale in the images is 25 μm. Data are means ± SE, which were derived from three experiments and at least triplicate wells in each experiment.*$p < 0.05$ vs. cardiomyocytes that treated with vehicle control. **$p < 0.01$ vs. cardiomyocytes that treated with vehicle control. #$p < 0.05$ vs. cardiomyocytes that treated with Ang II.

<0.05 were taken as significant. Significance levels are given in the text.

RESULTS

Blockade of PI3KC1 Attenuated Ang II-Induced Cardiac Hypertrophy in Rats

First, we determined the role of PI3KC1 in Ang II-induced cardiac hypertrophy by overexpressing the dominant negative class I PI3-kinase p85α subunit (DNp85) or GFP (control) using a viral vector-mediated gene-transfer technique in rat hearts through coronary arterial and cardiac injection. After injection, Ang II (200 ng/kg/min) or normal 0.9% saline were subcutaneously infused using osmotic pumps. After 4-weeks treatment with saline + Lv-GFP, saline + Lv-DNp85, Ang II + Lv-GFP, or Ang II + Lv-DNp85, the rats were euthanized and the cardiac tissue was collected. The PI3KC1 activity was detected using conventional Western Blots with antibodies against phosphorylated Akt (p-Akt) or total Akt. The results (**Figures 1A,B**) demonstrated that 4-weeks infusion of Ang II significantly increased the ratio of p-Akt vs. total Akt (0.38 ± 0.07 in the saline + Lv-GFP group vs. 0.59 ± 0.12 in the Ang II + Lv-GFP group, n = 6, $p < 0.05$), suggesting a chronic stimulatory effect of Ang II on PI3KC1 activity. Lentiviral vector-mediated overexpression of DNp85 dramatically attenuated Ang II infusion-induced phosphorylation of Akt (0.59 ± 0.12 in the Ang II + Lv-GFP group vs. 0.36 ± 0.06 in the Ang II + Lv-DNp85 group, n = 6, $p < 0.05$). The results demonstrate that chronic overexpression of Lv-DNp85 attenuates Ang II infusion-associated activation of PI3KC1.

The effects of Ang II infusion and Lv-DNp85 cardiac transduction on cardiac hypertrophy were evaluated in these four groups of rats by examining the morphology of cardiac myocytes in heart sections using H&E staining. The results are presented in **Figures 1C,D**, demonstrating that Ang II infusion significantly increased the diameter of cardiomyocytes, thus inducing severe cardiac hypertrophy (15.5 ± 0.5 μm in the Saline + Lv-GFP group vs. 22.5 ± 1.2 μm in the Ang II + Lv-

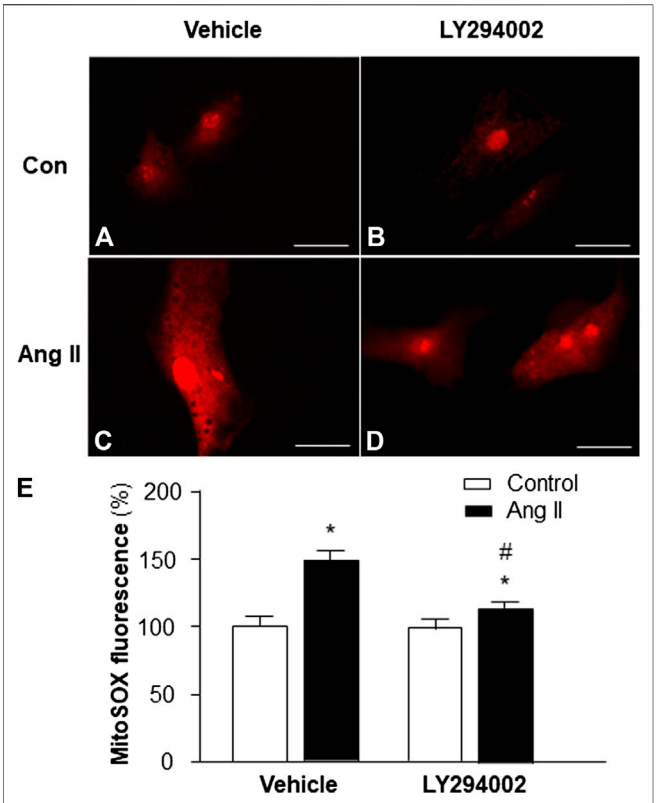

FIGURE 4 | Effect of Ang II and blockade of PI3KC1 on mitochondrial ROS production in cardiomyocytes. Mitochondrial ROS levels were determined using the oxidant-sensitive fluorogenic probe, MitoSOX, in cardiomyocytes treated with vehicle control, Ang II (10^{-6} M) with or without the PI3C1 inhibitor, LY294002 (10^{-6} M). **(A–D)** Representative fluorescence micrographs of cultured cardiomyocytes probed by MitoSOX after treatments. **(E)** Bar graphs summarizing the mitochondrial ROS levels in cardiomyocytes treated with the conditions described above. The scale in the images is 25 μm. Data are presented as means ± SE, which were derived from three experiments and at least triplicate wells in each experiment. *$p < 0.01$ vs. cardiomyocytes treated vehicle control. #$p < 0.05$ vs. cardiomyocytes treated with Ang II.

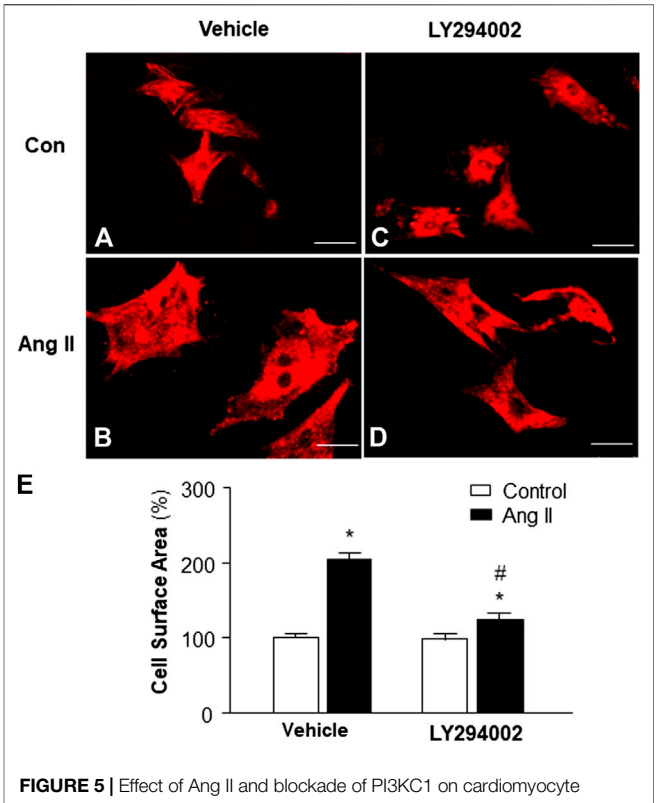

FIGURE 5 | Effect of Ang II and blockade of PI3KC1 on cardiomyocyte hypertrophy. Morphology of cardiomyocytes were determined by immunocytochemistry using an α-sarcomeric actin antibody in cardiomyocytes after treated with vehicle control, Ang II (10^{-6} M) with or without the PI3KC1 inhibitor, LY294002 (10^{-6} M) for 24 h **(A–D)** Representative fluorescence micrographs of cultured cardiomyocytes stained with α-sarcomeric actin antibody after treatments. **(E)** Bar graph summarizing the size of cardiomyocytes after the indicated treatment. Data are means ± SE, derived from three experiments and at least triplicate wells in each experiment. *$p < 0.05$ vs. control; #$p < 0.05$ vs. Ang II treatment.

GFP group, n = 6, $p < 0.05$). Ang II-induced increases in cardiomyocyte diameter were significantly attenuated by cardiac transduction of Lv-DNp85 (22.5 ± 1.2 μm in the Ang II + Lv-GFP group vs. 17.6 ± 1.1 μm in the Ang II + Lv-DNp85 group, n = 6, $p < 0.05$). The results demonstrate that blockade of PI3KC1 attenuates chronic Ang II infusion-associated cardiac hypertrophy.

Effect of Ang II on Cardiomyocyte Autophagy

Accumulating evidence indicates the possible involvement of autophagy in the pathophysiology of Ang II-induced cardiac hypertrophy (Zhou et al., 2016; Guo et al., 2017). Autophagy is a very important intracellular mechanism to protect cells from hazardous material accumulation by scavenging damaged mitochondria or proteins that produce reactive oxygen species (ROS). Intracellular ROS plays an important role in the pathogenesis of cardiac hypertrophy (Sag et al., 2014). Thus, the effect of Ang II on autophagy in cardiomyocytes was examined using immunofluorescence staining with antibodies against microtubule-associated protein light chain 3 (MAP-LC3), an autophagosome marker. The autophagesomes within cardiomyocytes were visualized as green fluorescent puncta, which are able to be counted under a microscope. The results (as shown in **Figure 2**) demonstrate that Ang II treatment caused autophagic alterations with two phases: an increasing phase at lower dosages and a decreasing phase at high dosages.

Effect of PI3KC1 and Ang II on Autophagy

To identify the role of PI3KC1 in Ang II-induced autophagy, autophagy was examined in cardiomyocytes treated with vehicle control or Ang II (10^{-6} M) with or without the presence of LY-294002, a PI3KC1 inhibitor. The results (as shown in **Figure 3**) demonstrate that Ang II (10^{-6} M) induced a significant elevation in autophagy in the presence of vehicle (DMSO, 0.1%, 1.00 ± 0.05 in control vs. 2.61 ± 0.12 in Ang II treatment, n = 3 experiments, $p < 0.05$). Treatment of cardiomyocytes with LY-294002 (10^{-6} M) significantly potentiated Ang II-induced autophagy by 46.4%

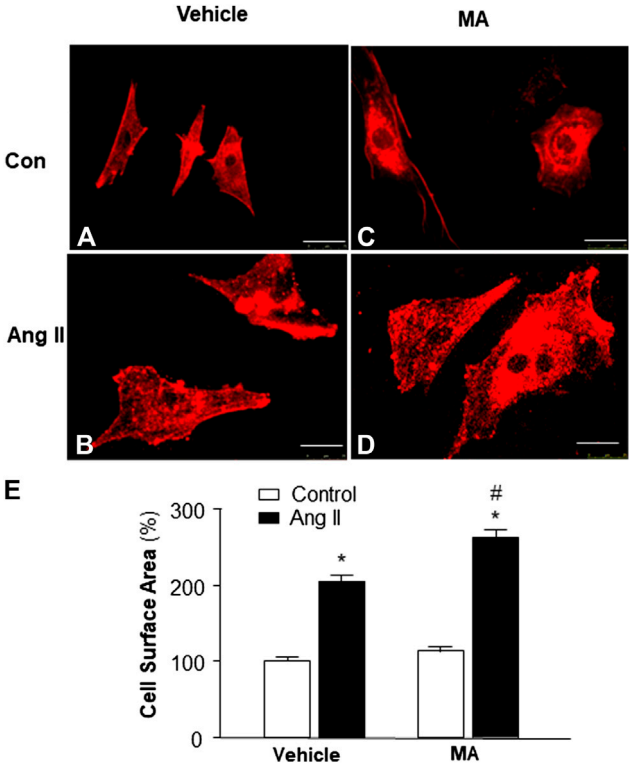

FIGURE 6 | Effect of Ang II and blockade of PI3KC3 on cardiomyocyte hypertrophy. Cell morphology of cardiomyocytes was determined by immunocytochemistry using an α-sarcomeric actin antibody in cardiomyocytes after treatment with vehicle control, Ang II (10^{-6} M) with or without the PI3KC3 inhibitor, 3-methyladenine (3-MA, 10^{-6} M) for 24 h **(A–D)** Representative fluorescence micrographs of cultured cardiomyocytes stained with α-sarcomeric actin antibodies after treatments. **(E)** Bar graph summarizing the size of cardiomyocytes after the indicated treatment. Data are means ± SE, which were derived from three experiments and at least triplicate wells in each experiment. *$p < 0.05$ vs. control; #$p < 0.05$ vs. Ang II treatment.

(1.06 ± 0.07 in LY-294002 alone vs. 3.82 ± 0.13 in LY-294002 plus Ang II, n = 3 experiments, $p < 0.05$). In addition, treatment with LY-294002 alone did not alter basal autophagy in cardiomyocytes. These results indicated that blockade of PI3KC1 significantly increased Ang II-induced autophagy in cardiomyocytes, suggesting that PI3KC1 plays an inhibitory role in Ang II-induced autophagy.

Role of PI3KC1 in Ang II-Induced ROS Production

Based on the results in the experiment above, showing that PI3KC1 has an inhibitory effect on Ang II-induced autophagy, we can propose that PI3KC1-mediated inhibition of autophagy could cause accumulation of damaged mitochondria, leading to elevation in intracellular ROS levels. Therefore, we next determined the role of PI3KC1 in Ang II-induced mitochondrial ROS production. Mitochondrial ROS production was measured using the MitoSox fluorescence approach in cardiomyocytes treated by control or Ang II (10^{-6} M) with or without the PI3KC1 inhibitor, LY-294002 (10^{-6} M). The results are presented in **Figure 4**, demonstrating that treatment of cardiomyocytes with Ang II significantly increased mitochondrial ROS production in the presence of vehicle (DMSO, 0.1%) as expected (100 ± 2.4% in control vs 149.3 ± 3.6% in Ang II, n = 3 experiments, $p < 0.01$). More interestingly, treatment with LY-294002 dramatically attenuated Ang II-induced increases in mitochondrial ROS accumulation by 31.7% in cardiomyocytes (95.3 ± 2.2% in LY-294002 alone vs. 115.6 ± 3.0% in LY-294002 plus Ang II, n = 3 experiments, $p < 0.05$). In addition, treatment with LY-294002 alone did not alter basal mitochondrial ROS production. These results suggest that PI3KC1-induced inhibition of autophagy may contribute to the Ang II treatment-associated elevation in intracellular ROS levels in cardiomyocytes.

Role of PI3KC1 in Ang II-Induced Cardiac Hypertrophy

Increasing evidence indicates that elevated mitochondrial ROS is involved in Ang II-induced cardiac hypertrophy (Guo et al., 2017). Considering the result from the experiment above, showing that PI3KC1 contributes to Ang II-induced elevation in intracellular ROS levels, we thus examined the role of PI3KC1 in Ang II-induced cardiac hypertrophy. The cell surface area was measured under a fluorescence microscope in cardiomyocytes stained with α-sarcomeric actin antibodies after treatment with control or Ang II (10^{-6} M) with or without a PI3KC1 inhibitor, LY-294002 (10^{-6} M). The results are presented in **Figure 5**, showing that treatment with Ang II significantly increased the cell surface area by 2-fold and that co-treatment with LY294002 significantly attenuated the Ang II-induced increase in cell surface area. In addition, LY2940002 alone did not alter the basal size of the cells. These results demonstrate that blockade of PI3KC1 significantly attenuated Ang II-induced cardiac hypertrophy, suggesting that activation of PI3KC1 contributes to Ang II-induced cardiac hypertrophy.

Role of PI3KC3 in Ang II-Induced Cardiac Hypertrophy

Previous studies demonstrate that mice with a PI3KC3 gene deletion have increased heart size (Jaber et al., 2012). Thus, we examined the role of PI3KC3 in Ang II-induced cardiac hypertrophy. The size of cardiomyocytes was measured under a fluorescence microscope in cardiomyocytes stained with α-sarcomeric actin antibodies after treatment with control or Ang II (10^{-6} M) with or without a PI3KC3 inhibitor, 3-methyladenine (3-MA, 10^{-6} M). The results are presented in **Figure 6**, demonstrating that treatment of cardiomyocytes with Ang II significantly increased the cell surface area as expected. More interestingly, co-treatment with 3-MA significantly facilitated Ang II-induced increases in cell surface area. Treatment with 3-MA alone did not significantly alter the basal size of the cells. These results demonstrate that blockade of PI3KC3 significantly promotes Ang II-induced cardiac

hypertrophy, suggesting that PI3KC3 activation may have a protective effect on Ang II-induced cardiac hypertrophy.

Role of PI3KC3 in Ang II-Induced ROS Production

Previous studies demonstrate that increased intracellular ROS production contributes to cardiac hypertrophy (Sag et al., 2014); thus, we examined the hypothesis that PI3KC3 reduces intracellular ROS production, leading to a protective effect on Ang II-induced cardiac hypertrophy. Mitochondrial ROS levels were detected using MitoSOX staining in cardiomyocytes after treatment with control or Ang II (10^{-6} M) with or without PI3KC3 inhibitor, 3-MA (10^{-6} M). The results are presented in **Figure 7A**, demonstrating that Ang II treatment significantly increased MitoSOX fluorescence density, suggesting elevated ROS levels, as expected. More interestingly, co-incubation with 3-MA significantly facilitated Ang II-induced increases in mitochondrial ROS production. However, treatment with 3-MA alone did not significantly alter basal ROS production. These results demonstrate that blockade of PI3KC3 promoted Ang II-induced mitochondrial ROS production, suggesting that activation of PI3KC3 may exert a protective effect on Ang II-induced ROS generation in cardiomyocytes.

Role of PI3KC3 in Ang II-Induced Autophagy

We next examined whether the protective effect of PI3KC3 on Ang II-induced ROS production is mediated by facilitating autophagy, leading to increased scavenging of damaged mitochondria, which is a major source of intracellular ROS. Autophagy was detected with MAP-LC3 antibody immunofluorescence by counting intracellular puncta as formation of autophagesomes in cardiomyocytes treated with control or Ang II (10^{-6} M) with or without 3-MA (10^{-6} M), a PI3KC3 inhibitor. The results are presented in **Figure 7B**, demonstrating that treatment of cardiomyocytes with Ang II significantly increased autophagy as compared with control. Co-treatment with 3-MA significantly attenuated Ang II-induced increases in autophagy. Treatment with 3-MA alone did not significantly alter the basal autophagy levels. These results demonstrate that blockade of PI3KC3 significantly attenuated Ang II-induced increases in autophagy, suggesting that activation of PI3KC3 contributes to Ang II-induced autophagy, facilitating salvage of damaged mitochondria, and thereby leading to reduced ROS production in cardiomyocytes.

DISCUSSION

The present study provides the first evidence that PI3KC1 contributes to Ang II-induced cardiac hypertrophy by inhibiting autophagy and increasing mitochondrial ROS production, and that PI3KC3 has a protective effect on Ang II-induced cardiac hypertrophy by promoting autophagy-mediated scavenging of mitochondrial ROS in cardiomyocytes (as summarized in **Figure 8**). This conclusion is supported by the following evidence: 1) blockade of PI3KC1 promotes Ang II-induced autophagy; in contrast, blockade of PI3KC3 attenuates Ang II-induced autophagy; 2) blockade of PI3KC1 diminishes Ang II-induced increases in mitochondrial ROS production and hypertrophy; 3) blockade of PI3KC3 promotes the Ang II-induced increase in mitochondrial ROS production and hypertrophy; and 4) inhibition of PI3KC1 by viral vector-mediated over-expression of the dominant negative p85 subunit significantly attenuated Ang II-induced cardiac hypertrophy in the heart. Collectively, these findings are consistent with the idea that Class I and Class II PI3-kinases play a different role in Ang II-induced cardiac hypertrophy by regulating autophagy-mediated scavenging of mitochondrial ROS generation.

Previous studies have demonstrated that increased production of ROS is involved tou in Ang II-induced cardiac hypertrophy. It has been proposed that NADPH oxidase is the major source of Ang II-stimulated ROS generation in cardiomyocytes. This

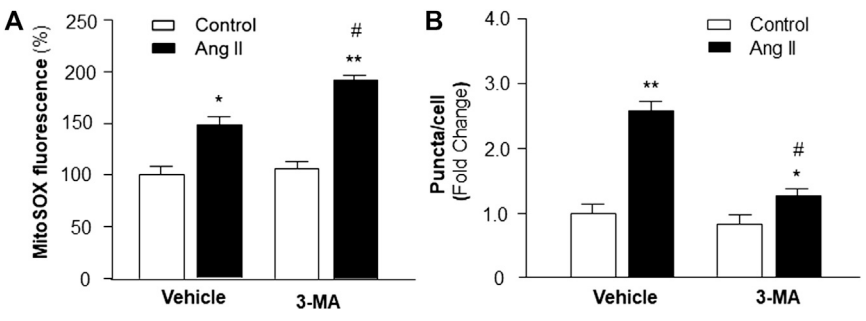

FIGURE 7 | Effect of Ang II and blockade of PI3KC3 on mitochondrial ROS production and autophagy in cardiomyocytes. Mitochondrial ROS levels were determined using the oxidant-sensitive fluorogenic probe, MitoSOX and autophagy was examined using MAP-LC3 antibodies in cardiomyocytes treated with vehicle control, Ang II with or without the PI3KC3 inhibitor, 3-methyladenine (3-MA). **(A)** Bar graphs summarizing the mitochondrial ROS levels in cardiomyocytes treated with vehicle control, Ang II (10^{-6} M), 3-MA (10^{-6} M), and Ang II + 3-MA. Data are presented as means ± SE, which were derived from three experiments and at least triplicate wells in each experiment. *$p < 0.05$ and **$p < 0.01$ vs. cardiomyocytes treated vehicle control. #$p < 0.05$ vs. cardiomyocytes treated with Ang II. **(B)** Bar graphs summarizing quantitative analysis of autophagic alterations in cardiomyocytes treated with vehicle control, Ang II (10^{-6} M), 3-MA (10^{-6} M), and Ang II + 3-MA. Data are means ± SE, which were derived from three experiments and at least triplicate wells in each experiment. *$p < 0.05$ and **$p < 0.01$ vs. cardiomyocytes that treated with vehicle control. #$p < 0.05$ vs. cardiomyocytes that treated with Ang II.

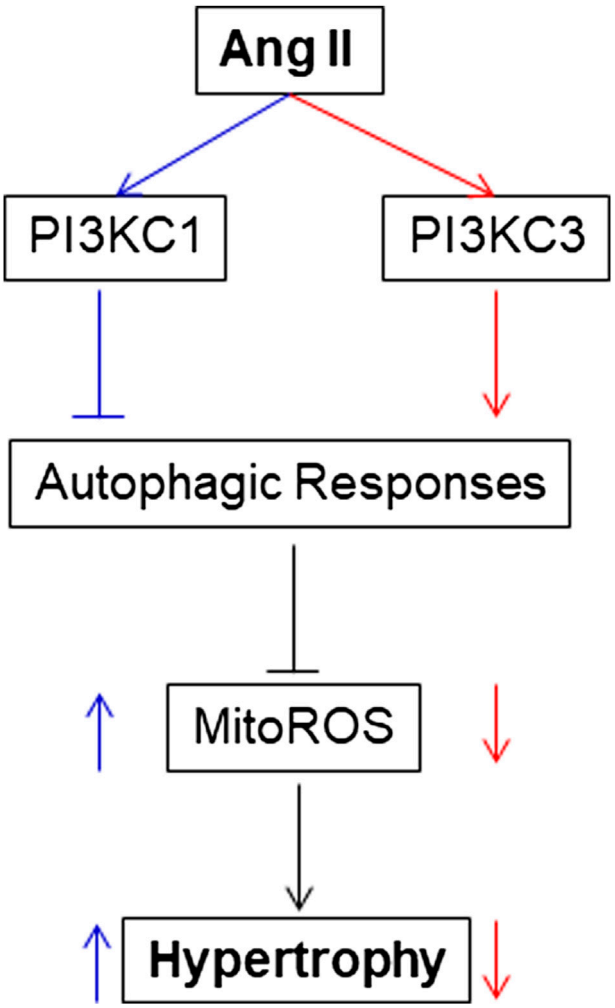

FIGURE 8 | Proposed intracellular mechanisms involved in the action of PI3KC1 vs. PI3KC3 in the Ang II-induced cardiac hypertrophy. PI3KC1, PI3-kinase Class I; PI3KC3, PI3-kinase Class III; ROS, reactive oxygen species; MitoROS, mitochondrial ROS.

hypothesis is supported by a previous study showing that blockade of gp91^{phox}, a subunit of NADPH oxidase, attenuates Ang II infusion-associated-hypertension and cardiac hypertrophy (Bendall et al., 2002). However, blockade of gp91^{phox} associated ROS production has no preventive effect on cardiac hypertrophy in Ang II over-production mice with transgenic overexpression of renin (Touyz et al., 2005). In this regard, mitochondrial dysfunction has been proposed as another source of ROS. It has been reported that ROS derived from damaged mitochondria are involved in cardiac hypertrophy induced by hypertension and myocardial infarction (Pei et al., 2016). This hypothesis is supported by the results from the present study, showing that Ang II treatment significantly increased mitochondrial ROS generation in cardiomyocytes. Furthermore, increased mitochondrial ROS generation was associated with impaired autophagy, a vital intracellular scavenging mechanism for damaged mitochondria that generate ROS. More interestingly, this impaired autophagy induced by Ang II was attenuated by blockade of PI3KC1 in cardiomyocytes. Thus, inhibition of the PI3KC1 signaling pathway could generate a protective effect on cardiac hypertrophy. This hypothesis is validated in our study, which demonstrates that inhibition of PI3KC1 by viral vector-mediated overexpression of dominant negative p85 PI3KC1 subunit (Lv-DNp85) significantly attenuated Ang II perfusion-induced cardiac hypertrophy in rats. These results suggest that the PI3KC1 signaling pathway could be a potential target for the treatment or prevention of cardiac hypertrophy.

One major question that arises from our study concerns the signaling pathways involved in the inhibitory effect of PI3KC1 on autophagy. It has been shown that PI3KC1 phosphorylates protein kinase B/Akt and that Akt induces activation of mTOR, which regulates several cellular functions such as cell growth, proliferation, and autophagy (Vanhaesebroeck et al., 2012; Sciarretta et al., 2018). This observation is consistent with the results from the current study showing that blockade of PI3KC1 with Lv-DNp85 significantly attenuated Ang II-induced phosphorylation of Akt in the heart of rats. In the heart, pharmacological inhibition of mTOR with rapamycin reverses cardiac hypertrophy induced by Akt overexpression (Shioi et al., 2002; Shiojima et al., 2015). In addition, it has been reported that activation of the mTOR signaling pathway inhibits autophagy activity in the heart (Shiojima et al., 2015; Nakai et al., 2007). Therefore, we can propose that the Akt/mTOR signaling pathway could be involved in the PI3KC1 activation-associated impairment of autophagy in cardiomyocytes. This hypothesis needs be verified in future studies.

This study demonstrates, for the first time, that the protective effects of PI3KC3 on Ang II-induced cardiac hypertrophy and mitochondrial ROS production are mediated by promoting autophagy activity. The autophagy mechanism includes the formation of double membraned autophagosomes, the fusion of autophagosomes to late endosomes/lysosomes, and the digestion of the enclosed contents by lysosomal hydrolases. Autophagy functions as an intracellular scavenging procedure by eliminating misfolded proteins and damaged organelles, such as damaged mitochondria, in order to maintain cellular homeostasis. The damaged mitochondria could increase ROS generation, leading to cardiac hypertrophy and heart failure (Bao et al., 2007). It has been reported that impaired autophagy is involved in the development of cardiac hypertrophy (Wang and Cui, 2017). In the current study, we observed that blockade of PI3KC3 significantly inhibited Ang II-induced autophagy activity, leading to increased ROS generation and cardiomyocyte hypertrophy. These findings suggest that PI3KC3 has a protective role in Ang II-induced cardiac hypertrophy by suppression of mitochondrial ROS via up-regulation of autophagy activity. This conclusion is supported by a previous investigation, from Jaber et al. (Jaber et al., 2012), demonstrating that mice with ablation of PI3KC3 Vps34 develop severe cardiac hypertrophy and reduced heart contractility. However, this conclusion will require verification in future studies using animal models.

In summary, we provide the first evidence that both PI3KC1 and PI3KC3 are involved in Ang II-induced cardiac hypertrophy, with each kinase playing a different role: Activation of PI3KC1 negatively regulates autophagy activity, leading to increased mitochondrial ROS production and cardiac hypertrophy. In contrast, activation of PI3KC3 increases autophagy activity, leading to reduced mitochondrial ROS generation and a protective effect on Ang II-induced cardiac hypertrophy. An interesting question that arose from the current studies is why Ang II treatment causes autophagic alterations with two phases: an increasing phase at lower dosages and a decreasing phase at high dosages. The possible underlying mechanism may be due to activation of different PI3Ks. At lower dosage, Ang II predominantly activates PI3KC3, leading to increases in autophagic responses and a protective effect on mitochondrial ROS accumulation. This protective effect may contribute to the compensatory cardiac hypertrophy effect under physiological conditions. It will be very interesting to study whether this protective signaling pathway induced by Ang II at lower dosages is mediated by stimulation of AT2 receptors since activation of AT2 receptors is reported to exhibit a protective effect from cardiac hypertrophy (Castoldi et al., 2019). At higher dosages, Ang II may predominantly activates PI3KC1, besides PI3KC3, leading to inhibition of autophagic responses and accumulation of mitochondrial ROS, which results in a detrimental effect and hypertrophy in the heart. However, this hypothesis needs further investigation in the future. Taken together, the results indicate that the shift from PI3KC3 to PI3KC1 may be involved in the conversion from cardiac compensation to decompensation in pathophysiological conditions; therefore, PI3KC1 and PI3KC3 may be novel therapeutic targets for the prevention or treatment of cardiac hypertrophy.

DATA AVAILABILITY STATEMENT

The raw data supporting the conclusions of this article will be made available by the authors, without undue reservation.

ETHICS STATEMENT

The animal study was reviewed and approved by the North Dakota State University Institutional Animal Care and Use Committee.

AUTHOR CONTRIBUTIONS

TZ and ZW contributed equally to this work. All authors contributed to the article and approved the submitted version.

FUNDING

The contents of this study are solely the responsibility of the authors and do not necessarily represent the official view of NIH.

ACKNOWLEDGMENTS

This work was supported by Grants from National Institutes of Health (NIH, NS55008, HL143519). Some of the data presented in this manuscript was from the Doctoral Thesis of Tiecheng Zhong at North Dakota State University (Zhong, 2018).

REFERENCES

Bao, W., Behm, D. J., Nerurkar, S. S., Ao, Z., Bentley, R., Mirabile, R. C., et al. (2007). Effects of p38 MAPK Inhibitor on angiotensin II-dependent hypertension, organ damage, and superoxide anion production. *J.* Cardiovasc. Pharmacol. 49, 362–368. doi:10.1097/FJC.0b013e318046f34a

Bendall, J. K., Cave, A. C., Heymes, C., Gall, N., and Shah, A. M. (2002). Pivotal role of a gp91(phox)-containing NADPH oxidase in angiotensin II-induced cardiac hypertrophy in mice. *Circulation* 105, 293–296. doi:10.1161/hc0302.103712

Castoldi, G., di Gioia, C. R. T., Roma, F., Carletti, R., Manzoni, G., Stella, A., et al. (2019). Activation of angiotensin type 2 (AT2) receptors prevents myocardial hypertrophy in Zucker diabetic fatty rats. *Acta Diabetol.* 56 (1), 97–104. doi:10.1007/s00592-018-1220-1

Guo, L., Yin, A., Zhang, Q., Zhong, T., O'rourke, S. T., and Sun, C. (2017). Angiotensin-(1-7) attenuates angiotensin II-induced cardiac hypertrophy via a Sirt3-dependent mechanism. *Am. J. Physiol. Heart Circ. Physiol.* 312, H980–H991. doi:10.1152/ajpheart.00768.2016

Harvey, P. A., and Leinwand, L. A. (2011). The cell biology of disease: cellular mechanisms of cardiomyopathy. *J. Cell Biol.* 194, 355–365. doi:10.1083/jcb.201101100

Hill, J. A., and Olson, E. N. (2008). Cardiac plasticity. *N. Engl. J. Med.* 358, 1370–1380. doi:10.1056/NEJMra072139

Hou, X., Hu, Z., Xu, H., Xu, J., Zhang, S., Zhong, Y., et al. (2014). Advanced glycation endproducts trigger autophagy in cadiomyocyte via RAGE/PI3K/AKT/mTOR pathway. *Cardiovasc. Diabetol.* 13, 78. doi:10.1186/1475-2840-13-78

Hunyady, L., and Catt, K. J. (2006). Pleiotropic AT1 receptor signaling pathways mediating physiological and pathogenic actions of angiotensin II. *Mol. Endocrinol.* 20, 953–970. doi:10.1210/me.2004-0536

Iwanaga, Y., Hoshijima, M., Gu, Y., Iwatate, M., Dieterle, T., Ikeda, Y., et al. (2004). Chronic phospholamban inhibition prevents progressive cardiac dysfunction and pathological remodeling after infarction in rats. *J. Clin. Invest.* 113, 727–736. doi:10.1172/JCI18716

Jaber, N., Dou, Z., Chen, J. S., Catanzaro, J., Jiang, Y. P., Ballou, L. M., et al. (2012). Class III PI3K Vps34 plays an essential role in autophagy and in heart and liver function. *Proc. Natl. Acad. Sci. U.S.A.* 109, 2003–2008. doi:10.1073/pnas.1112848109

Misawa, H., Ohtsubo, M., Copeland, N. G., Gilbert, D. J., Jenkins, N. A., and Yoshimura, A. (1998). Cloning and characterization of a novel class II phosphoinositide 3-kinase containing C2 domain. *Biochem. Biophys. Res. Commun.* 244, 531–539. doi:10.1006/bbrc.1998.8294

Nakai, A., Yamaguchi, O., Takeda, T., Higuchi, Y., Hikoso, S., Taniike, M., et al. (2007). The role of autophagy in cardiomyocytes in the basal state and in response to hemodynamic stress. *Nat. Med.* 13, 619–624. doi:10.1038/nm1574

Pei, H., Yang, Y., Zhao, H., Li, X., Yang, D., Li, D., et al. (2016). The role of mitochondrial functional proteins in ROS production in ischemic heart diseases. *Oxid. Med. Cell. Longev.* 2016, 5470457. doi:10.1155/2016/5470457

Sadoshima, J., Xu, Y., Slayter, H. S., and Izumo, S. (1993). Autocrine release of angiotensin II mediates stretch-induced hypertrophy of cardiac myocytes *in vitro*. *Cell* 75, 977–984. doi:10.1016/0092-8674(93)90541-w

Sag, C. M., Santos, C. X., and Shah, A. M. (2014). Redox regulation of cardiac hypertrophy. *J. Mol. Cell. Cardiol.* 73, 103–111. doi:10.1016/j.yjmcc.2014.02.002

Sciarretta, S., Forte, M., Frati, G., and Sadoshima, J. (2018). New insights into the role of mTOR signaling in the cardiovascular System. *Circ. Res.* 122, 489–505. doi:10.1161/CIRCRESAHA.117.311147

Shioi, T., Kang, P. M., Douglas, P. S., Hampe, J., Yballe, C. M., Lawitts, J., et al. (2000). The conserved phosphoinositide 3-kinase pathway determines heart size in mice. *EMBO J.* 19, 2537–2548. doi:10.1093/emboj/19.11.2537

Shioi, T., McMullen, J. R., Kang, P. M., Douglas, P. S., Obata, T., Franke, T. F., et al. (2002). Akt/protein kinase B promotes organ growth in transgenic mice. *Mol. Cell Biol.* 22, 2799–2809. doi:10.1128/mcb.22.8.2799-2809.2002

Shiojima, I., Sato, K., Izumiya, Y., Schiekofer, S., Ito, M., Liao, R., et al. (2015). Disruption of coordinated cardiac hypertrophy and angiogenesis contributes to the transition to heart failure. *J. Clin. Invest.* 115, 2108–2118. doi:10.1172/JCI24682

Sun, C., Zubcevic, J., Polson, J. W., Potts, J. T., Diez-Freire, C., Zhang, Q., et al. (2009). Shift to an involvement of phosphatidylinositol 3-kinase in angiotensin II actions on nucleus tractus solitarii neurons of the spontaneously hypertensive rat. *Circ. Res.* 105, 1248–1255. doi:10.1161/CIRCRESAHA.109.208926

Touyz, R. M., Mercure, C., He, Y., Javeshghani, D., Yao, G., Callera, G. E., et al. (2005). Angiotensin II-dependent chronic hypertension and cardiac hypertrophy are unaffected by gp91phox-containing NADPH oxidase. *Hypertension* 45, 530–537. doi:10.1161/01.HYP.0000158845.49943.5e

Vanhaesebroeck, B., Stephens, L., and Hawkins, P. (2012). PI3K signalling: the path to discovery and understanding. *Nat. Rev. Mol. Cell Biol.* 13, 195–203. doi:10.1038/nrm3290

Wang, X., and Cui, T. (2017). Autophagy modulation: a potential therapeutic approach in cardiac hypertrophy. *Am. J. Physiol. Heart Circ. Physiol.* 313, H304–H319. doi:10.1152/ajpheart.00145.2017

Wenzel, S., Abdallah, Y., Helmig, S., Schäfer, C., Piper, H. M., and Schluter, K. D. (2006). Contribution of PI 3-kinase isoforms to angiotensin II- and alpha-adrenoceptor-mediated signalling pathways in cardiomyocytes. *Cardiovasc. Res.* 71, 352–362. doi:10.1016/j.cardiores.2006.02.004

Yan, W., Guo, L., Zhang, Q., Sun, W., O'Rourke, S. T., Liu, K., et al. (2015). Chronic blockade of class I PI3-kinase attenuates Ang II-induced cardiac hypertrophy and autophagic alteration. *Eur. Rev. Med. Pharmacol. Sci.* 19, 772–783.

Yao, F., Sumners, C., O'rourke, S. T., and Sun, C. (2008). Angiotensin II increases GABAB receptor expression in nucleus tractus solitarii of rats. *Am. J. Physiol. Heart Circ. Physiol.* 294, H2712–H2720. doi:10.1006/bbrc.1998.829410.1152/ajpheart.00729.2007

Yao, F., Sun, C., and Chang, S. K. (2010). Morton lentil extract attenuated angiotensin II-induced cardiomyocyte hypertrophy via inhibition of intracellular reactive oxygen species levels *in vitro*. *J. Agric. Food Chem.* 58, 10382–10388. doi:10.1021/jf101648m

Zhao, H., Qi, G., Han, Y., Shen, X., Yao, F., Xuan, C., et al. (2015). 20-Hydroxyeicosatetraenoic acid is a key mediator of angiotensin II-induced apoptosis in cardiac myocytes. *J. Cardiovasc. Pharmacol.* 66, 86–95. doi:10.1097/FJC.0000000000000248

Zhong, T. (2018). Ang II-induced cardiac remodeling: role of PI3-kinase-dependent autophagy. Dissertation/Doctoral Thesis. Fargo (ND): North Dakota State University.

Zhou, L., Ma, B., and Han, X. (2016). The role of autophagy in angiotensin II-induced pathological cardiac hypertrophy. *J. Mol. Endocrinol.* 57, R143–R152. doi:10.1530/JME-16-0086

Conflict of Interest: The authors declare that the research was conducted in the absence of any commercial or financial relationships that could be construed as a potential conflict of interest.

Advantages of publishing in Frontiers

OPEN ACCESS
Articles are free to read for greatest visibility and readership

FAST PUBLICATION
Around 90 days from submission to decision

HIGH QUALITY PEER-REVIEW
Rigorous, collaborative, and constructive peer-review

TRANSPARENT PEER-REVIEW
Editors and reviewers acknowledged by name on published articles

Frontiers
Avenue du Tribunal-Fédéral 34
1005 Lausanne | Switzerland

Visit us: www.frontiersin.org
Contact us: frontiersin.org/about/contact

REPRODUCIBILITY OF RESEARCH
Support open data and methods to enhance research reproducibility

DIGITAL PUBLISHING
Articles designed for optimal readership across devices

FOLLOW US
@frontiersin

IMPACT METRICS
Advanced article metrics track visibility across digital media

EXTENSIVE PROMOTION
Marketing and promotion of impactful research

LOOP RESEARCH NETWORK
Our network increases your article's readership